

AD-A139 953

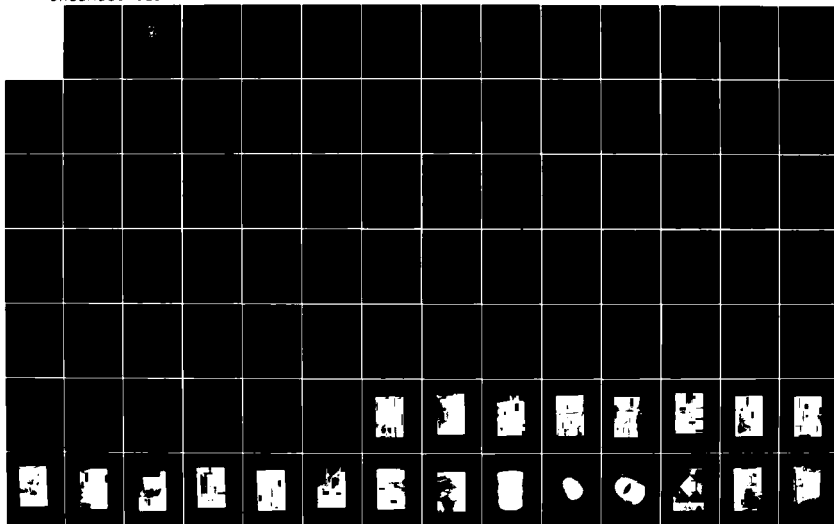
OPERATIONAL PERFORMANCE CHARACTERISTICS OF A
MULTIPLY-SHROUDED ANGLED-DIF... (U) NAVAL POSTGRADUATE
SCHOOL MONTEREY CA R E STAPLES SEP 83

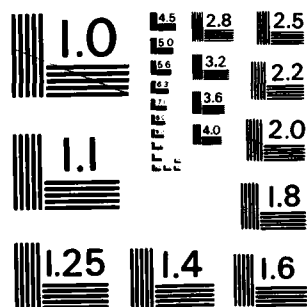
1/2

UNCLASSIFIED

F/G 21/5

NL





MICROCOPY RESOLUTION TEST CHART
NATIONAL BUREAU OF STANDARDS-1963-A

2

NAVAL POSTGRADUATE SCHOOL

Monterey, California

AD A139953



THESIS

OPERATIONAL PERFORMANCE CHARACTERISTICS OF
A MULTIPLY-SHROUDED, ANGLED-DIFFUSER STACK
GAS EDUCTOR IN TURBULENT CROSS-FLOW

by

Ralph Eugene Staples, Jr.

September 1983

Thesis Advisor:

P. F. Pucci

DTIC
SELECTED
APR 10 1984
S E

DTIC FILE COPY

Approved for public release; distribution unlimited.

84 04 09 199

Unclassified

SECURITY CLASSIFICATION OF THIS PAGE (When Data Entered)

REPORT DOCUMENTATION PAGE		READ INSTRUCTIONS BEFORE COMPLETING FORM
1. REPORT NUMBER	2. GOVT ACCESSION NO. AD-N139 953	3. RECIPIENT'S CATALOG NUMBER
4. TITLE (and Subtitle) Operational Performance Characteristics of a Multiply-Shrouded, Angled-Diffuser Stack Gas Eductor in Turbulent Cross-Flow		5. TYPE OF REPORT & PERIOD COVERED Master's Thesis; September 1983
		6. PERFORMING ORG. REPORT NUMBER
7. AUTHOR(s) Ralph Eugene Staples, Jr.		8. CONTRACT OR GRANT NUMBER(s)
9. PERFORMING ORGANIZATION NAME AND ADDRESS Naval Postgraduate School Monterey, California 93943		10. PROGRAM ELEMENT, PROJECT, TASK AREA & WORK UNIT NUMBERS
11. CONTROLLING OFFICE NAME AND ADDRESS Naval Postgraduate School Monterey, California 93943		12. REPORT DATE September 1983
		13. NUMBER OF PAGES 218
14. MONITORING AGENCY NAME & ADDRESS (if different from Controlling Office)		15. SECURITY CLASS. (of this report) Unclassified
		15a. DECLASSIFICATION/DOWNGRADING SCHEDULE
16. DISTRIBUTION STATEMENT (of this Report) Approved for public release; distribution unlimited.		
17. DISTRIBUTION STATEMENT (of the abstract entered in Block 20, if different from Report)		
18. SUPPLEMENTARY NOTES		
19. KEY WORDS (Continue on reverse side if necessary and identify by block number)		
Gas Eductor	Diffuser Rings	Cooling
Multiple Nozzle	Hot Flow	Secondary Flow
Mixing Stack	Hot Primary Flow	Tertiary Flow
Shroud	Exhaust	Turbulent Cross-Flow
20. ABSTRACT (Continue on reverse side if necessary and identify by block number)		
<p>Performance characteristics of two multiple-ring diffuser eductors were determined from collected data. The performance characteristics of a five ring diffuser model were compared with a geometrically similar model tested in cold flow. Model similarity for comparison was maintained through the mach number.</p>		

DD FORM 1 JAN 73 1473

EDITION OF 1 NOV 65 IS OBSOLETE 1
S/N 0102-LP-014-6601

Unclassified

SECURITY CLASSIFICATION OF THIS PAGE (When Data Entered)

Unclassified

SECURITY CLASSIFICATION OF THIS PAGE (When Data Entered)

Both models were tested in a turbulent cross-flow simulating a 29.5 knot relative wind. Minor improvement in the pumping coefficient was seen to occur when cross-flow was introduced.

External surface temperature measurements along the model assembly were recorded by two methods for comparative analysis. The effect of cross-flow is seen in a significant surface temperature reduction in the shroud assembly while apparent degradation of film cooling effectiveness at the diffuser rings resulted in minimal temperature change.

Accession For	
NTIS GPRM	<input checked="checked" type="checkbox"/>
DTIC TAB	<input type="checkbox"/>
Unannounced	<input type="checkbox"/>
Justification	
By _____	
Distribution/	
Availability Codes	
Avail and/or	
Dist	Special
A-1	

DTIC
COPY
INSPECTED
1

Approved for public release; distribution unlimited.

Operational Performance Characteristics of a
Multiply-Shrouded, Angled-Diffuser Stack Gas
Eductor in Turbulent Cross-Flow

by

Ralph E. Staples, Jr.
Lieutenant Commander, United States Navy
B.S. Mar.Eng., Maine Maritime Academy, 1971

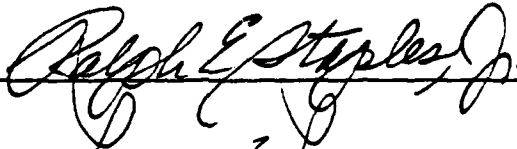
Submitted in partial fulfillment of the
requirements for the degree of

MASTER OF SCIENCE IN MECHANICAL ENGINEERING


from the

NAVAL POSTGRADUATE SCHOOL
September 1983

Author



Approved by:


Thesis Advisor


Chairman, Department of Mechanical Engineering


Dean of Science and Engineering

ABSTRACT

Performance characteristics of two multiple-ring diffuser eductors were determined from collected data. The performance characteristics of a five ring diffuser model were compared with a geometrically similar model tested in cold flow. Model similarity for comparison was maintained through the Mach number.

Both models were tested in a turbulent cross-flow simulating a 29.5 knot relative wind. Minor improvement in the pumping coefficient was seen to occur when cross-flow was introduced.

External surface temperature measurements along the model assembly were recorded by two methods for comparative analysis. The effect of cross-flow is seen in a significant surface temperature reduction in the shroud assembly while apparent degradation of film cooling effectiveness at the diffuser rings resulted in minimal temperature change.

TABLE OF CONTENTS

I.	INTRODUCTION -----	20
II.	BACKGROUND -----	22
	A. THE TEST FACILITIES -----	22
	B. INITIAL INVESTIGATIONS AT NPS -----	23
	C. IMPROVEMENTS IN MIXING STACK CONFIGURATION ----	24
	D. CURRENT OBJECTIVES -----	24
III.	THEORY AND MODELING -----	26
	A. MODELING TECHNIQUE -----	26
	B. ONE-DIMENSIONAL ANALYSIS OF A SIMPLE EDUCTOR -----	27
	C. NON-DIMENSIONAL FORM OF THE SIMPLE EDUCTOR EQUATION -----	34
	D. EXPERIMENTAL CORRELATION -----	37
	E. PUMPING COEFFICIENT -----	38
IV.	EXPERIMENTAL APPARATUS -----	40
	A. COMBUSTOR AIR PATH -----	40
	B. FUEL SYSTEM -----	42
	1. System Arrangement -----	42
	2. Fuel System Flow Rate Measurement and Control -----	43
	C. THE MEASUREMENT PLENUM -----	45
	1. The Rear Seal -----	45
	2. The Forward Seal -----	45
	3. Model Installation and Alignment -----	45

D.	INSTRUMENTATION -----	46
1.	Temperature Measurement -----	46
2.	Pressure Measurement -----	47
E.	THE MODELS -----	47
1.	Model A -----	48
2.	Model A Modified -----	49
F.	THE CROSS-FLOW CENTRIFUGAL FAN -----	49
1.	Installation and Configuration -----	49
2.	Performance Capabilities -----	50
V.	EXPERIMENTAL RESULTS -----	52
A.	MODEL A RESULTS -----	52
1.	Pumping Performance -----	52
2.	Mixing Stack Temperatures -----	52
3.	Mixing Stack Pressures -----	54
4.	Shroud and Diffuser Temperatures -----	54
5.	Exit Plane Temperatures -----	57
B.	MODEL A MODIFIED RESULTS -----	58
1.	Pumping Performance -----	58
2.	Mixing Stack Temperatures -----	59
3.	Mixing Stack Pressures -----	59
4.	Shroud and Diffuser Temperatures -----	59
5.	Exit Plane Temperatures -----	60
VI.	CONCLUSIONS -----	61
VII.	RECOMMENDATIONS -----	62
	FIGURES -----	63
	TABLES -----	162

APPENDIX A: GAS GENERATOR OPERATION -----	191
APPENDIX B: CALIBRATION -----	210
APPENDIX C: UNCERTAINTY ANALYSIS -----	212
LIST OF REFERENCES -----	214
INITIAL DISTRIBUTION LIST -----	216

LIST OF TABLES

I.	Rotameter Calibration Data -----	162
II.	Thermocouple Display Channel Assignments, Type K -----	163
III.	Thermocouple Display Channel Assignments, Type T -----	164
IV.	Model Characteristics -----	165
V.	Pumping Coeff. Data, Model A (175 F) - No Cross-Flow -----	166
VI.	Pumping Coeff. Data, Model A (650 F) - No Cross-Flow -----	167
VII.	Pumping Coeff. Data, Model A (850 F) - No Cross-Flow -----	168
VIII.	Pumping Coeff. Data, Model A (850 F) - Cross-Flow -----	169
IX.	Pumping Coeff. Data, Model A (950 F) - No Cross-Flow -----	170
X.	Pumping Coeff. Data, Model A (950 F) - Cross-Flow -----	171
XI.	Pumping Coeff. Data, Model A Mod (850 F) - No Cross-Flow -----	172
XII.	Pumping Coeff. Data, Model A Mod (850 F) - Cross-Flow -----	173
XIII.	Pumping Coeff. Data, Model A Mod (950 F) - No Cross-Flow -----	174
XIV.	Pumping Coeff. Data, Model A Mod (950 F) - Cross-Flow -----	175
XV.	Mixing Stack Pressure Data, Model A -----	176
XVI.	Mixing Stack Pressure Data, Model A Modified -----	177

XVII.	Mixing Stack Temperature Data, Model A -----	178
XVIII.	Mixing Stack Temperature Data, Model A Mod -----	179
XIX.	Shroud and Diffuser Temp. Data, Model A -----	180
XX.	Shroud and Diffuser Temp. Data, Model A Mod -----	181
XXI.	Exit Plane Temperature Data, Model A -----	182
XXII.	Exit Plane Temperature Data, Model A Mod -----	183
XXIII.	Exit Plane Horiz. Pitot Traverse Data -----	184
XXIV.	24 in. Standoff - Pitot Horiz. Traverse -----	185
XXV.	24 in. Standoff - Pitot Vertical Traverse -----	186
XXVI.	24 in. Standoff - 4.5 in Pitot Vert. Traverse ----	187
XXVII.	Pumping Coefficient Results -----	188
XXVIII.	Air Mass Flow Calibration Data -----	189
XXIX.	Air Mass Flow vs. Pressure Product Data -----	190

LIST OF FIGURES

1.	Simple Nozzle Eductor System -----	63
2.	Plan of Uptake, Model, and Measurement Plenum -----	64
3.	Dimensional Diagram of Slotted Mixing Stack -----	65
4.	Schematic of Model A - Shroud and Diffuser Rings ---	66
5.	Schematic of Model A Modified - Shroud and Diffuser Rings -----	67
6.	Characteristic Eductor Dimensions -----	68
7.	Gas Generator Arrangement -----	69
8.	Schematic Diagram of Pressure Measurement System ---	70
9.	Schematic Diagram of Temperature Measurement System -----	71
10.	Gas Generator Electrical System -----	72
11.	Gas Generator Fuel System -----	73
12.	Gas Generator Control Station -----	74
13.	Main Power Supply and Control Panel -----	75
14.	Manometer Installation -----	76
15.	Hot Flow Test Facility -----	77
16.	Air Supply Standpipe and Valving -----	78
17.	Combustor Air Piping -----	79
18.	Uptake Section -----	80
19.	Carrier Air Compressor -----	81
20.	Air Compressor Suction Valve -----	82
21.	Air Cooling Bank and Bypass Discharge -----	83
22.	Cooling Water Pump and Tower Fan Controllers -----	84

23.	Auxiliary Oil Pump Control -----	85
24.	Fuel Pump Installation -----	86
25.	H. P. Fuel Piping and Valves -----	87
26.	Model Installation -----	88
27.	Model Alignment -----	89
28.	Model A -----	90
29.	Model A Entrance -----	91
30.	Model A Exit -----	92
31.	Model A Installed -----	93
32.	Cross-Flow Fan with Model A Installed -----	94
33.	Exit Plane Temperature Measurement -----	95
34.	Tilted-Angled Nozzle Plate -----	96
35.	Tilted Nozzle Geometry -----	97
36.	External Temperature Measurement Points, Model A ---	98
37.	External Temperature Measurement Points, Model A Mod -----	99
38.	Schematic of Cross-Flow Fan Pitot Tube Traverses ---	100
39.	Cross-Flow Fan Nozzle Geometry -----	101
40.	Rotameter Calibration Curve -----	102
41.	Air Mass Flow Rate Calibration Curve -----	103
42.	Sample Pumping Coefficient Plot -----	104
43.	Pumping Coefficient, Model A (175 F) - No Cross-Flow -----	105
44.	Pumping Coefficient, Model A (650 F) - No Cross-Flow -----	106
45.	Pumping Coefficient, Model A (850 F) - No Cross-Flow -----	107

46.	Pumping Coefficient, Model A (850 F) - Cross-Flow --	108
47.	Pumping Coefficient, Model A (950 F) - No Cross-Flow -----	109
48.	Pumping Coefficient, Model A (950 F) - Cross-Flow --	110
49.	Pumping Coefficient, Model A Mod (850 F) - No Cross-Flow -----	111
50.	Pumping Coefficient, Model A Mod (850 F) - Cross-Flow -----	112
51.	Pumping Coefficient, Model A Mod (950 F) - No Cross-Flow -----	113
52.	Pumping Coefficient, Model A Mod (950 F) - Cross-Flow -----	114
53.	Mixing Stack Temp., Model A (650 F) - No Cross-Flow -----	115
54.	Mixing Stack Temp., Model A (850 F) - No Cross-Flow -----	116
55.	Mixing Stack Temp., Model A (850 F) - Cross-Flow ---	117
56.	Mixing Stack Temp., Model A (950 F) - No Cross-Flow -----	118
57.	Mixing Stack Temp., Model A (950 F) - Cross-Flow ---	119
58.	Mixing Stack Temp., Model A Mod (850 F) - No Cross-Flow -----	120
59.	Mixing Stack Temp., Model A Mod (850 F) - Cross-Flow -----	121
60.	Mixing Stack Temp., Model A Mod (950 F) - No Cross-Flow -----	122
61.	Mixing Stack Temp., Model A Mod (950 F) - Cross-Flow -----	123
62.	Mixing Stack Press., Model A (650 F) - No Cross-Flow -----	124
63.	Mixing Stack Press., Model A (850 F) - No Cross-Flow -----	125

64.	Mixing Stack Press., Model A (850 F) - Cross-Flow --	126
65.	Mixing Stack Press., Model A (950 F) - No Cross-Flow -----	127
66.	Mixing Stack Press., Model A (950 F) - Cross-Flow --	128
67.	Mixing Stack Press., Model A Mod (850 F) - No Cross-Flow -----	129
68.	Mixing Stack Press., Model A Mod (850 F) - Cross-Flow -----	130
69.	Mixing Stack Press., Model A Mod (950 F) - No Cross-Flow -----	131
70.	Mixing Stack Press., Model A Mod (950 F) - Cross-Flow -----	132
71.	Type T External Temp., Model A (650 F) - No Cross-Flow -----	133
72.	Type T External Temp., Model A (850 F) - No Cross-Flow -----	134
73.	Type T External Temp., Model A (850 F) - Cross-Flow--	135
74.	Type T External Temp., Model A (950 F) - No Cross-Flow -----	136
75.	Type T External Temp., Model A (950 F) - Cross-Flow--	137
76.	Type T Ext. Temp., Model A Mod (850 F) - No Cross-Flow -----	138
77.	Type T Ext. Temp., Model A Mod (850 F) - Cross-Flow--	139
78.	Type T Ext. Temp., Model A Mod (950 F) - No Cross-Flow -----	140
79.	Type T Ext. Temp., Model A Mod (950 F) - Cross-Flow--	141
80.	Omega External Temp., Model A (650 F) - No Cross-Flow -----	142
81.	Omega External Temp., Model A (850 F) - No Cross-Flow -----	143
82.	Omega External Temp., Model A (850 F) - Cross-Flow--	144

83.	Omega External Temp., Model A (950 F) - No Cross-Flow -----	145
84.	Omega External Temp., Model A (950 F) - Cross-Flow--	146
85.	Omega Ext. Temp., Model A Mod (850 F) - No Cross-Flow -----	147
86.	Omega Ext. Temp., Model A Mod (850 F) - Cross-Flow--	148
87.	Omega Ext. Temp., Model A Mod (950 F) - No Cross-Flow -----	149
88.	Omega Ext. Temp., Model A Mod (950 F) - Cross-Flow--	150
89.	Exit Plane Temp., Model A (650 F) - No Cross-Flow---	151
90.	Exit Plane Temp., Model A (850 F) - No Cross-Flow---	152
91.	Exit Plane Temp., Model A (850 F) - Cross-Flow -----	153
92.	Exit Plane Temp., Model A (950 F) - No Cross-Flow---	154
93.	Exit Plane Temp., Model A (950 F) - Cross-Flow -----	155
94.	Exit Plane Temp., Model A Mod (850 F) - No Cross-Flow -----	156
95.	Exit Plane Temp., Model A Mod (850 F) - Cross-Flow--	157
96.	Exit Plane Temp., Model A Mod (950 F) - No Cross-Flow -----	158
97.	Exit Plane Temp., Model A Mod (950 F) - Cross-Flow--	159
98.	Exit Plane Temp. Comparison, Model A (950 F) -----	160
99.	Exit Plane Temp. Comparison, Model A Mod (950 F) ---	161

TABLE OF SYMBOLS

ENGLISH LETTER SYMBOLS

A	- Area, in ² , ft ²
B	- Atmospheric pressure, in Hg
c	- Sonic velocity, ft/sec
C	- Coefficient of discharge
D	- Diameter, in (as a reference quantity, refers to the inside diameter of the mixing stack)
DELPN	- Pressure drop across the entrance reducing section, in H ₂ O
DELPU	- Pressure drop across the burner U-tube, in H ₂ O
f	- Friction factor
F _{fr}	- Wall skin-friction force, lbf
g	- Proportionality factor in Newton's Second Law g = 32.174 lbm-ft/lbf-sec ²
h	- Enthalpy, Btu/lbm
l	- Arbitrary length, in
L	- Length of the mixing stack assembly, in
P	- Pressure, in H ₂ O
PMS	- Static pressure in the mixing stack, referenced to atmospheric, in H ₂ O
PNH	- Inlet air pressure upstream of the reducing section, in Hg
PPLN	- Pressure differential across the measurement plenum secondary flow nozzles, in H ₂ O

PUPT - Pressure in the uptake, in H_2O

r - Radial distance from the axis of the mixing stack, in

R - Gas Constant, for air = 53.34 ft-lbf/lbm- $^{\circ}R$

ROTA - Fuel mass flow rotameter reading

Rms - Interior radius of the mixing stack, in

s - Entropy, Btu/lbm-R

S - Standoff, distance between the discharge plane of the primary nozzles and the entrance plane of the mixing stack, in

T - Temperature, $^{\circ}F$, $^{\circ}R$

TAMB - Ambient temperature, $^{\circ}F$

TAMBR - Ambient temperature, $^{\circ}R$

TBURN - Burner temperature, $^{\circ}F$

TEP - Exit plane temperature, $^{\circ}F$

TMS - Mixing stack wall temperature, $^{\circ}F$

TNH - Inlet air temperature, $^{\circ}F$

TNHR - Inlet air temperature, $^{\circ}R$

TSURF - Surface temperature of shroud and diffusers, $^{\circ}F$

TUPT - Uptake temperature, $^{\circ}F$

TUPTR - Uptake temperature, $^{\circ}R$

u - Internal Energy (Btu/lbm)

U - Velocity, ft/sec

UM - Average velocity in the mixing stack, ft/sec

UP - Primary flow velocity at nozzle exit, ft/sec

UU - Primary flow velocity in uptake, ft/sec

v - Specific volume (ft³/lbm)

W - Mass flow rate, lbm/sec
 WF - Mass flow rate of fuel, lbm/sec
 WP - Primary mass flow rate, lbm/sec
 WS - Secondary mass flow rate, lbm/sec
 WPA - Mass flow rate of primary air, lbm/sec
 X - Axial distance from mixing stack entrance, in

DIMENSIONLESS GROUPINGS

A* - Secondary flow area to primary flow area ratio
 A * - Tertiary flow area to primary flow area ratio
 K_e - Kinetic energy correction factor
 K_m - Momentum correction factor at mixing stack exit
 K_p - Momentum correction factor at primary nozzle exit
 M, UMACH - Mach number
 P* - Pressure Coefficient for secondary flow
 P * - Pressure coefficient for tertiary flow
 PMS* - Pressure coefficient for mixing stack pressures
 Re - Reynolds number
 T* - Secondary flow absolute temperature to primary
 flow absolute temperature ratio
 T_t* - Tertiary flow absolute temperature to primary
 flow absolute temperature ratio
 W* - Secondary mass flow rate to primary mass flow
 rate ratio
 W_t* - Tertiary mass flow rate to primary mass flow
 rate ratio

- ρ^* - Secondary flow density to primary flow
density ratio
- ρ^* - Tertiary flow density to primary flow
density ratio

GREEK LETTER SYMBOLS

- β - $K + (f/2) * (A / A)$
- β - Ratio of ASME long radius metering nozzle
throat diameter to inlet diameter
- γ - Ratio of specific heats for air
- μ - Absolute viscosity, lbf-sec/ft²
- ρ - density, lbm/ft³
- ϕ - "Function of"

SUBSCRIPTS

- 0 - Section within the measurement plenum
- 1 - Section at primary nozzle exit
- 2 - Section at mixing stack exit
- a - Atmospheric
- b - Burner
- m - Mixed flow
- ms - Mixing stack
- or - orifice
- P - Primary
- s - Secondary
- t - Tertiary
- u - Uptake
- w - Mixing stack wall

ACKNOWLEDGEMENTS

Completion of the research contained in this thesis is owed in a large part to the advice, assistance and support of a number of other people. In particular, I would like to express my sincere appreciation to the following:

Professor Paul F. Pucci, of the Mechanical Engineering Department, my thesis advisor, whose support and guidance made this such a worthwhile experience.

Mr. John Moulton, modelmaker and craftsman, whose detailed work provided the foundation of this research.

Mr. Ron Longueira, laboratory technician, whose hard work and good humor provided much support in the accomplishment of this work.

Lieutenant Steve Daughety, USN, a friend and classmate, who, in spite of his own duties, was always ready to lend a hand.

And, most importantly, my wife, Danna, whose support, patience, and incredible flexibility have meant so much to me during my career.

I. INTRODUCTION

The increased introduction of marine gas turbines into naval ship propulsion plants has presented several problems associated with the attendant high mass flow rates and escalating operating temperatures presented by these units. Exhaust gas temperatures above 900 degrees Fahrenheit develop an exhaust plume with an intense infrared signature providing a target source for heat seeking offensive weapons. Additionally, these high temperatures can significantly degrade the performance of mast mounted electronic equipments, and provide an undesirable environment for helicopter operations.

Investigations conducted at the Naval Postgraduate School have shown considerable promise in alleviation of these problems by reducing the exhaust gas temperatures through the use of multiply-shrouded eductor systems which induce both secondary and tertiary air into the primary flow stream under turbulent conditions. Significant temperature reductions have been realized with this relatively simple apparatus with latest developments resulting in both size and weight reductions. It is important to note that these temperature reductions have been achieved without an unacceptable degradation of engine performance.

The gas eductor system has proven more feasible than the alternatives of water injection or energy recovery systems (when specifically utilized with the main propulsion engines). It should be noted however that significant promise exists for an energy recovery system such as RACER (Rankine Cycle Energy Recovery) which is currently receiving some interest for installation in the follow-on ships of the DDG-51 class.

The mixing process under the turbulent conditions encountered in the gas eductor is complex and not well understood although significant research efforts are being directed at a better understanding of the phenomenon. Dividing operation of gas eductors into three regimes on the basis of Mach number, the first regime ($M \geq 1.0$) becomes of interest in applications such as thrust augmentation for aircraft and rocket engines, the second regime ($0.4 \leq M \leq 0.6$) is especially relevant to thrust enhancement in Vertical Takeoff or Landing (VTOL) aircraft, and the last regime ($M \leq 0.2$) is the range of interest in dilution cooling of engine exhaust gases. This latter regime is of direct interest to this research and that of ongoing research at the Naval Postgraduate School.

II. BACKGROUND

Naval combatant vessels having marine gas turbine propulsion units currently utilize simple gas eductor systems. The design of gas eductors for destroyers of the DD-963 class was guided by Charwat [Ref. 1] at the University of California at Los Angeles and uses a solid wall mixing stack which relies on the length of the mixing stack to provide complete mixing. Initial investigations at the Naval Postgraduate School, which began in 1976, involved determination of the effects of various parameters on the pumping and mixing performance of gas eductors. The ultimate objectives of both past and present research is to effect reductions in the size and weight of the fabricated eductor structure while optimizing eductor performance specifically in terms of plume temperature and stack surface temperature.

A. THE TEST FACILITIES

To carry out the aforementioned research objectives, two test facilities have been constructed. The first facility, the "cold flow" facility, readily permits rapid evaluation of a wide variety of eductor configurations. Its primary benefit is the expediency of data collection resulting from easily fabricated models which do not undergo high temperatures in the testing cycle. Additionally, inexpensive

materials afford evaluation of numerous models at minimal cost. The second test facility, the "hot flow" facility, is designed to test models at actual operating temperatures. In addition to confirming the pumping characteristics of geometrically similar models tested in cold flow, it provides the needed data on exhaust temperatures and stack surface temperatures.

B. INITIAL INVESTIGATIONS AT NPS

The initial investigation of gas eductor performance at the Naval Postgraduate School was undertaken by Ellin [Ref. 2]. This work was based on a simple one dimensional gas eductor model developed by Pucci [Ref. 3]. Testing three basic eductor geometries, Ellin attempted to determine the effects of varying the area of the primary jet with respect to the area of the mixing stack. Ellin verified a correlation between dimensionless parameters representing the pressure depression in and the induced flow from a secondary environment by the eductor. These parameters were suggested by a one dimensional analytic model. Ellin's work was followed by Moss [Ref. 4], and Harrell [Ref. 5].

The work of Ellin, Moss, and Harrell was conducted exclusively in the cold flow facility, and it was considered essential that actual operating conditions be investigated to verify these results. Ross [Ref. 6] undertook the actual construction, calibration, and test verification of the hot

flow test facility. Under the recommendations of the previous researchers, Welch [Ref. 7] conducted the initial hot flow testing using a four nozzle, solid walled mixing stack eductor.

C. IMPROVEMENTS IN MIXING STACK CONFIGURATION

Reports of significant pressure depression throughout the length of the original straight, solid walled mixing stacks suggested that additional, or tertiary flow could be induced into the mixing stack along its length. Additionally, it was considered that this flow could be used to reduce externally detectable surface temperatures by means of film cooling. Staehli and Lemke [Ref. 8] investigated the use of cooling ports in the mixing stack at the cold flow facility to determine its potential.

Hill [Ref. 9] followed Welch in hot flow testing and considered the performance of a slotted mixing stack under actual operating parameters. Eick [Ref. 10] and Kavalis [Ref. 11] conducted follow-on research in the hot flow test facility using the slotted mixing stack with multiply-shrouded eductors and observed excellent results confirming the cold flow analysis.

D. CURRENT OBJECTIVES

The objectives of this investigation were to verify the high temperature performance of an eductor configuration

tested by Pritchard [Ref. 12] in the cold flow facility, conduct calibration of the entrance nozzle for more accurate determination of air mass flow rates, and determine the effects of turbulent cross-flow on eductor performance.

III. THEORY AND MODELING

Eductors are relatively simple devices in which a jet of fluid (primary jet) is directed into a co-axial mixing chamber in such a manner that a volume of secondary fluid becomes entrained in the flow and a pumping action occurs. The fluids may be in liquid or gaseous form, or a combination.

The eductor described in this research is used to pump gases at relatively low velocities. Of specific consideration is the ability of a relatively hot primary gas jet to entrain and mix with a cooler ambient fluid (air) to produce a uniform flow at some desirable intermediate temperature. Mach number similarity has been chosen as the link in dynamic similarity between the primary gas flow rates of the models and the prototype. Dimensionless parameters controlling the flow are used throughout the analysis. These parameters were derived from a one-dimensional analysis of a simple eductor.

A. MODELING TECHNIQUE

Based on the average flow properties of the eductor prototype, the air flow in the mixing stack eductor system is turbulent ($Re > 10^5$). As a consequence of this turbulence, momentum exchange is predominant over shear interaction, and the kinetic and internal energy terms are more influential on the flow than are viscous forces. It can be shown that

the Mach number is a more significant parameter than Reynolds number in describing this turbulent flow; therefore, as stated previously, it is the Mach number which has been maintained to more accurately represent the primary flow relationship between prototype and model.

B. ONE-DIMENSIONAL ANALYSIS OF A SIMPLE EDUCTOR

The theoretical analysis of an eductor may be approached in two ways. One method attempts to analyze the details of the mixing process of the primary and secondary air streams as it takes place inside the mixing stack. This requires an interpretation of the mixing phenomenon which, when applied to a multiple nozzle system, becomes extremely complex. The other method, which was chosen here, analyzes the overall performance of the eductor system and is not concerned with the actual mixing process. To avoid repetition of previous reports only the main parameters and assumptions will be presented here. A complete derivation of the analysis used can be found in [Ref. 2] and [Ref. 3]. The one-dimensional flow analysis of the simple eductor system (Fig. 1) described depends on the simultaneous solution of the continuity, momentum, and energy equations coupled with the equation of state, all compatible with specific boundary conditions.

The idealizations made for simplifying the analysis are as follows:

- 1) The flow is steady state and incompressible.

2) Adiabatic flow exists throughout the eductor with isentropic flow of the secondary stream from the plenum (at section 0) to the throat of entrance of the mixing stack (at section 1) and irreversible adiabatic mixing of the primary and secondary streams occurs in the mixing stack (between sections 1 and 2).

3) Isentropic flow of the tertiary flow exists from the tertiary plenum to the minimum area at Section 2, with irreversible adiabatic mixing of the flows between Sections 2 and 3.

4) The static pressure across the flow at the entrance and exit planes of the mixing-tube (at sections 1 and 2) is uniform.

5) At the mixing stack entrance (section 1) the primary flow velocity U_p and temperature T_p are uniform across the primary stream, and the secondary flow velocity U_s and temperature T_s are uniform across the secondary stream, but U_p does not equal U_s , and T_p does not equal T_s .

6) At Section 2, the mixing of primary and secondary air has an average velocity, U_x , and an average temperature, T_x .

7) Incomplete mixing of the primary, secondary, and tertiary streams in the mixing stack is accounted for by the use of a non-dimensional momentum correction factor K_m which relates the actual momentum rate to the pseudo-rate based on the bulk-average velocity and density and by the

use of a non-dimensional kinetic energy correction factor K_e which relates the actual kinetic energy rate to the pseudo-rate based on the bulk-average velocity and density.

8) Both gas flows behave as perfect gases.

9) Changes in gravitational potential energy are negligible.

10) Pressure changes P_{os} to P_1 , P_{ot} to P_2 , P_1 to P_2 and P_2 to P_3 ($=P_a$) are small relative to the static pressure, so that the gas density is essentially dependent upon temperature and atmospheric pressure.

11) Wall friction in the mixing stack is accounted for with the conventional pipe friction factor term based on the bulk-average flow velocity U_m and the mixing stack wall area A_w .

The following parameters, defined here for clarity, will be used in the following development.

$\frac{A_p}{A_M}$ ratio of primary flow area to mixing stack
cross section area

$\frac{A_w}{A_M}$ ratio of wall friction area to mixing stack
cross sectional area

K_p momentum correction factor for primary mixing

K_M momentum correction factor mixed flow

f wall friction factor

Based on the continuity equation, the conservation of mass principle for steady flow yields

$$W_M = W_P + W_S + W_T \quad (\text{eqn 3.1})$$

where

$$\begin{aligned} W_P &= \rho_P U_P A_P \\ W_S &= \rho_S U_S A_S \\ W_T &= \rho_T U_T A_T \\ W_M &= \rho_M U_M A_M \end{aligned} \quad (\text{eqn 3.2})$$

All of the above velocity and density terms, with the exception of ρ_M and U_M , are defined without ambiguity by virtue of idealizations (4) and (5) above. Combining equations (3.1) and (3.2) above, the bulk average velocity at the exit plane of the mixing stack becomes

$$U_M = \frac{W_s + W_t + W_p}{\rho_M A_M} \quad (\text{eqn 3.3})$$

where A_M is fixed by the geometric configuration and

$$\rho_M = \frac{P_a}{RT_M} \quad (\text{eqn 3.4})$$

where T_M is calculated as the bulk average temperature from the energy equation (3.11) below. The momentum equation

stems from Newton's second and third laws of motion and is the conventional force and momentum-rate balance in fluid mechanics.

$$K_p \left(\frac{W_p U_p}{g_c} \right) + \left(\frac{W_s U_s}{g_c} \right) + \left(\frac{W_t U_t}{g_c} \right) + P_1 A_1 = K_M \left(\frac{W_m U_m}{g_c} \right) + P_2 A_2 + F_{fr} \quad (\text{eqn 3.5})$$

Note the introduction of idealizations (4) and (7). To account for a possible non-uniform velocity profile across the primary nozzle exit, the momentum correction factor K_p is introduced here. It is defined in a manner similar to that of K_M and by idealization (5), supported by work conducted by Moss, it is set equal to unity. K_p is carried through this analysis only to illustrate its effect on the final result. The momentum correction factor for the mixing stack is defined by the relation

$$K_M = \frac{1}{W_m U_m} \int_0^A U_3^2 \rho_3 dA \quad (\text{eqn 3.6})$$

where U is evaluated as the bulk-average velocity from equation (3.3). The wall skin friction force F can be related to the flow stream velocity by

$$F_{fr} = f A_w \left(\frac{U_m^2 \rho_m}{2 g_c} \right) \quad (\text{eqn 3.7})$$

using idealization (11). As a reasonably good approximation for turbulent flow, the friction factor may be calculated from the Reynolds number

$$F = 0.046 (Re_m)^{-0.2} \quad (\text{eqn 3.8})$$

Applying the conservation of energy principle to the steady flow system in the mixing stack between the entrance and exit plane,

$$\begin{aligned} W_p \left(h_p + \frac{U_p^2}{2g_c} \right) + W_s \left(h_s + \frac{U_s^2}{2g_c} \right) + W_t \left(h_t + \frac{U_t^2}{2g_c} \right) \\ = W_m \left(h_m + Ke \frac{U_m^2}{2g_c} \right) \end{aligned} \quad (\text{eqn 3.9})$$

neglecting potential energy of position changes (idealization 9). Note the introduction of the kinetic energy correction factor Ke , which is defined by the relation

$$Ke = \frac{1}{W_m U_m^2} \int_0^{A_m} U_3^2 \rho_3 dA \quad (\text{eqn 3.10})$$

It may be demonstrated that for the purpose of evaluating the mixed mean flow temperature T_m , the kinetic energy terms may be neglected to yield

$$h_m = \frac{W_p}{W_m} h_p + \frac{W_s}{W_m} h_s + \frac{W_t}{W_m} h_t \quad (\text{eqn 3.11})$$

where $T_m = \phi(h_m)$ only, with the idealization (8).

The energy equation for the isentropic flow of the secondary air flow from the plenum to the entrance of the mixing stack may be shown to reduce to

$$\frac{P_{os} - P_s}{\rho_s} = \frac{U_s^2}{2g_c} \quad (\text{eqn 3.12})$$

similarly, the energy equation for the tertiary air flow reduces to

$$\frac{P_o - P_t}{\rho_t} = \frac{U_t^2}{2g_c} \quad (\text{eqn 3.13})$$

The previous equations may be combined to yield the vacuum produced by the eductor action in either secondary or tertiary air plenums. Letting $P_3 = P_m = P_a$ and assuming that $A_3 = A_m \approx A_2 \approx A_1$ and assuming the friction between sections 2 and 3 is negligible, the vacuum produced for the secondary air plenum is

$$P_a - P_{os} = \frac{1}{g_c A_m} \left[K_p \frac{W_p^2}{A_p \rho_p} + \frac{W_s^2}{A_s \rho_s} \left(1 - 1/2 \frac{A_m}{A_s} \right) + \frac{W_t^2}{A_t \rho_t} - \frac{W_m}{A_m \rho_m} \left(K_m + \frac{f}{2} \frac{A_m}{A_m} \right) \right] \quad (\text{eqn 3.14})$$

where it is understood that A_p and ρ_p apply to the primary flow at the entrance to the mixing stack, A_s and ρ_s apply to the secondary flow at this same section, and A_m and ρ_m apply

to mixed flow at the exit of the mixing stack system. P_a is atmospheric pressure, and is equal to the pressure at the exit of the mixing stack. A_w is the area of the inside wall of the mixing stack.

For the tertiary air plenum, the vacuum produced is

$$P_a - P_{ot} = \frac{1}{g_c A_m} \left[K_2 \left(\frac{W_p + W_s}{\rho_2 A_m} \right)^2 + \frac{W_t^2}{\rho_t A_m} \left(1 - 1/2 \frac{A_m}{A_t} \right) - K_m \frac{W_m^2}{\rho_m A_m} \right] \quad (\text{eqn 3.15})$$

where the primary flow now consists of both the primary and secondary air flows, and where K_2 is the momentum correction factor at section 2.

C. NON-DIMENSIONAL FORM OF THE SIMPLE EDUCTOR EQUATION

In order to satisfy the criteria of geometrically similar flows, the non-dimensional parameters which govern the flow must be determined. The means chosen for determining these parameters was to normalize equations (3.14) and (3.15) with the following dimensionless groupings.

$$P^* = \frac{\frac{P_a - P_{os}}{\rho_s}}{\frac{U_p^2}{2g_c}} \quad \text{a pressure coefficient which compares the pumped head } (P_a - P_{os}) \text{ for the secondary flow to the driving head } (U_p^2 / 2g_c) \text{ of the primary flow}$$

$$PT^* = \frac{\frac{P_a - P_{ot}}{\rho_t}}{\frac{U_p^2}{2g_c}} \quad \text{a pressure coefficient which compares the pumped head } (P_a - P_{ot}) \text{ for the tertiary flow to the driving head } (U_p^2 / 2g_c) \text{ of the primary flow}$$

$$W^* = \frac{W_s}{W_p}$$

a flow rate ratio, secondary to primary
mass flow rate

$$WT^* = \frac{W_t}{W_p}$$

a flow rate ratio, tertiary to primary
mass flow rate, W_t^*

$$T^* = \frac{T_s}{T_p}$$

an absolute temperature ratio, secondary
to primary

$$TT^* = \frac{T_t}{T_p}$$

an absolute temperature ratio, tertiary
to primary, T_t^*

$$\rho_s^* = \frac{\rho_s}{\rho_p}$$

a flow density ratio of the secondary to
primary flow. Note that since the fluids
are considered perfect gases,

$$\rho_s^* = \frac{T_p}{T_s} = \frac{1}{T_s^*}; P_s \approx P_p \text{ and } P_t \approx P_p$$

$$\rho_t^* = \frac{\rho_t}{\rho_p}$$

a flow density ratio of the tertiary or film
cooling flow to primary flows. (Note that
since the fluids are considered perfect gases

$$\rho_t^* = \frac{T_p}{T_t} = \frac{1}{T_t^*})$$

$$A_s^* = \frac{A_s}{A_p}$$

a ratio of secondary flow area to primary
flow area

$$A_t^* = \frac{A_t}{A_p}$$

a ratio of tertiary flow area to primary
flow area

With these non-dimensional groupings, equations (3.14) and
(3.15) can be rewritten in dimensionless form.

$$\frac{P^*}{T^*} = 2 \frac{A_p}{A_m} \left\{ \left(K_p - \frac{A_p}{A_m} \beta \right) - W^* (1+T^*) \frac{A_p}{A_m} \beta + \frac{W_t^* T_t^*}{A_t^*} \right. \\ \left. + W^{*2} T^* \left(\frac{1}{A^*} \left(1 - \frac{A_m}{2A^* A_p} \right) - \frac{A_p}{A_m} \beta \right) \right\} \quad (\text{eqn 3.16})$$

where

$$\beta = K_m + f_2 \frac{A_w}{A_m} \quad (\text{eqn 3.17})$$

This may be rewritten as

$$\frac{P^*}{T^*} = C_1 + C_2 W^* (T^*+1) + C_3 W^* T + C_4 W_t^{*2} T_t^* \quad (\text{eqn 3.18})$$

where

$$C_1 = 2 \frac{A_p}{A_m} \left(K_p - \frac{A_p}{A_m} \beta \right), \quad (\text{eqn 3.19})$$

$$C_2 = -2 \left(\frac{A_p}{A_m} \right)^2 \beta, \quad (\text{eqn 3.20})$$

$$C_3 = 2 \frac{A_p}{A_m} \left\{ \frac{1}{A^*} \left(1 - \frac{A_m}{2A^* A_p} \right) \beta - \frac{A_p}{A_m} \beta \right\}, \quad (\text{eqn 3.21})$$

$$\text{and } C_4 = \frac{1}{A_t^*} \quad (\text{eqn 3.22})$$

The additional dimensionless quantities listed below have been used in past research to correlate the static pressure distribution down the length of the mixing stack.

$$PMS = \frac{\frac{PMS}{\rho_s}}{\frac{U_p^2}{2g_c}}$$

a pressure coefficient which compares the pumping head (PMS/ρ_s) for the secondary flow to the driving head ($U_p^2/2g_c$) of the primary flow, where PMS = static pressure along the mixing stack length

$$\frac{X}{D}$$

ratio of the axial distance from the mixing stack entrance to the diameter of the mixing stack

D. EXPERIMENTAL CORRELATION

For the geometries and flow rates investigated, it was confirmed by Ellin [Ref. 2] and Moss [Ref. 4] that a satisfactory correlation of the variable P^* , T^* and W^* takes the form

$$\frac{P^*}{T^*} = \phi (W^* T^{*n}) \quad (\text{eqn 3.23})$$

where the exponent "n" was determined to be equal to 0.44. The details of the determination of $n = 0.44$ as the correlating exponent for the geometric parameters of the gas eductor model being tested is given by Ellin. To obtain a gas eductor model's pumping characteristic curve, the experimental data is correlated and analyzed by using equation (3.23), that is, P^*/T^* is plotted as a function of $W^* T^{*0.44}$. This correlation is used to predict the open to the environment operating point for the gas eductor model. Variations in the model's geometry will change the pumping ability,

which can be evaluated from the plot of equation (3.23). The value of parameter $W \cdot T^{0.44}$ when $P^*/T^* = 0$ is referred to as the pumping coefficient. Since the tertiary flow is much less than the secondary flow, it has been demonstrated by Lemke and Staehli [Ref. 8], and Drucker [Ref. 13] that the pumping characteristic is relatively insensitive to tertiary flow.

E. PUMPING COEFFICIENT

The pumping coefficient derived from non-dimensional parameters provides a basis for analyzing the eductor's pumping capability. Changes in stack geometries such as L/D ratio, slotting, shrouding, diffuser rings, and spacing between stack and shroud, and between shroud and diffuser rings will alter the eductor's pumping performance and the pumping coefficient. The pumping coefficients for the model should correspond to the coefficients for the shipboard eductor system. At the shipboard operating point, the eductor is exposed to no restrictions in the secondary or tertiary air flows. In the model, this is simulated by completely opening the air plenums which provides an open-to-the-environment simulation. Unfortunately, at this condition and secondary and/or tertiary air flow rates cannot be measured. The eductor model's characteristics are first established over the measurable flow range and then extrapolated to the desired operation point.

The data for this extrapolation is established by varying the associated induced air flow rate, either secondary or tertiary, from zero to its maximum measurable rate. These rates are determined by sequentially opening the ASME flow nozzles mounted to the plenum and recording the pressure drop across the nozzles. Values for nozzle cross sectional areas, pressure drops, induced flow are temperatures, and barometric pressure are then used to calculate the dimensionless parameters P^*/T^* , and $W^*T^{*0.44}$. The dimensionless parameters are then plotted as illustrated in Figure 42. Data point (1) is the maximum vacuum which is produced by the eductor with no secondary flow, obtained by closing all ASME flow nozzles. Data points in region (2) correspond to opening most of the ASME flow nozzles and the final point corresponds to opening all flow nozzles. Although the data points in region 2 appear to be zero or nearly so, they do have a small finite value. The uncertainty associated with these points is relatively high with the data collected in this research considered qualitatively accurate to within ± 0.05 of the reported value which was obtained via linear regression. The data points in region (3) provide the most consistent and accurate data. Extrapolation of the pumping characteristic curve to intersect with the abscissa at $P^*/T^*=0$ locates the appropriate operating point for the eductor model configuration.

IV. EXPERIMENTAL APPARATUS

The test facility apparatus currently in use was designed, fabricated, and installed by Ross [Ref. 6] and used by all follow-on researchers for hot primary flow analysis. A Boeing 502 gas turbine engine combustor section and turbine nozzle were used to construct the gas generator. Various components of the engine's fuel system were modified by Ross to support a simplified combustor layout. Air for combustion is supplied by a Carrier centrifugal air compressor (three stage) which is located in building 230 of the Naval Postgraduate School Annex. The actual model testing and gas generator operation is controlled from the hot test facility, building 249. Appendix A provides detailed instructions for safe and proper operation of the gas generator.

A. COMBUSTOR AIR PATH

Combustion air and cooling air supplied by the centrifugal air compressor pass from the compressor discharge via underground pipe between buildings 230 and 249. Air enters the test facility through a vertical standpipe containing an eight inch butterfly valve in parallel with a remote-manual bypass globe valve (Figure 16). This butterfly valve is normally closed with flow through the bypass valve being of sufficient volume to operate the gas generator. Figure 7 is the layout of the gas generator. At the top of the standpipe is a "T"

connection. In one direction flow passes through an eight inch butterfly valve and enters a short section of piping which is used by the Aeronautical Engineering Department to supply various experiments. The second arm of the "T" supplies the combustion gas generator through an eight inch to four inch reducing section (entrance nozzle). The flow characteristics of this entrance nozzle were determined from calibration data collected by this researcher and are presented in Appendix B. The pressure drop across this section is used to determine the mass flow rate of air through the gas generator assembly. A linear curve was fit to the data of Table XXIX for use in data reduction programs. The correlation is presented in Figure 41. Air flow next passes through a manual isolation valve and enters a splitter section.

In the splitter section, a portion of the air flow is directed through the motor operated burner air control valve and the U-tube to the combustor section. The flow characteristics of this section as determined by Ross are presented in [Ref. 6]. The remaining air passes through the motor operated cooling air bypass valve and enters the mixing section. The mixing section was fabricated by Ross from the nozzle box of the Boeing engine. A device was installed in the nozzle box to introduce a swirl into the cooling air which is counter to that produced by the nozzles. Hot gases from the combustion section enter the mixing section through

the nozzles and the effect of the counter-rotating flow is to produce rapid and thorough mixing. Downstream of the mixing section is a flow straightener which is followed by an uptake section which delivers the gas flow to the primary nozzles.

B. FUEL SYSTEM

1. System Arrangement

Service fuel is stored in a 55 gallon drum mounted on an elevated stand adjacent to the building. Fuel flows from the storage tank through a tank isolation valve to a bulkhead isolation valve located inside building 249. A tank stripping and drain connection is located in the supply line outside the building. Adjacent to the interior bulkhead valve is a thermocouple connection for measuring fuel temperature. Fuel then passes through the flow measuring rotameter to a fuel filter. Taking suction on the filter is a 24V DC motor driven fuel supply pump. This positive displacement pump contains an internal bypass and pressure regulating feature. Normal pump discharge pressure is 14-16 PSIG.

The supply pump provides positive suction head for the high pressure pump. This pump has no internal bypass and must be provided with an external recirculation loop when in operation. Valves placed in the recirculation are used to control the pump discharge pressure and thus, the

flow of fuel to the burner nozzle. Downstream of the recirculation connection is a system drain valve and a manually operated discharge valve, Figure 25. From the discharge valve, fuel is piped to an electrically operated solenoid valve located at the entrance to the combustor.

2. Fuel System Flow Rate Measurement and Control

A Fischer Porter Model 10A3565A rotameter is installed to monitor fuel flow rate. Calibration was performed in place by Eick using the fuel supply pump to discharge fuel into a container for a fixed period of time. The quantity of fuel discharged was weighed on a gram scale and the mass determined. Flow rate was controlled using a needle valve at the pump outlet. Rotameter calibration data is given in Table I. Figure 40 plots fuel mass flow against rotameter reading. A linear curve fit to the data results in the expression

$$WF = -3.076 + 0.4048 * ROTA \quad (\text{eqn 4.1})$$

Hill [Ref. 9] had recommended that the system's fuel control valve be replaced with a needle valve to improve sensitivity and control. The existing arrangement used a ball valve mounted on the pump table as a fuel control valve. A long mechanical linkage extended across the building to the control station. Not only did this linkage seriously impede access around the gas generator, but this arrangement made accurate adjustment of the fuel flow difficult; therefore,

a 3/8 inch stainless steel tubing was used to extend the high pressure pump recirculation line to the control station. The ball valve was retained as the control valve and mounted on the bench at the control station. This valve permits the operator to rapidly select any desired operating pressure in a single motion.

To increase the sensitivity of the fuel control valve, a needle valve was installed in parallel with it close to the high pressure pump, Figure 25. This valve, which is always partially open, permits flow through the recirculation line even when the fuel control valve is fully closed. Thus flow through the pump is assured even when both the fuel control and the pump discharge valves are closed.

This needle valve ("trimmer" valve) is used to establish the range of control for the fuel control valve. When properly adjusted this system provides smooth operation over a range of high pressure pump discharge pressures from 80 to 350 psig. Since the high pressure pump's maximum output pressure is specified to be 375 psig, control is obtained over most of the pump's useful range. Fuel pressure is easily adjusted to within 5 psig of a desired setpoint and with some care can accurately be varied in increments as small as 2 psig.

C. THE MEASUREMENT PLENUM

1. The Rear Seal

A flexible seal is installed at the rear wall. This diaphragm seal is formed from a rubberized fabric. The fabric is bedded in a layer of silicone sealant and clamped to the uptake with a band clamp. A similar layer of sealant is applied to the plenum rear wall and the seal attached with a split clamping ring. Figure 18 is a view of the plenum interior showing the finished uptake and the diaphragm seal. The rear seal provides uniformity in uptake gas temperature, with temperatures between the uptake mid-section and the primary nozzle now varying less than two degrees F.

2. The Forward Seal

The forward seal bulkhead is within the plenum and seal plates are provided to clamp to the entrance section of the mixing stack. A double O-ring assembly is utilized on the outer circumference of the inlet to the mixing stack to provide proper sealing.

3. Model Installation and Alignment

An adjustable support stand was designed and constructed to support the mixing stack assembly independently of the seal plates. This stand facilitates model installation and alignment. Alignment is accomplished by mounting the model on the stand, installing centering plates in each end of the mixing stack and in the open of the uptake pipe, and adjusting the stand until the alignment bar passes

freely through holes in the centering plates. The alignment apparatus can be seen in Figure 27. Standoff distance is then set by installing the straight primary nozzles on the uptake and measuring the required distance from the nozzle exit plane to the mixing stack entrance plane (the termination of the entrance radius -- 0.5 inch) using a combination square. This adjustment normally requires no more than 0.125 inch movement of the model when a 0.5 standoff distance is desired.

Due to the longitudinal expansion observed by Eick, the installed standoff distance was modified from 3.5610 inches to 3.6875 inches to compensate accordingly.

D. INSTRUMENTATION

1. Temperature Measurement

Two types of thermocouple displays are installed with each having the capability to accept eighteen (18) channels. A type K display provides data on combustion temperatures, uptake temperatures and mixing stack wall temperatures. Table II gives the current channel assignments. The type T display is used to measure inlet air, ambient air, fuel, and shroud and diffuser temperatures. Table III gives the current channel assignments. The display installation is shown in Figure 12.

2. Pressure Measurement

Five manometers, shown in Figure 14, are installed for gas generator operation and data collection. They include a 20 inch water manometer for measurement of differential pressure across the inlet reducing section (DELPN), an oil manometer (range 0-17 inches water) for measuring uptake pressure (PUPT), a 20 inch mercury manometer for measuring inlet air pressure (PNH), a 2 inch inclined water manometer used to measure the differential pressure across the burner U-tube (DELPN), and a 6 inch inclined water manometer connected to a distribution manifold. Five individual manifolds located in the main control panel (Figure 13) are interconnected to permit measurement of plenum and mixing stack pressures with respect to atmospheric pressure. Mixing stack pressures both above and below atmospheric can be displayed.

E. THE MODELS

Two eductor models were tested. Both models were tested with and without a cross-flow. Each model consisted of a primary nozzle plate mounted on the end of the uptake piping and a mixing stack, shroud and diffuser assembly. Characteristic eductor dimensions are given in Figure 6. In both models tested the mixing stack interior diameter "D", was 7.122 inches. This dimension is the same as used in previous hot primary flow testing and is 0.6087 scale of the cold flow models. Both models tested employed a standoff ratio, "S/D", of 0.5. Table IV provides a comparison of the key model characteristics.

1. Model A

Model A is shown in the test installation apparatus in Figure 31. This configuration includes a primary nozzle plate with four (15/20) tilted and angled nozzles. The configuration of the nozzles refers to the characteristic angles. The tilt of the nozzle is 15 degrees from the vertical with the nozzle being rotated or "angled in" 20 degrees from the tangential direction. Figure 35 details these angles for clarification. The ratio of the mixing stack area to primary nozzle area is 2.5.

The mixing stack is enclosed in a low carbon, cold rolled sheet steel shroud extending from $X/D = 0.15$ to $X/D = 1.125$. Five sheet steel diffuser rings 0.375 diameters long are installed to bring the overall length of the assembly to 1.5 diameters. Film cooling clearance between the stack and the shroud varies along the length of the model while the film cooling clearance between the diffuser rings is 0.188 inches. The dimensions of this model are shown in Figure 4. One row of thermocouples was installed along the length of the shroud and diffusers oriented ninety degrees from a horizontal plane passing through the model's centerline axis. These twelve (12) type T thermocouple readouts were used as a comparison to external readings obtained from an Omega Engineering 871 digital thermocouple with fully remote probing capability.

2. Model A Modified

The second model tested was a modified version of the first in that an extra diffuser ring was located outside the fifth ring of Model A. This ring was of the same thickness, material and length, and was geometrically concentric to diffuser ring number five of model A. The annular clearance between diffuser rings five and six was 0.188 inches. The dimensions of the modified model are shown in Figure 5.

F. THE CROSS-FLOW CENTRIFUGAL FAN

1. Installation and Configuration

The fan used to model the relative wind (cross-flow) was of the centrifugal type. It was manufactured by the Joy Manufacturing Company, General Products Division, New Philadelphia, Ohio.

The centrifugal fan was installed at the experimental site to be as mobile and portable as practicable considering its weight. To afford mobility for proper standoff positioning in relation to the model and facilitate certain data collection, the fan was mounted on a platform having heavy duty ball bearing casters. The lower section of the platform facilitated installation of a "step-up" transformer and provided adequate stowage of the power cable when the fan was not in service.

A converging nozzle was attached to the fan exit volute to provide directional stability to the air discharge,

and additionally to provide a datum for theoretical determination of discharge velocity. The fan nozzle exit area was chosen arbitrarily to provide a nozzle discharge area to model discharge area ratio of 3:1.

The fan is driven by a Reliance Duty Master AC motor. The motor is a 440V, 3 phase, 4.8 amp, 60 Hz unit designed for continuous duty at 1755 RPM when connected to the high speed windings as was the case for this research.

Since the test facility, Bldg 249, does not have 440V power available, it was necessary to utilize 220V power provided to a step-up transformer to provide the necessary voltage. Once proper electrical connection and grounding was made, starting the stopping of the fan was facilitated safely by utilizing a five amp circuit breaker specifically installed for the fan 220V supply circuit. A picture of the cross-flow fan is shown in Figure 32.

2. Performance Capabilities

The cross-flow fan utilized has a nominal air flow rate of 3000 CFM at a total pressure of 3.0 inches of water. Maximum air flow rate is established at 4200 CFM at or below 1.0 inches of water total pressure. Since the total pressure developed by the installed convergent nozzle was not known, it was necessary to determine the fan's discharge velocity profile experimentally, and thereby determine a quasi-optimum nozzle to model standoff distance to provide a relatively

uniform flow field. Based upon theoretical calculations, discounting any losses, the maximum velocity achievable from the fan was estimated at thirty-five (35) knots.

To determine the actual velocity distribution at the exit plane of the fan nozzle and to determine a suitable standoff distance (nozzle to model), a flow measurement experiment using a pitot tube to measure total pressure was devised. The basic equation for estimation of the velocity in the flow stream is given by equation (7-53) of [Ref. 14].

$$p_o - p_\infty = 1/2 \rho U_\infty^2 \quad (\text{eqn 4.1})$$

Four sets of data were collected. One data set was collected for each of the following pitot traverses: horizontal traverse at the nozzle exit plane, horizontal traverse at a standoff distance of twenty-four inches, vertical traverse at a twenty-four inch standoff, and a 4.5 inch vertical traverse at the bottom of the model (diffuser ring 5 on the model centerline) to a horizontal plane coincident with the model support and alignment base. This data is presented in Tables XXIII through XXVI.

Based upon the collected data the standoff distance of twenty-four inches (nozzle exit plane to model centerline) was determined suitable in representing an average flow field velocity of 29.5 knots.

V. EXPERIMENTAL RESULTS

A. MODEL A RESULTS

1. Pumping Performance

The pumping performance of Model A is shown in Figures 43 through 48 with supporting data presented in Tables V through X. Using the correlation previously developed in section (d) of Chapter III, a linear regression technique was utilized to determine the pumping coefficient for the specific uptake test temperature and cross-flow condition. Given the inherent uncertainty of the linear fit, specifically considering the uncertainty and data scatter present in the lower plenum pressure differential regime, the data presented for pumping coefficients is considered qualitatively accurate to within ± 0.05 . The pumping coefficient comparison to a geometrically similar model tested by Pritchard [Ref. 12] at the cold flow facility is considered valid.

A table of comparative results is presented in Table XXVII.

2. Mixing Stack Temperatures

Figures 53 through 57 graphically present the data obtained from this model. Tabular results of the collected data are contained in Table XVII.

This model is equipped with twelve (12) type "K" thermocouples imbedded in the stack walls at various locations

to measure the film cooling effectiveness of the mixing stack slotted ports. The mixing stack thermocouple numbering system is referenced to a specific type "K" channel in Table II. Determination of film cooling effectiveness is achieved by referencing the appropriate temperature of thermocouples imbedded both upstream and downstream of the two selected cooling ports. As noted by Kavalis, [Ref. 11], it is suspected that due to the tilted angle of the nozzles, the flow is not uniform across the mixing stack and the sector between consecutive nozzles exhibit lower temperatures.

The data collected appears relatively consistent throughout when corrections for variation in ambient temperature are considered. The data reported has consistently higher temperatures than those reported by Eick [Ref. 10] and Kavalis [Ref. 11] who both used the tilted and angled primary nozzles with the slotted mixing stack but whose models used straight vice angled shrouds and diffusers. Since the entrance nozzle calibration conducted preliminary to actual model testing resulted in a lower air mass flow rate correlation, it is theorized that the lower temperatures observed by Eick and Kavalis were a result of the larger cooling effect from the induced tertiary air flow of the higher mixing stack air mass flow rates under which their investigations were conducted. The maximum wall temperatures reported by Eick and Kavalis are 306°F and 320°F respectively. This research resulted in a maximum wall temperature for Model A of 357°F.

Relative to cross-flow effects, no depression in temperature was noticeable throughout the data when correction for the effect of ambient temperature is considered.

3. Mixing Stack Pressures

The data obtained for mixing stack pressure is presented in Figures 62 through 66 and in Table XV.

As noted by Eick, due to the small size of the pressure tap and extremely long run of tubing (over 20 feet) to the manometer, a substantial period of time was required for the manometer reading to reach its final value. No oscillations were noticeable once a final value was reached. The data collection was found to be consistently stable and repeatable.

Comparison of the data is remarkably consistent throughout the range of uptake temperatures. This model compared to the straight shroud and diffuser models tested by Eick and Kavalis tends to show an increase in mixing stack pressure which might account for the increased wall temperatures noted. The effect of cross-flow appears to be an improvement in the mixing stack pressure profile. An average increase of 15% was noted.

4. Shroud and Diffuser Temperatures

Shroud and diffuser temperatures were obtained utilizing two methods. A type "T" thermocouple system having a digital output servicing twelve channels of interest was used in conjunction with a fully remote Omega Engineering model 871

thermocouple probe. The Omega remote reading thermocouple was a portable battery operated device with a hand-held surface probe and was of the type "K". Comparison between these two temperature monitoring devices in an equilibrium condition resulted in a mean temperature differential of $+0.5^{\circ}\text{F}$. This differential is acceptable under steady state conditions; however, the transient effects observed during the experimental data collection lead this researcher to believe that the type "T" thermocouple readings were more accurate. During data collection, and particularly during cross-flow data collection, significant oscillations in temperature were noticed with the remote probe device. When the Omega probe was used to determine shroud and diffuser external temperatures, an equilibrium condition did not appear achievable for recording of a discrete temperature. Initially, oscillation in the sensed temperature occurred rapidly and then damped somewhat although oscillation did continue. This necessitated that the recorded temperature be an average value with inherent error introduced as a function of the data recorder. Despite this drawback the surface probe did provide comparative data and it was decided to continue data collection with this device for a qualitative comparison with the type "T" data.

Using the "A" model for comparative analysis of the noted differential in shroud and diffuser temperature between the type "T" thermocouples and the Omega portable thermocouple

external probe readings, an uptake temperature of 950 degrees F was selected. In a no cross-flow condition (qualitatively normalizing the data to account for a difference in ambient temperature) relative to shroud temperatures, only a minimal differential is observed with exception of the far end of the shroud which exhibits approximately a 20 degree difference. The maximum difference noted in diffuser ring temperature occurs for rings three and five. This difference is ten (10) degrees F. When cross-flow was introduced, the difference in shroud temperatures was minimal with the exception of the shroud end closest to the diffusers which showed an approximately ten (10) degrees F difference. Diffuser ring temperature differential was more pronounced in the cross-flow relative to the two temperature sensors with a maximum deviation of 25 degrees F for diffuser ring five and a mean diffuser ring temperature differential of 15 degrees F.

The surface probe temperature measurements were taken along the model's length starting at diffuser ring five and working rearward toward the after section of the shroud. The point of each measurement was taken along the surface of the model coincident with the model's centerline and oriented 180 degrees from the cross-flow. The sequence of the temperature measurements and relative distance from the mixing stack entrance are given by the X/D parameter values as shown in Figure 36.

Figures 71 through 75 present the shroud and diffuser temperatures obtained via the type "T" thermocouples while Figures 80 through 84 present the external surface probe data.

Data collected for the shroud in the no cross-flow condition show a consistently increasing temperature with the most notable increase being at the $X/D = 1.068$ position. When cross-flow was introduced the slope of the temperature profile appeared to flatten somewhat but again the $X/D = 1.068$ position showed a sharp increase in temperature. Cross-flow did result in a significant reduction in this high temperature reducing it approximately fifty degrees.

The five diffuser rings showed good temperature reduction potential until the fourth ring was reached when the effects of film cooling appeared to be dissipating and a continued increase of diffuser ring temperature was noticeable.

The effects of cross-flow resulted in an overall increase in diffuser ring temperature and resulted in an erratic although predictable temperature profile. The ultimate effect of the cross-flow appeared to be an overall shroud and diffuser assembly temperature reduction with some distortion of film cooling effects being induced by the cross-flow.

5. Exit Plane Temperatures

Figures 89 through 93 display the exit plane temperature data. Table XXI is a compilation of the data points presented in these figures.

A comparison of exit plane temperature profiles, with and without cross-flow, is presented for the maximum uptake temperature of 950 degrees F. Good symmetry is observed in those profiles displayed with no cross-flow introduced with the exception of the 850°F uptake profile. It is considered that this asymmetry was caused by an inadvertent movement of the traversing mechanism which was noted during the data collection process.

Upon introduction of cross-flow it is noted that a depression of profile temperature takes place resulting in an average temperature reduction of greater than 50 degrees F. At the same time some increase in downstream profile temperature was noted in Model A.

The peak temperatures observed in Model A at uptake temperatures of 850°F and 950°F were 531°F (with cross-flow) and 586°F (no cross-flow) respectively.

B. MODEL A MODIFIED RESULTS

1. Pumping Performance

The pumping performance characteristics for the modified model were extremely close in comparison to those of Model A. A comparative summary is provided in Table XXVII.

Pumping coefficient plots are shown in Figures 49 through 52. Supporting tabular data is contained in Table XI.

2. Mixing Stack Temperatures

As anticipated, the modification of adding an additional diffuser ring to this model had little effect to change the mixing stack temperatures.

The temperature reduction noted upon introduction of cross-flow with Model A was also consistently noted for the data collected. It should be noted that any comparative analysis in this regard should be normalized to account for ambient temperature conditions.

Data collected for this model is presented in Figures 58 through 61 and Table XVIII.

3. Mixing Stack Pressures

This data which is presented in Figures 67 through 70 and Table XVI is consistent with the findings of Model A. The only minor exception being a slight reduction noted in the average pressure increase reported with the model under cross-flow conditions.

4. Shroud and Diffuser Temperatures

A reduction in temperature of approximately 20°F was noted for diffuser ring five (5) which directly received the effects of the film cooling resulting from the addition of an extra diffuser ring. This temperature reduction effect was present both with and without the cross-flow introduced.

Without cross-flow no appreciable modification in shroud and diffuser temperatures was noticeable when normalization for ambient temperature is considered with the exception

of ring five as noted above. In a cross-flow condition the added film cooling effect of the additional diffuser ring resulted in an overall reduction in diffuser ring temperatures.

5. Exit Plane Temperatures

Figures 94 through 97 present the exit plane temperature for the modified model. Table XXII is a compilation of this data.

No appreciable change in peak temperature was observed for the modified model in comparison with Model A. The temperature depression effect induced by the cross-flow noted in Model A was also evident. In contrast with Model A, however, no increase in downstream profile temperature was noted. This is shown in Figure 99.

VI. CONCLUSIONS

This investigation studied the thermal and pumping performance of two multiply-shrouded, angled-diffuser stack gas eductors with five and six diffuser rings and how cross-flow at a mean velocity of 29.5 knots affected such performance. Based on the data presented the following conclusions are drawn:

- 1) Pumping coefficient data obtained in this investigation correlates with that of a geometrically similar model tested in the cold facility.
- 2) Introduction of cross-flow results in a slight improvement in eductor pumping performance.
- 3) Cross-flow effects in the mean velocity range studied in this investigation (29.5 knots) result in an overall temperature reduction at the surface of the assembly but tend to result in some distortion or degradation of the desired diffuser film cooling effects.
- 4) Cross-flow did not appear to have any significant effect upon a modification of the peak exit plane temperature.
- 5) The modified model produced superior film cooling effects in comparison to Model A.
- 6) Improvements in overall eductor performance and reduction in exit plane temperature appear feasible by optimization of the angled diffuser design to account for maximum film cooling effectiveness.

VII. RECOMMENDATIONS

Considering the experience gained in the conduct of this research and specifically in view of the results obtained, the following research recommendations are offered for future investigations.

1) Diffuser ring number one should be extended to a length approximately twice the current length to attempt to reduce the high temperature noted at the end of the shroud.

2) The cross-flow fan should be modified for two speed operations and other nozzle designs should be tested to provide a range of cross-flow velocities for model evaluation.

3) Further investigation of the flow phenomenon at end around the model's shroud and diffuser assembly should be conducted to explain the noted intermittent degradation of film cooling effectiveness.

4) Additional research should be performed to determine the variation in induced tertiary air flow resulting from a modification in air mass flow rate.

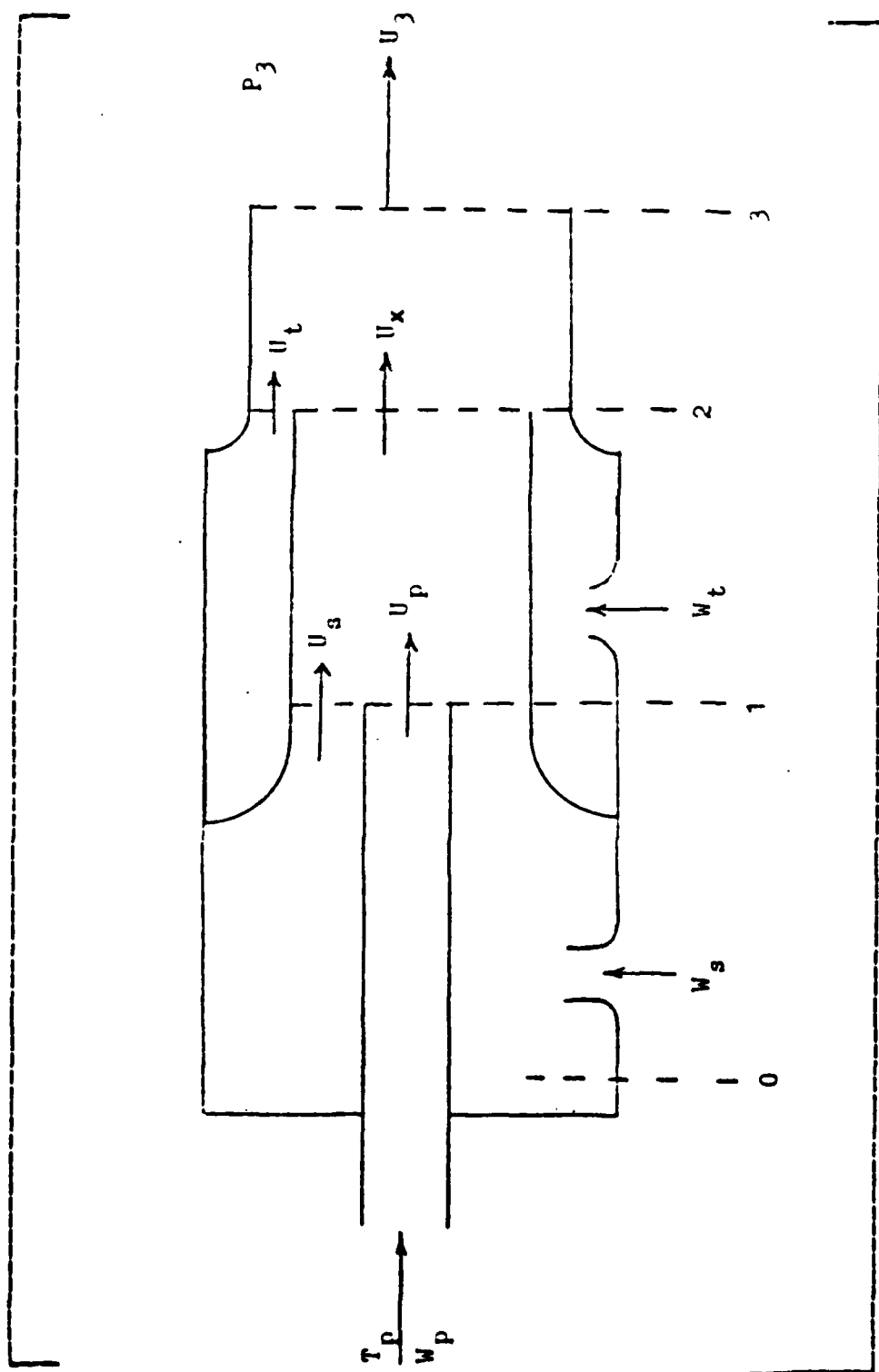


Figure 1. Simple Nozzle Ejector System.

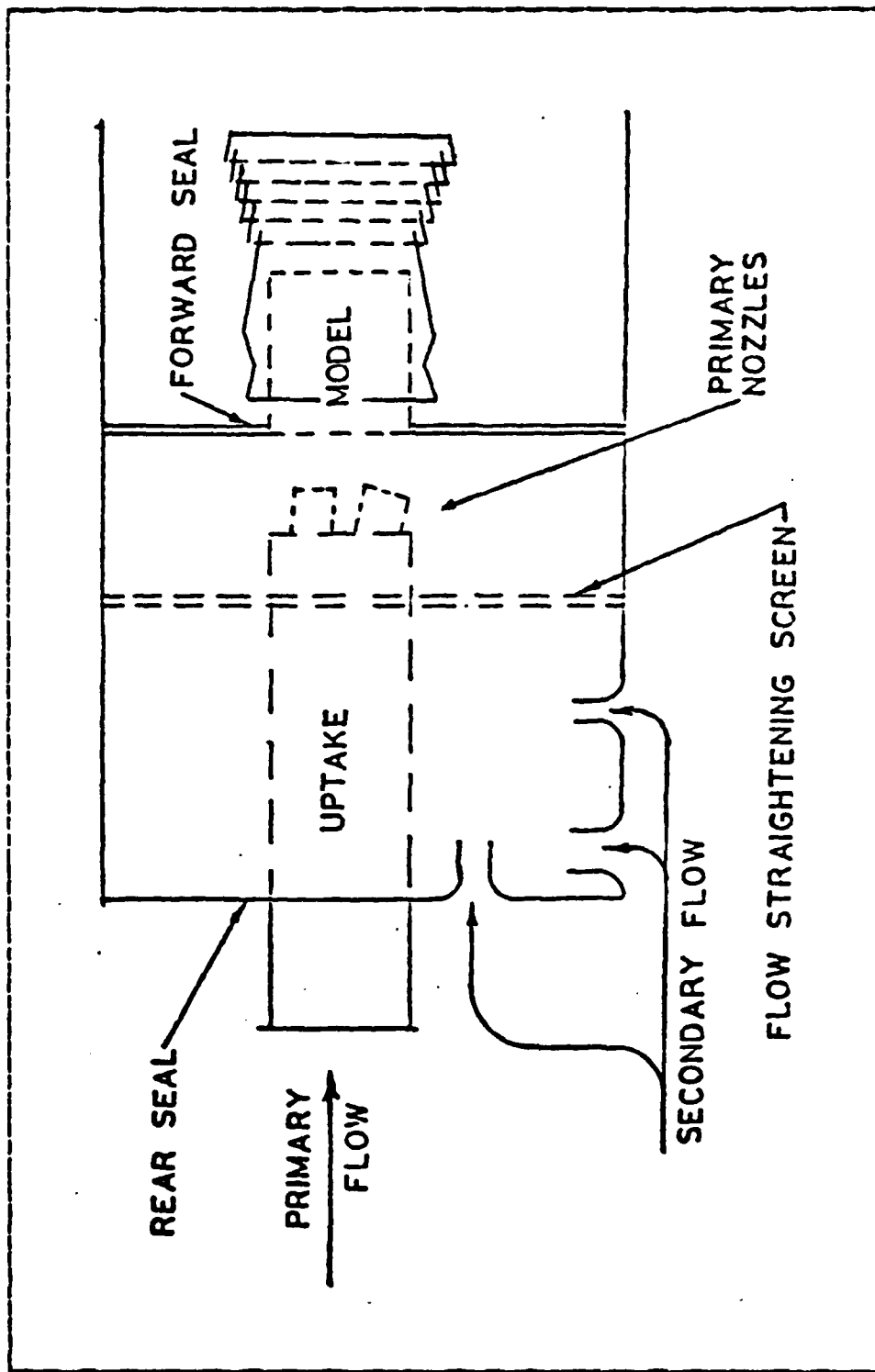


Figure 2. Plan of Uptake, Model, and Measurement Plenum.

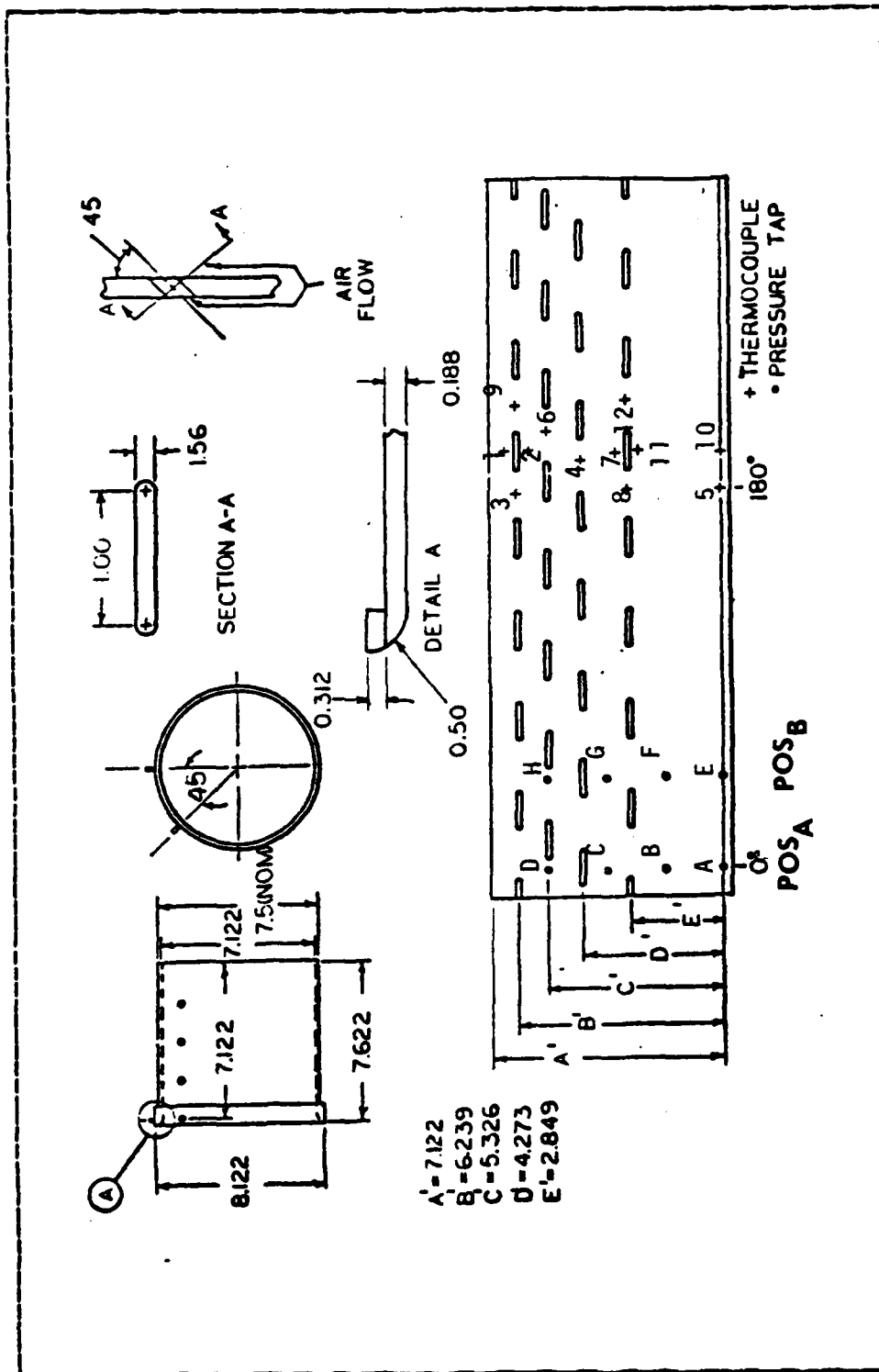


Figure 3. Dimensional Diagram of Slotted Mixing Stack.

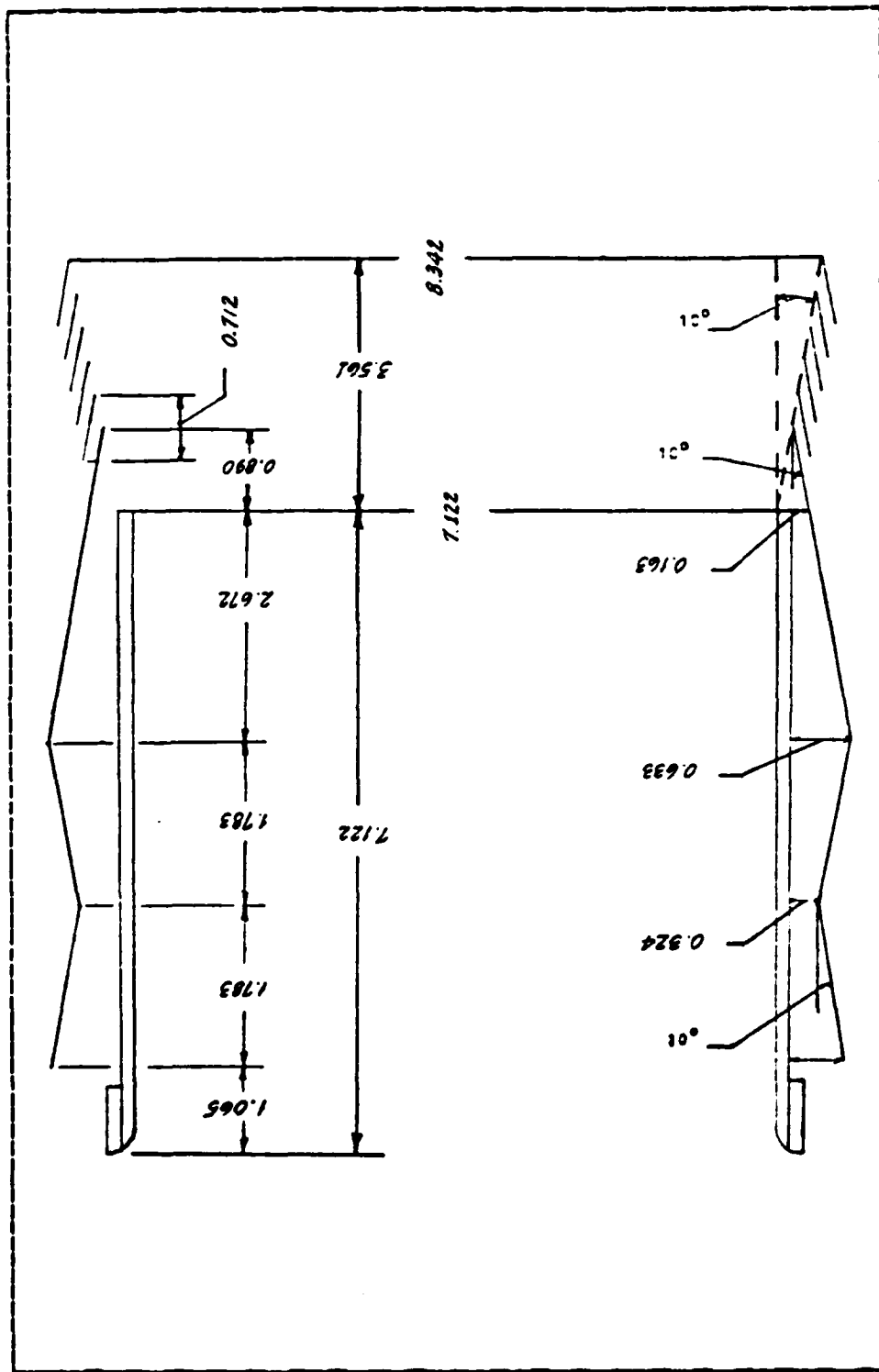


Figure 4. Schematic of Model A - Shroud and Diffuser Rings.

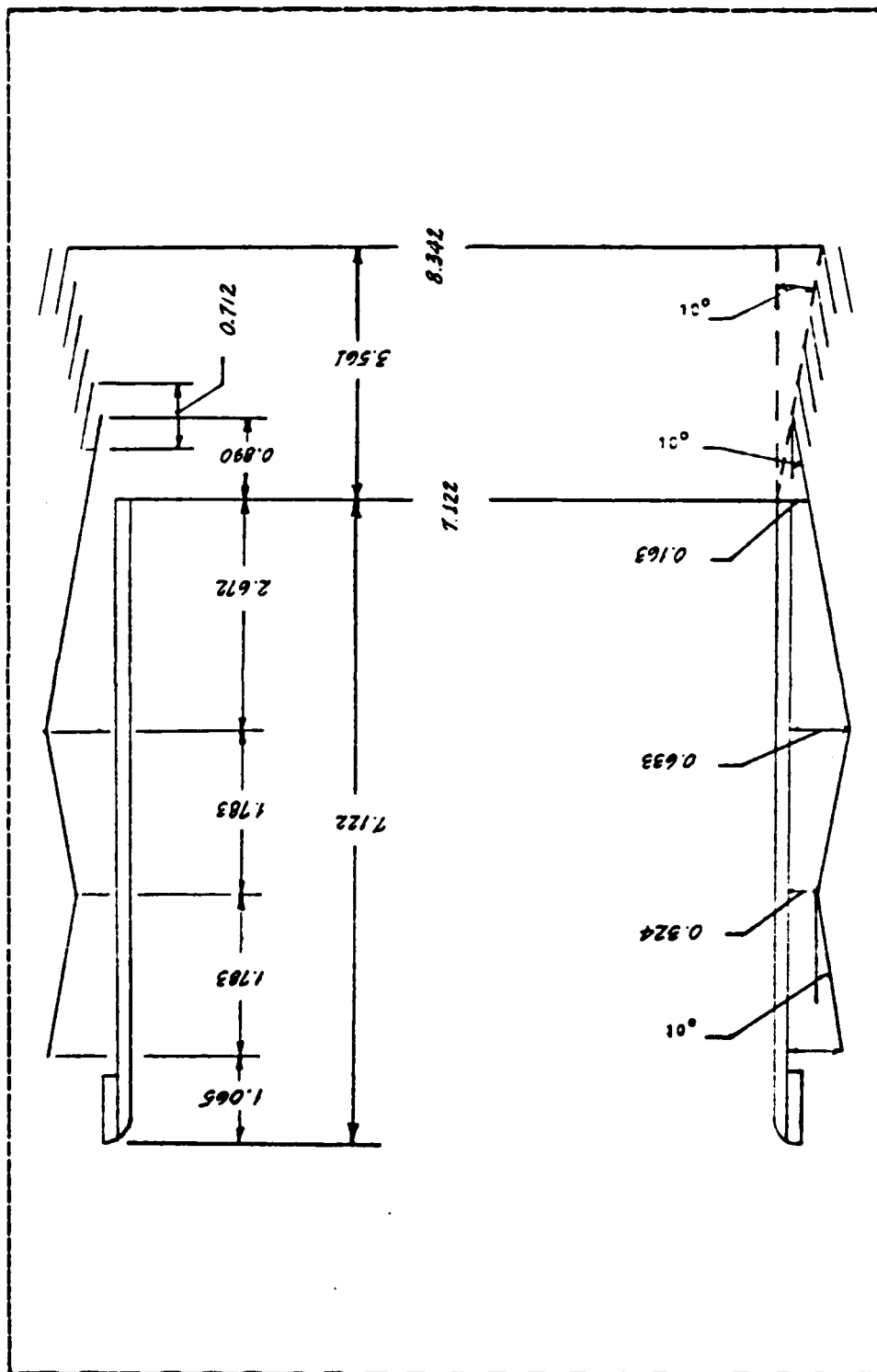


Figure 5. Schematic of Model A Modified - Shroud and Diffuser Rings.

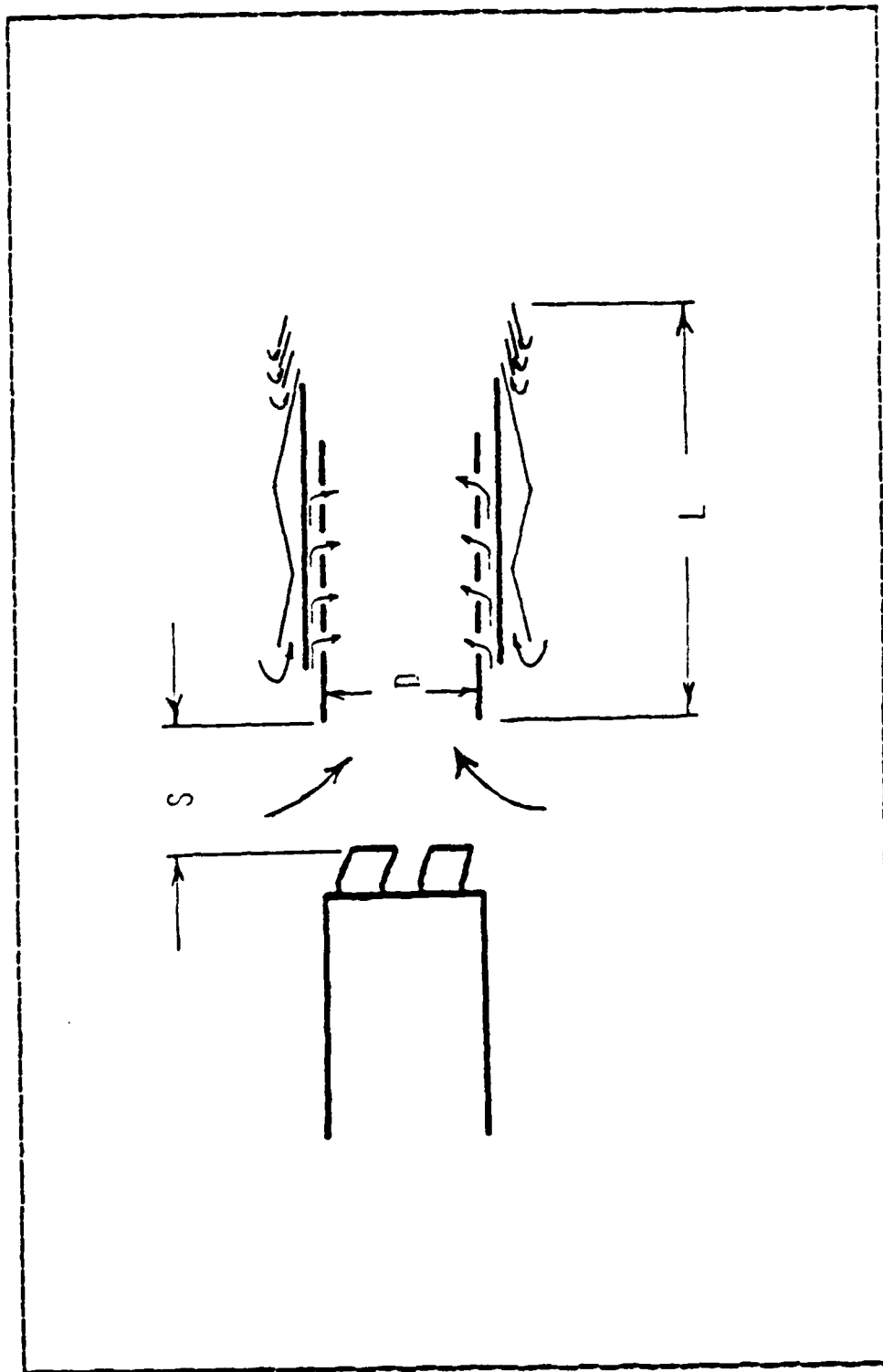


Figure 6. Characteristic Eductor Dimensions.

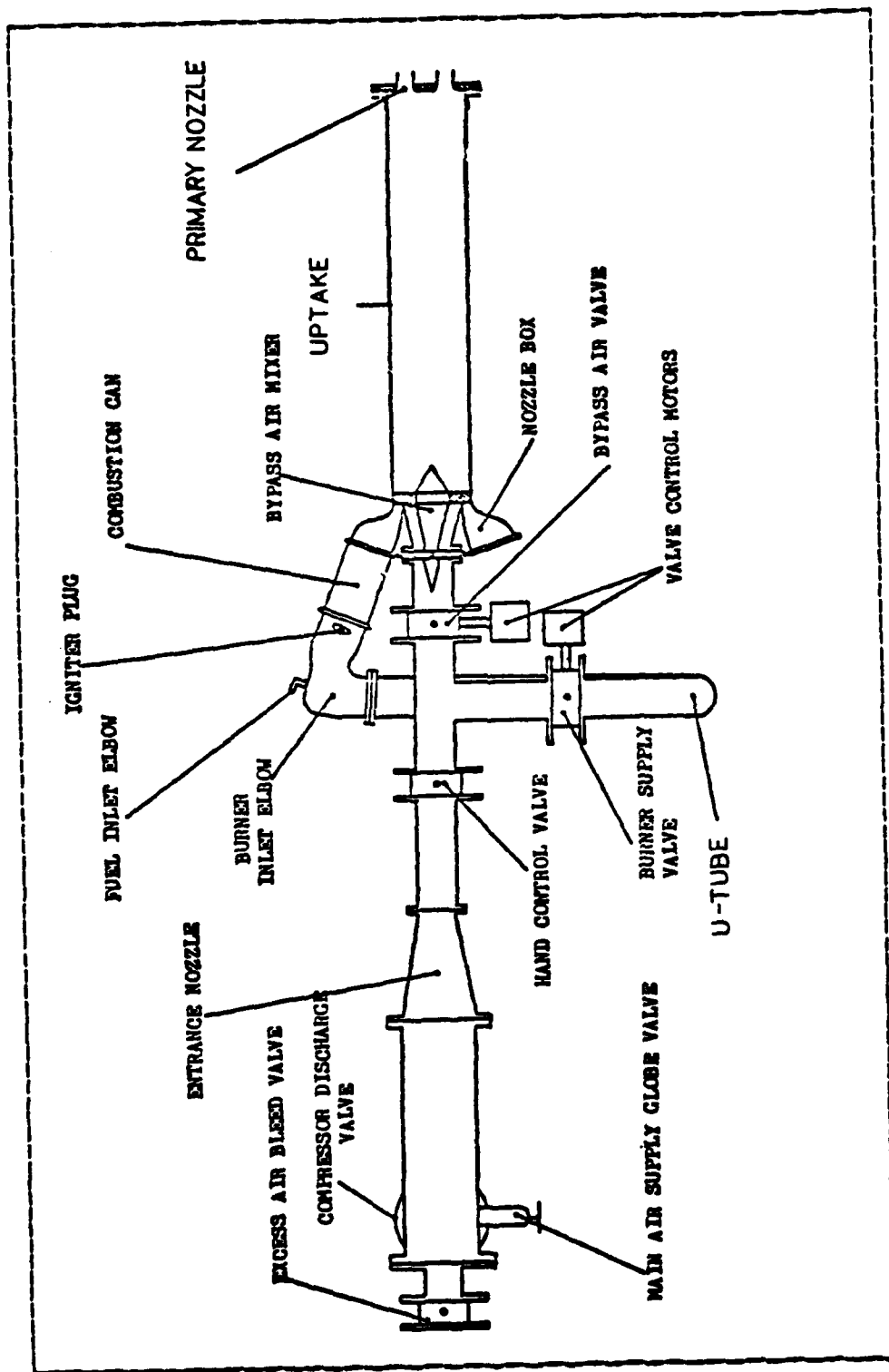


Figure 7. Gas Generator Arrangement.

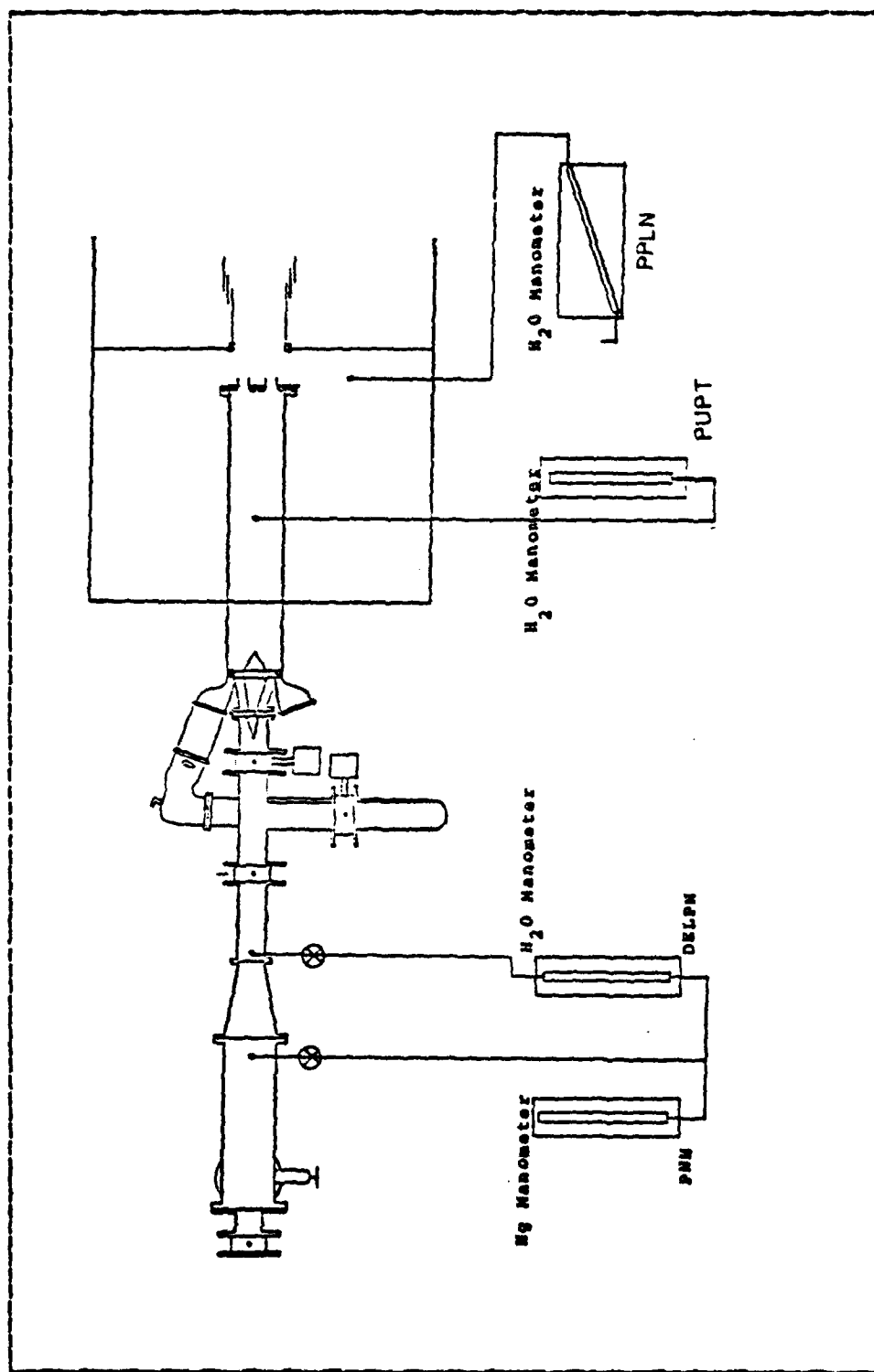


Figure 8. Schematic Diagram of Pressure Measurement System.

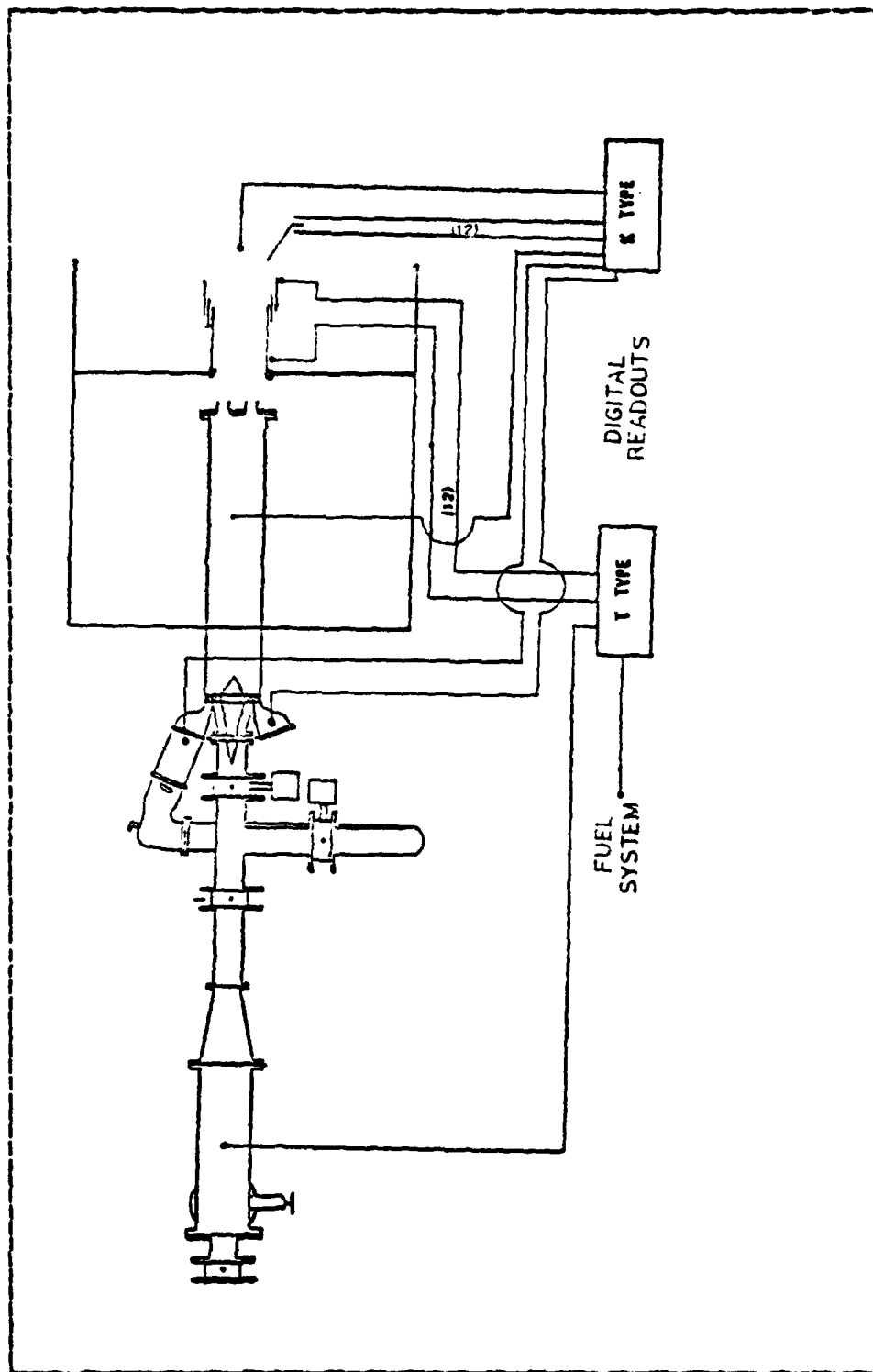


Figure 9. Schematic Diagram of Temperature Measurement System.

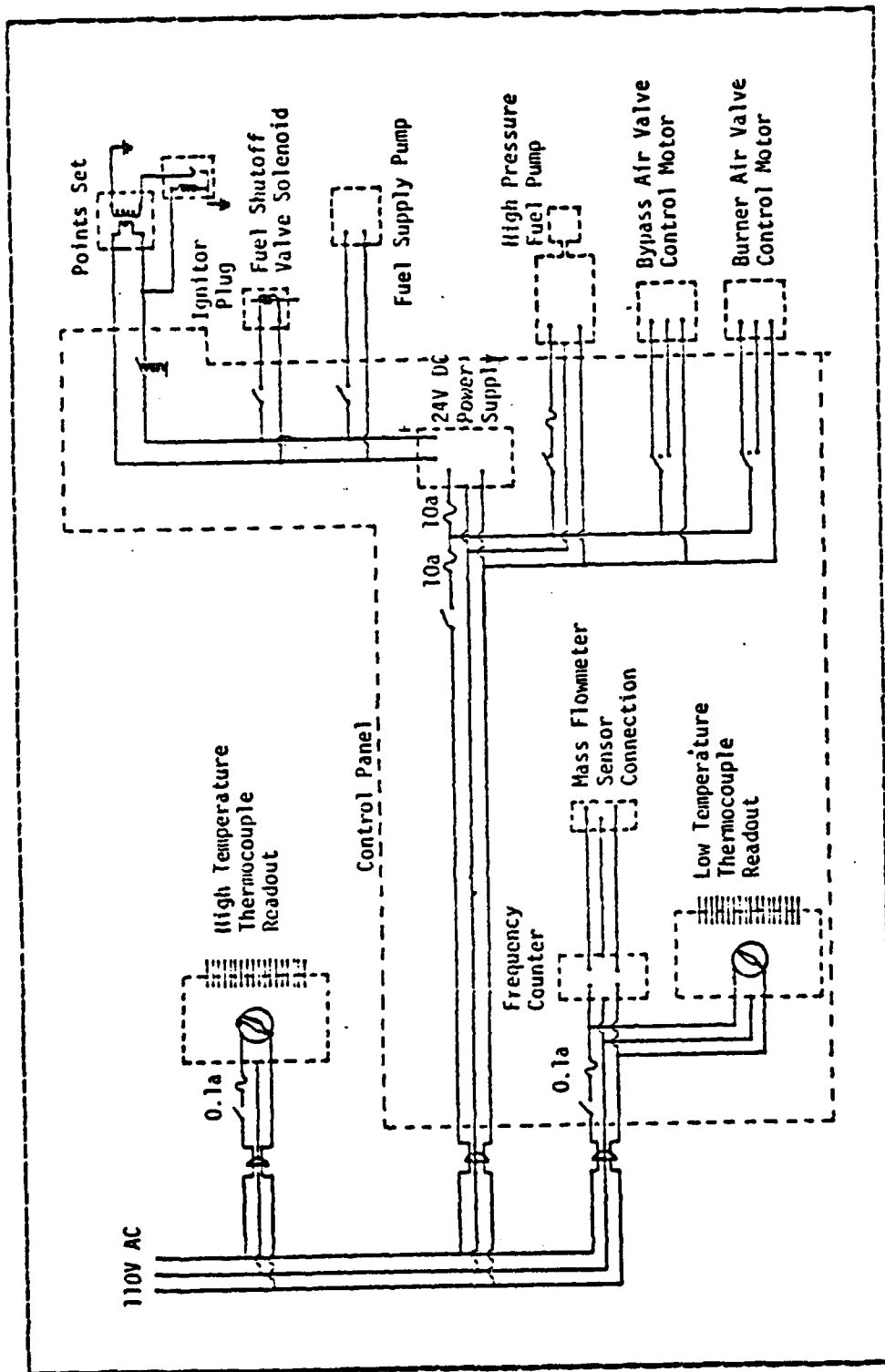


Figure 10. Gas Generator Electrical System.

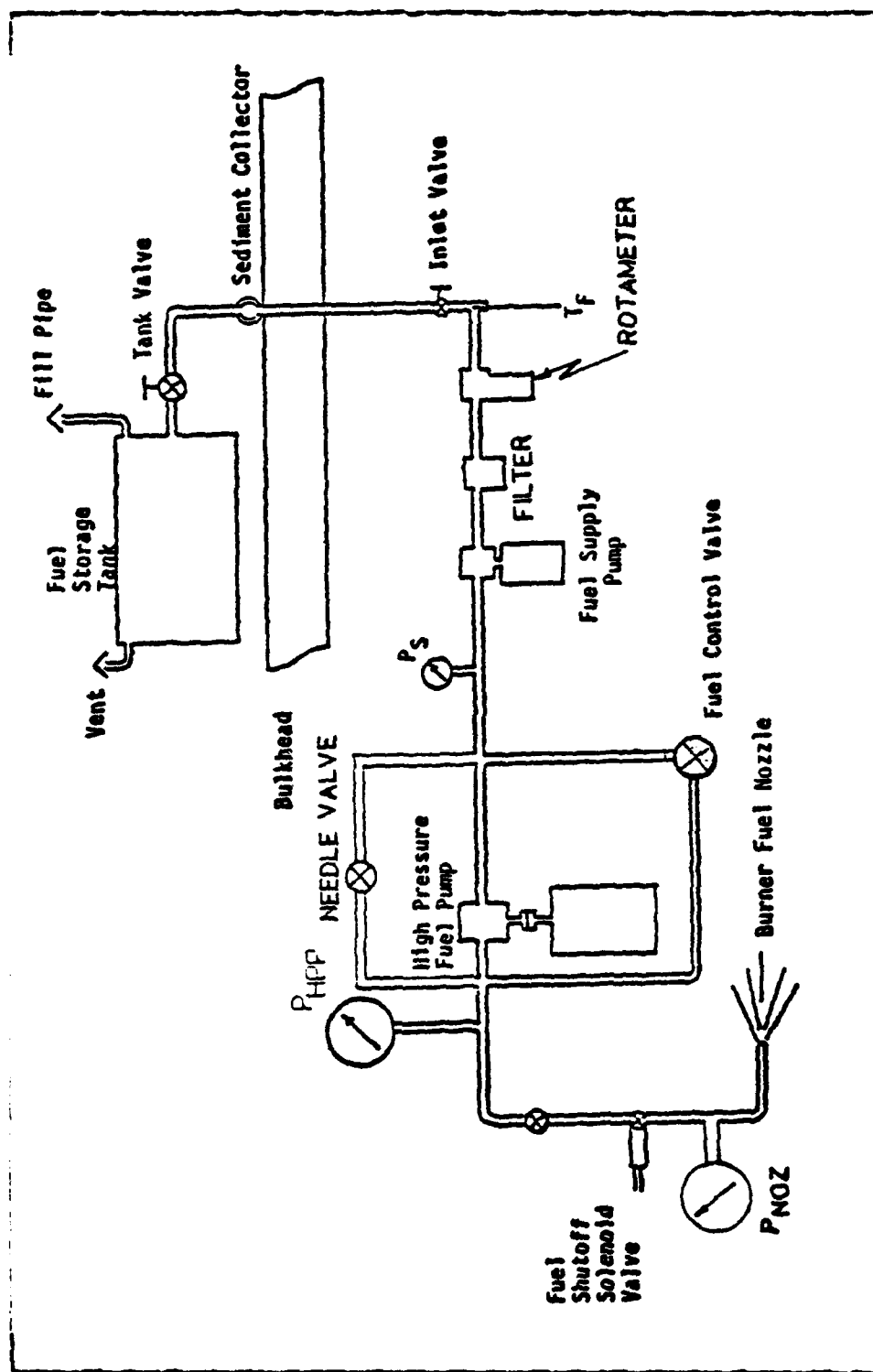


Figure 11. Gas Generator Fuel System.

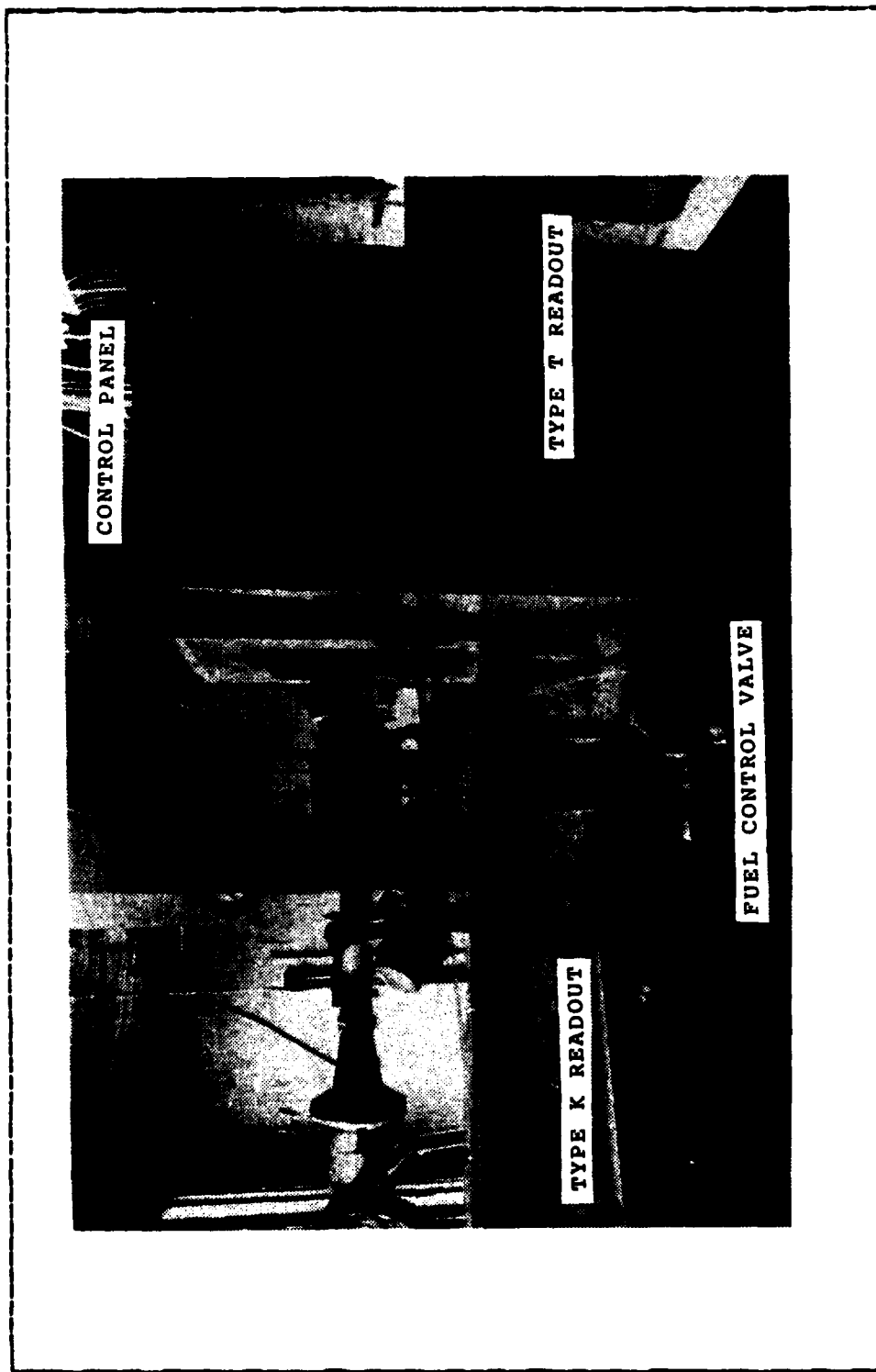


Figure 12. Gas Generator Control Station.



Figure 13. Main Power Supply and Control Panel.

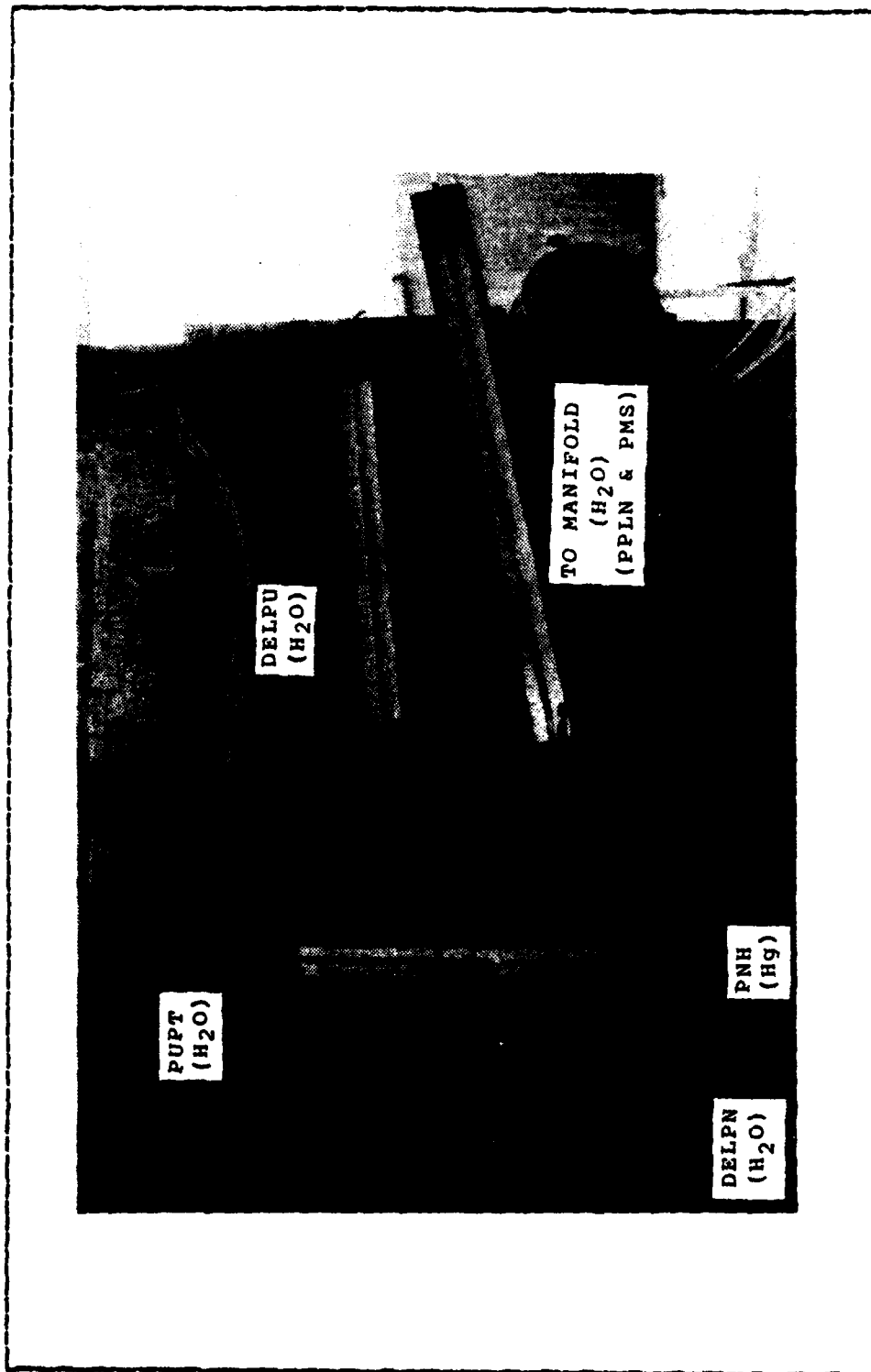


Figure 14. Manometer Installation.

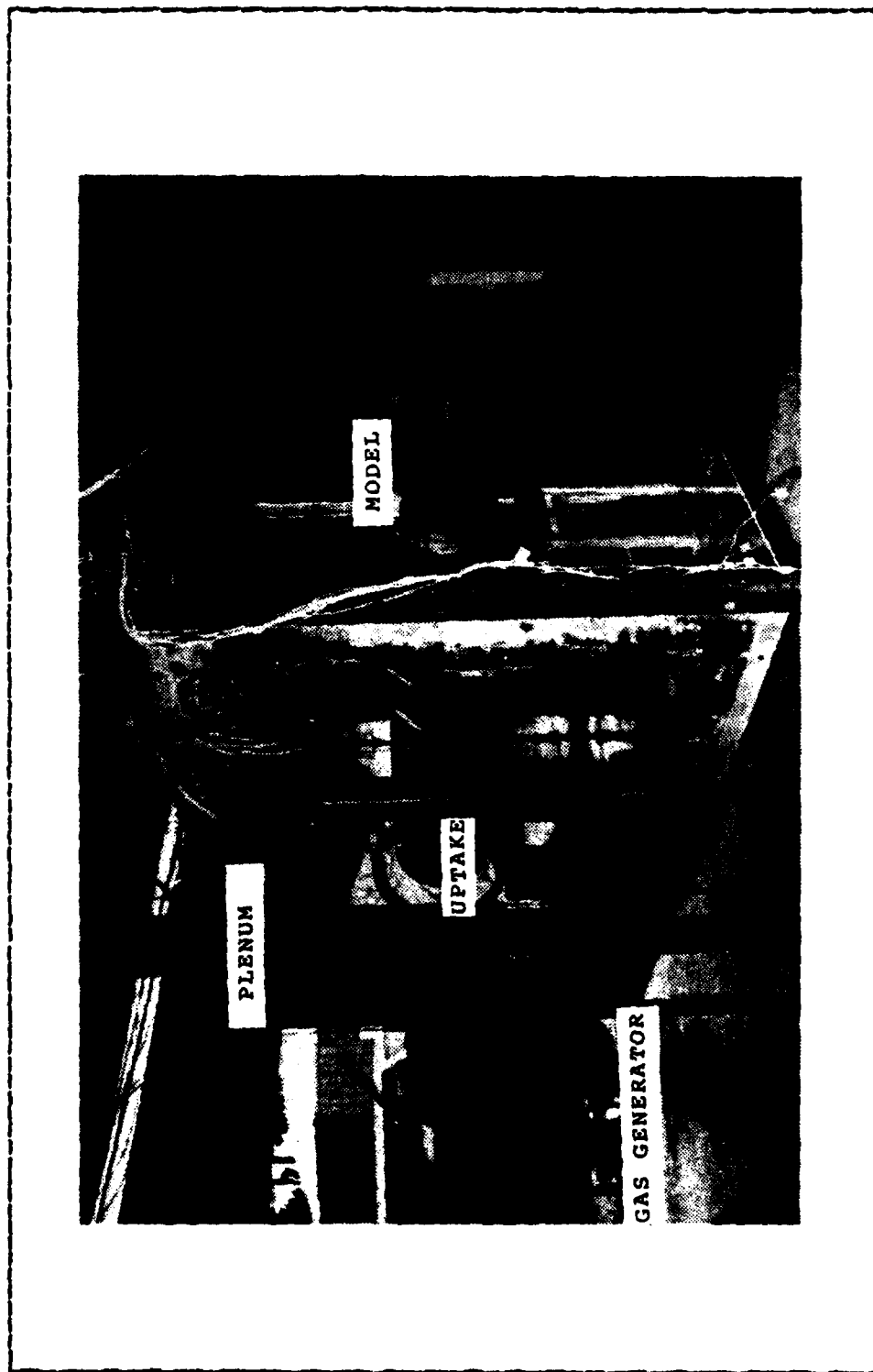


Figure 15. Hot Flow Test Facility.

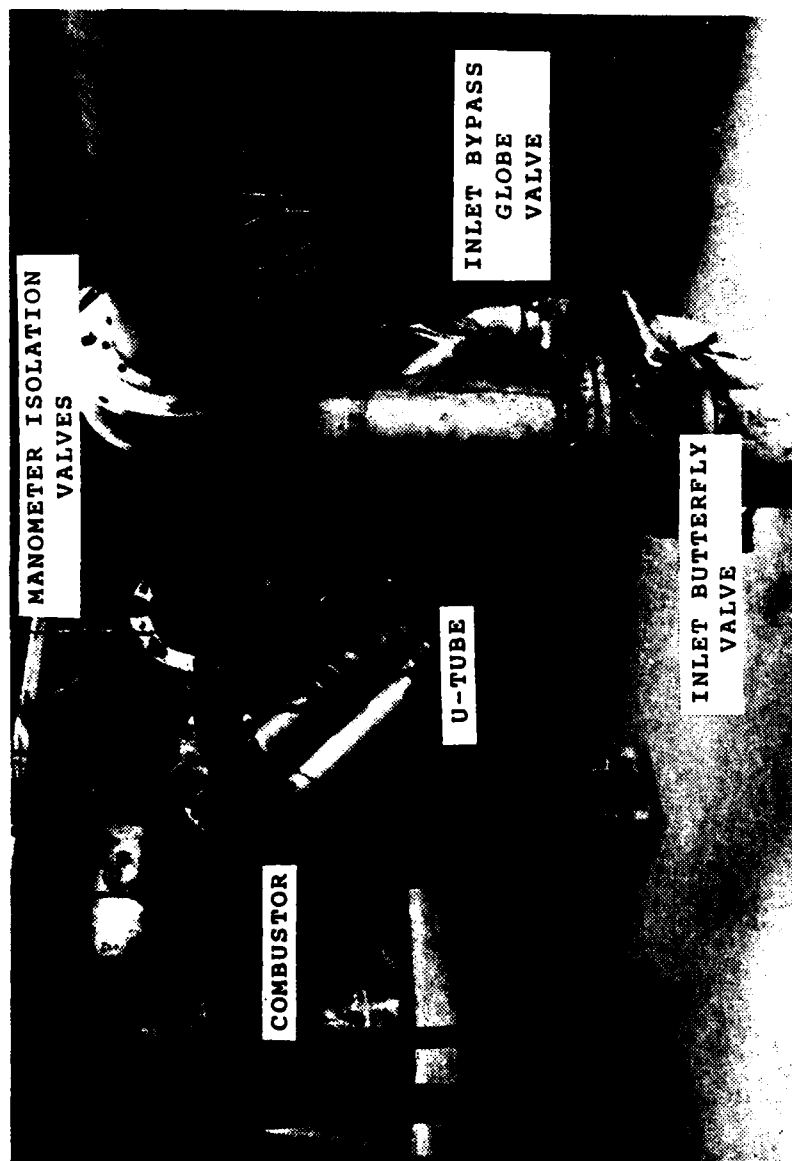


Figure 16. Air Supply Standpipe and Valving.

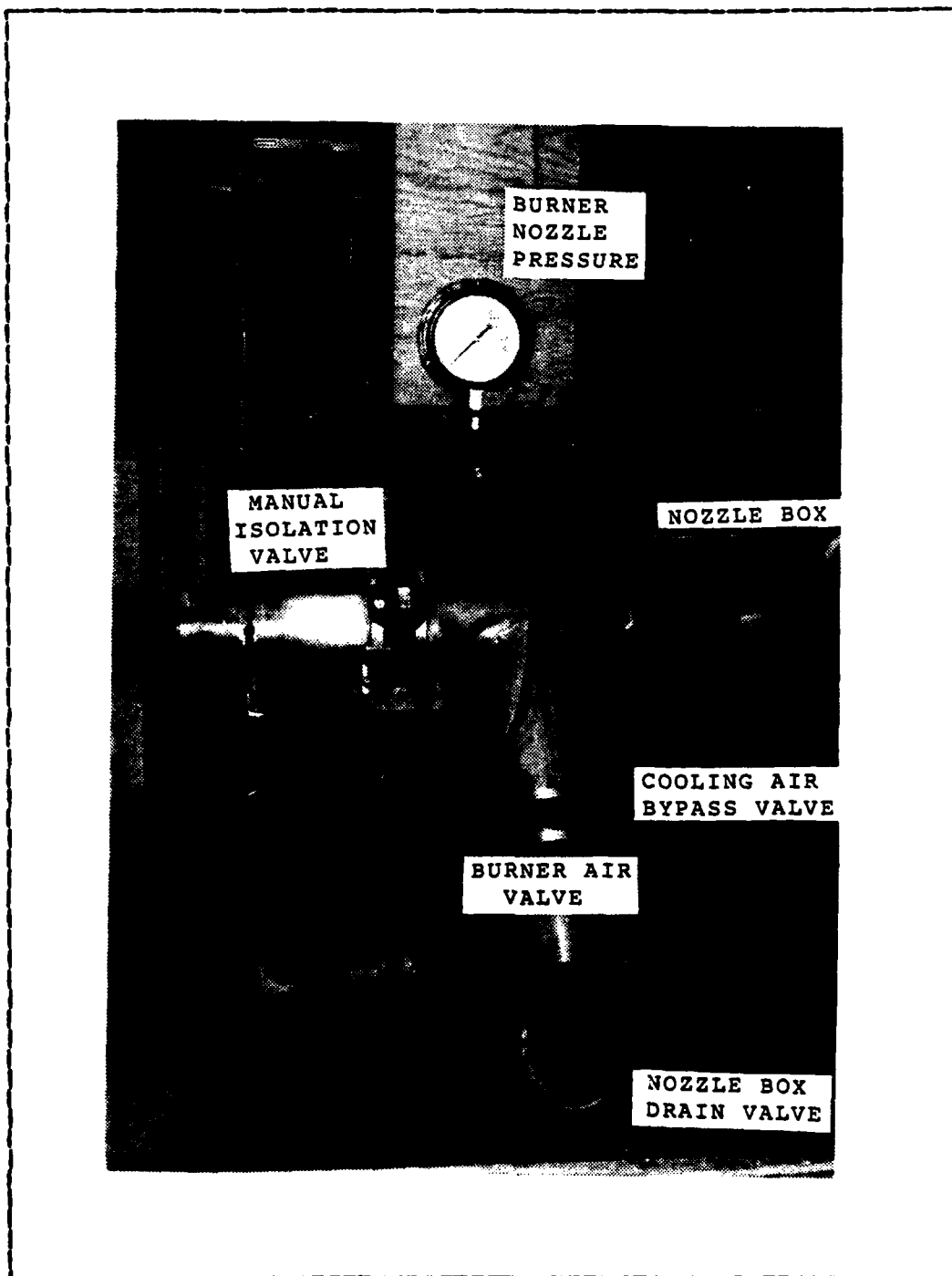


Figure 17. Combustor Air Piping.

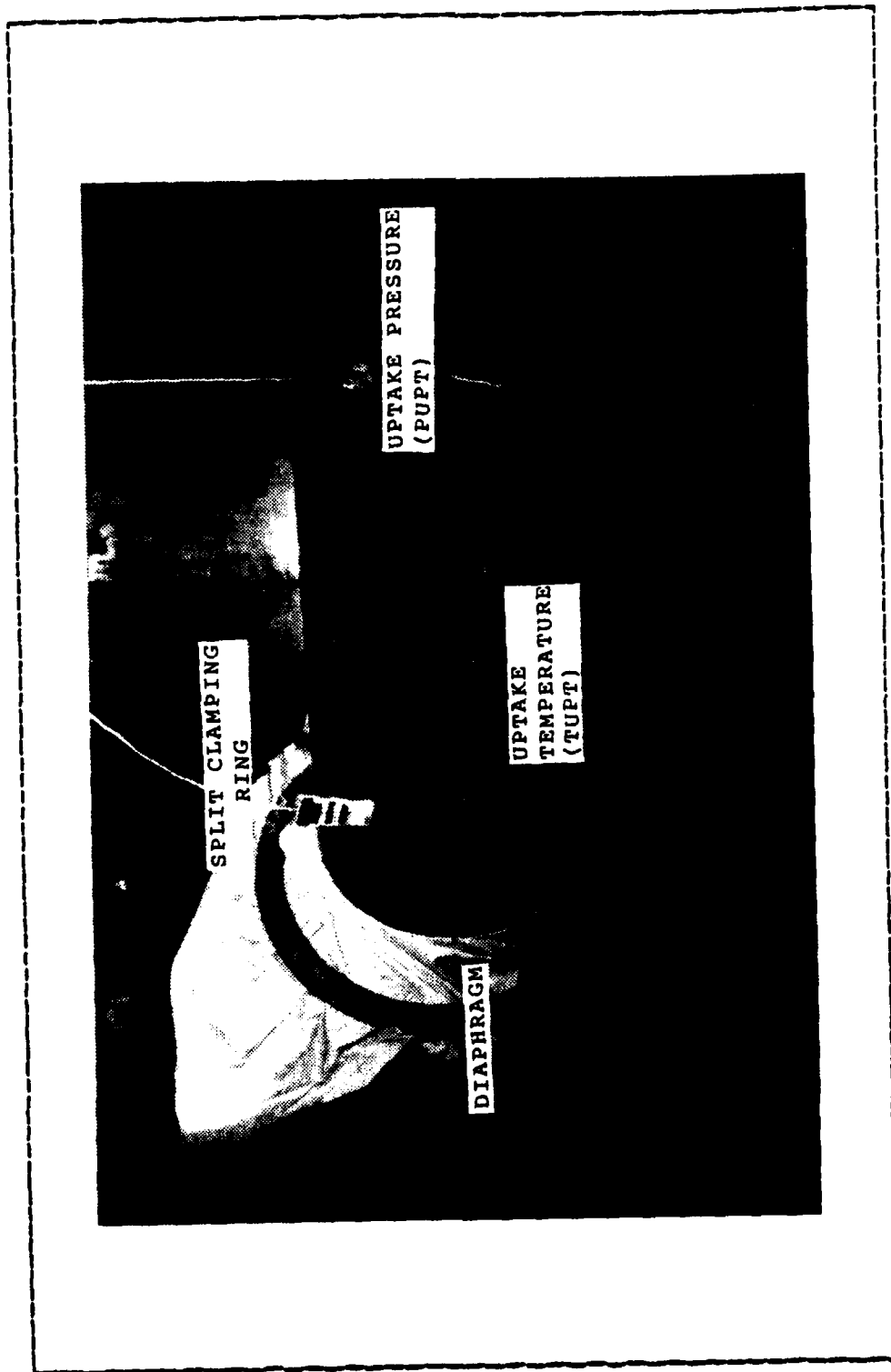


Figure 18. Uptake Section.

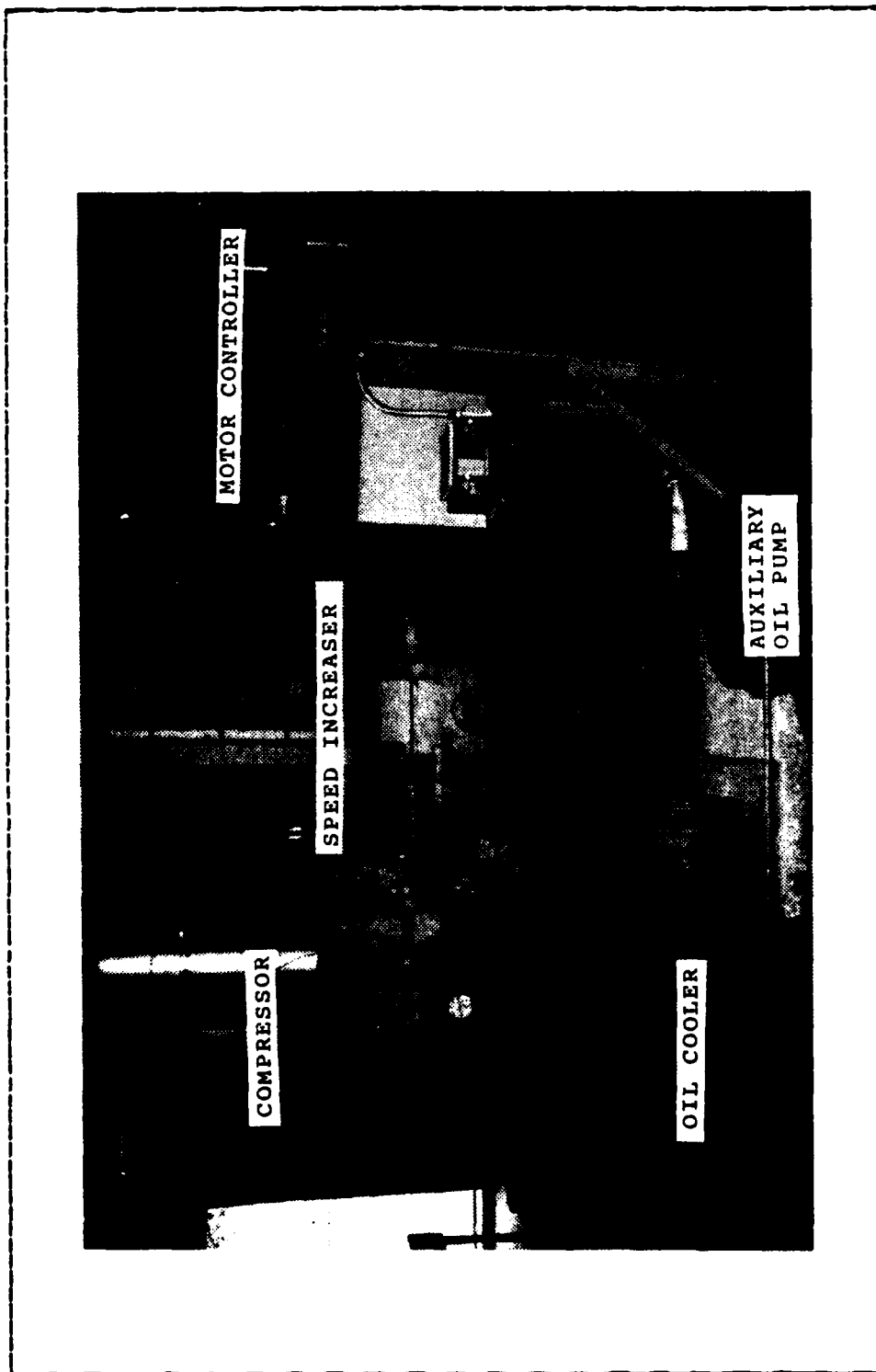


Figure 19. Carrier Air Compressor.

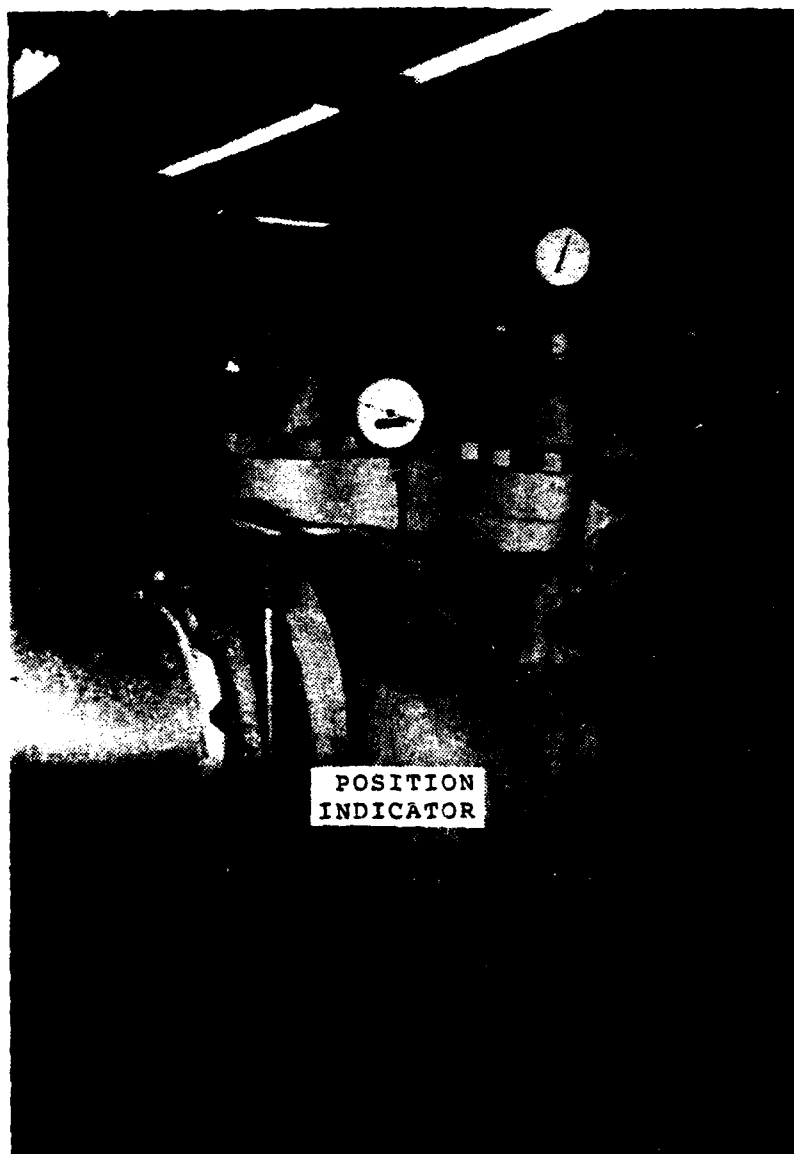


Figure 20. Air Compressor Suction Valve.

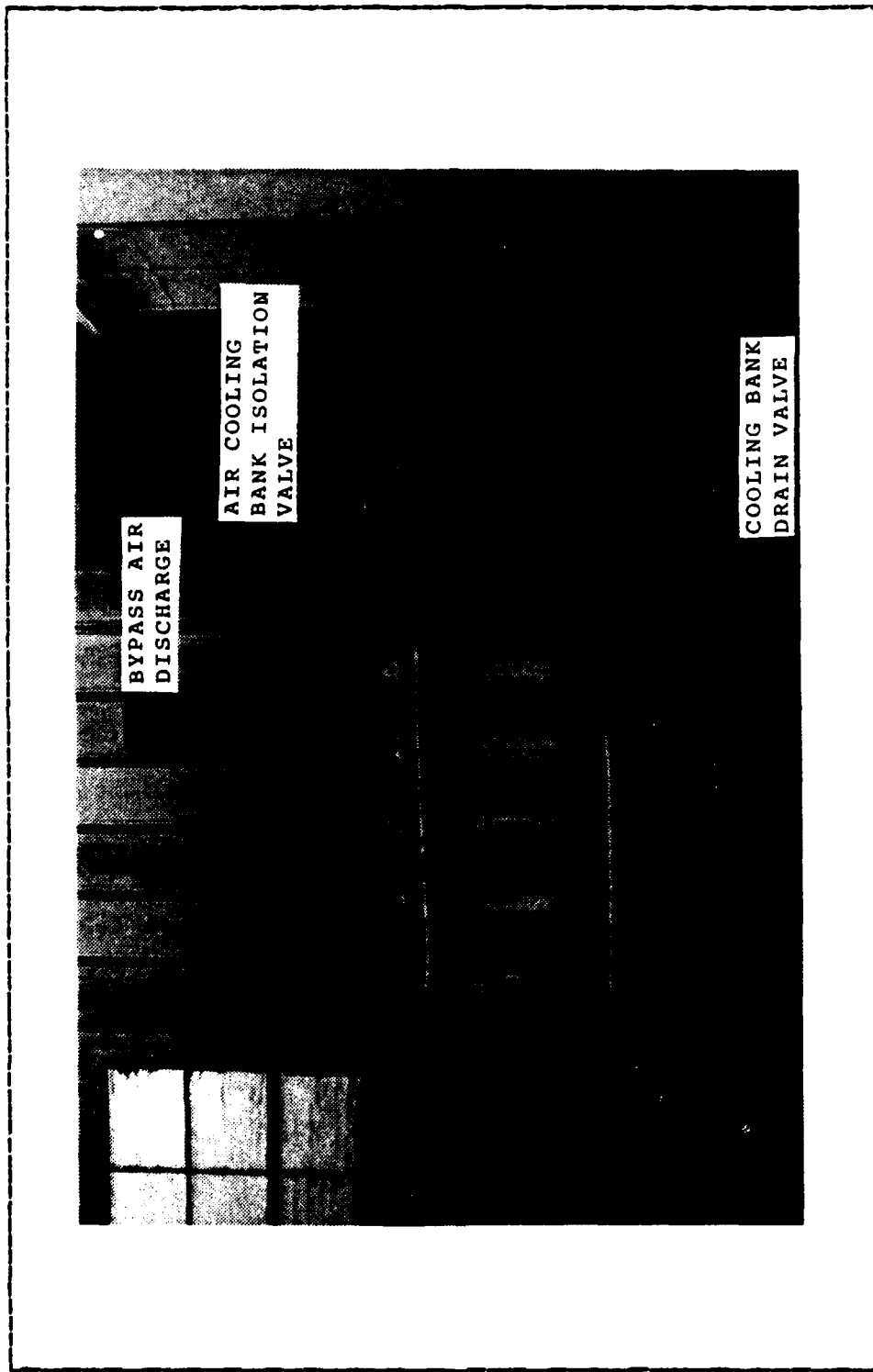


Figure 21. Air Cooling Bank and Bypass Discharge.

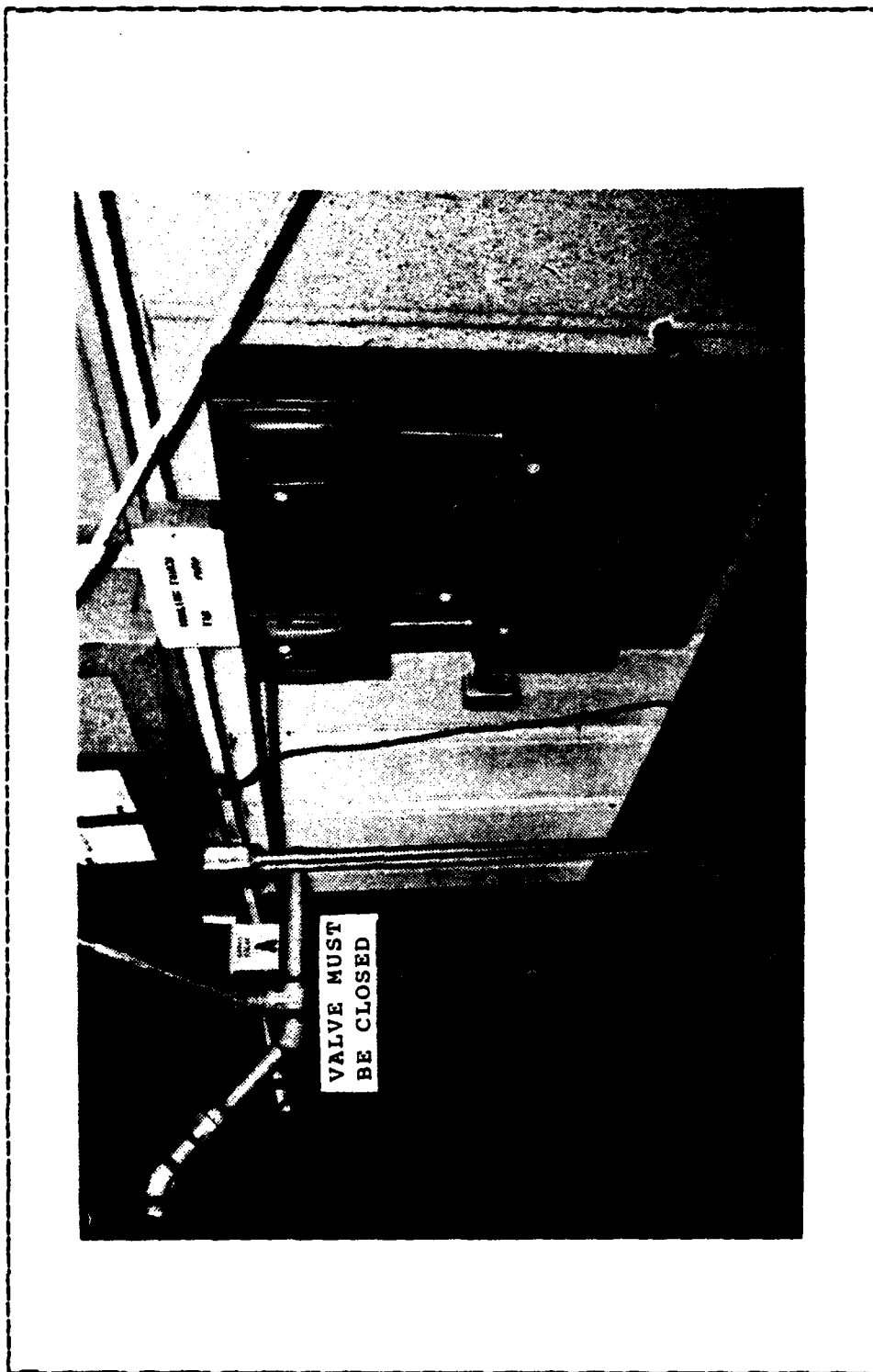


Figure 22. Cooling Water Pump and Tower Fan Controllers.

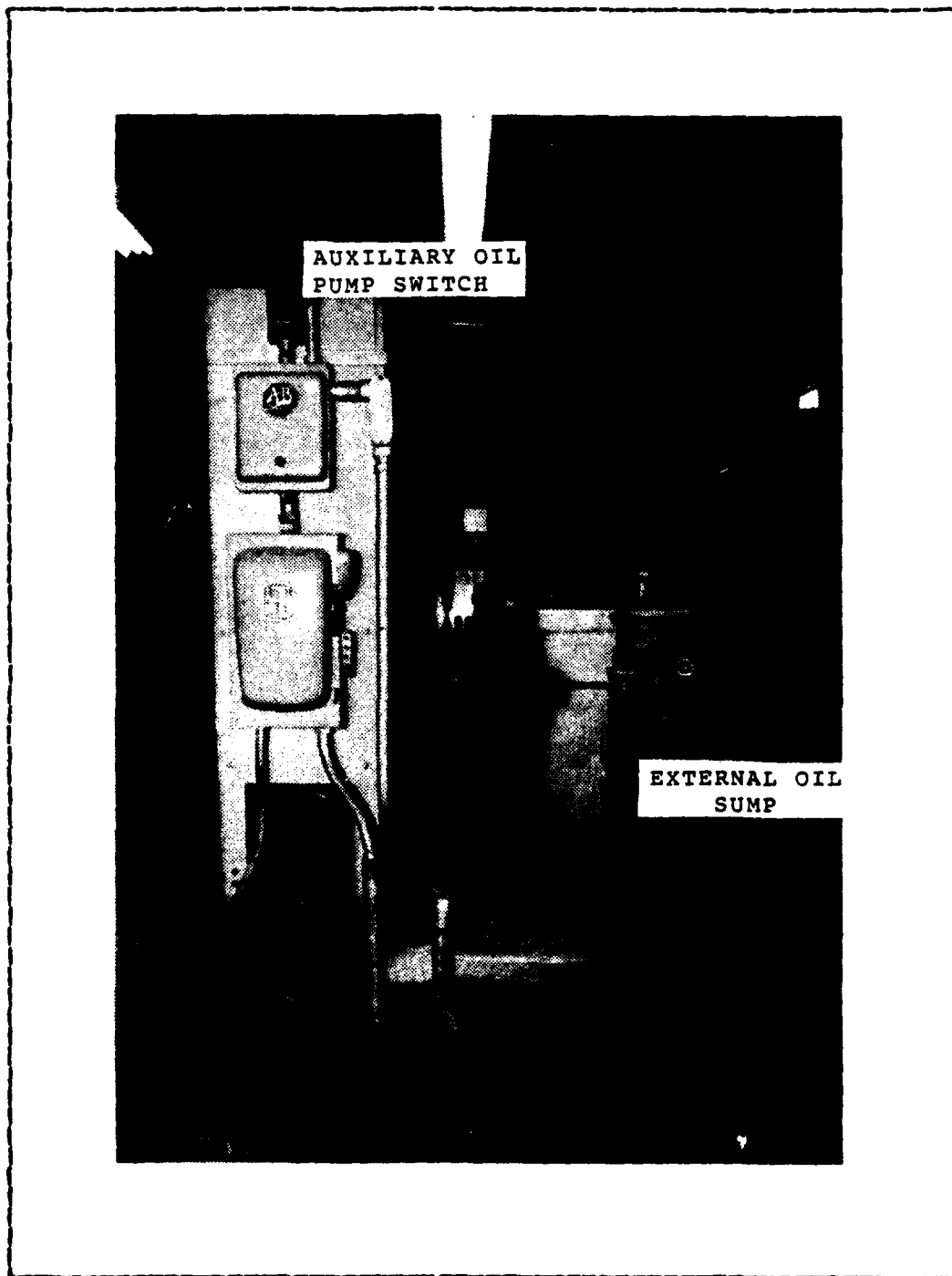


Figure 23. Auxiliary Oil Pump Control.

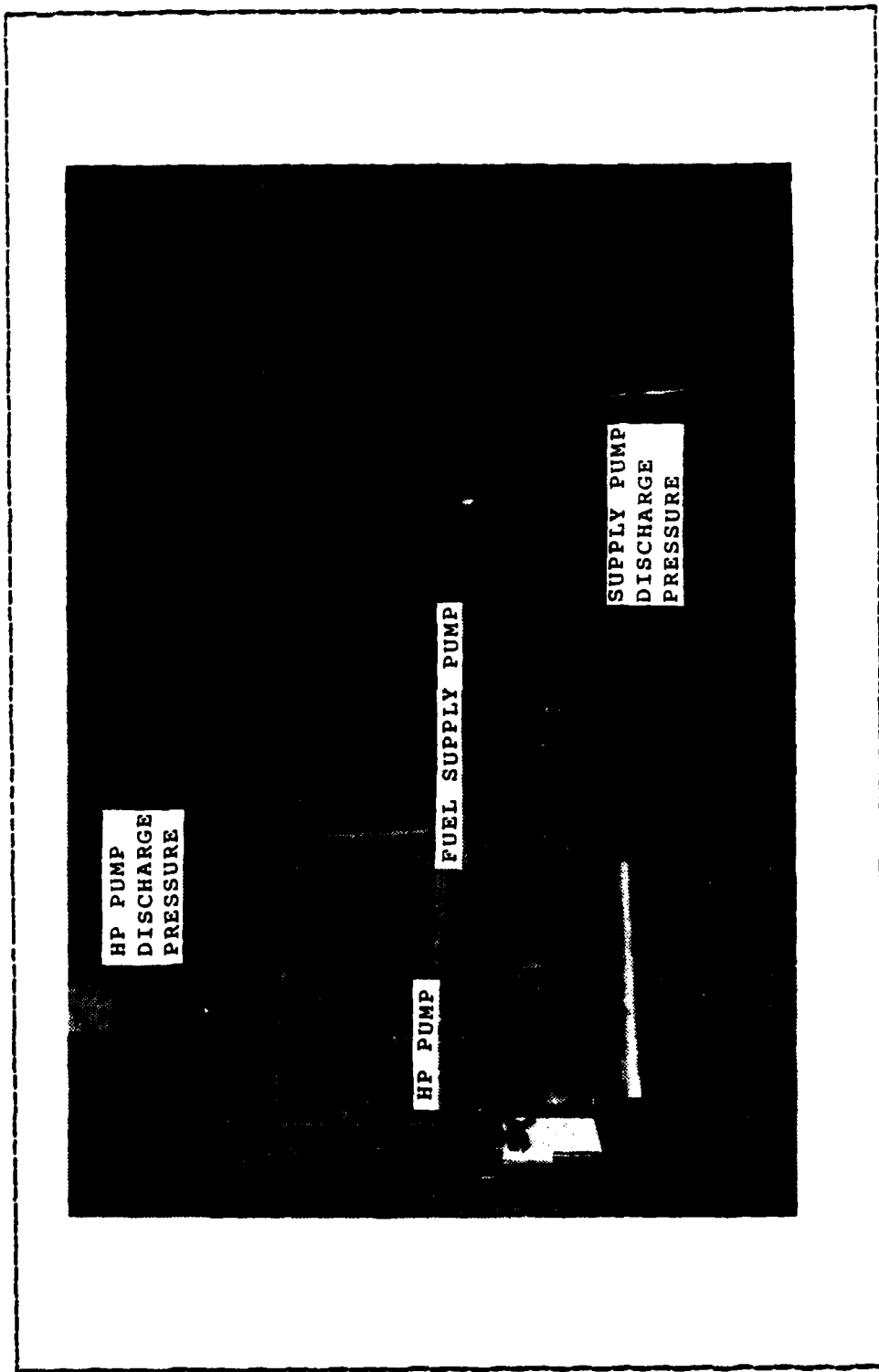


Figure 24. Fuel Pump Installation.

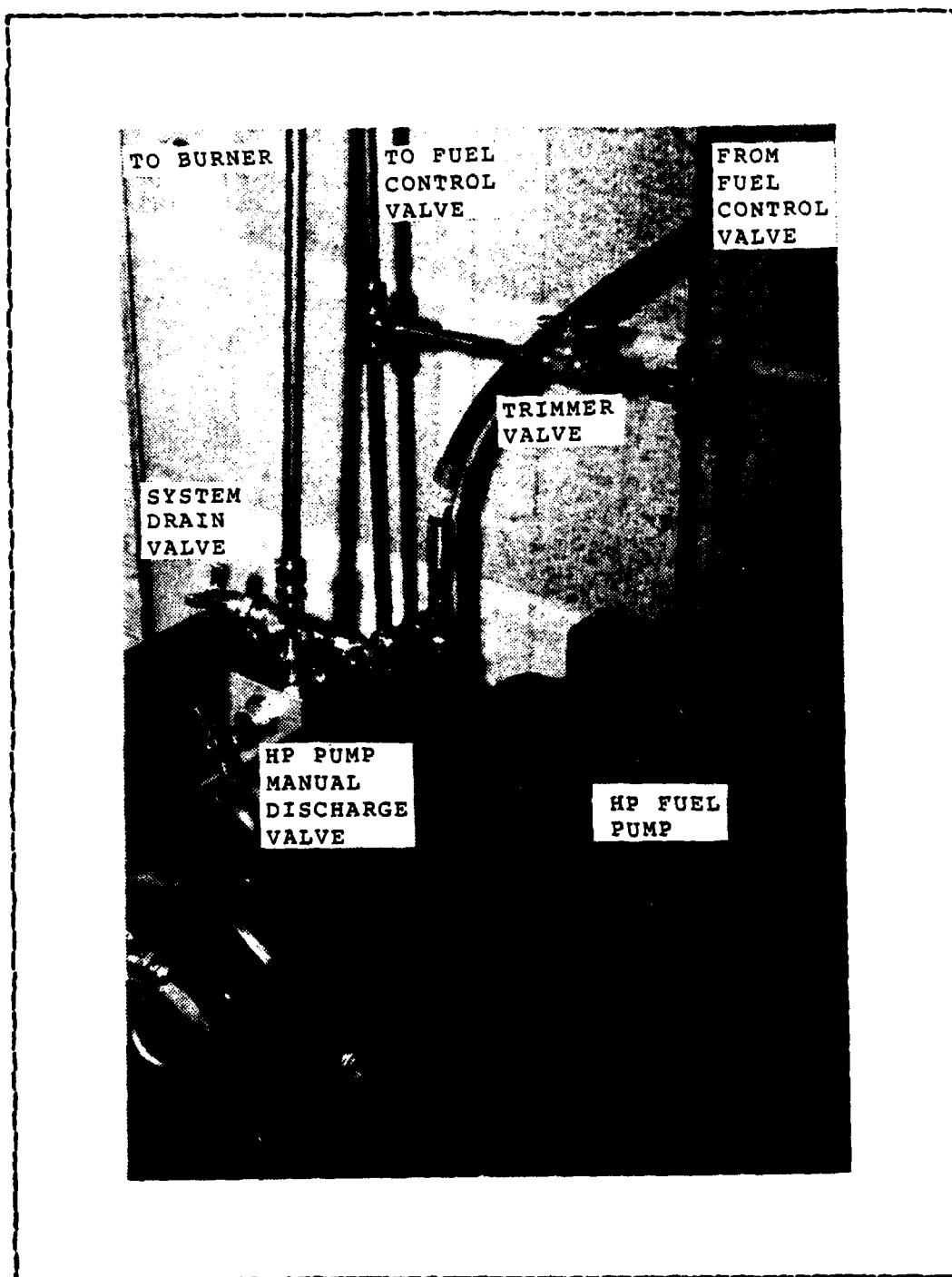


Figure 25. H. P. Fuel Piping and Valves.

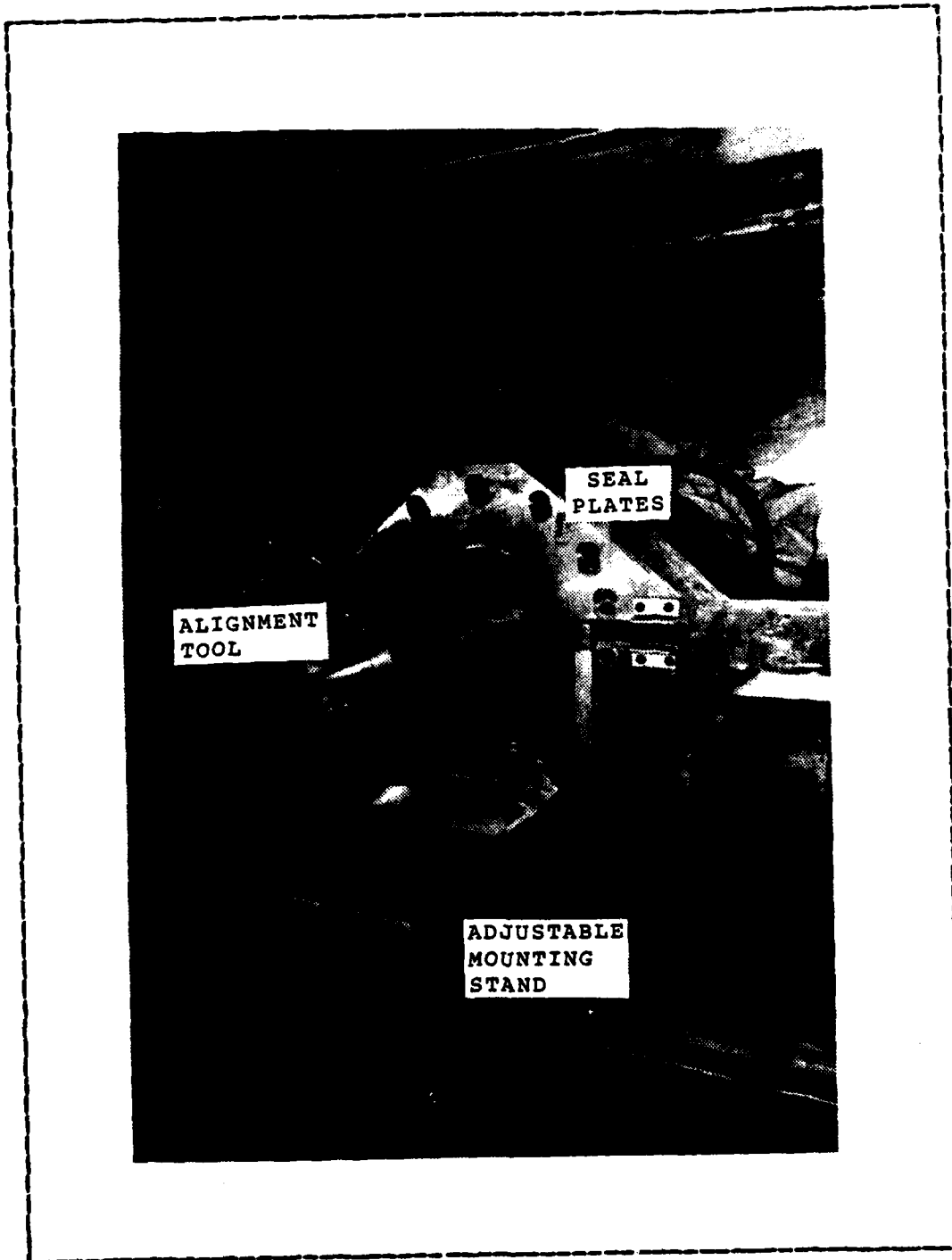


Figure 26. Model Installation.

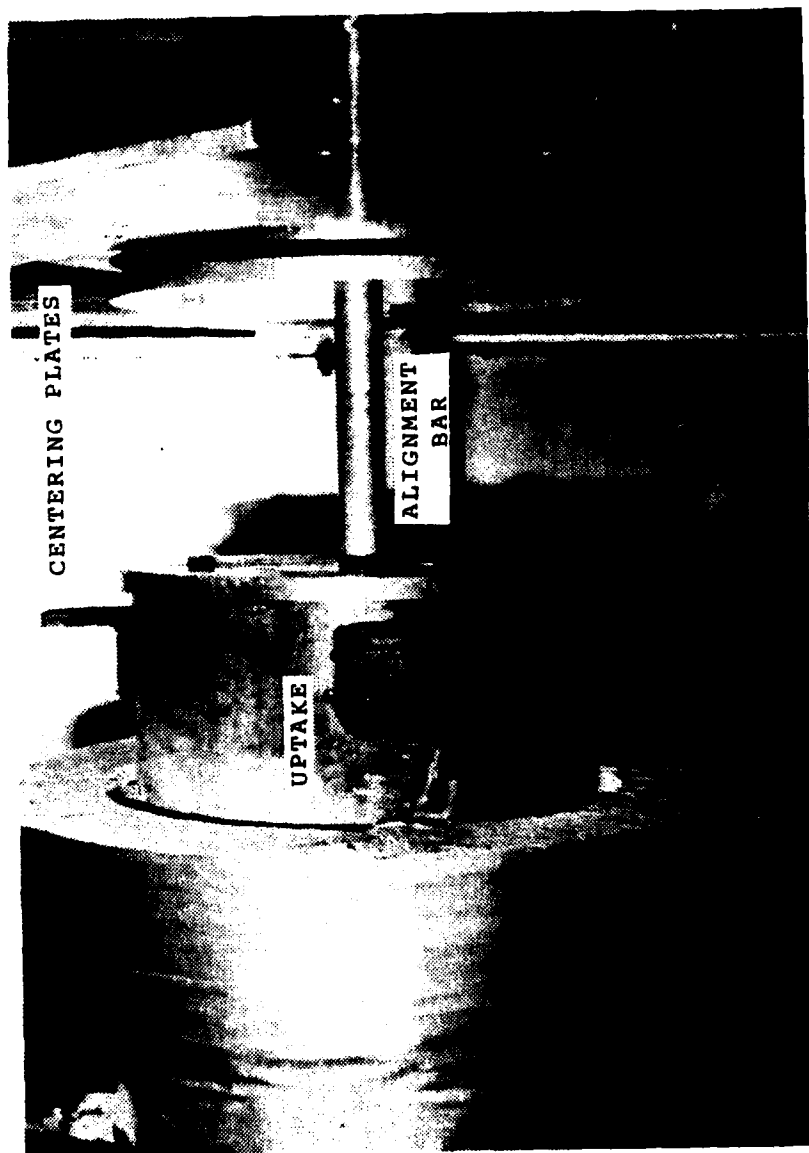


Figure 27. Model Alignment.

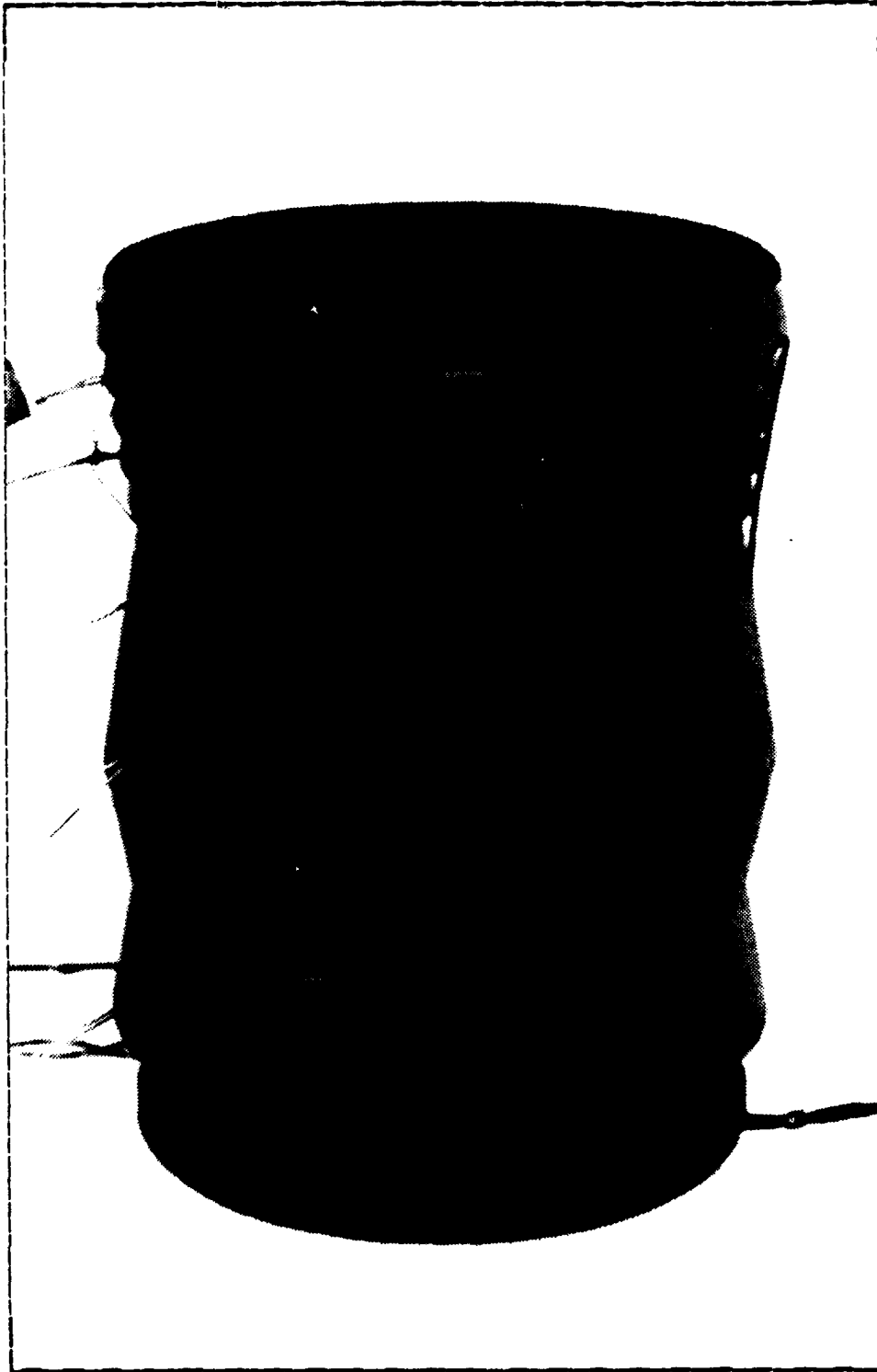


Figure 28. Model A.



Figure 29. Model A Entrance.

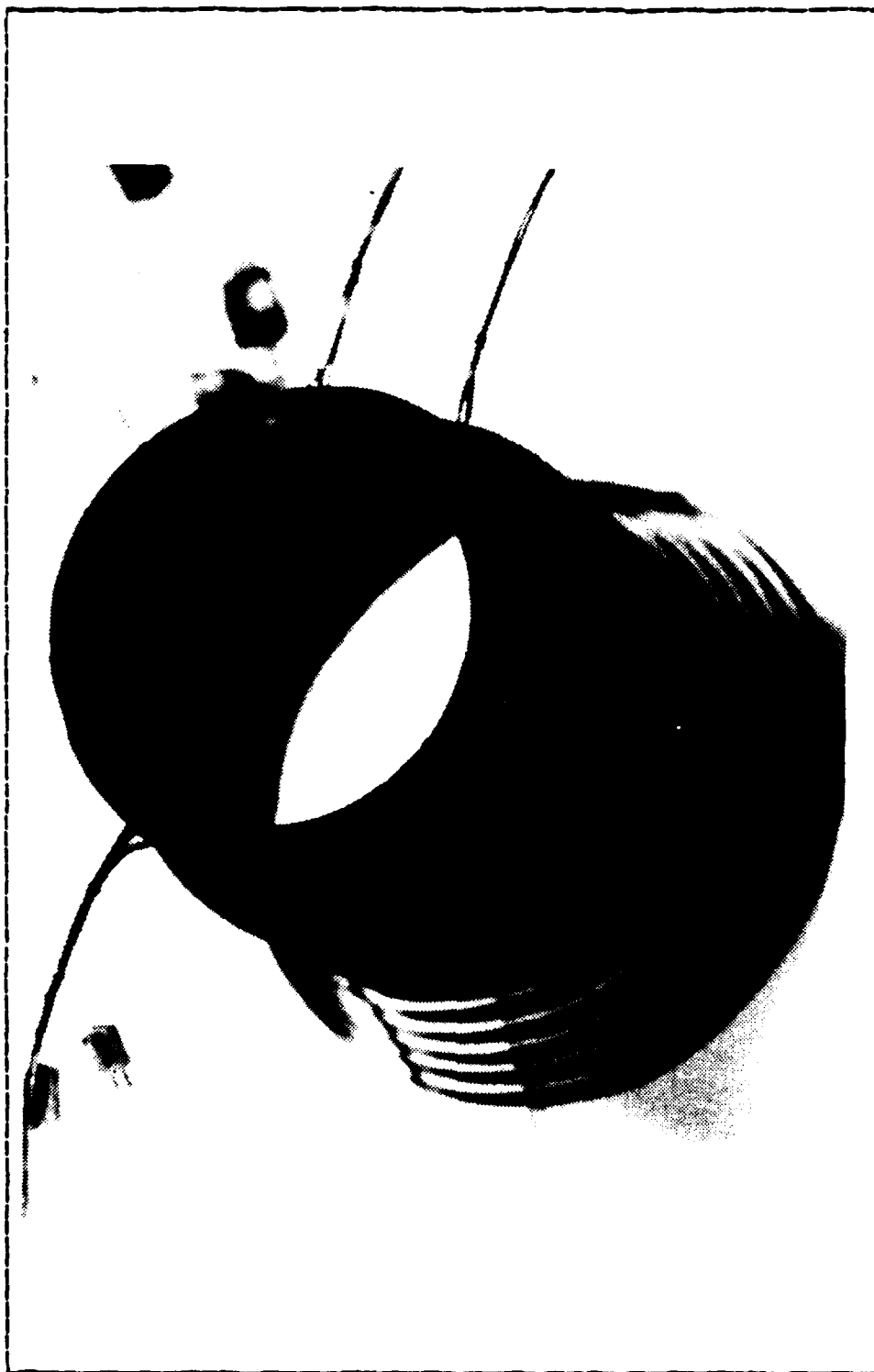


Figure 30. Model A Exit.



Figure 31. Model A Installed.



Figure 32. Crossflow Fan with Model A Installed.

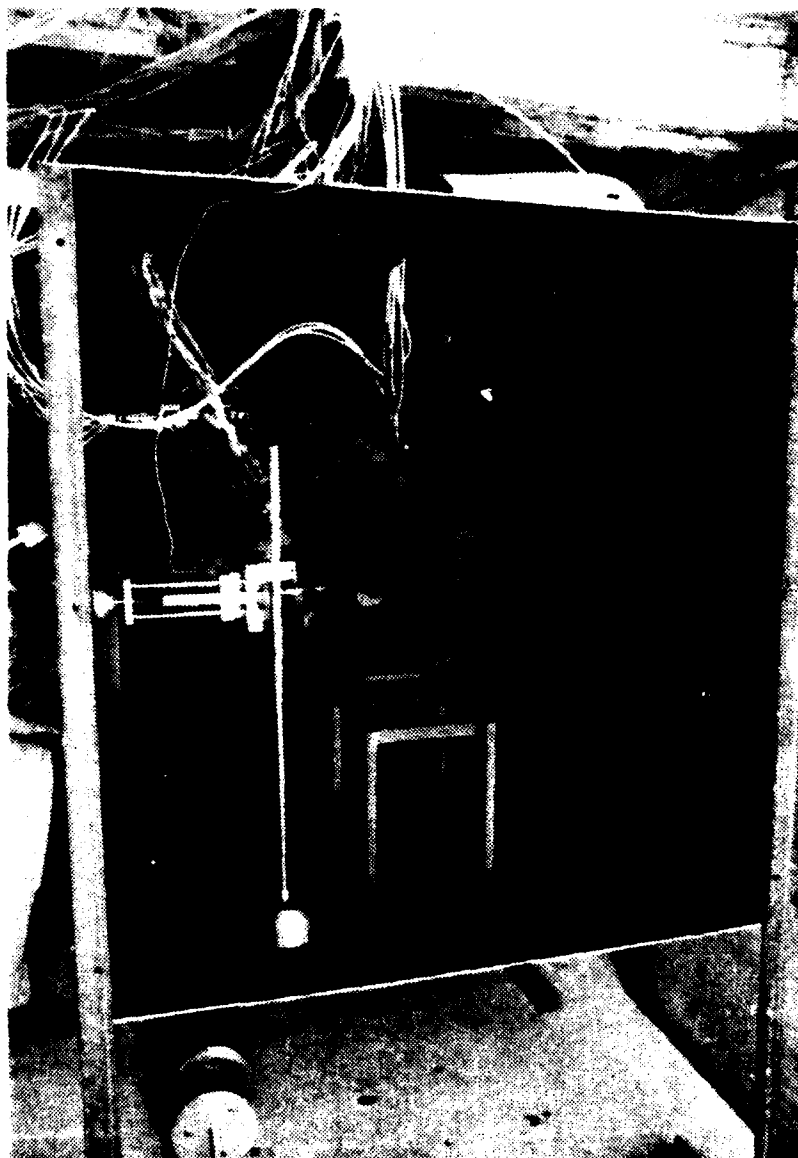


Figure 33. Exit Plane Temperature Measurement.

AD-A 139 953

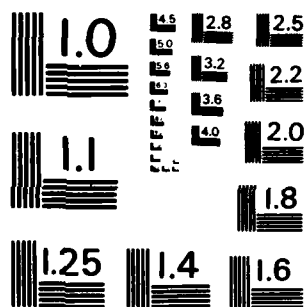
OPERATIONAL PERFORMANCE CHARACTERISTICS OF A
MULTIPLY-SHROUDED ANGLED-DIF. (U) NAVAL POSTGRADUATE
SCHOOL MONTEREY CA R E STAPLES SEP 83

2/3

UNCLASSIFIED

F/G 21/5

NL



MICROCOPY RESOLUTION TEST CHART
NATIONAL BUREAU OF STANDARDS-1963-A

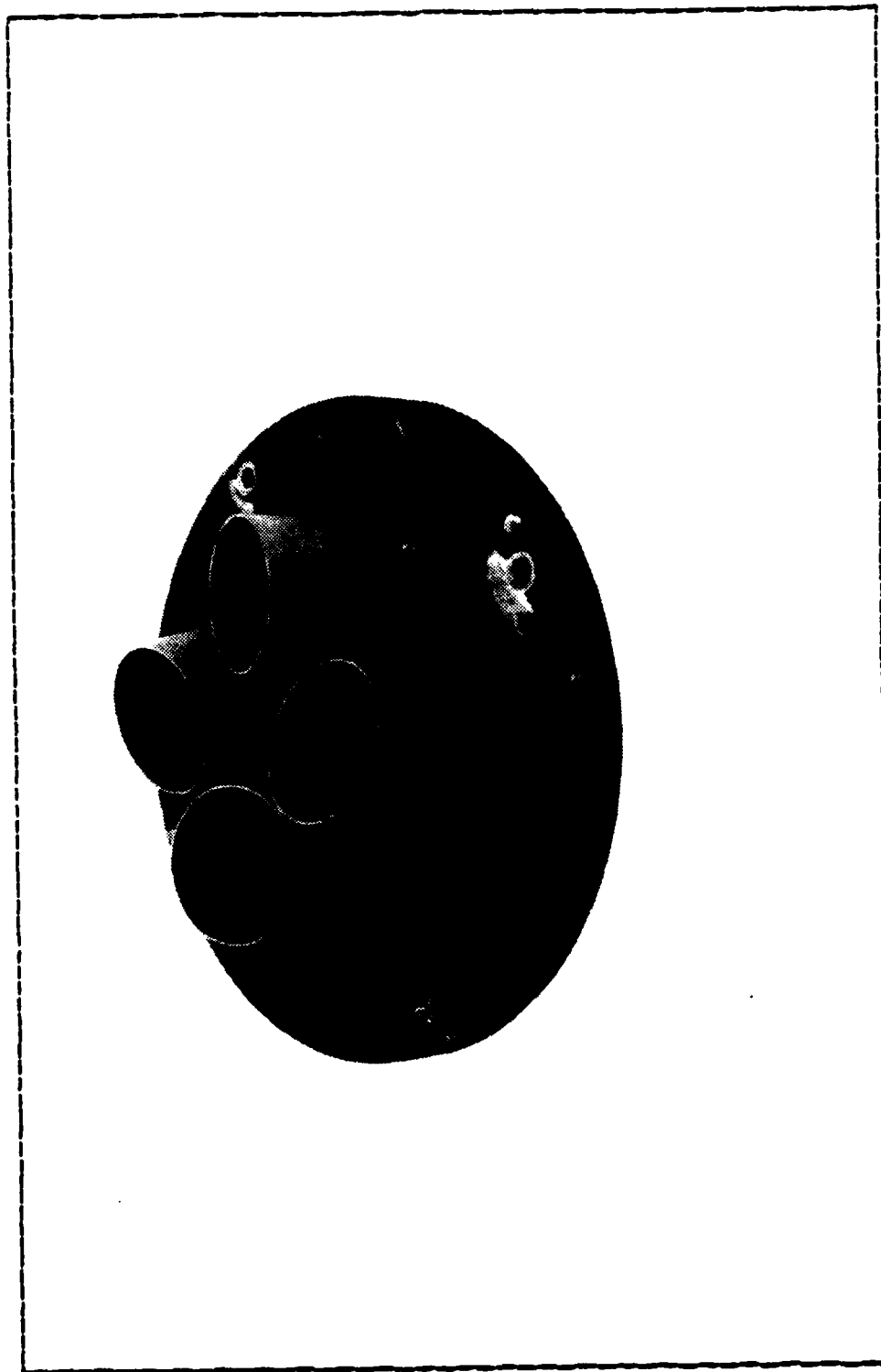


Figure 34. Tilted-Angled Nozzle Plate.

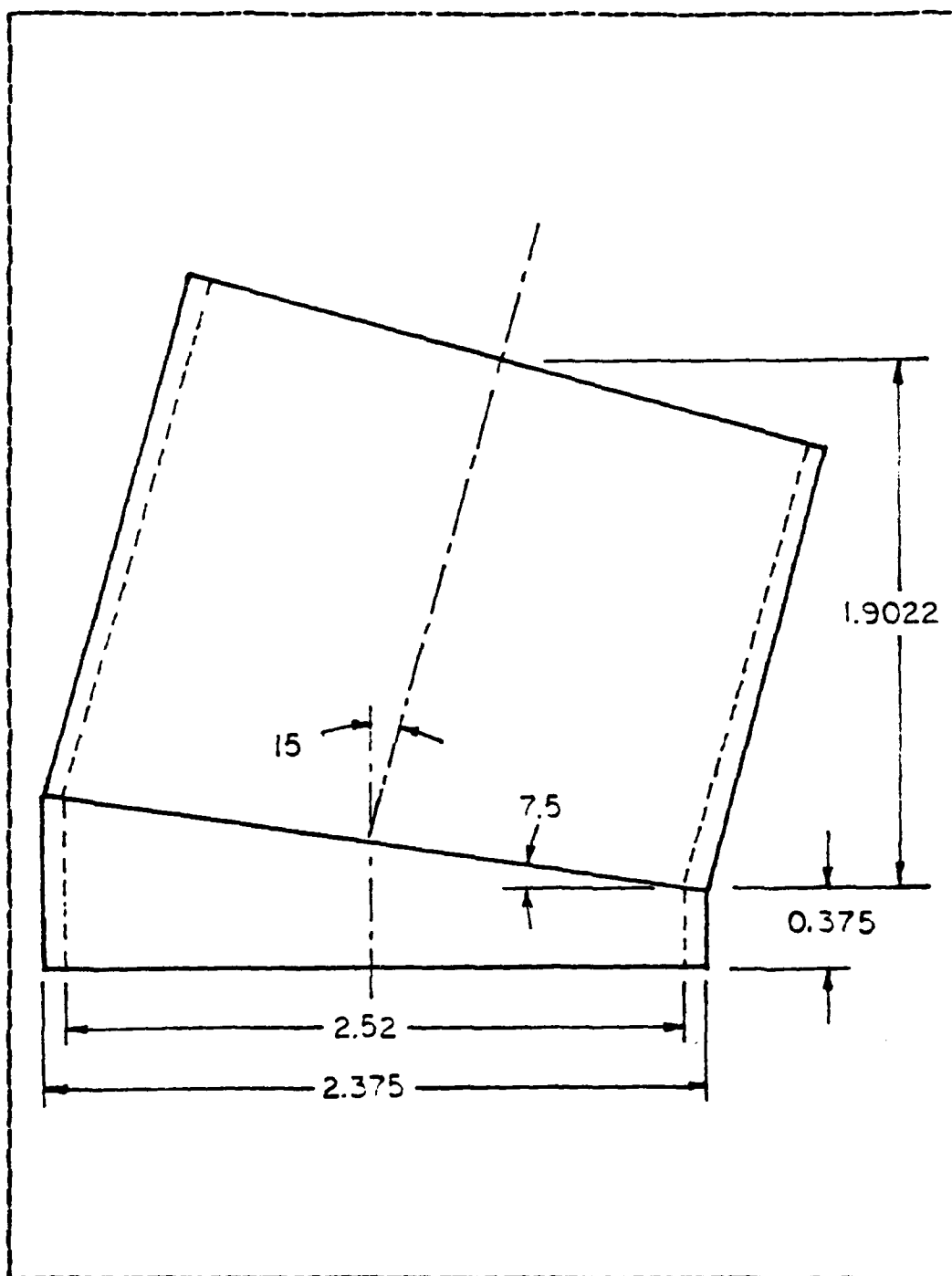


Figure 35. Tilted Nozzle Geometry.

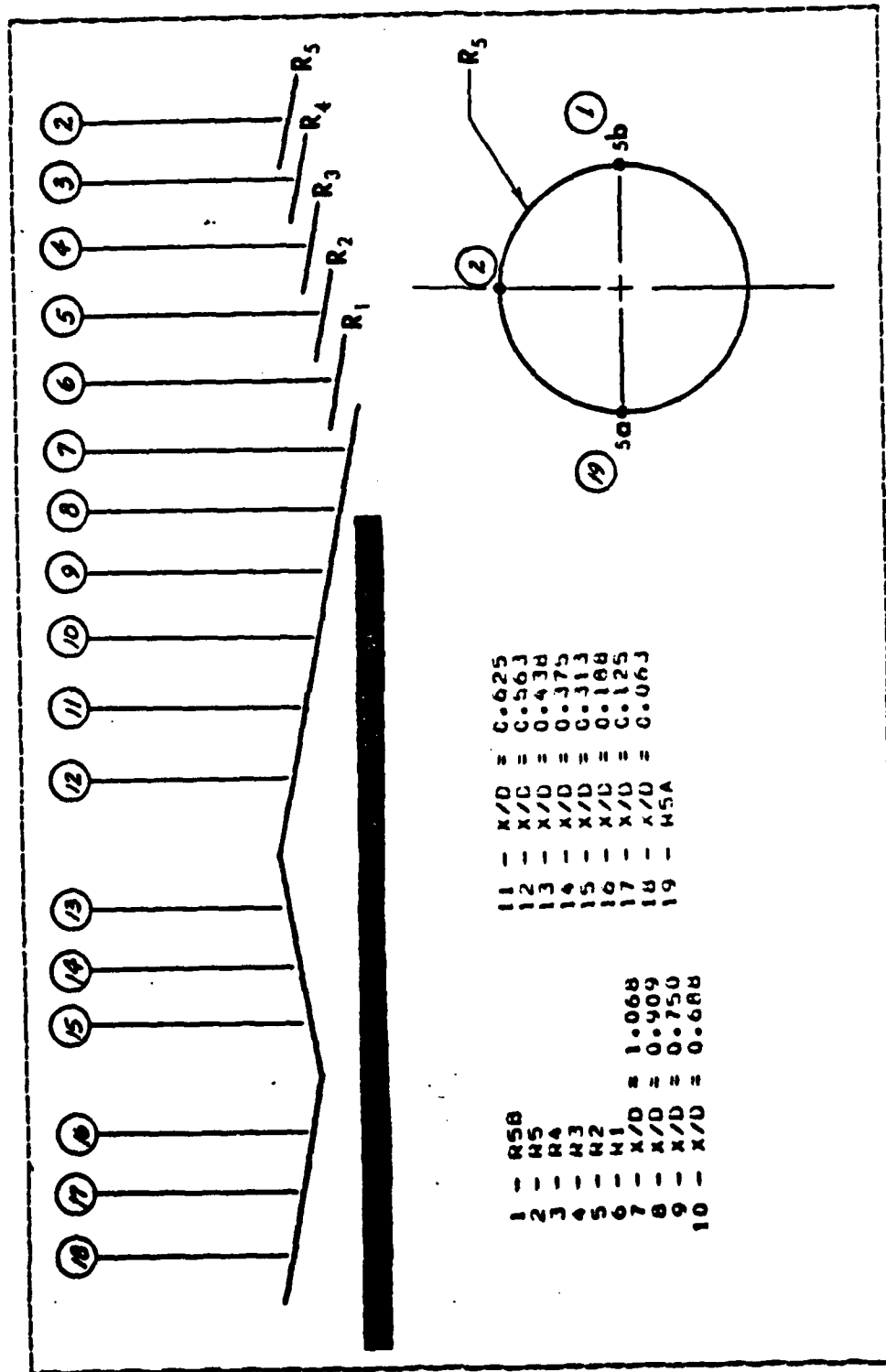


Figure 36. External Temperature Measurement Points, Model A.

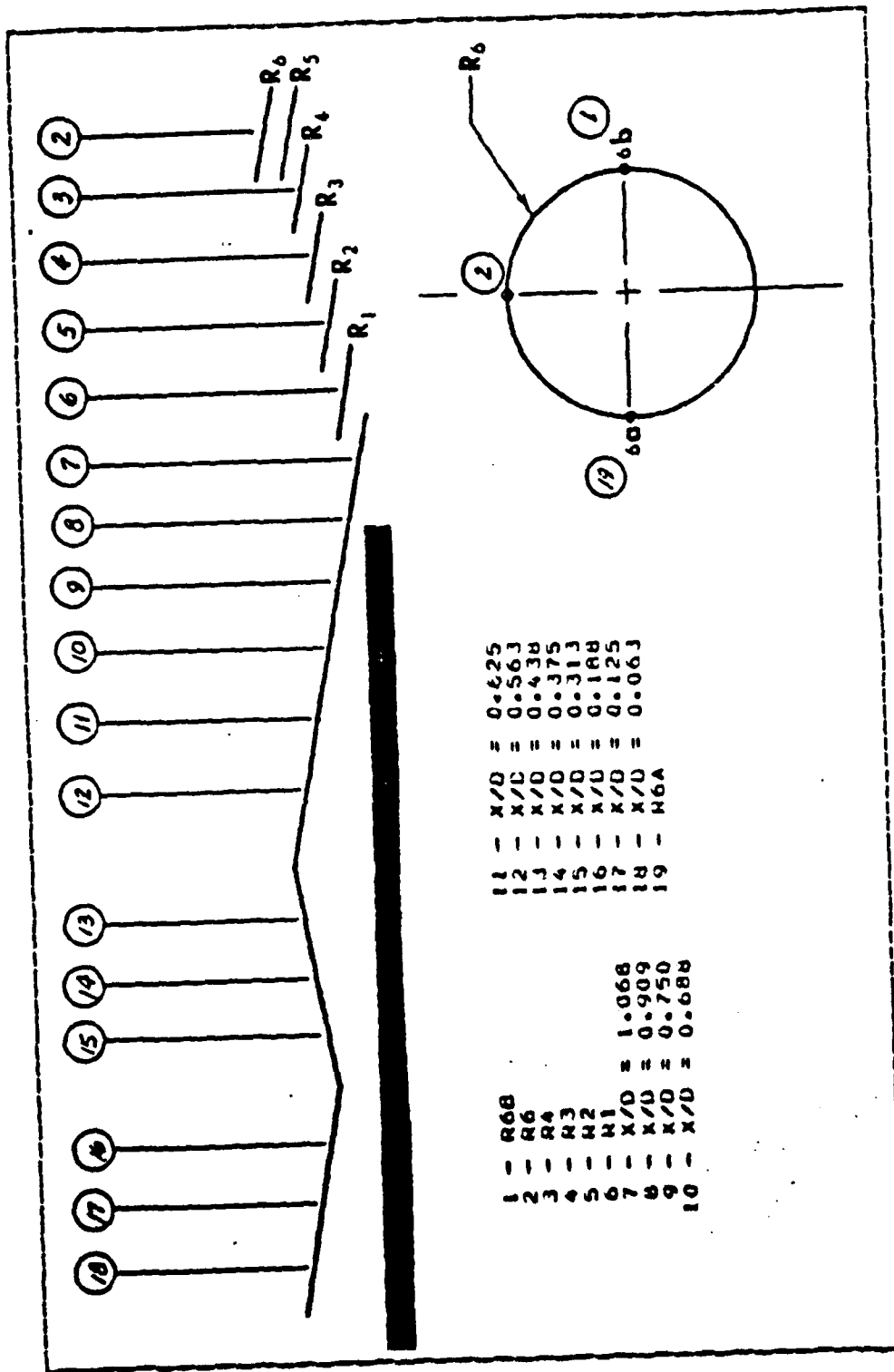


Figure 37. External Temperature Measurement Points, Model A Mod..

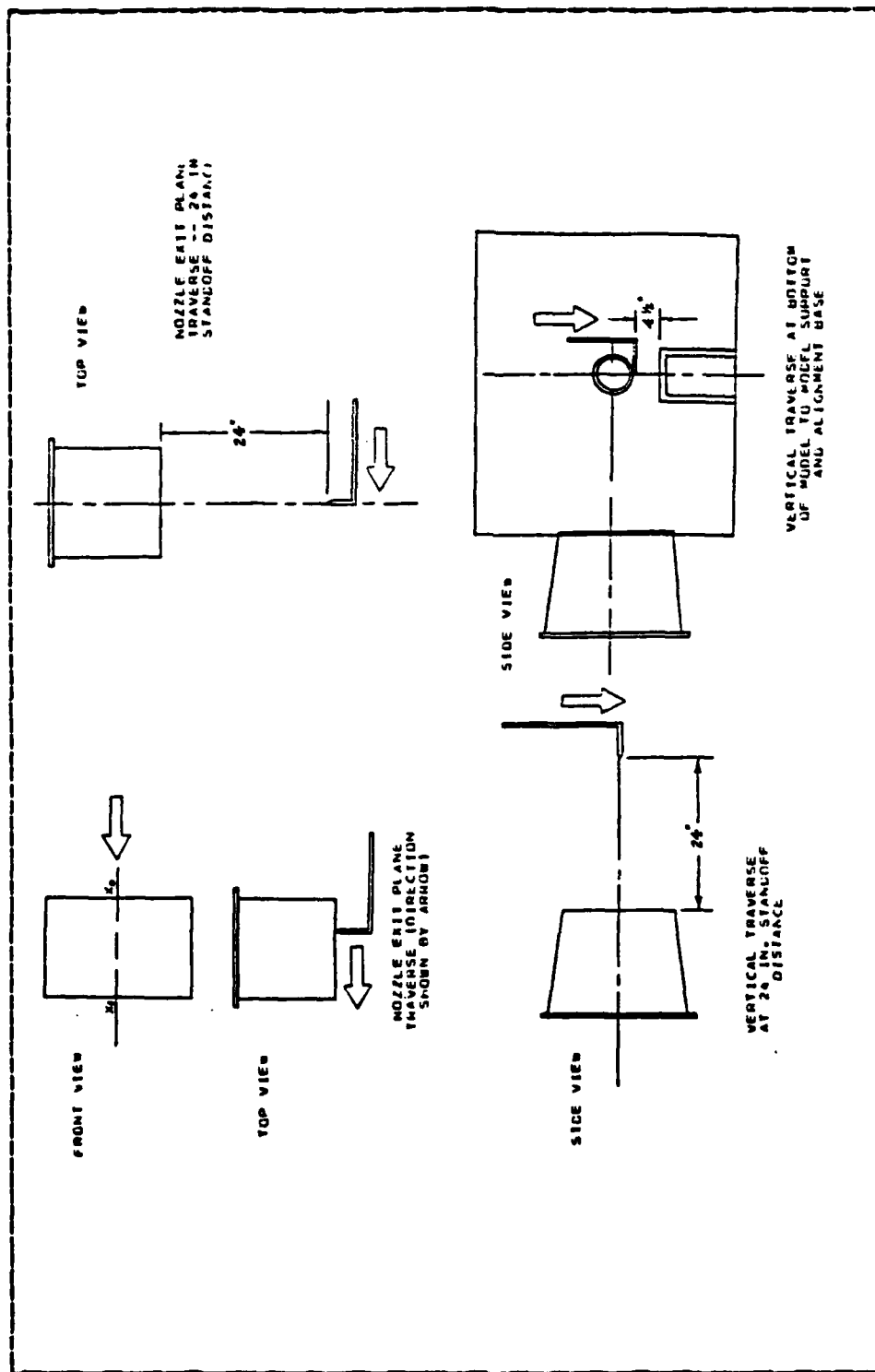
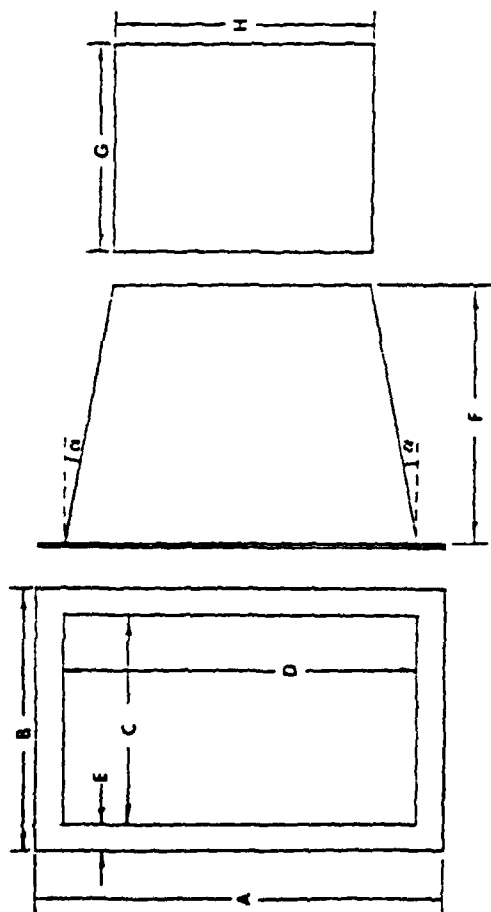


Figure 38. Schematic of Crossflow Pan Pitot Tube Traverses.



A=22.375
B=14.750
C=11.750
D=19.375
E=4.500
F=14.500
G=14.250
H=14.250
I=14.250

ALL DIMENSIONS IN INCHES

Figure 39. Crossflow Fan Nozzle Geometry.

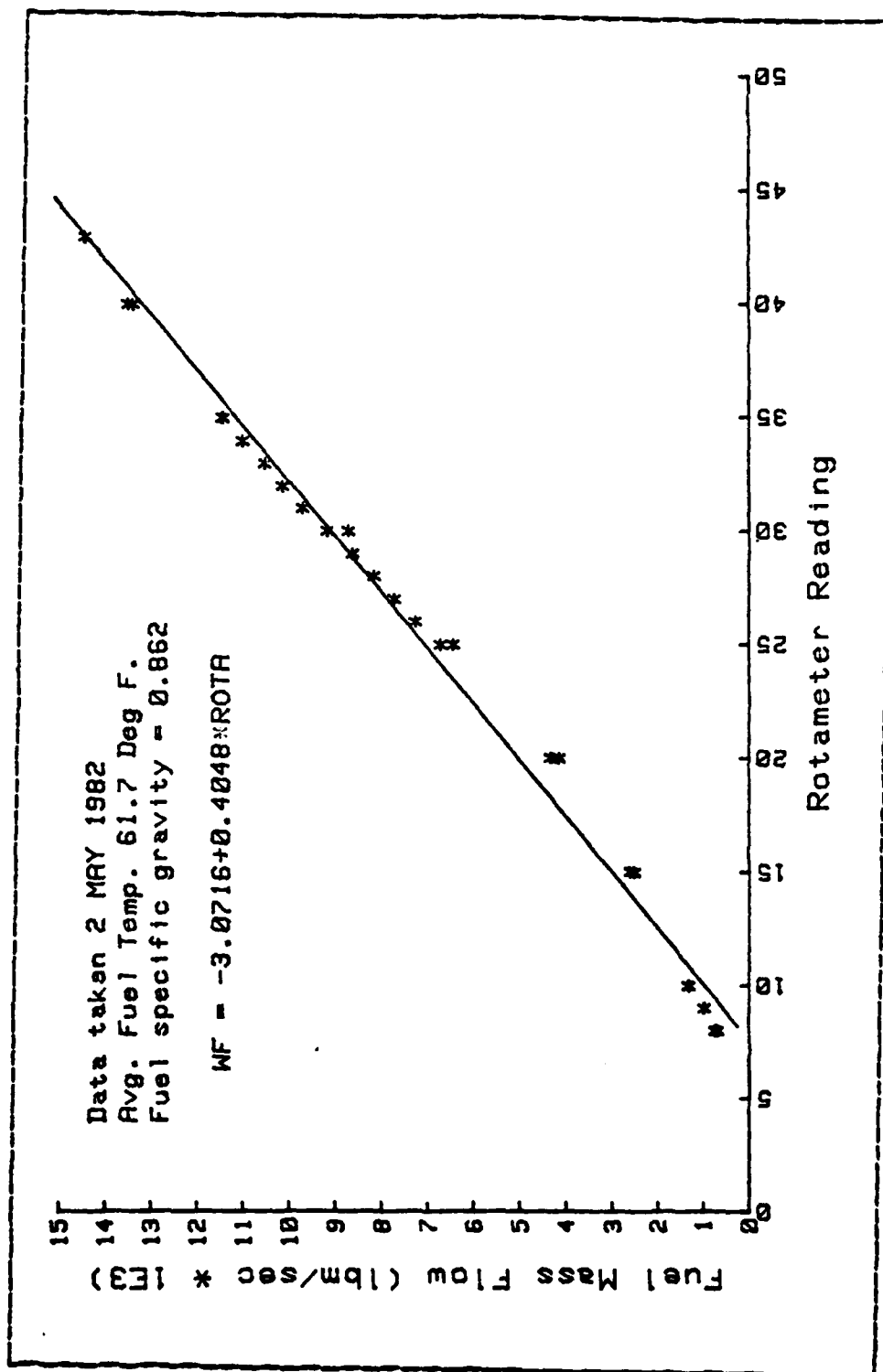


Figure 40. Rotameter Calibration Curve.

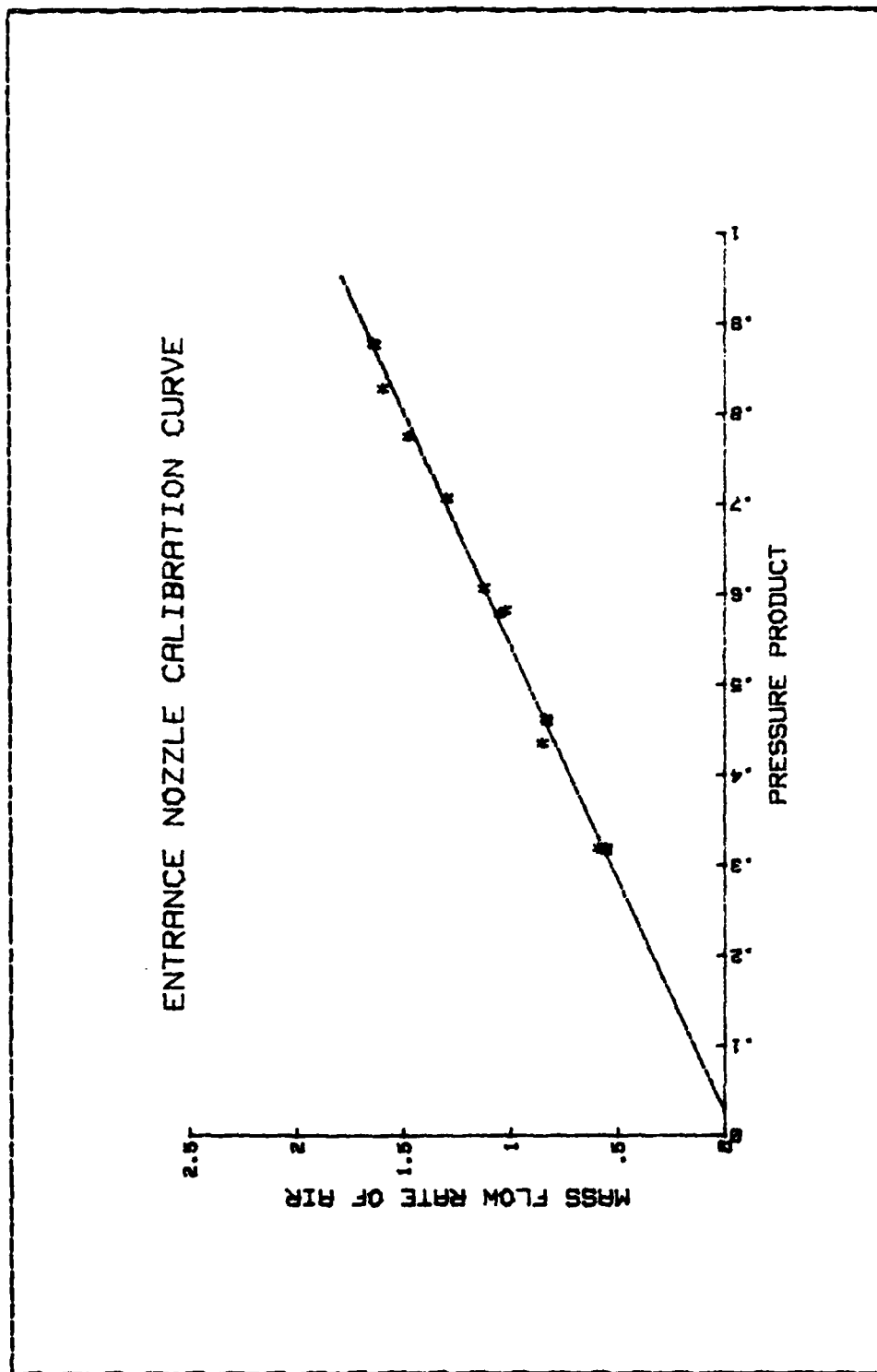


Figure 41. Air Mass Flow Rate Calibration Curve.

EXPERIMENTAL PUMPING COEFFICIENT COMPARISON

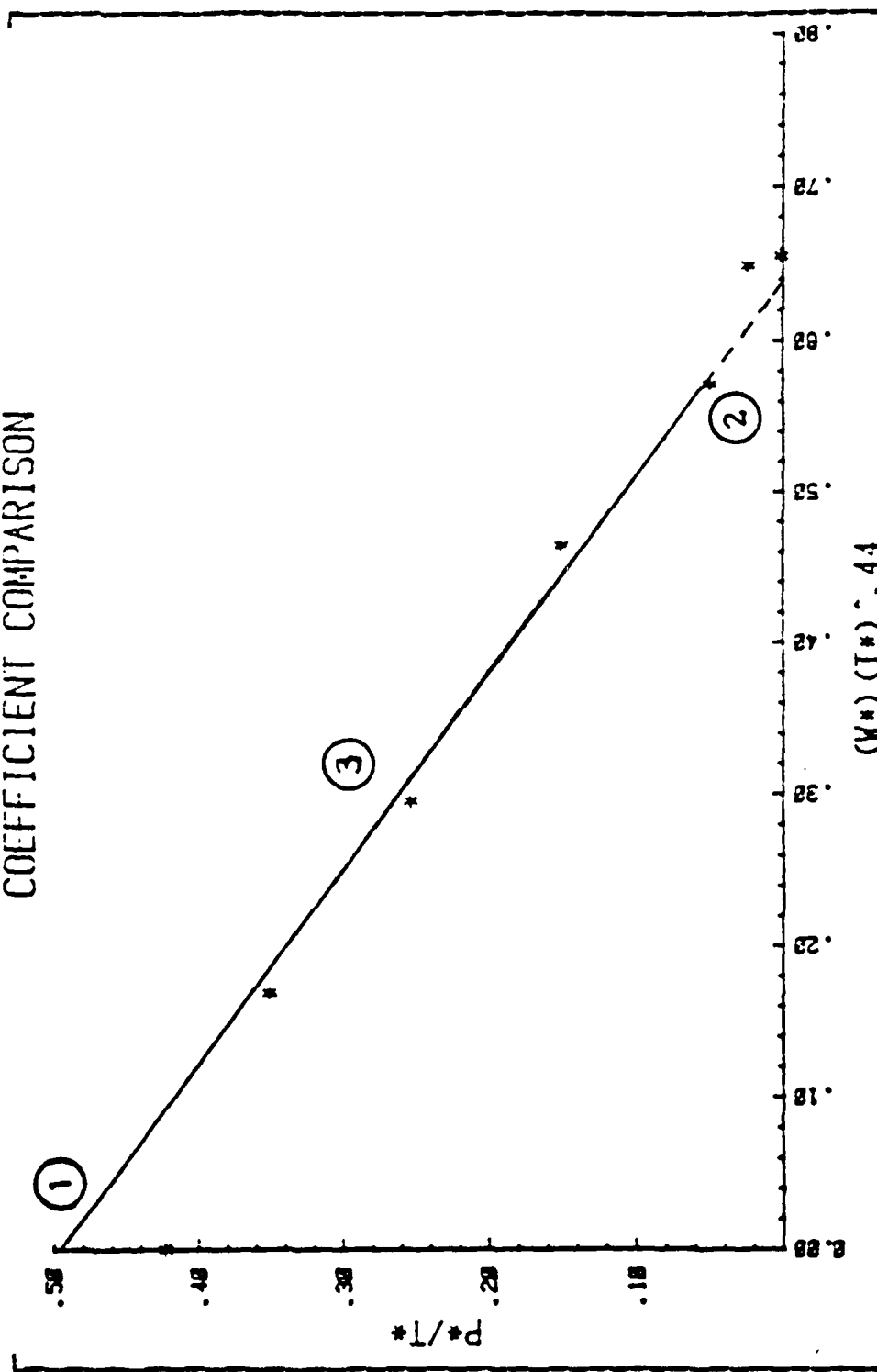


Figure #2. Sample Pumping Coefficient Plot.

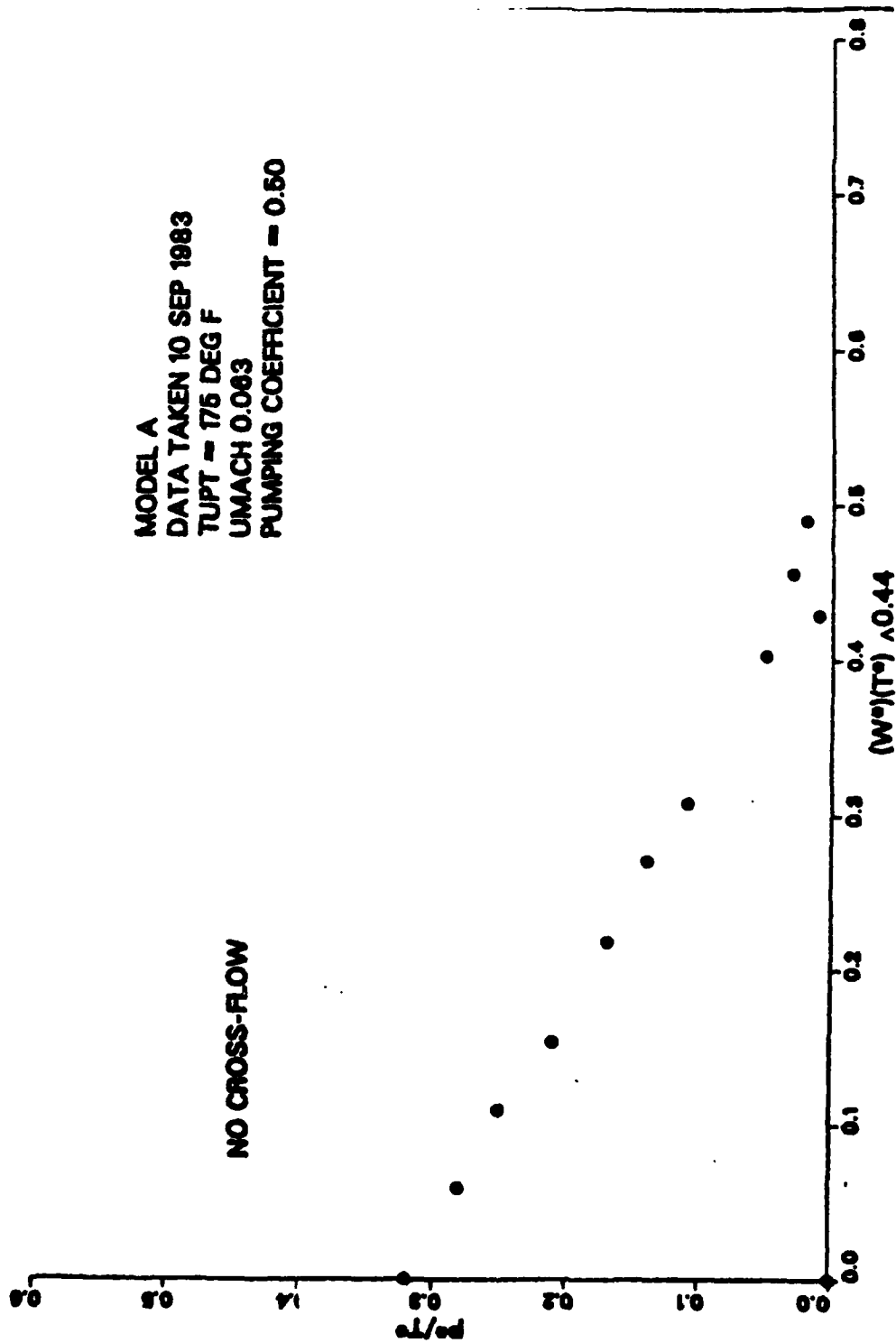


Figure 43. Pumping Coefficient, Model A (175 F) - No Crossflow.

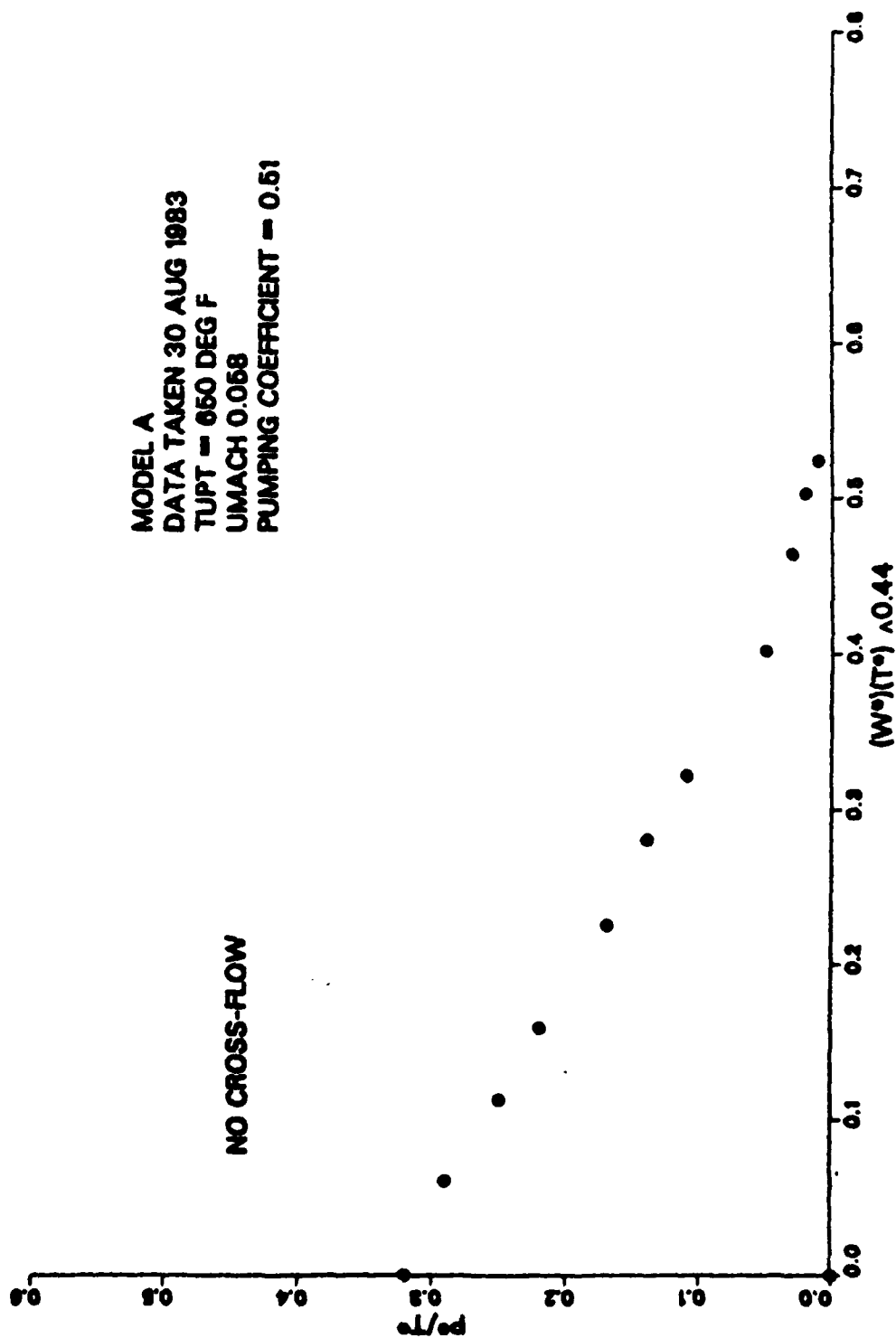


Figure 44. Pumping Coefficient, Model A (650 F) - No Crossflow.

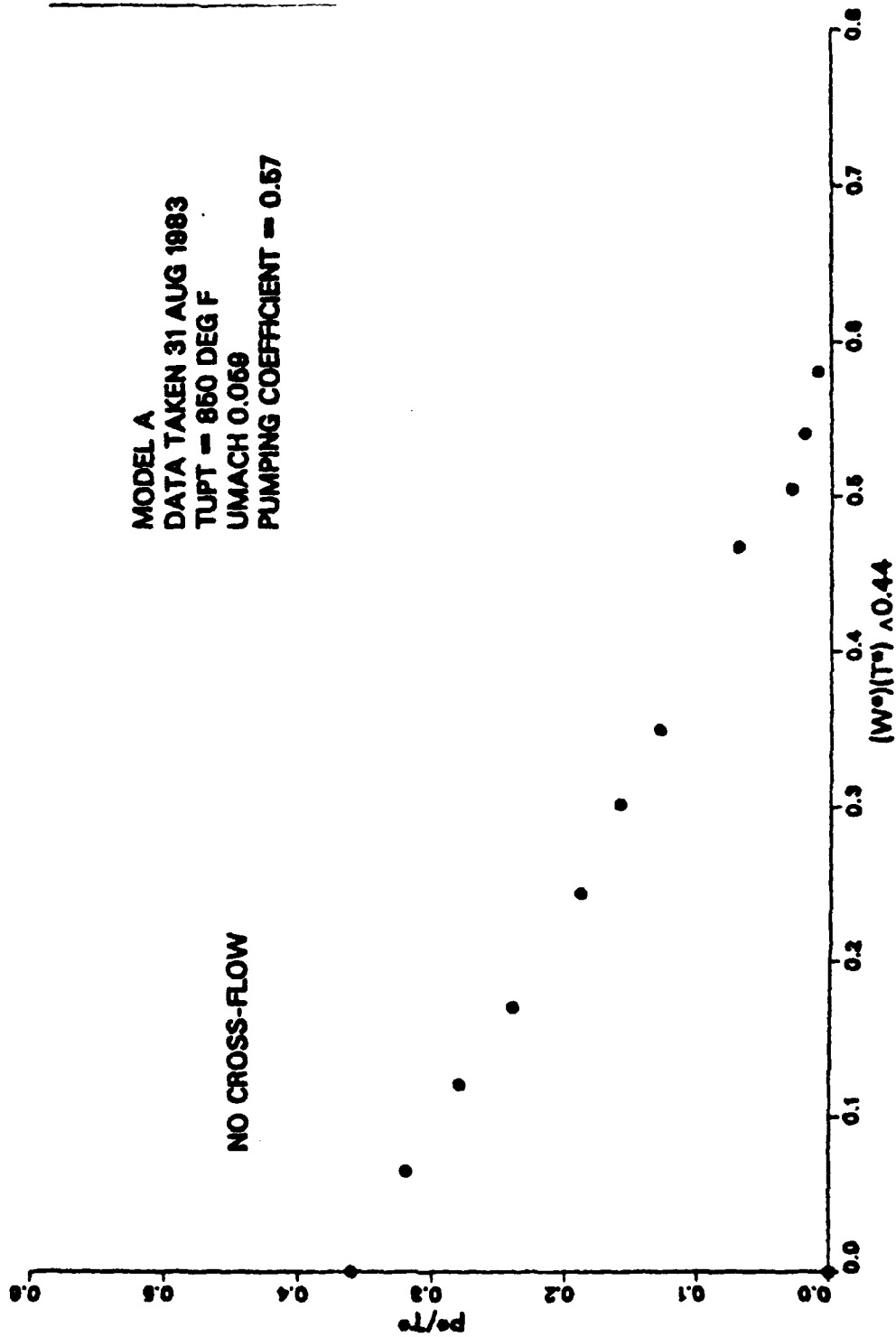


Figure 45. Pumping Coefficient, Model A (850 F) - No Crossflow.

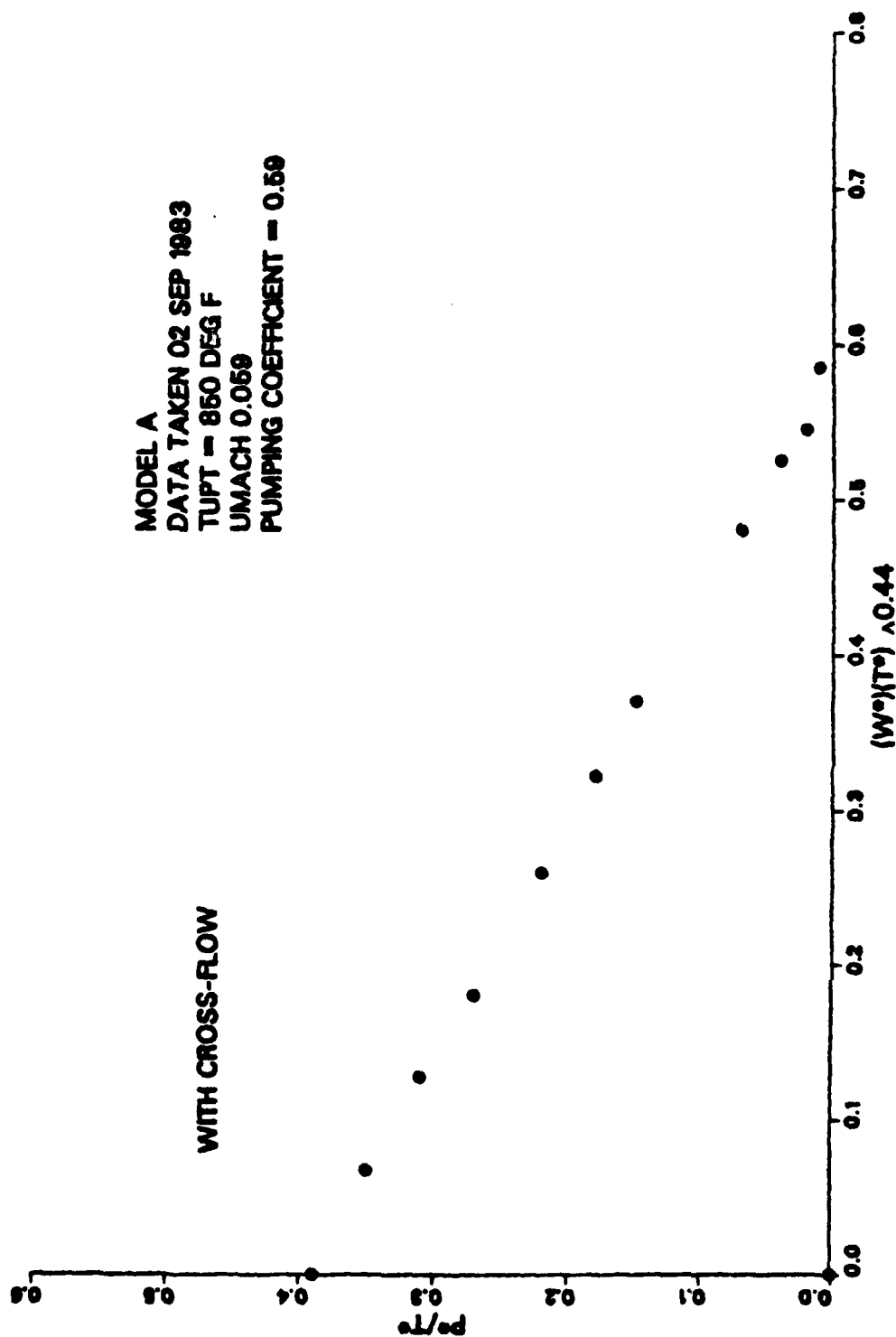


Figure 46. Pumping Coefficient, Model A (850 F) - Crossflow.

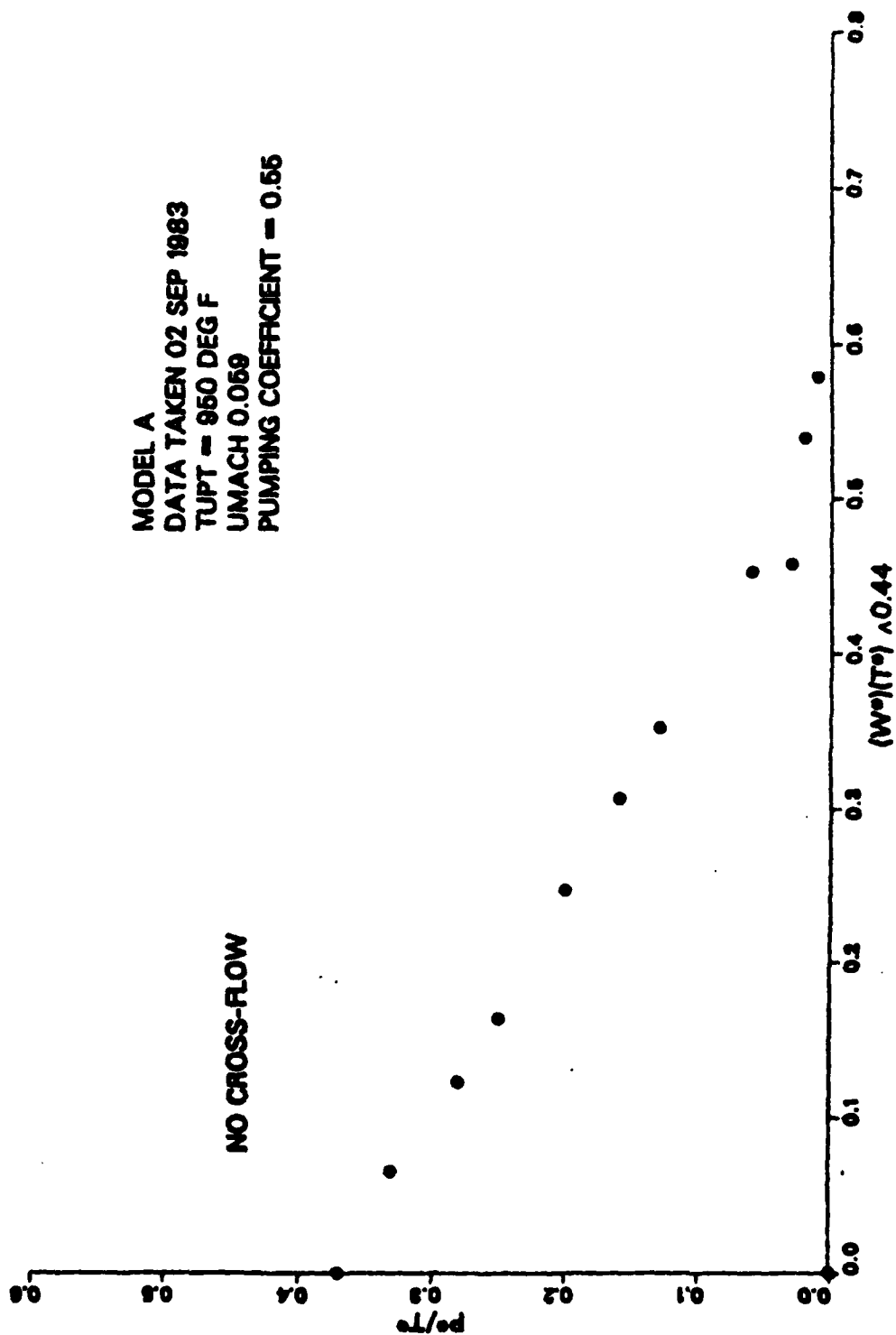


Figure 47. Pumping Coefficient, Model A (950 F) - No Crossflow.

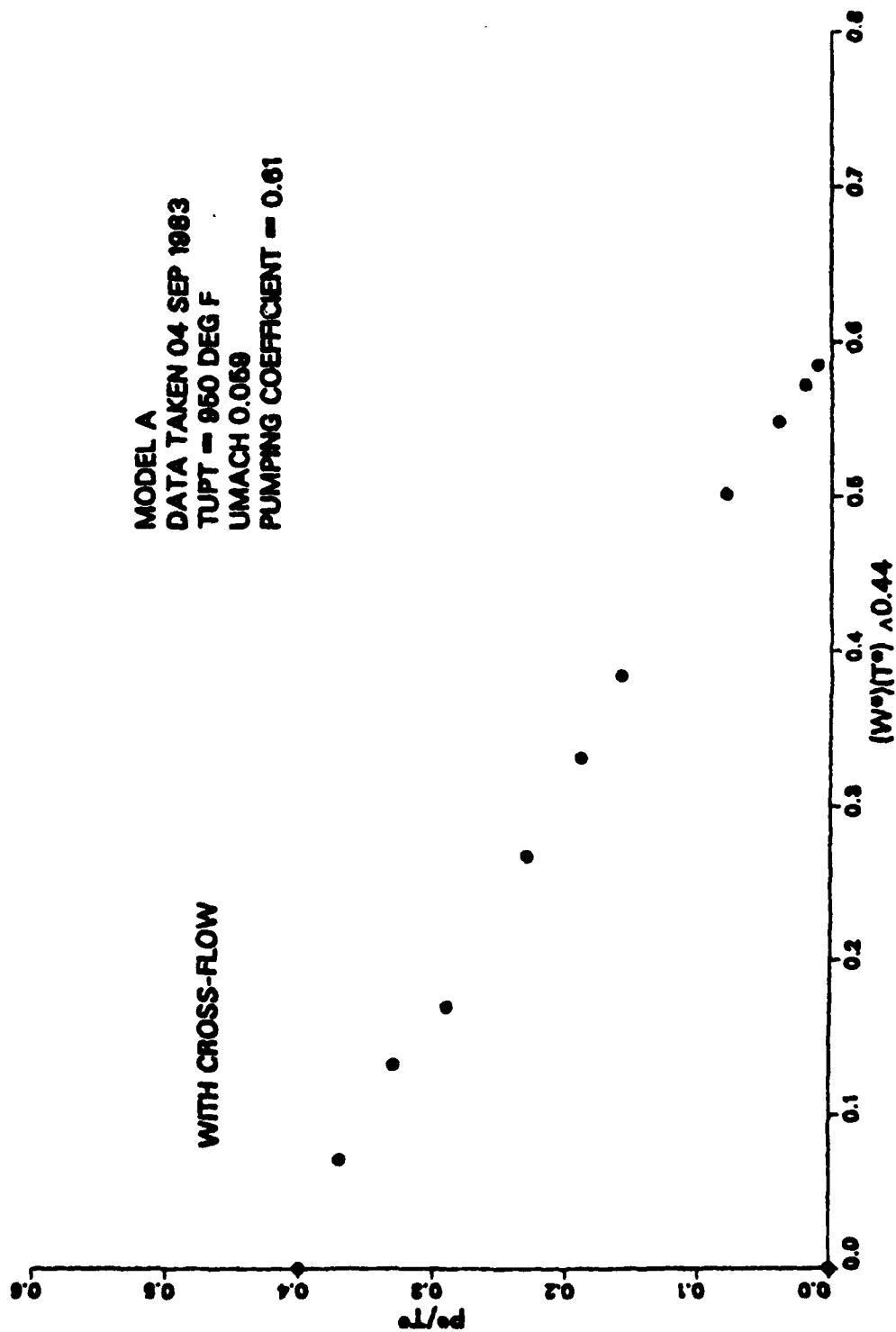


Figure #8. Pumping Coefficient, Model A (950 F) - Crossflow.

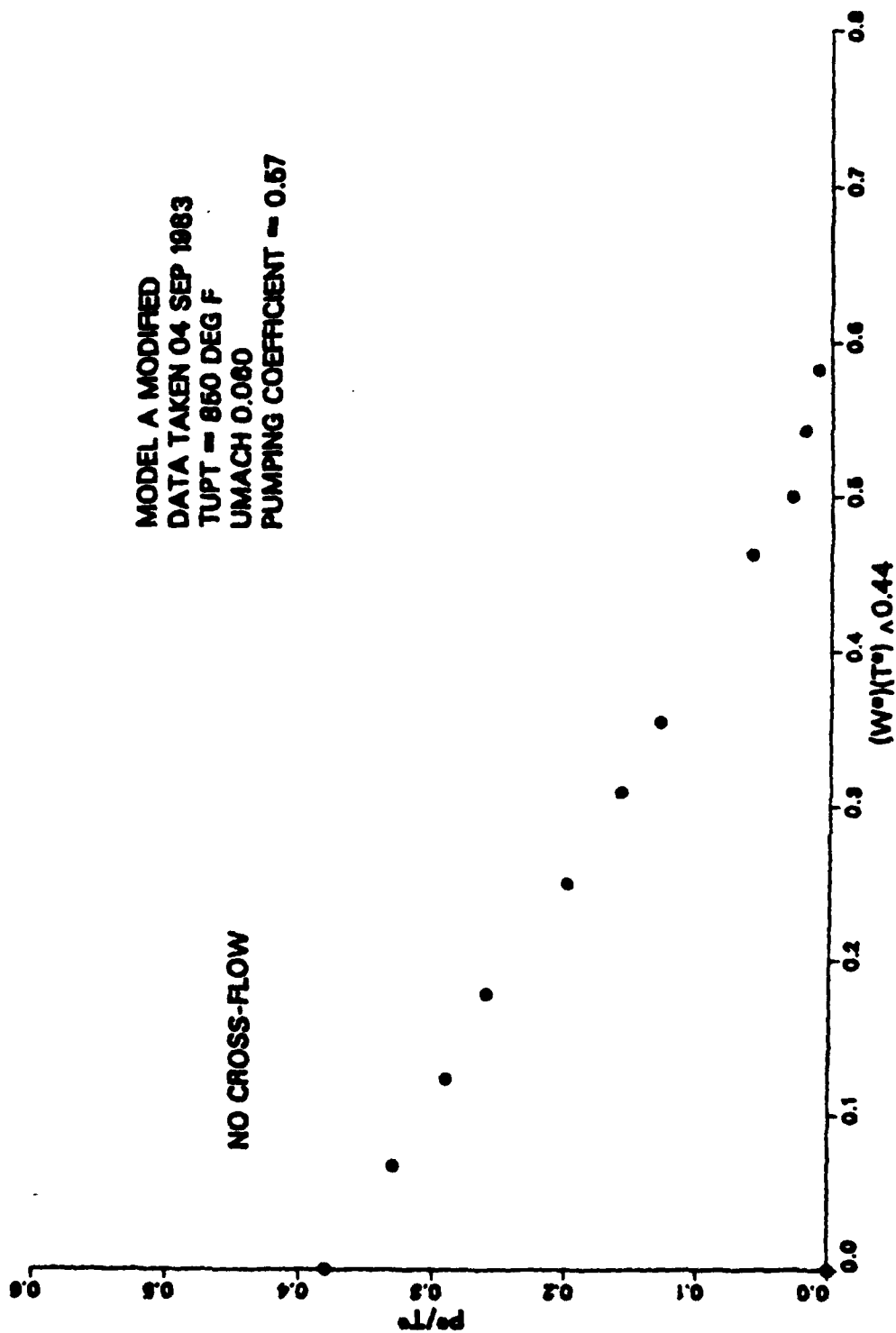


Figure 49. Pumping Coefficient, Model A Mod (850 F) - No Crossflow.

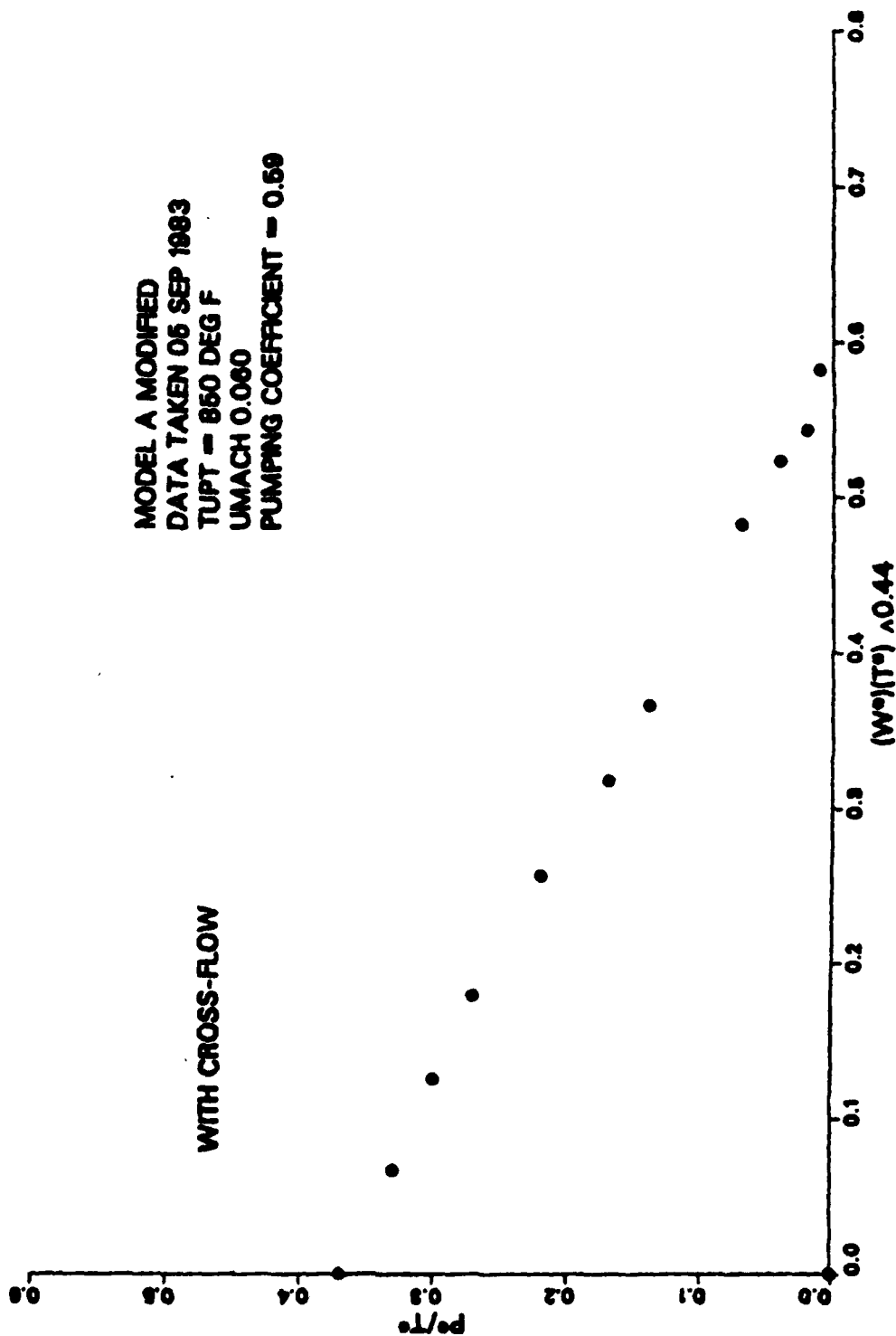


Figure 50. Pumping Coefficient, Model A Mod (850 F) - Crossflow.

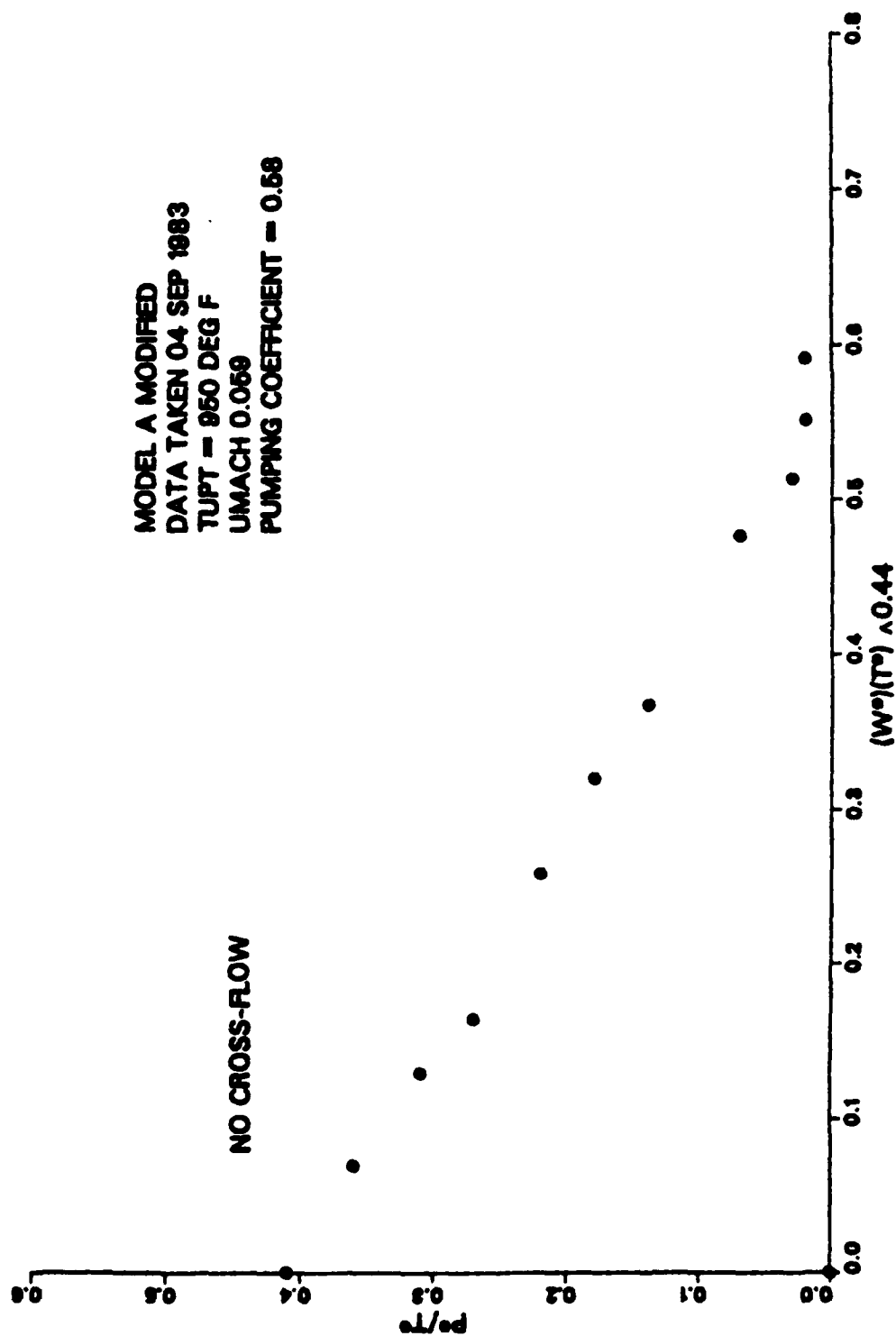


Figure 51. Pumping Coefficient, Model A Mod (950 F) - No Crossflow.

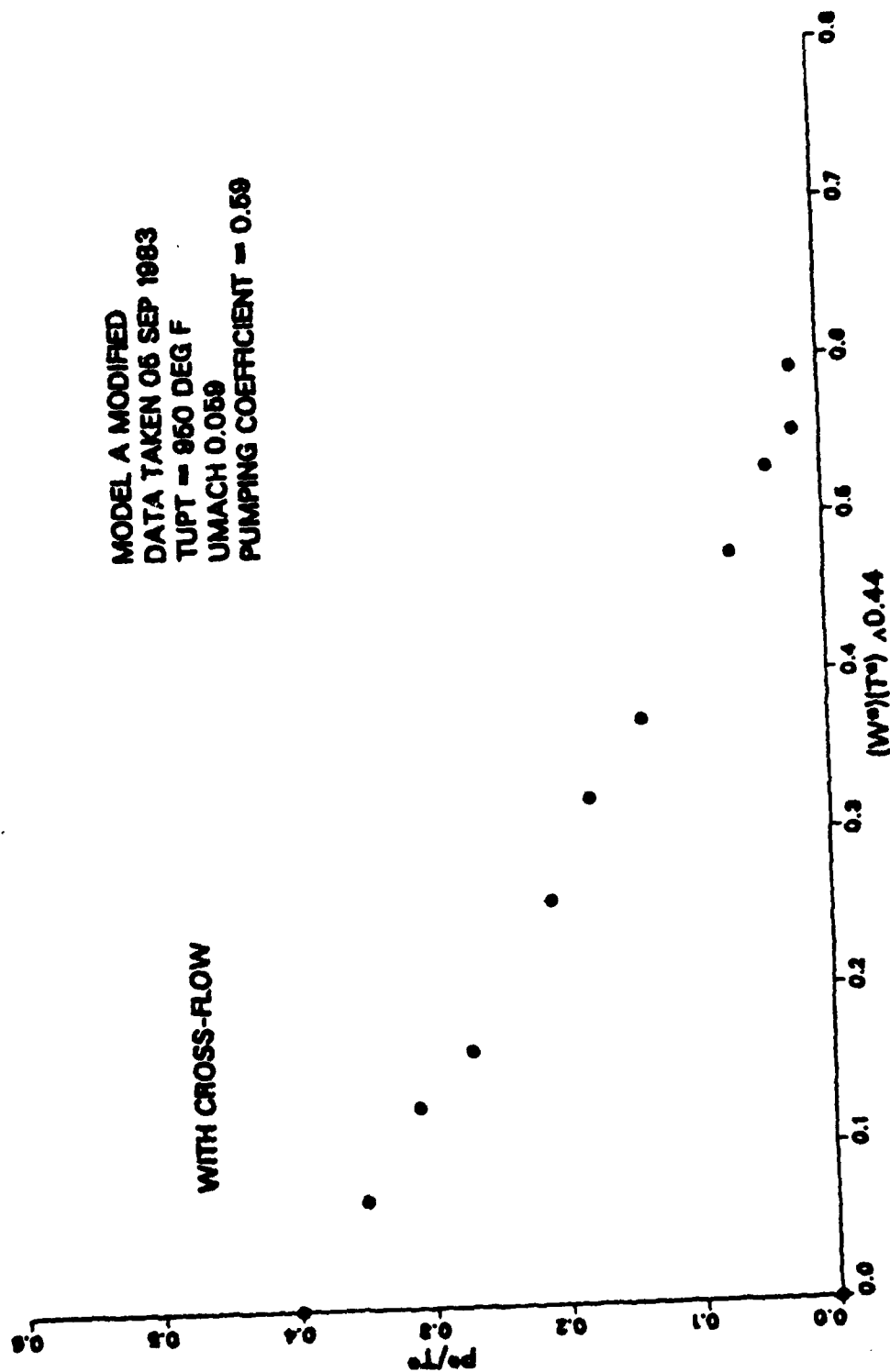


Figure 52. Pumping Coefficient, Model A Mod (950 F) - Crossflow.

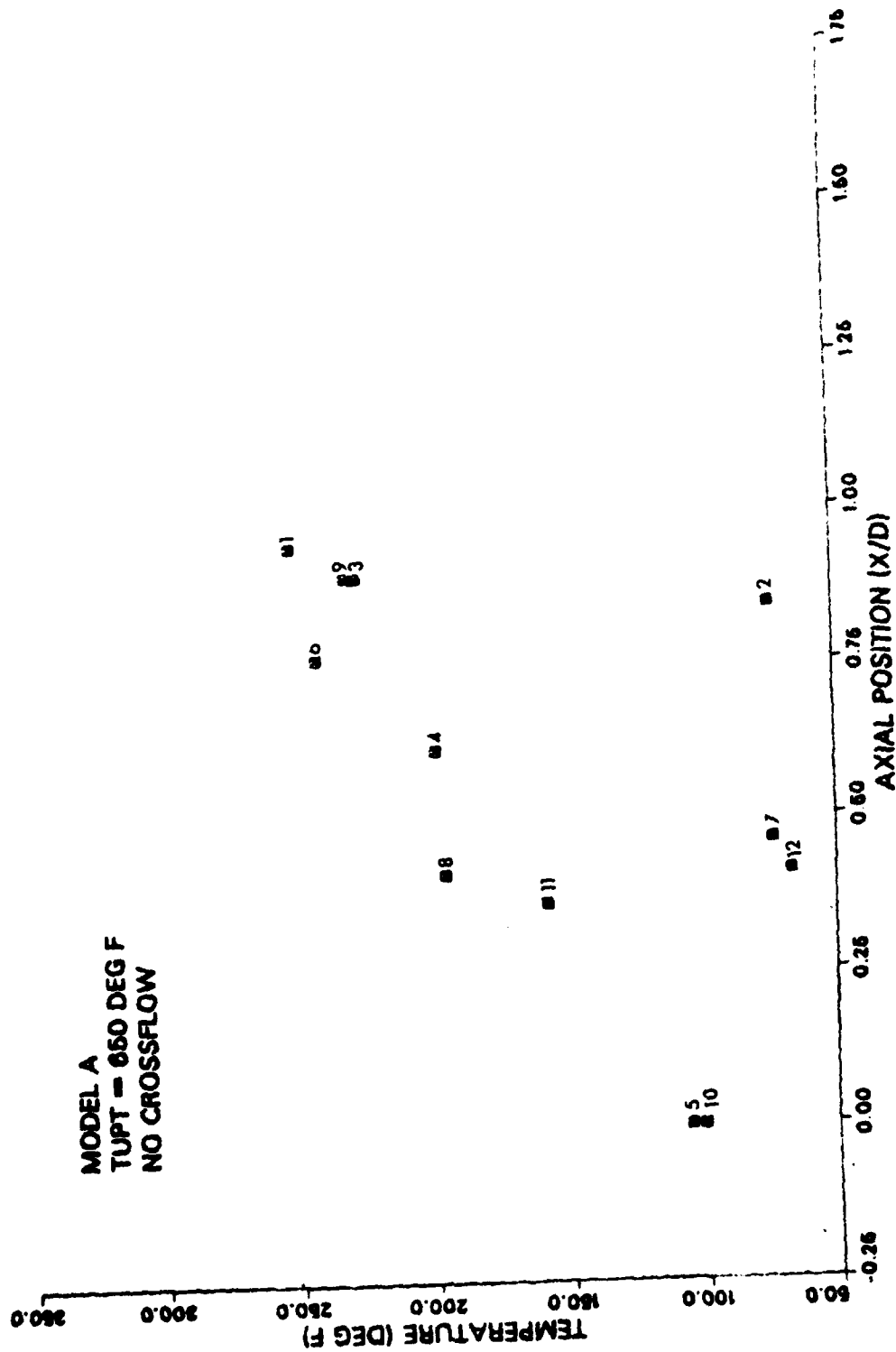


Figure 53. Mixing Stack Temp., Model A (650 F) - No Crossflow.

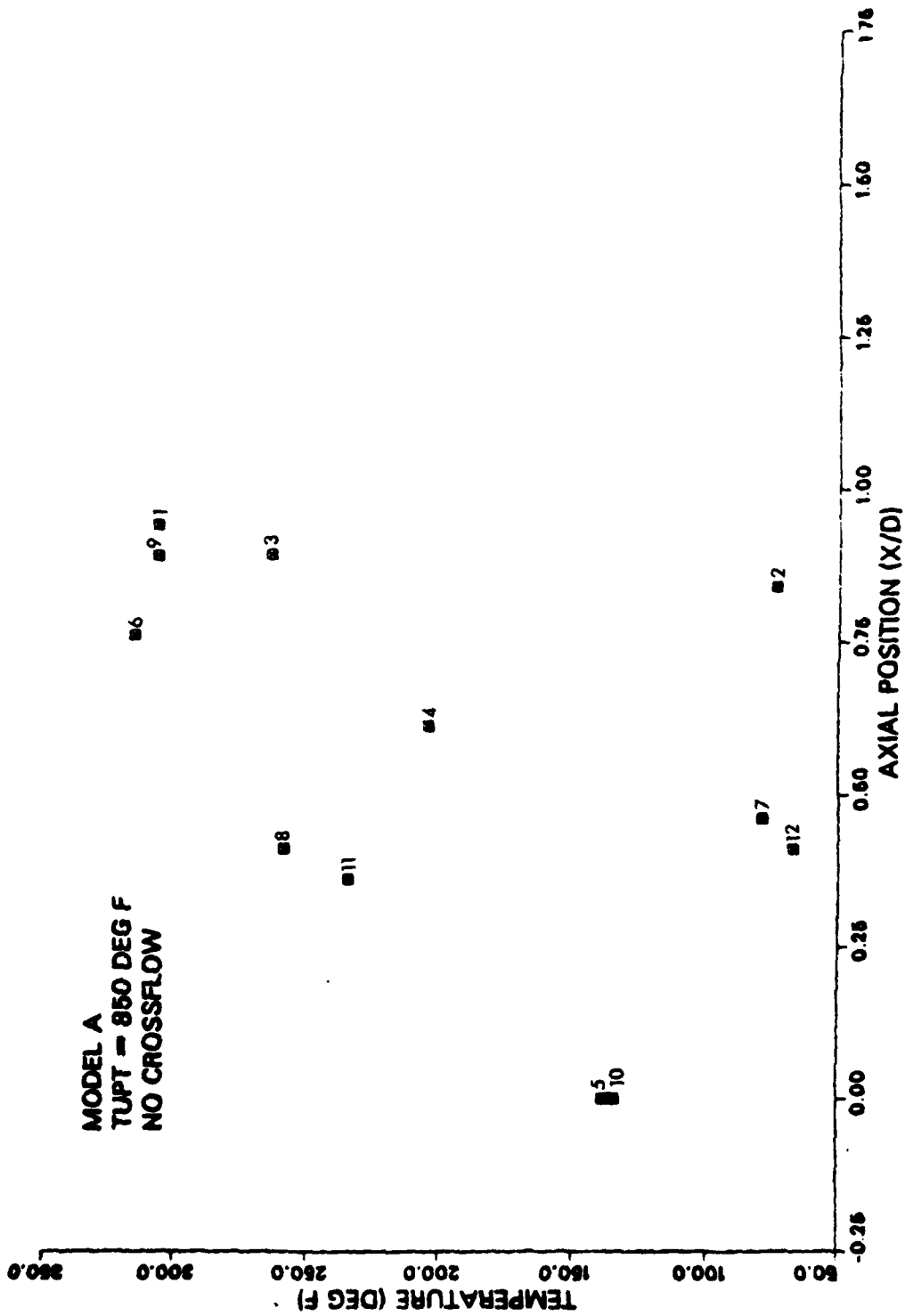


Figure 54. Mixing Stack Temp., Model A (850F) - No crossflow.

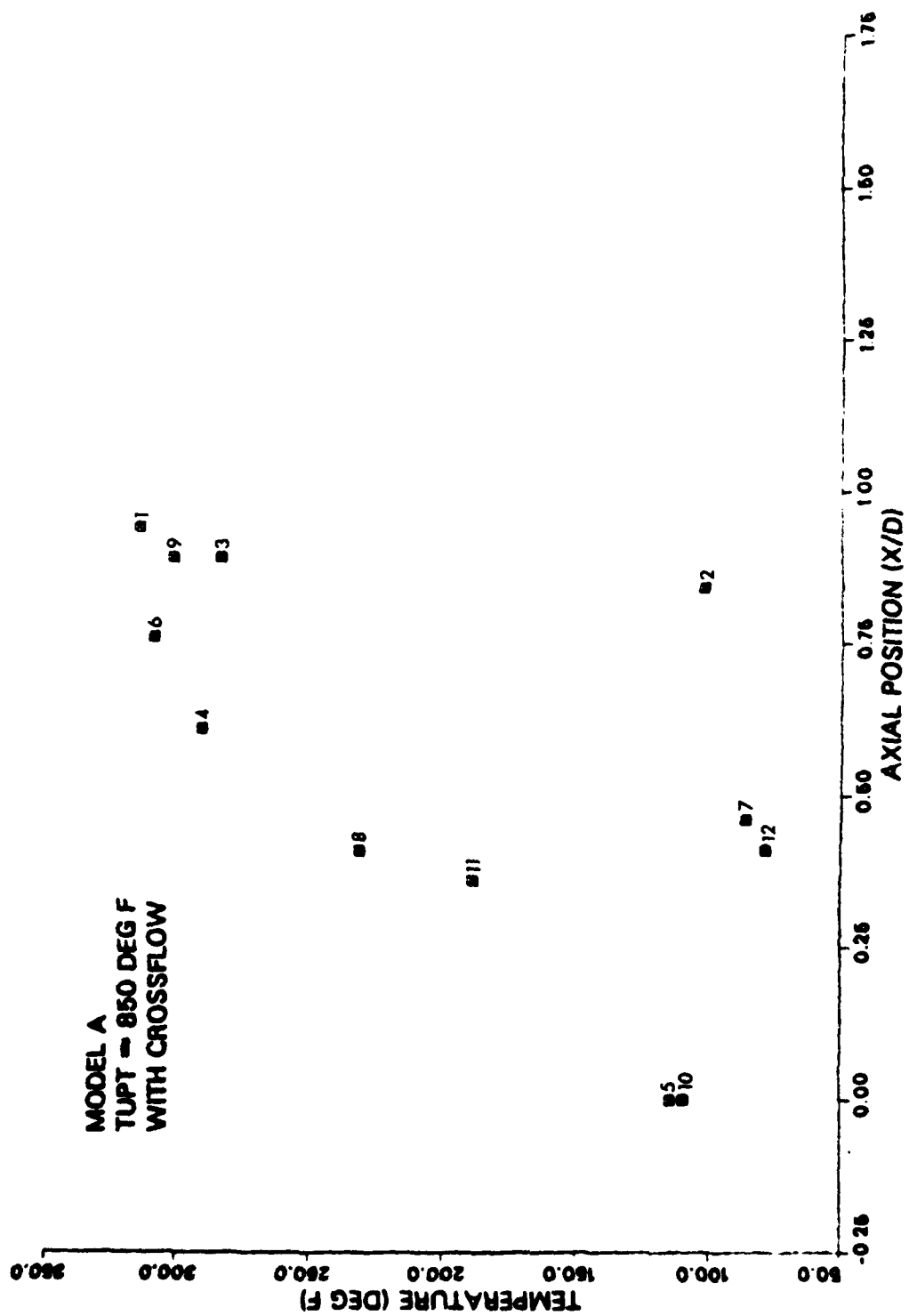


Figure 55. Mixing Stack Temp., Model A (850 F) - Crossflow.

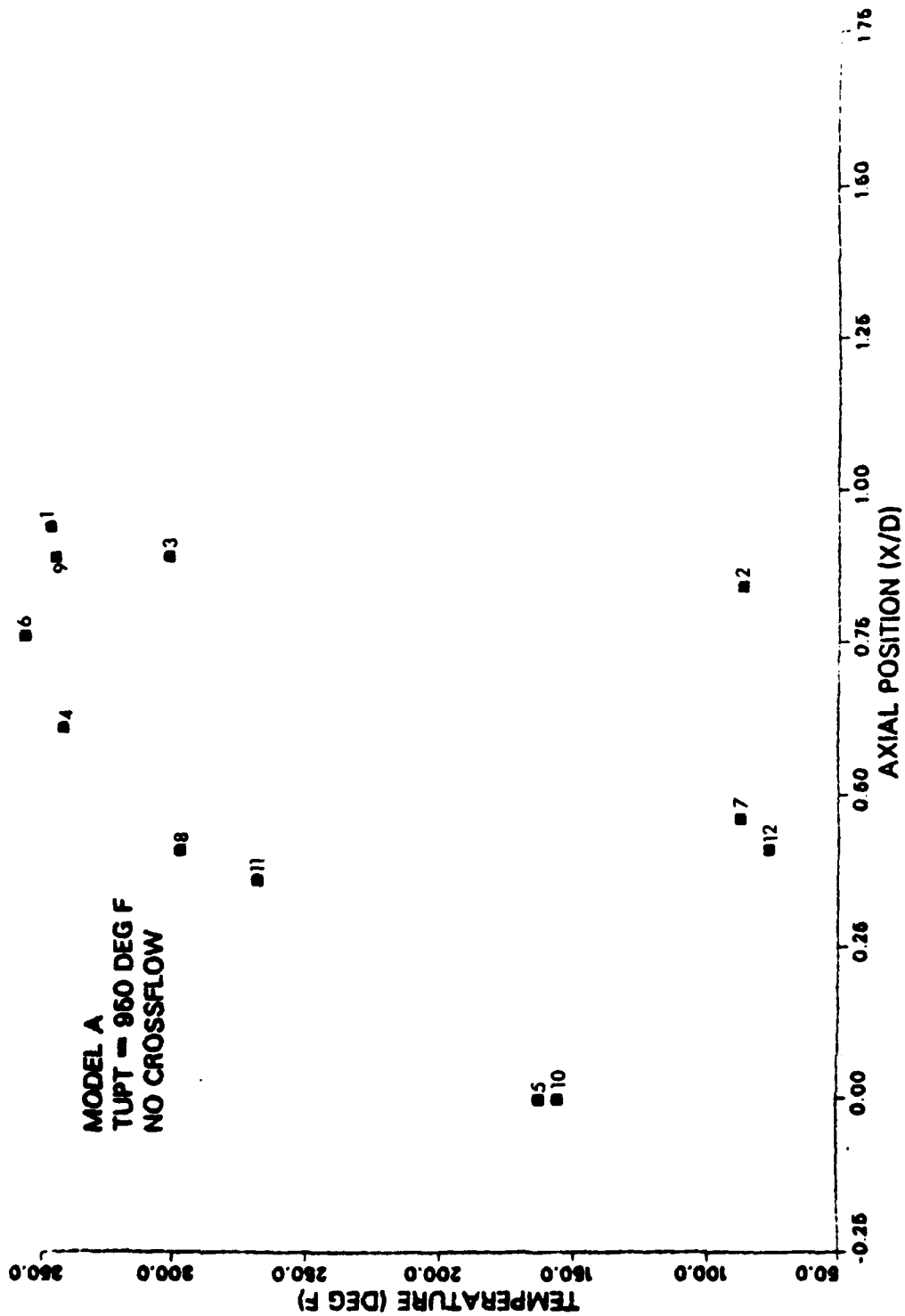


Figure 56. Mixing Stack Temp., Model A (950 F) - No Crossflow.

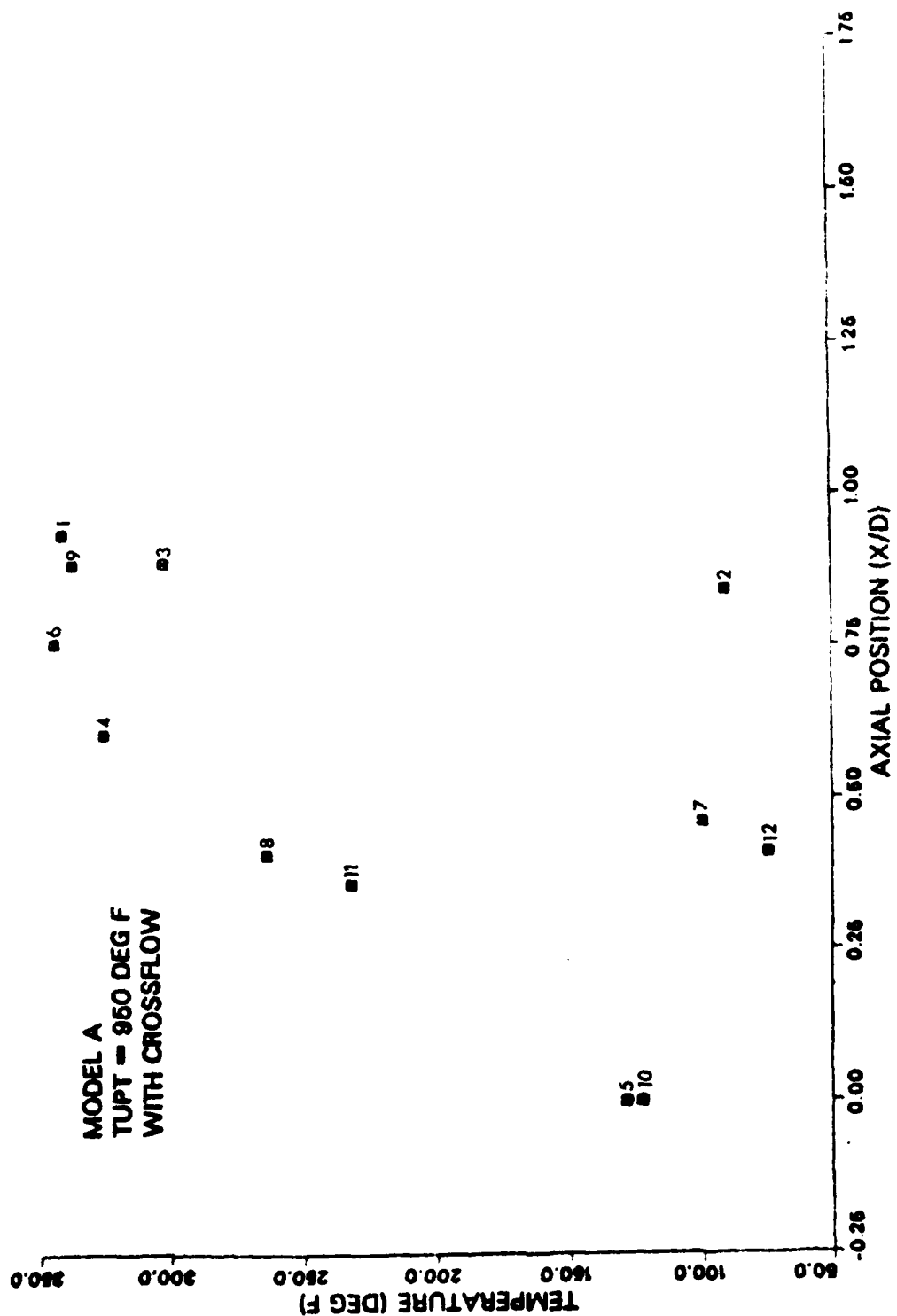


Figure 57. Mixing Stack Temp., Model A (950 F) - Crossflow.

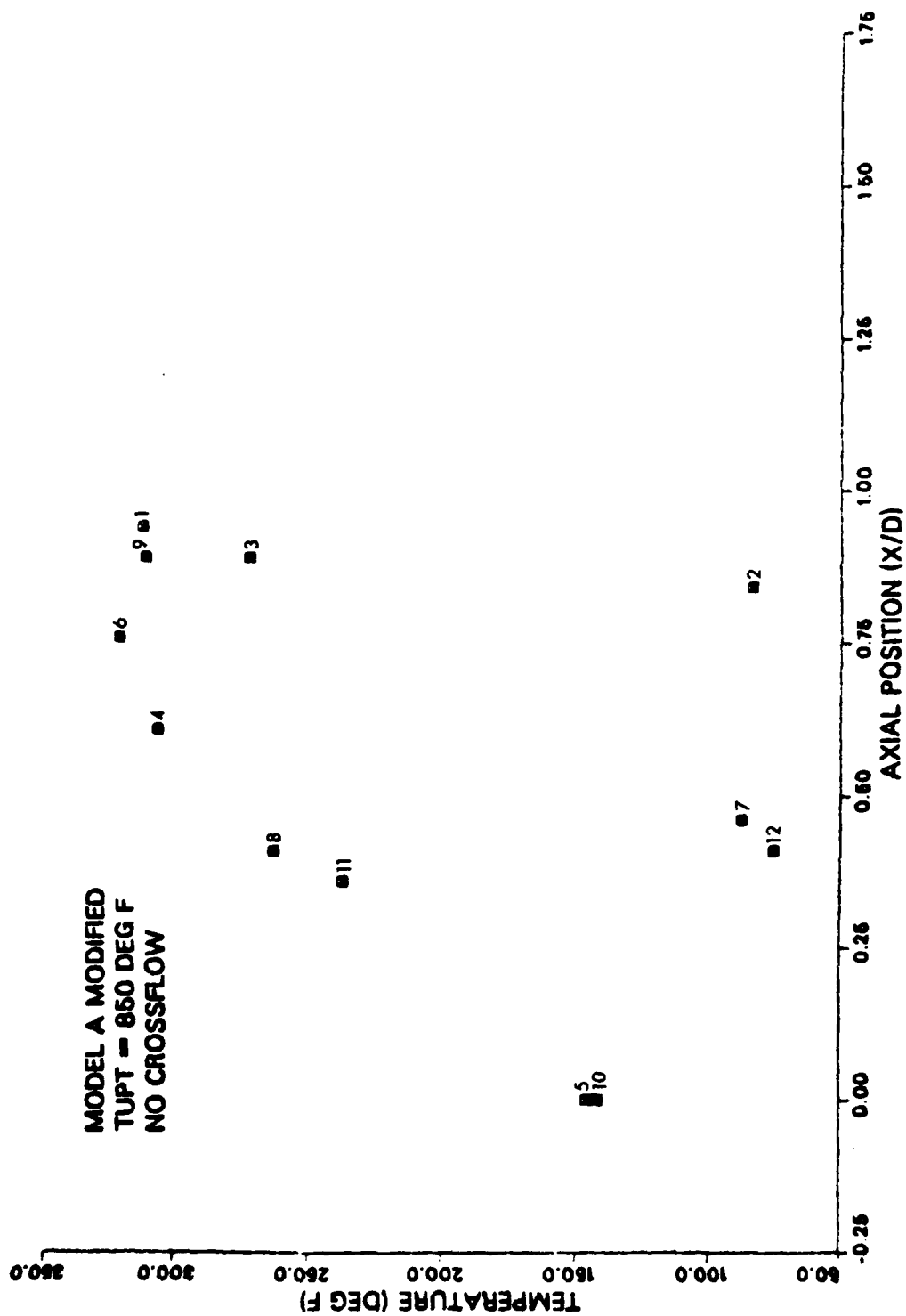


Figure 58. Mixing Stack Temp., Model A Mod (850 F) - No Crossflow.

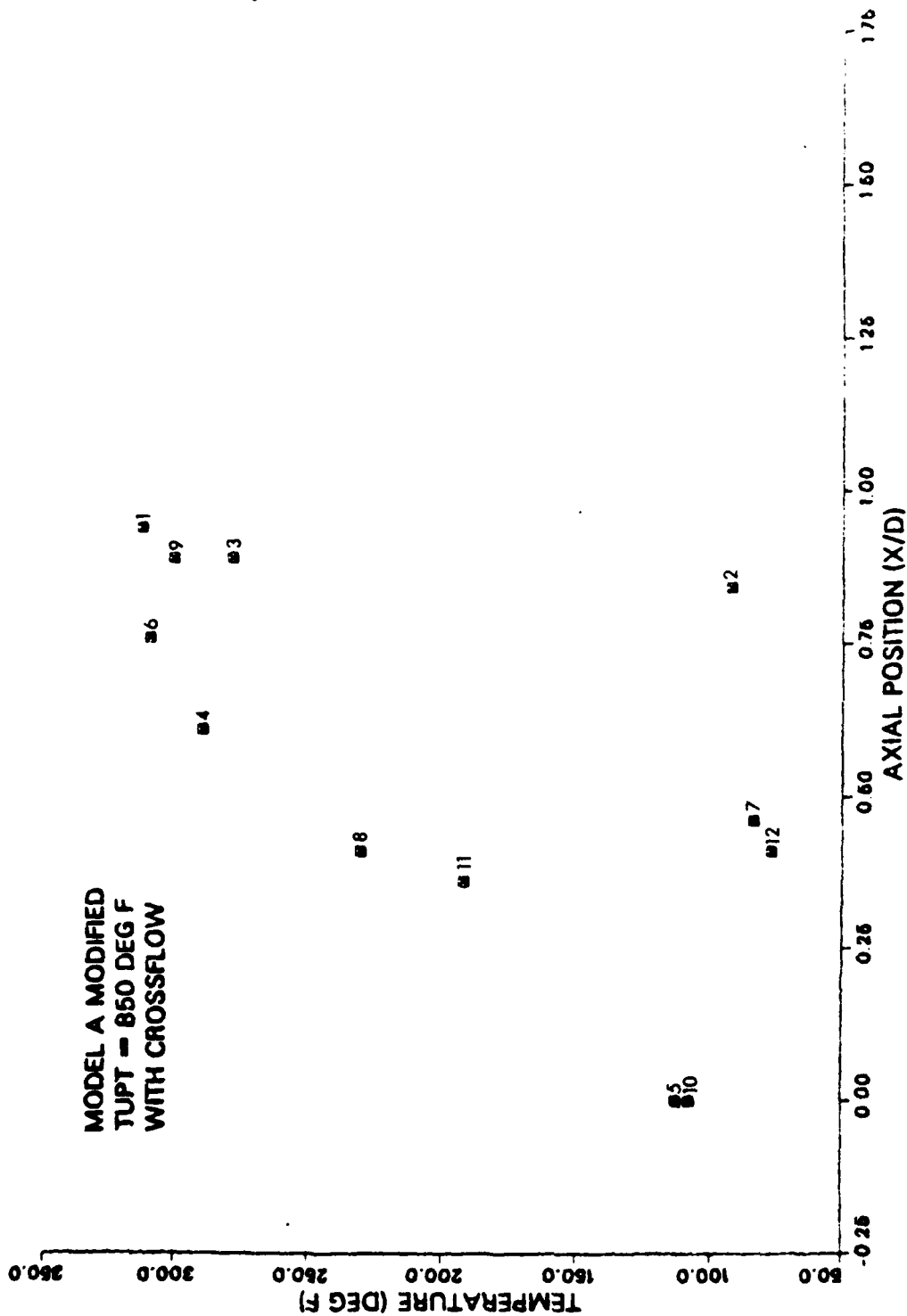


Figure 59. Mixing Stack Temp., Model A Mod (850 F) - Crossflow.

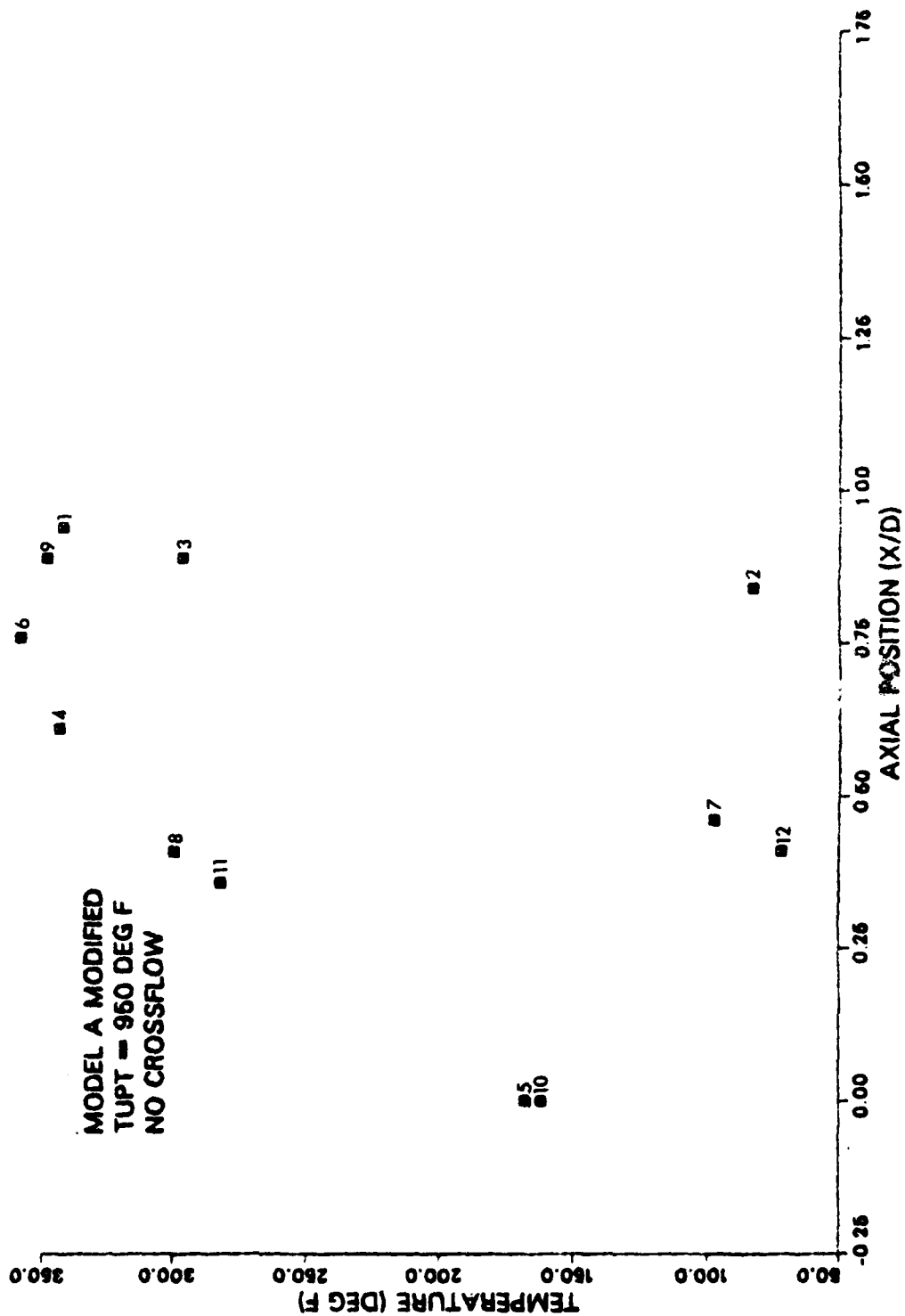


Figure 60. Mixing Stack Temp., Model A Mod (950 F) - No Crossflow.

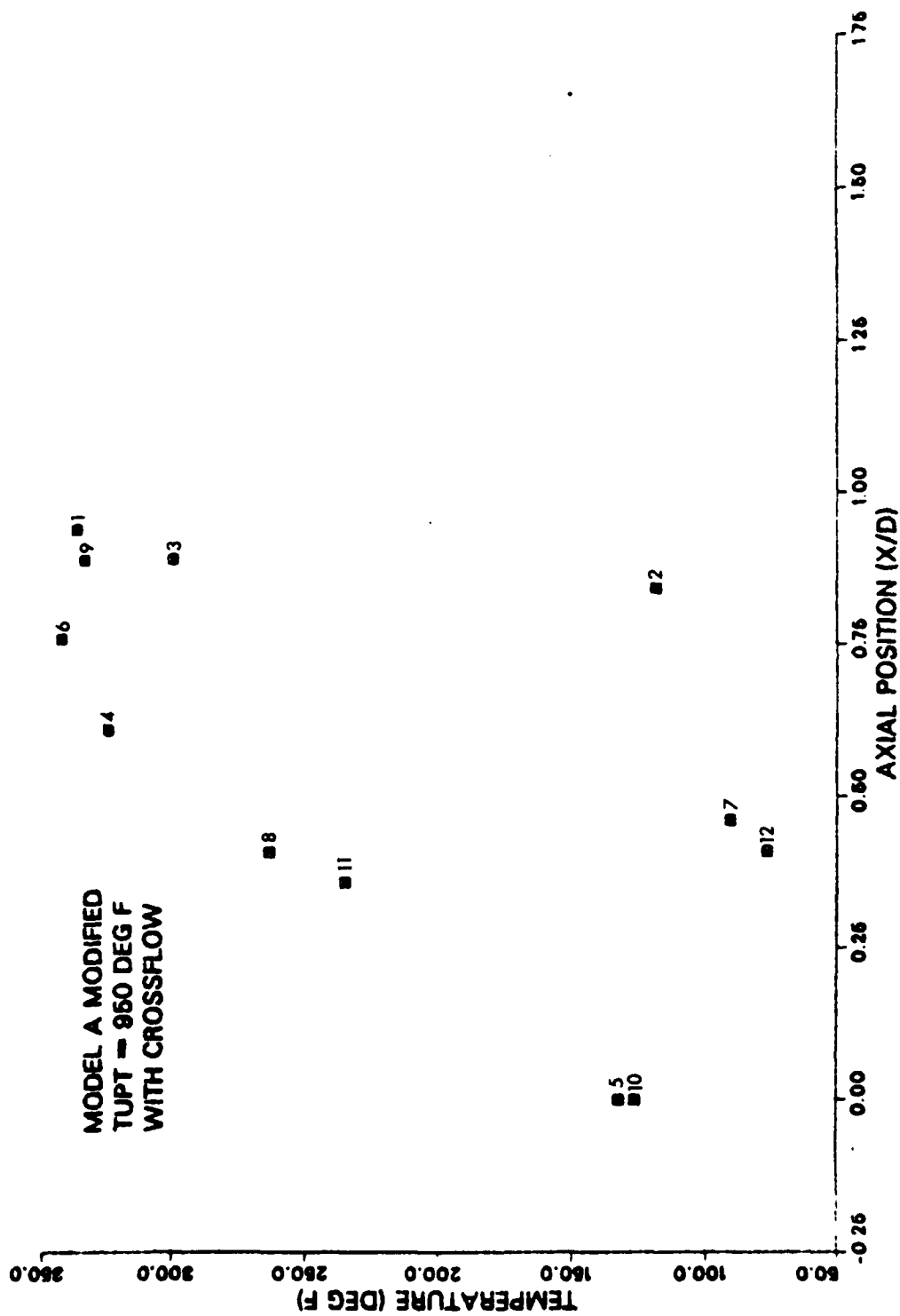


Figure 61. Mixing Stack Temp., Model A Mod (950 F) - Crossflow.

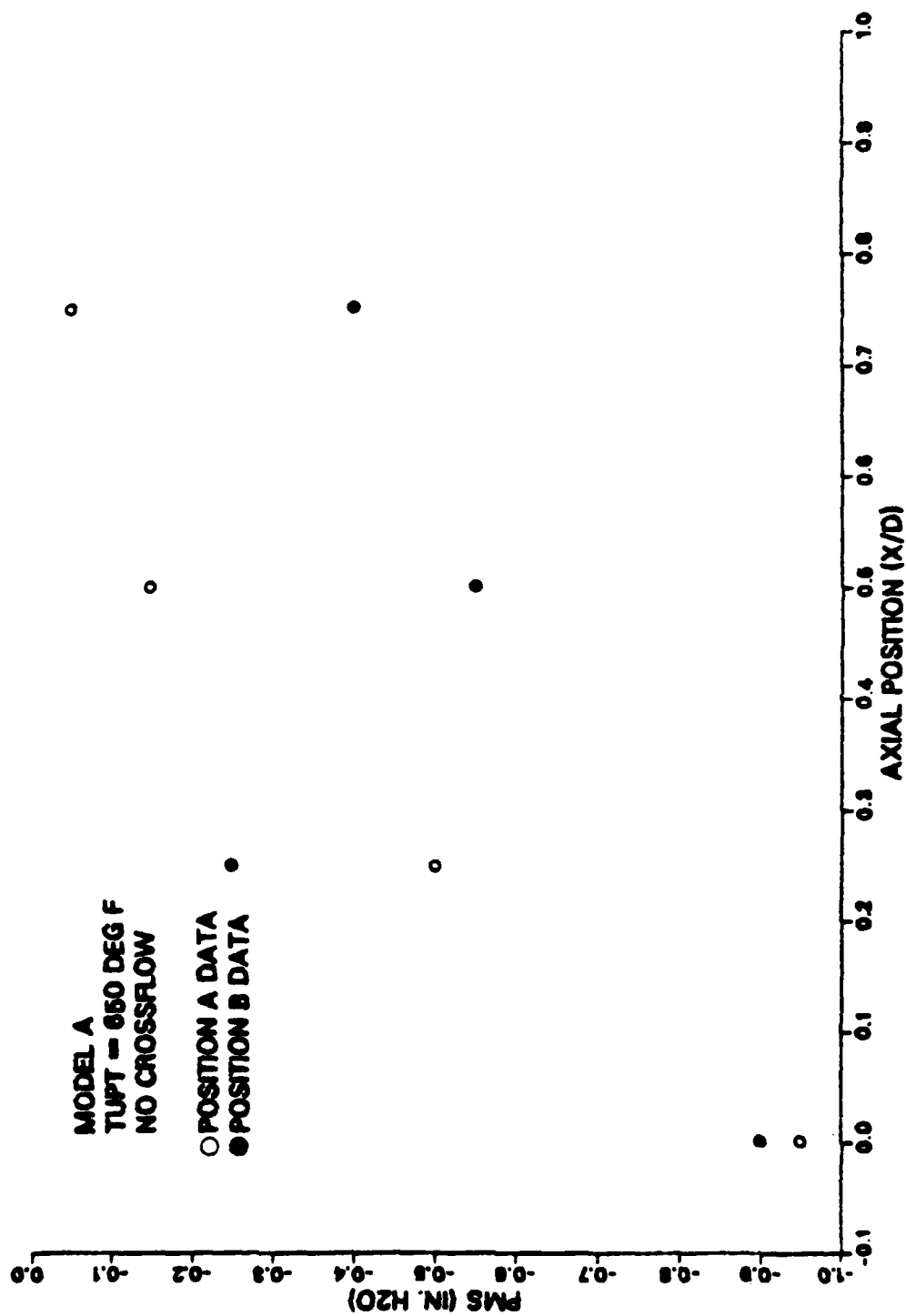


Figure 62. Mixing Stack Press., Model A (650 F) - No Crossflow.

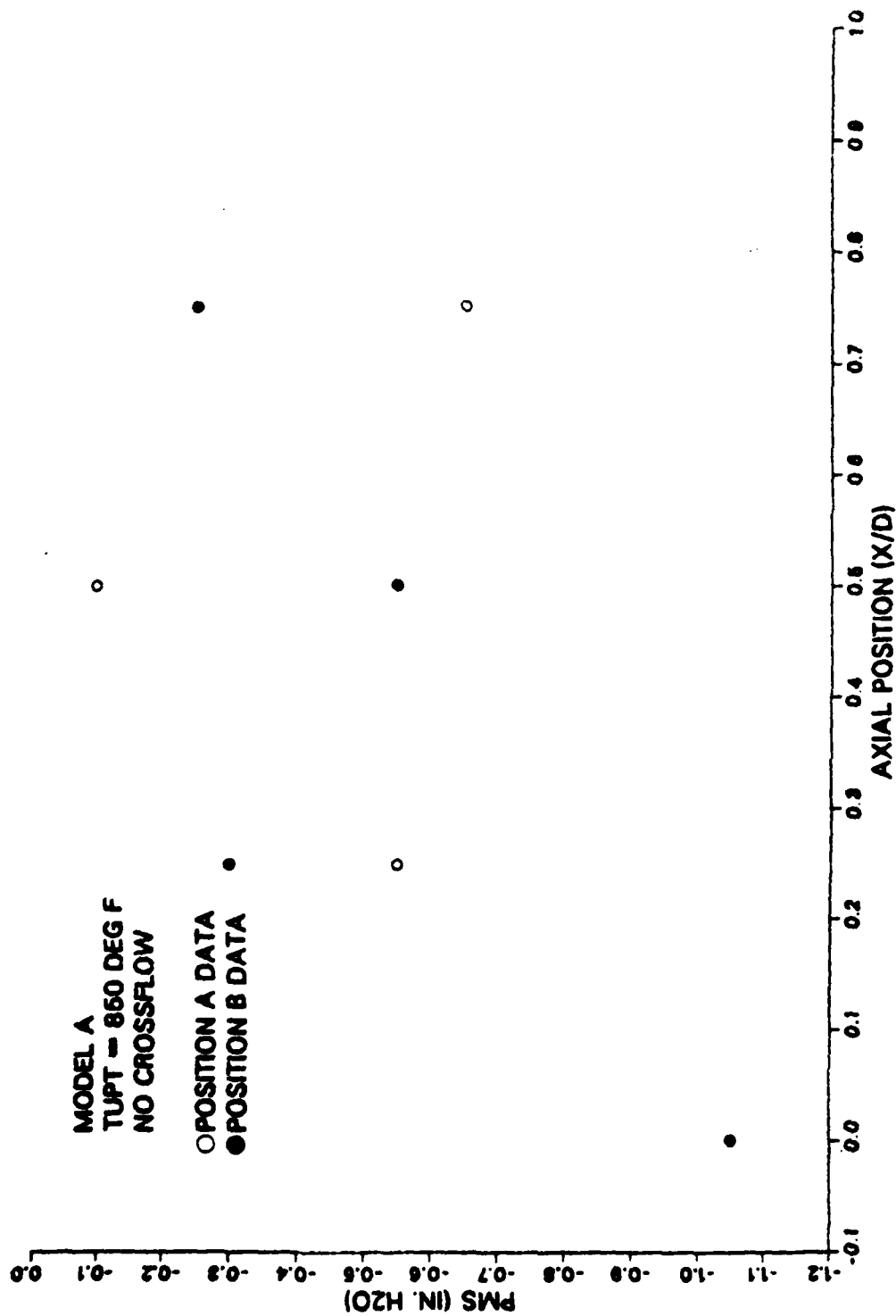


Figure 63. Mixing Stack Press., Model A (850 F) - No Crossflow.

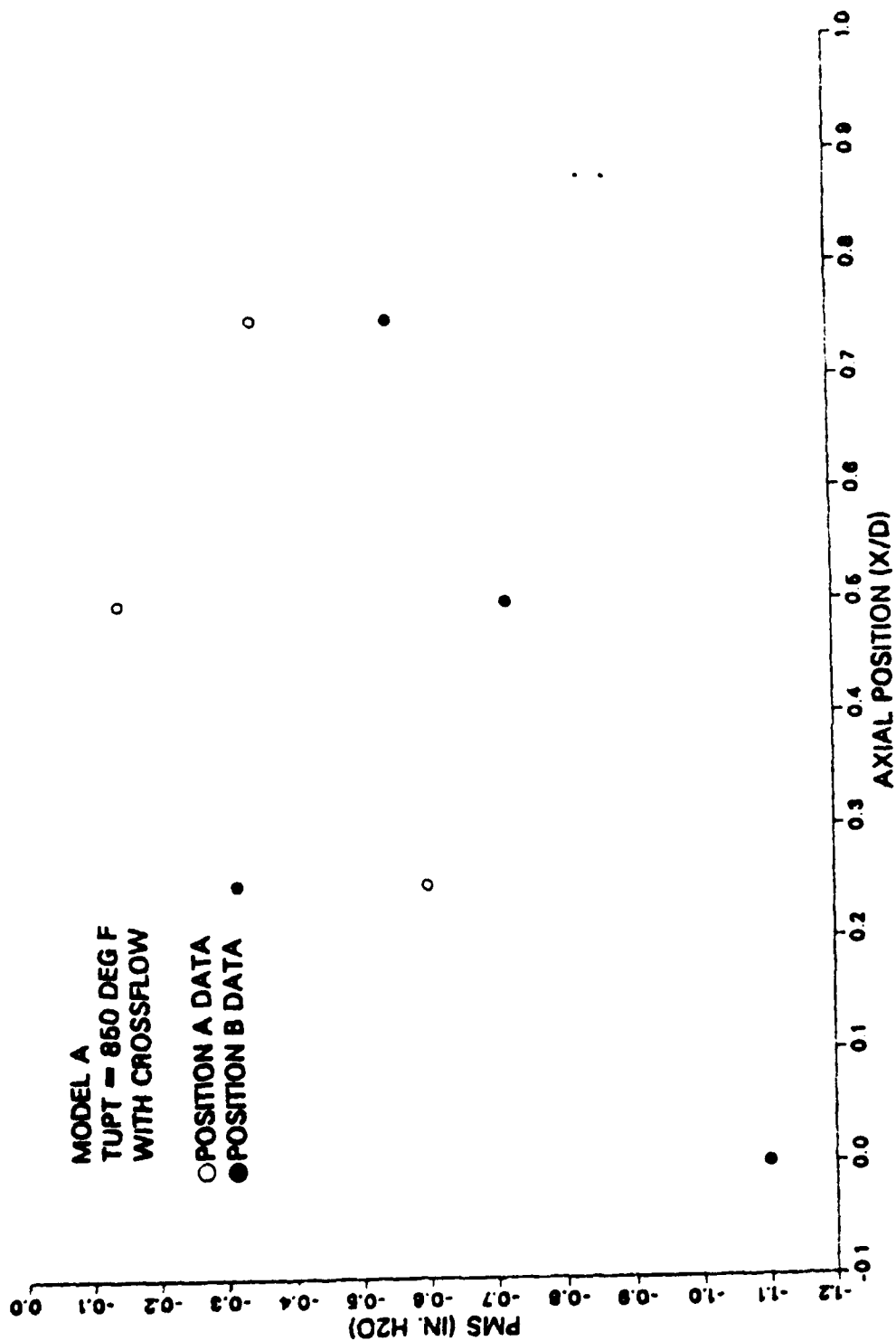


Figure 64. Mixing Stack Press., Model A (850 F) - Crossflow.

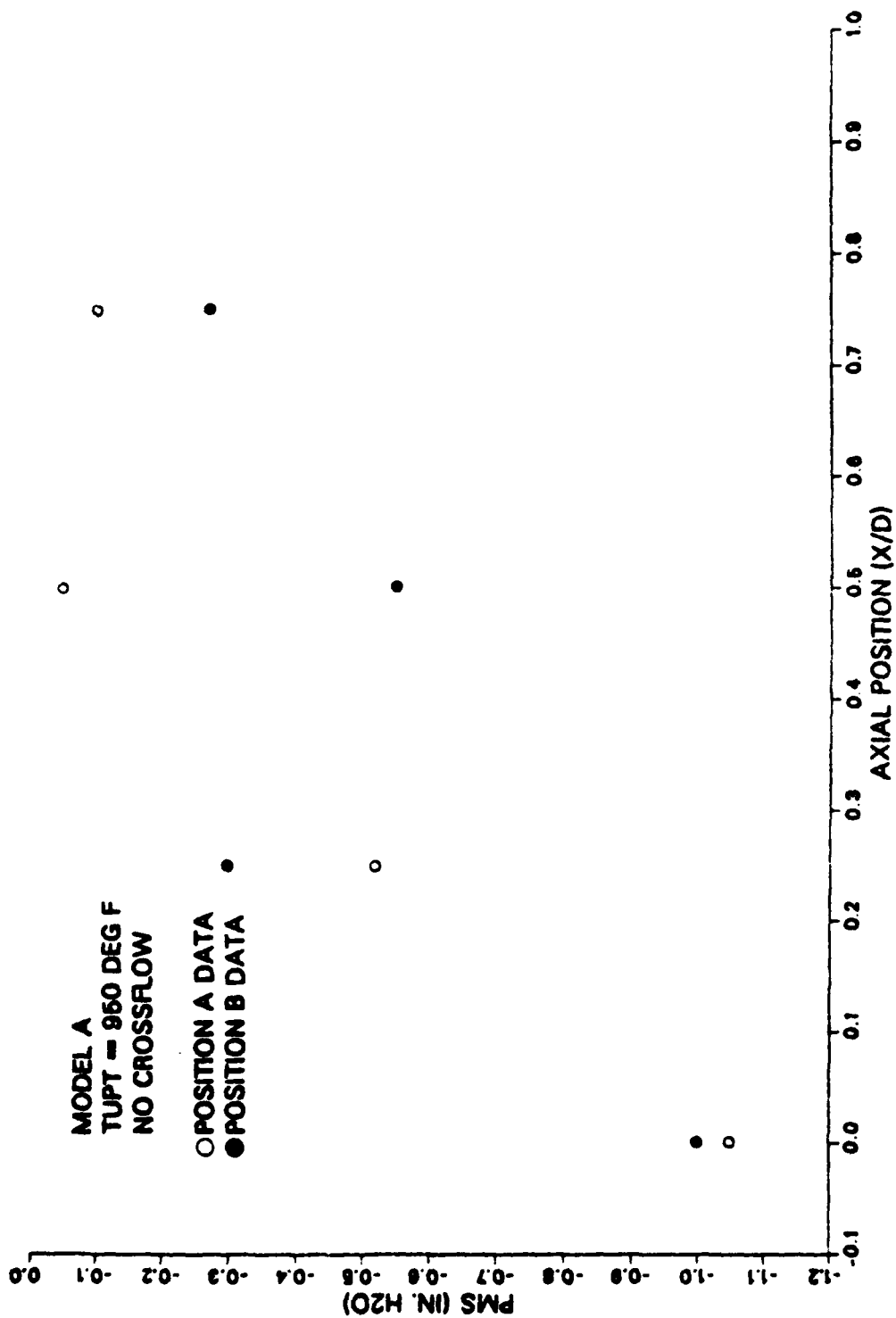


Figure 65. Mixing Stack Press., Model A (950 F) - No Crossflow.

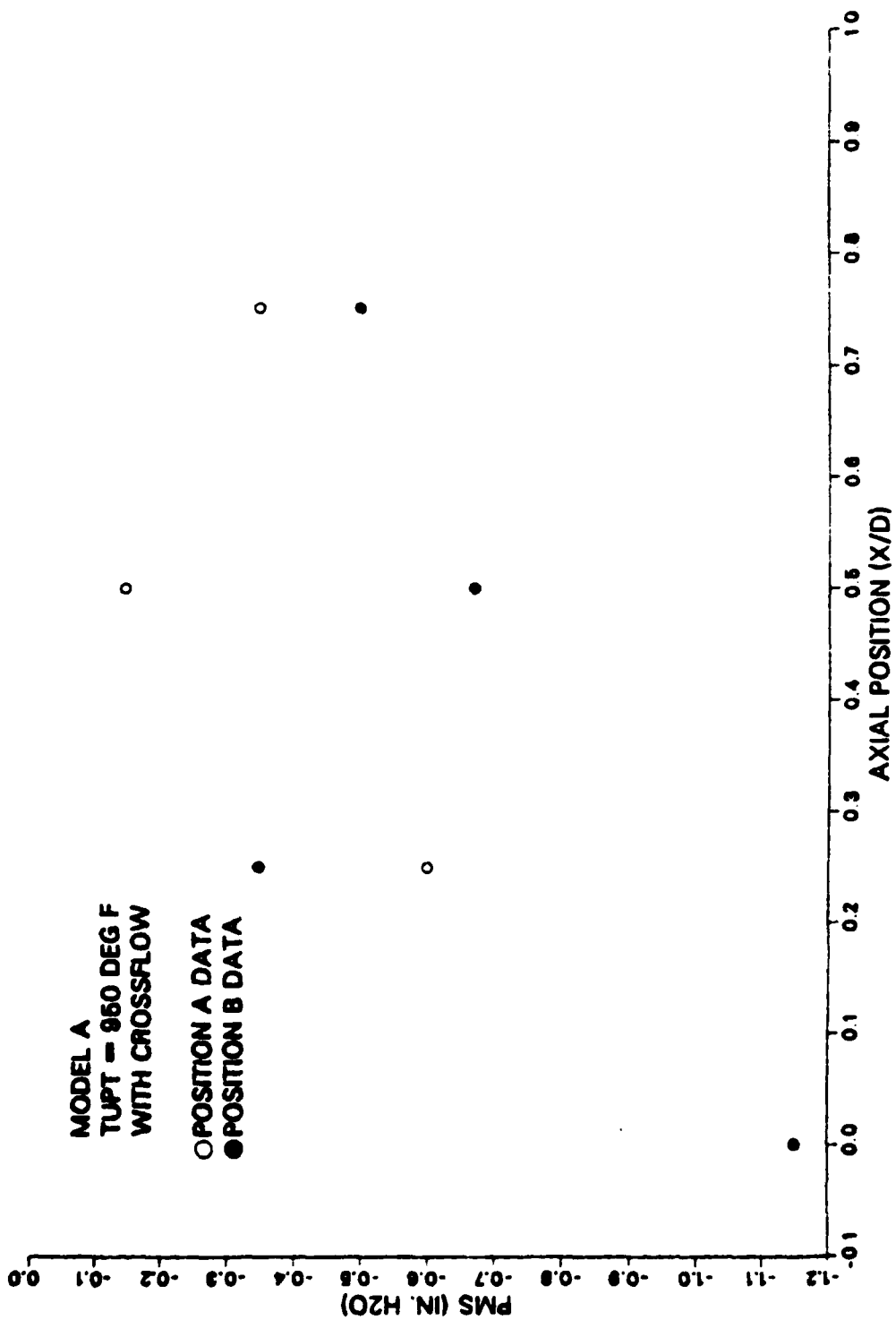


Figure 66. Mixing Stack Press., Model A (950 F) - Crossflow.

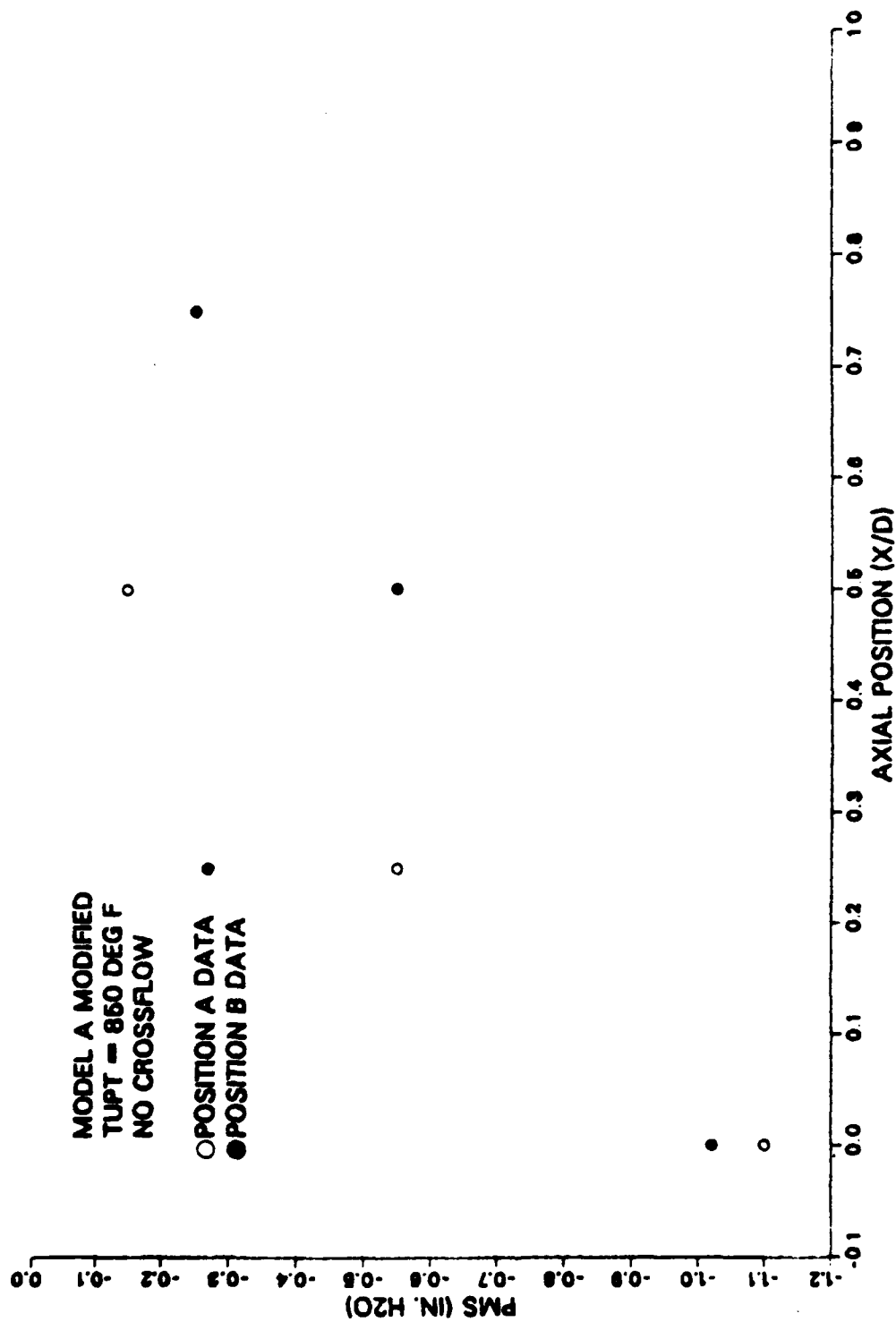


Figure 67. Mixing Stack Press., Model A Mod (850 F) - No Crossflow.

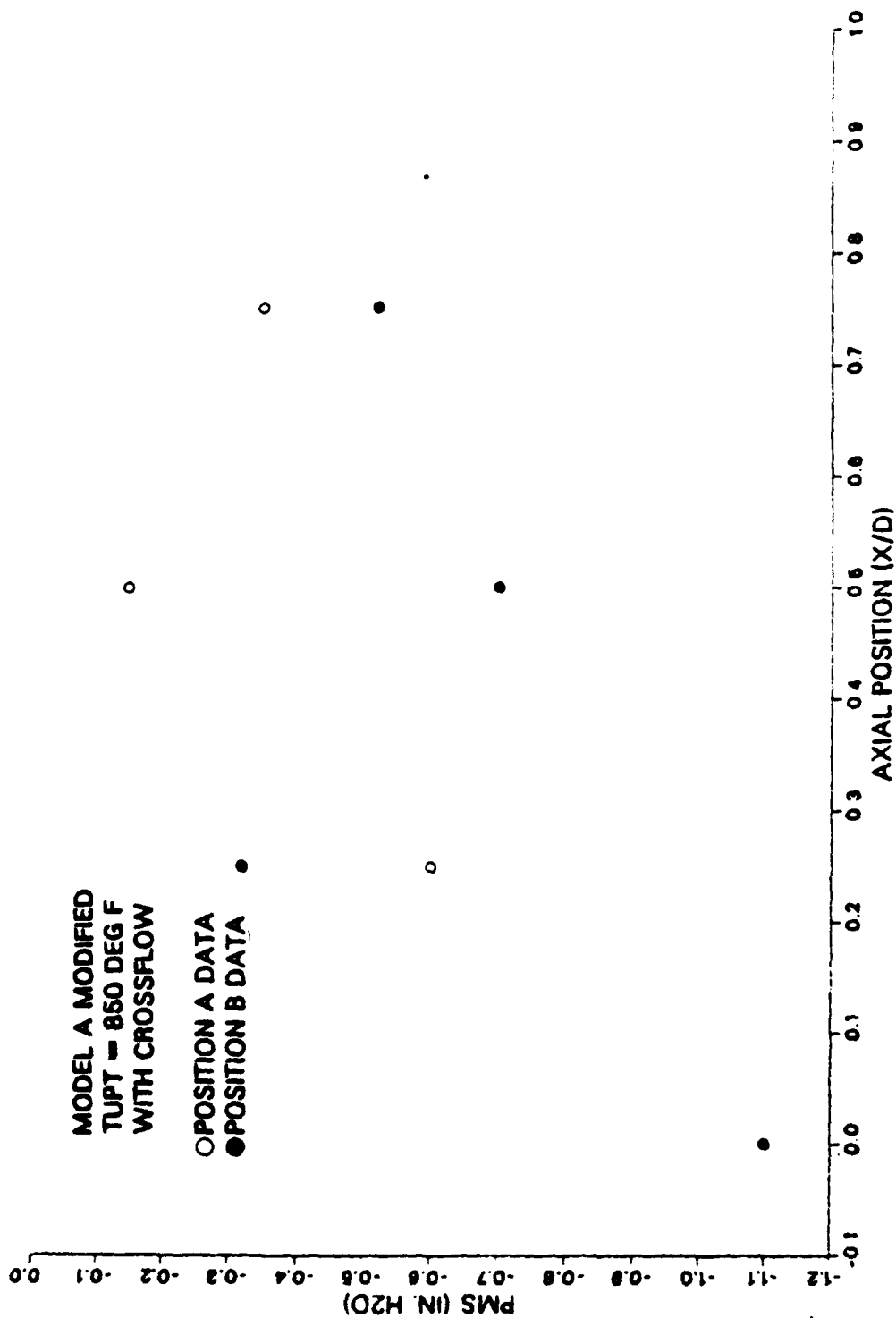


Figure 68. Mixing Stack Press., Model A Mod (850 F) - Crossflow.

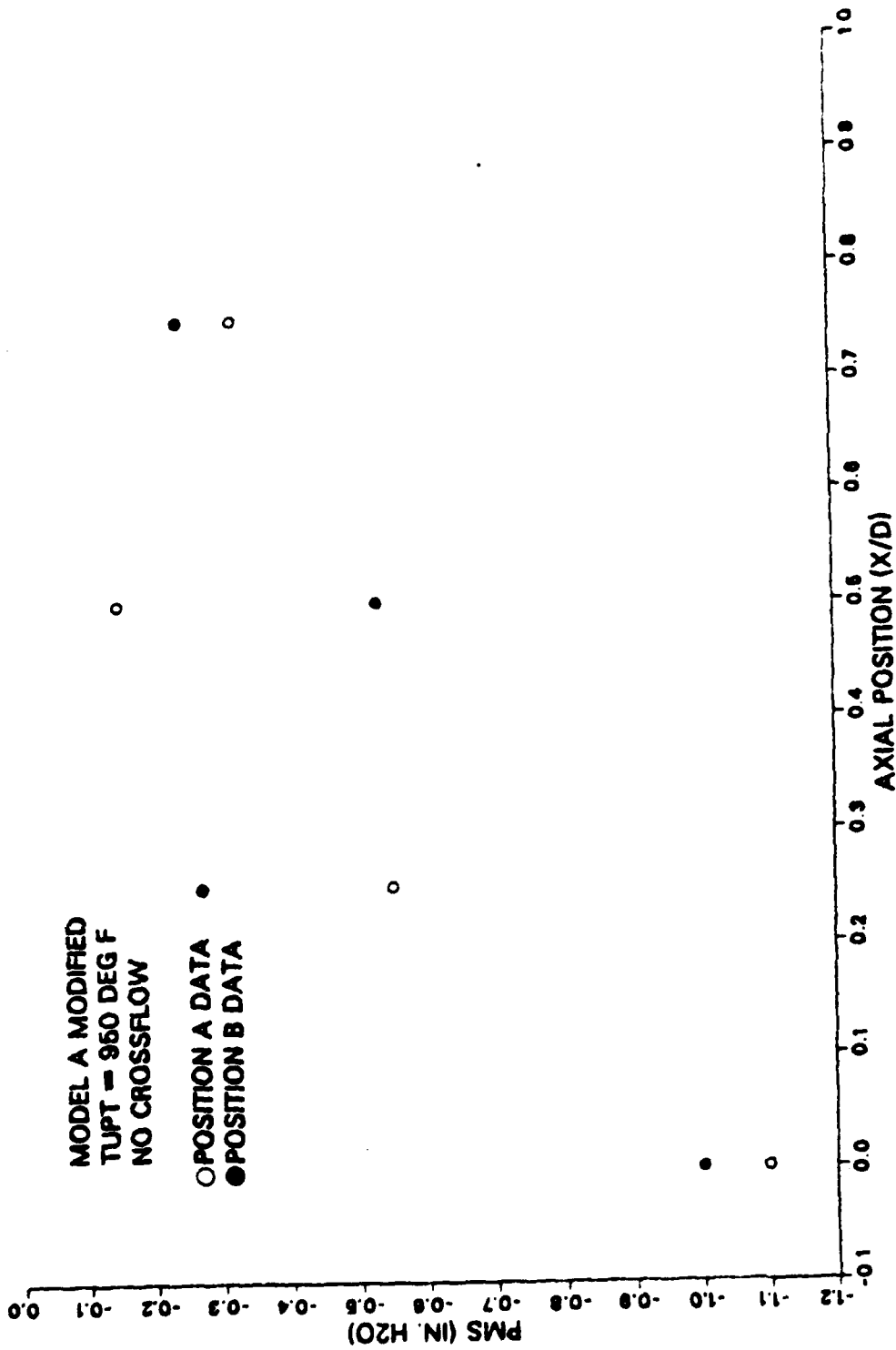


Figure 69. Mixing Stack Press., Model A Mod (950 F) - No Crossflow.

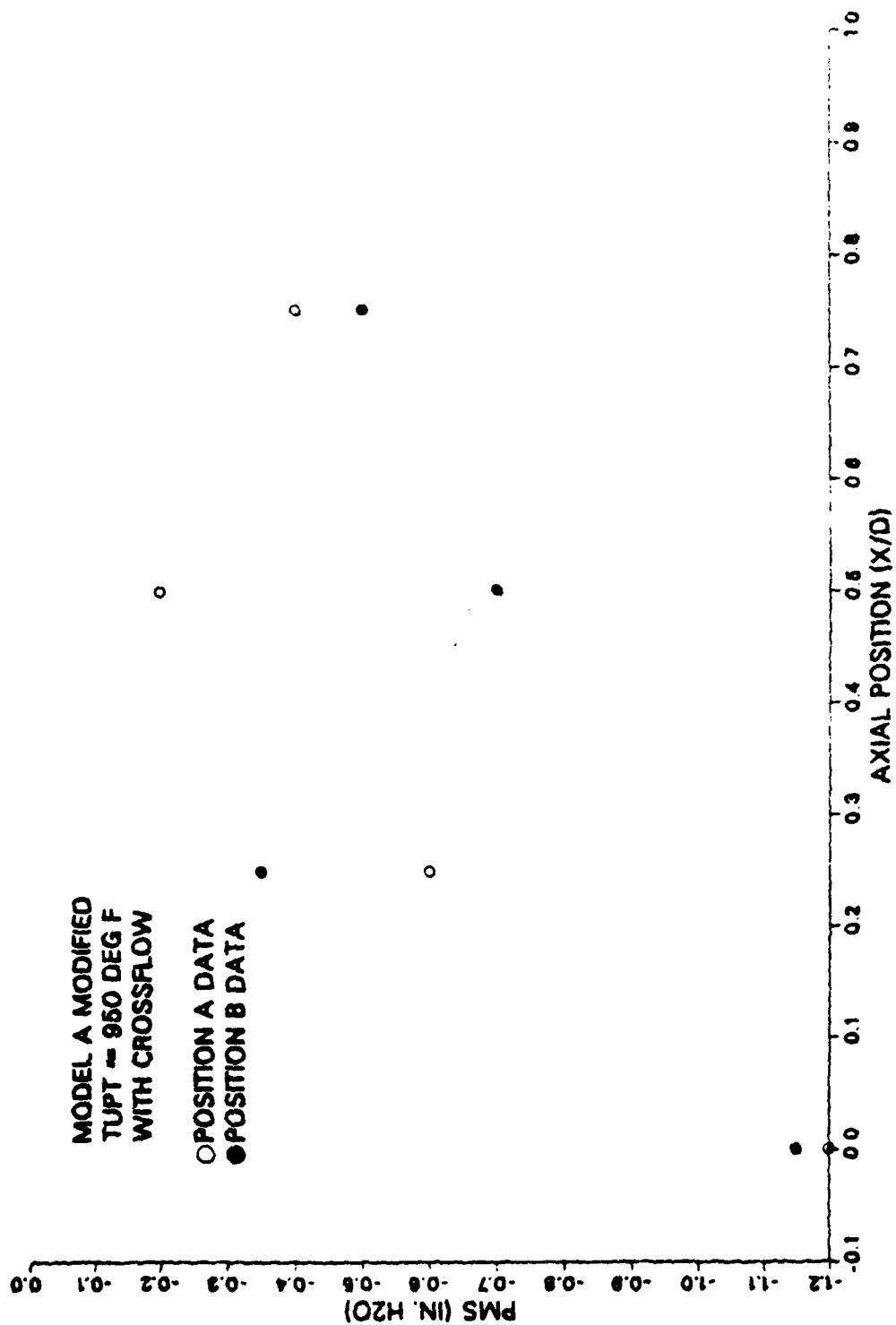


Figure 70. Mixing Stack Press., Model A Mod (950 F) - Crossflow.

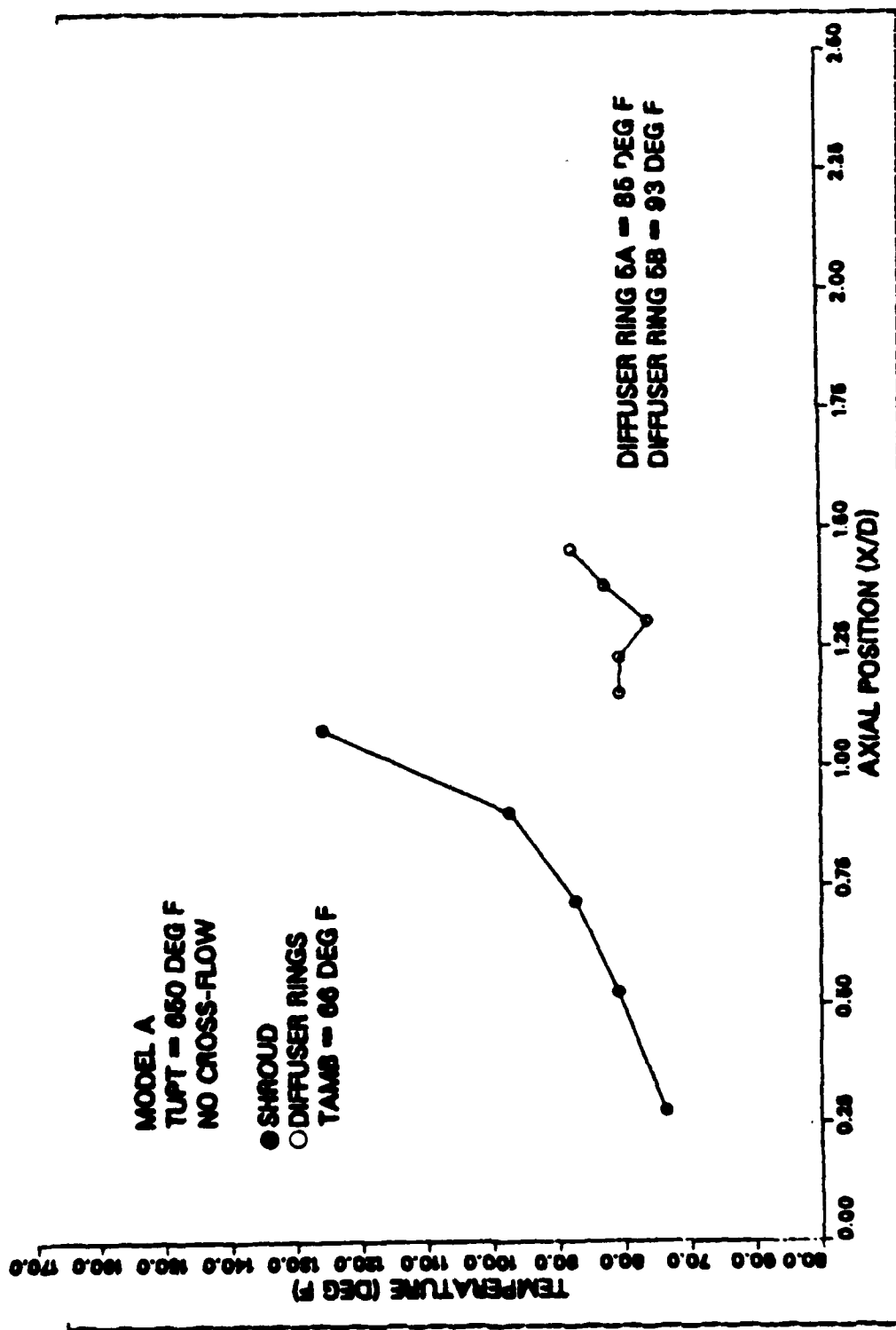


Figure 71. Type T External Temp., Model A (650 F) - No Crossflow.

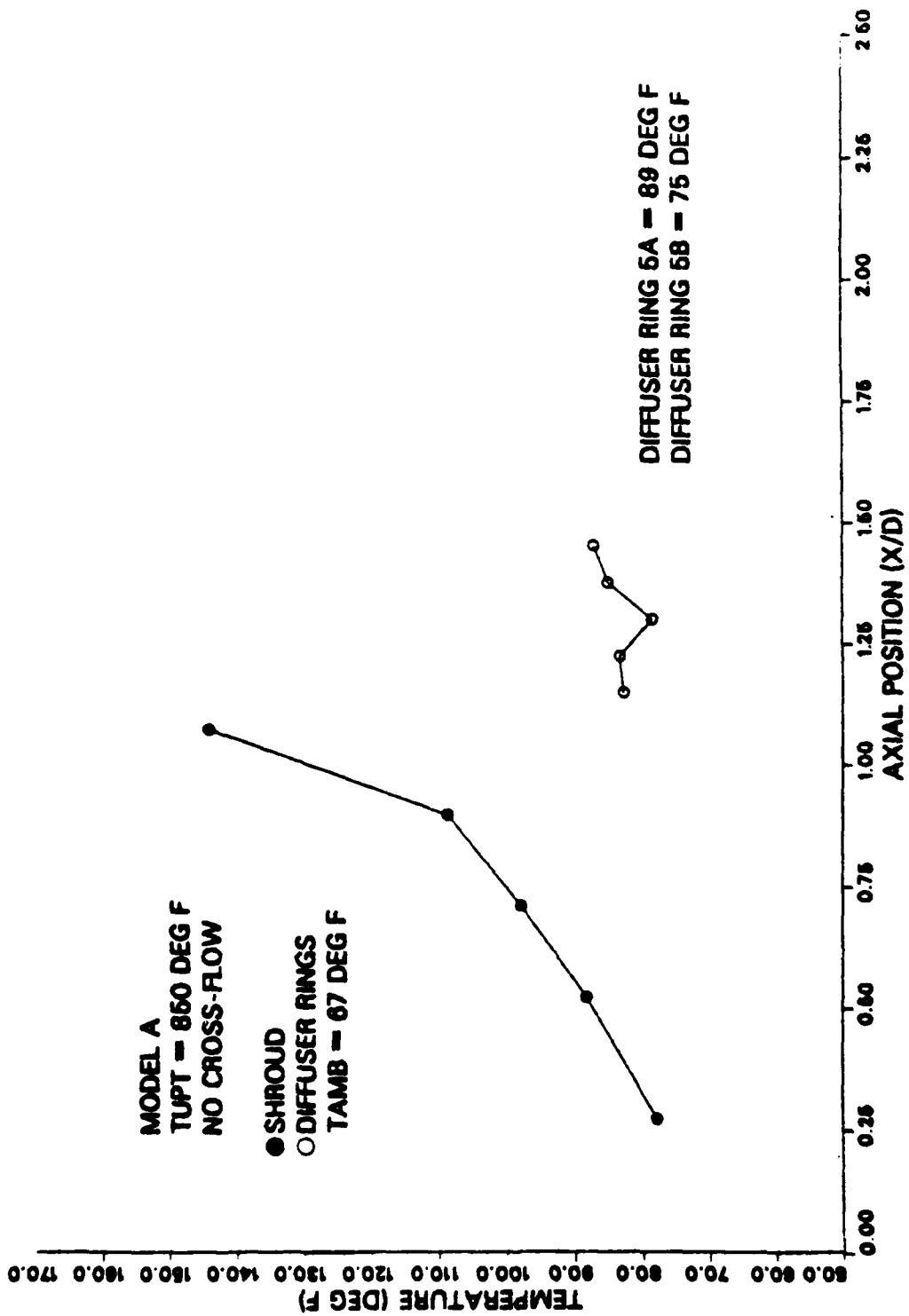


Figure 72. Type T External Temp., Model A (850 F) - No Crossflow.

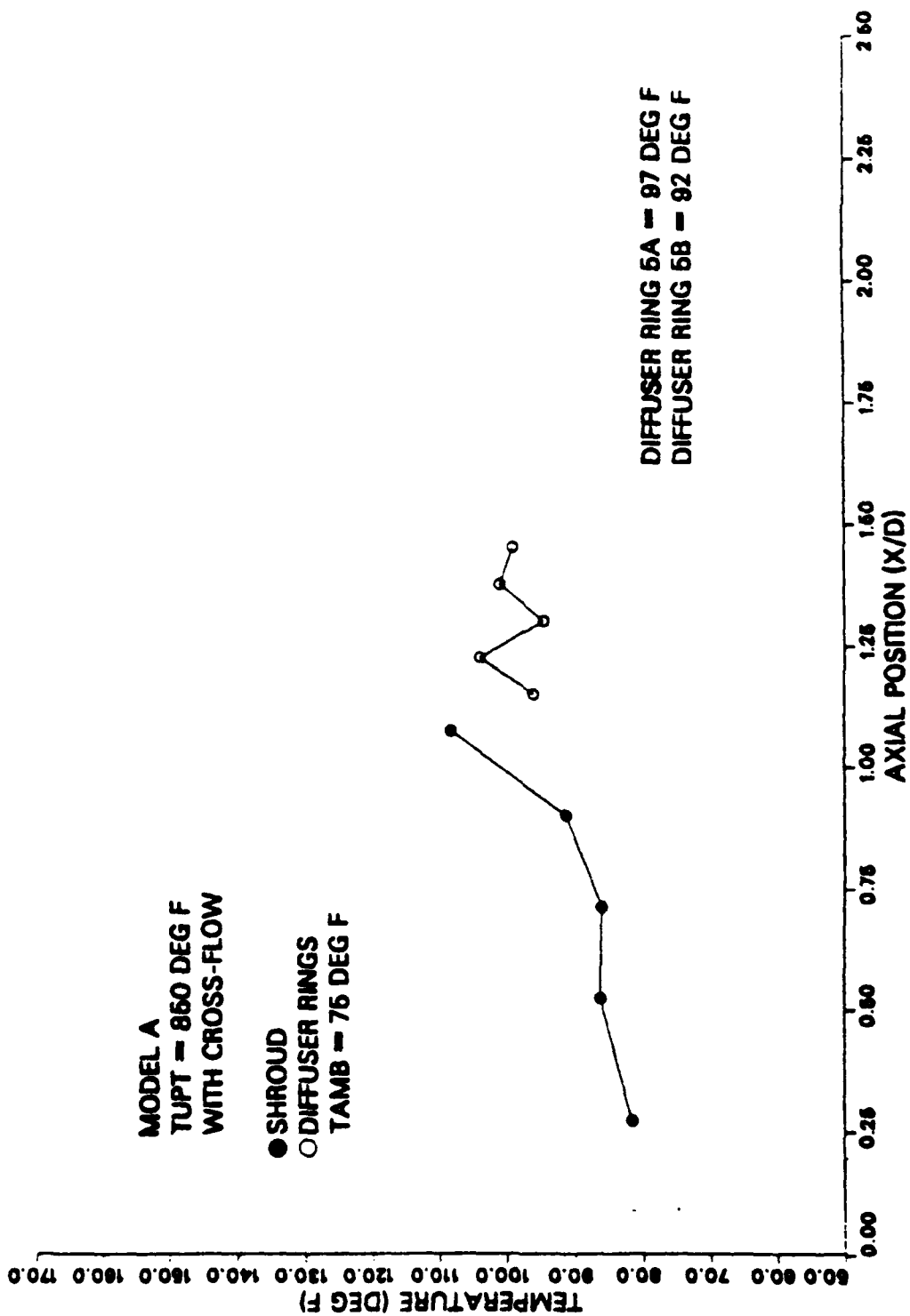


Figure 73. Type T External Temp., Model A (850 F) - Crossflow.

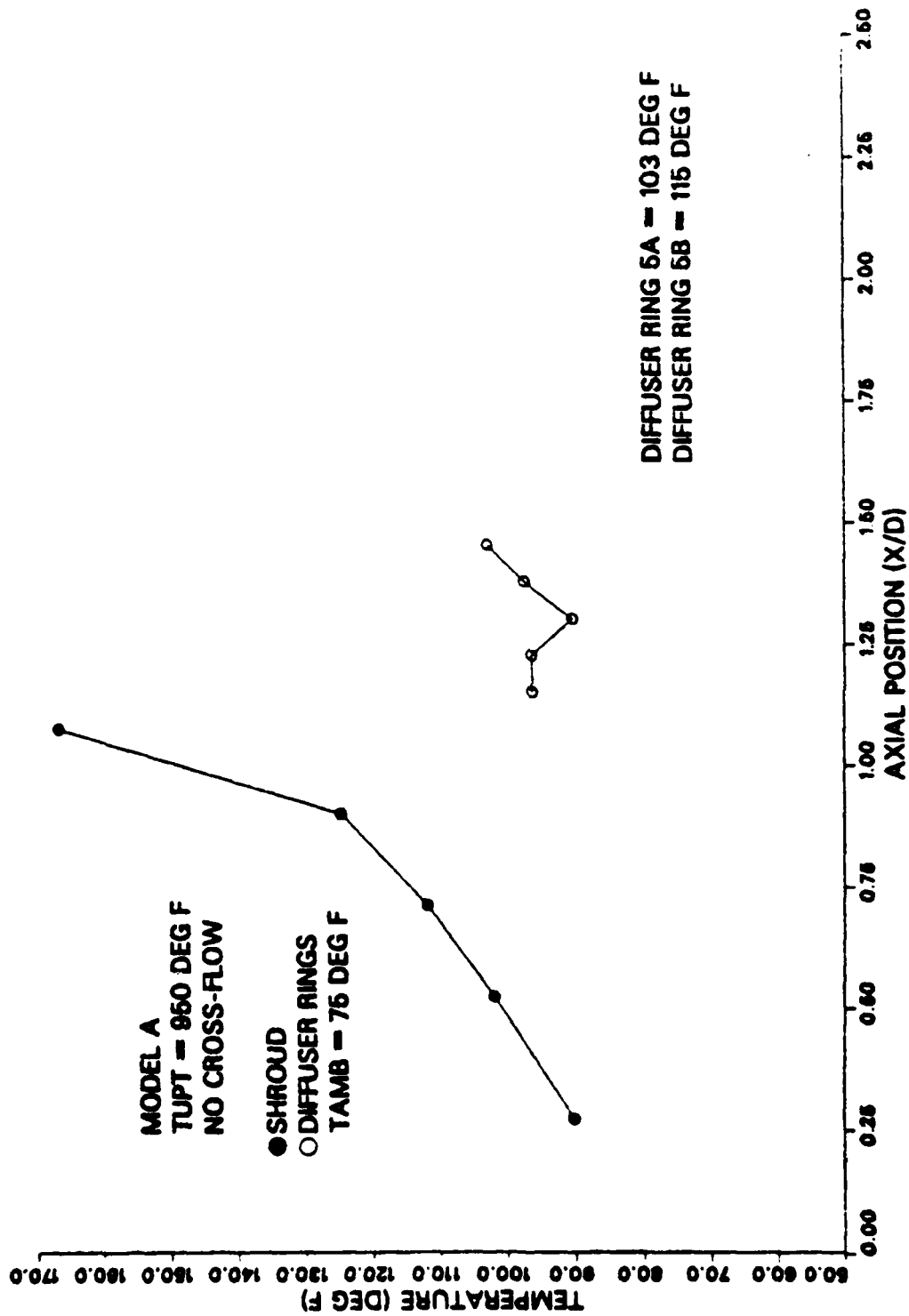


Figure 74. Type T External Temp., Model A (950 F) - No Crossflow.

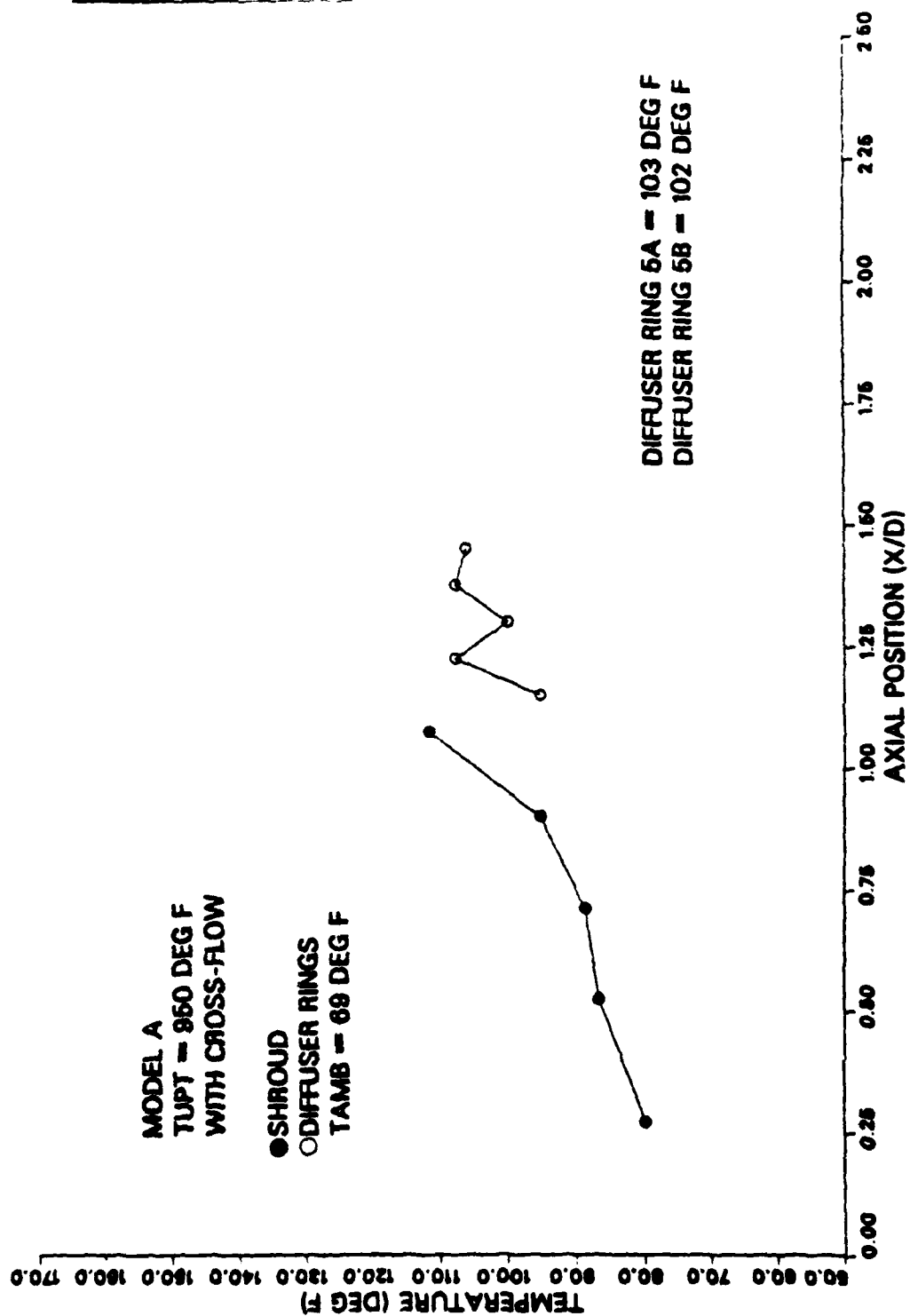


Figure 75. Type T External Temp., Model A (950 F) - Crossflow.

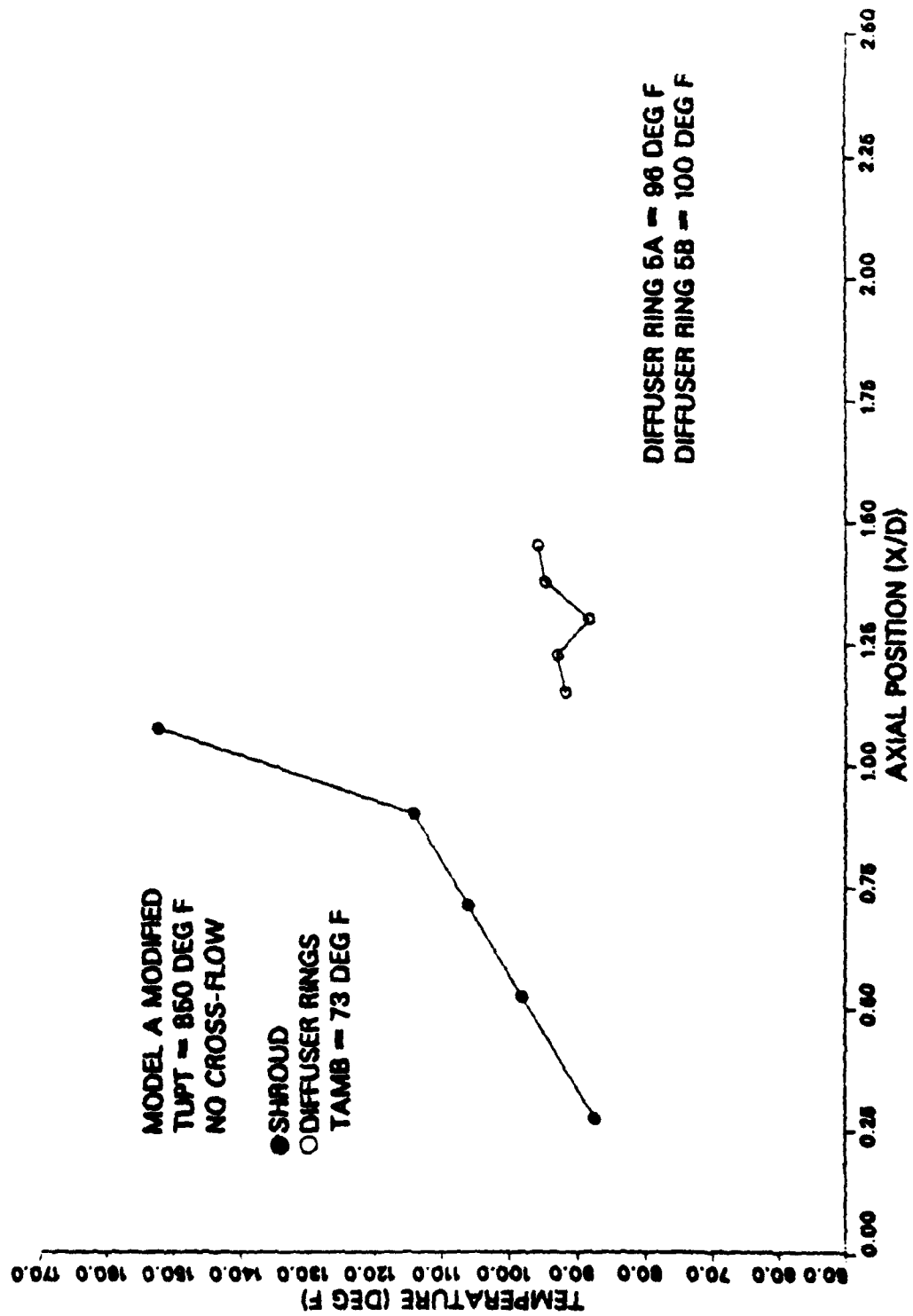


Figure 76. Type T Ext. Temp., Model A Mod (850 F) - No Crossflow.

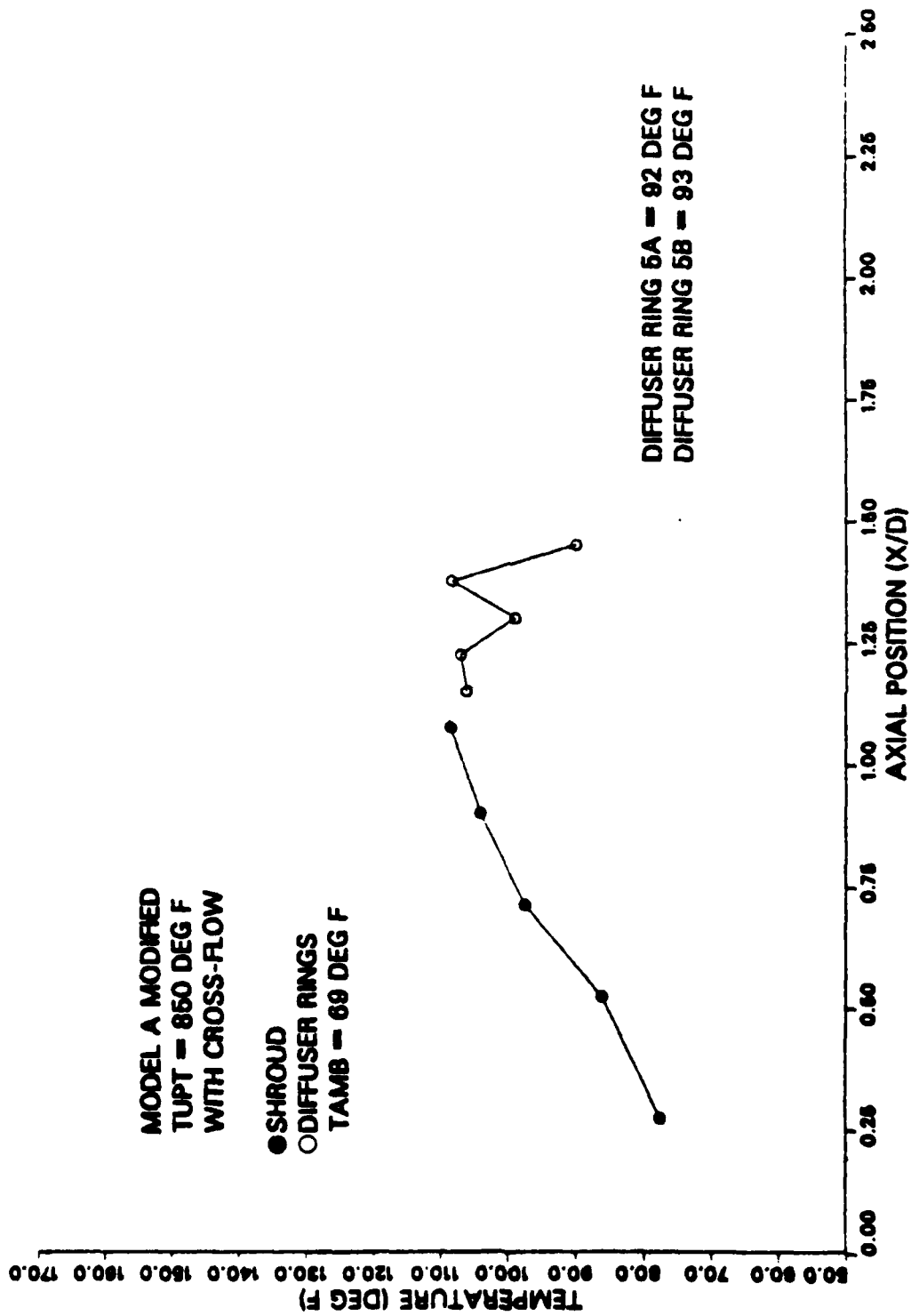


Figure 77. Type T Ext. Temp., Model A Mod (850 F) - Crossflow.

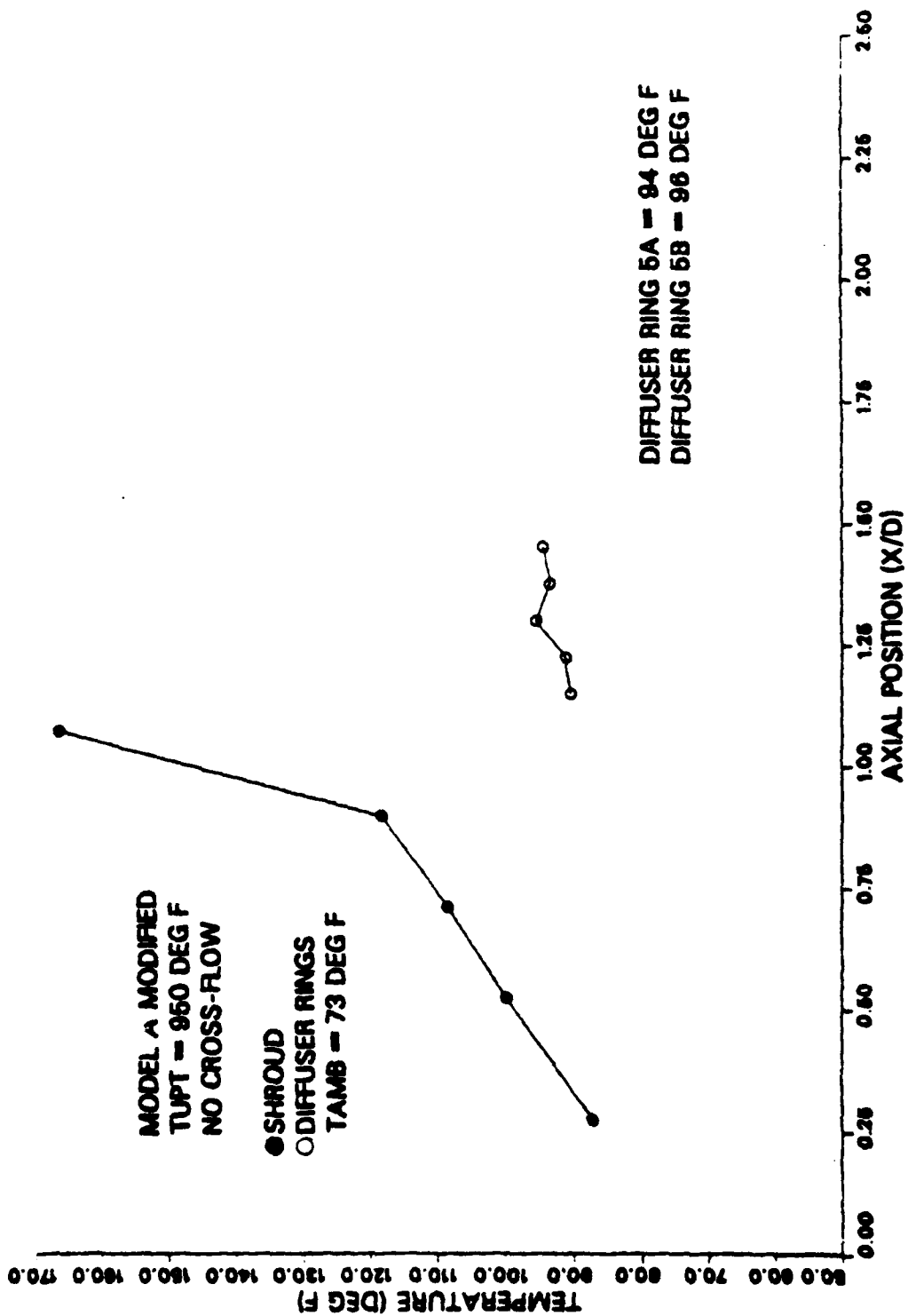


Figure 78. Type T Ext. Temp., Model A Mod (950 F) - No Crossflow.

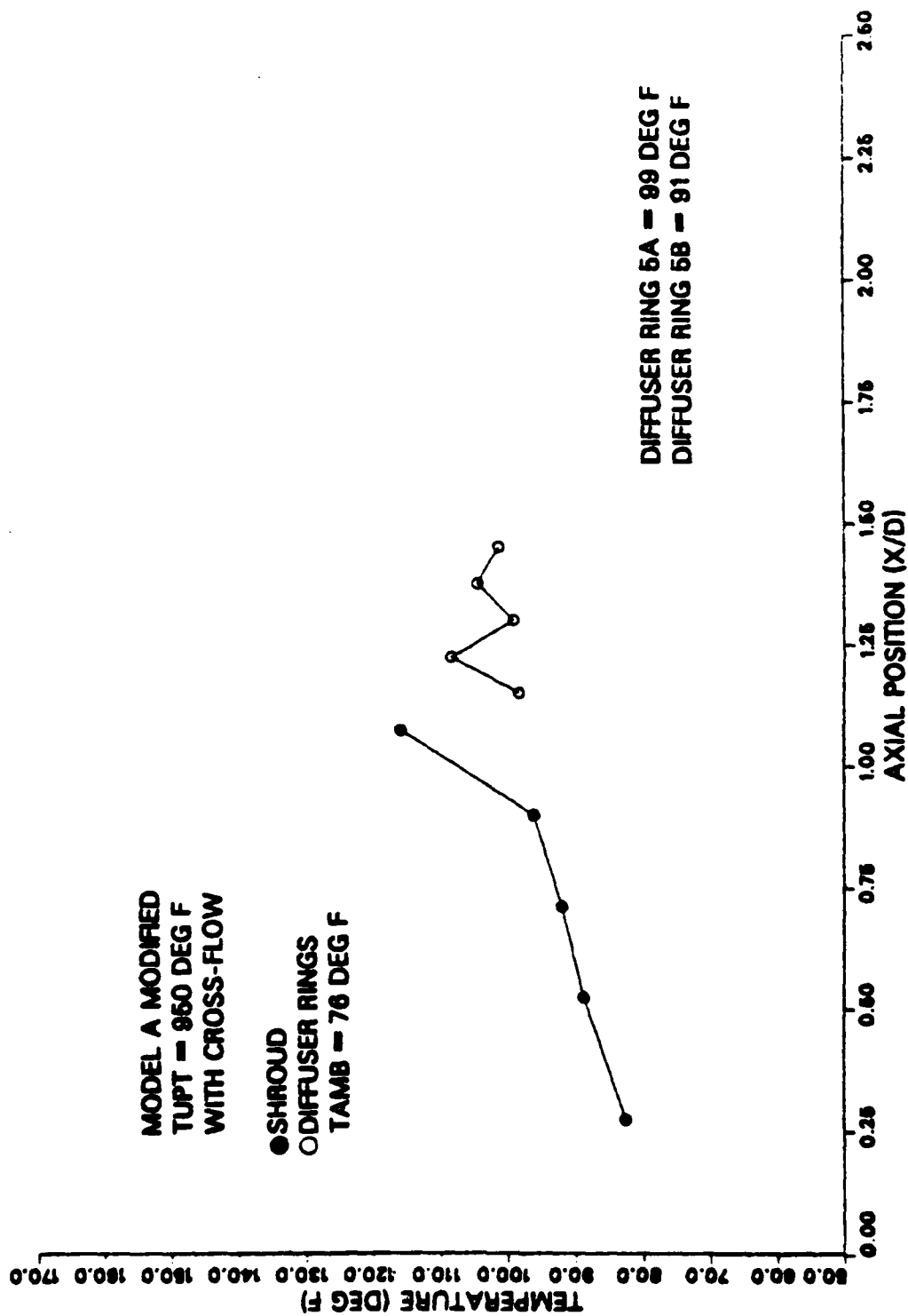


Figure 79. Type T Ext. Temp., Model A Mod (950 F) - Crossflow.

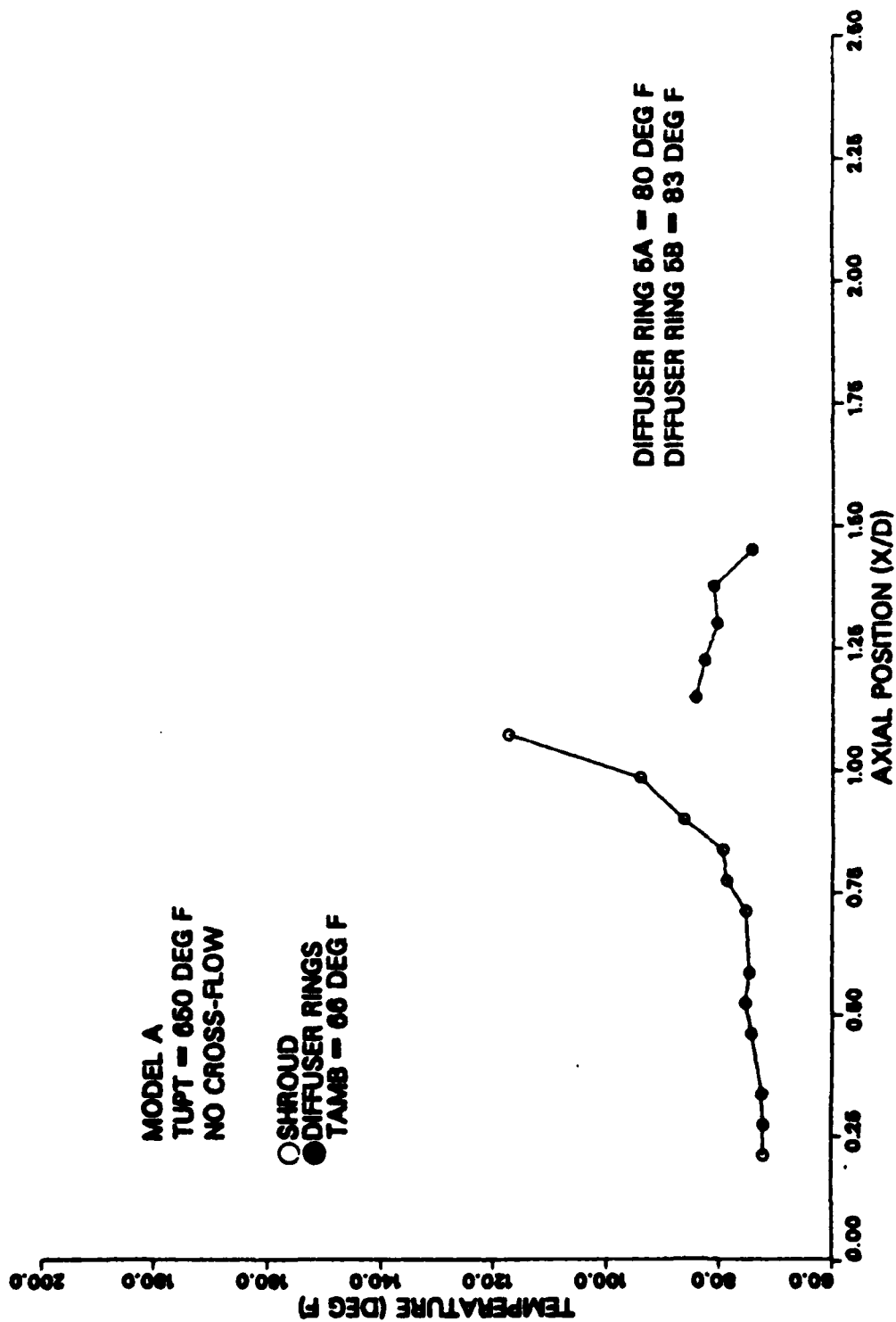


Figure 80. Omega External Temp., Model A (650 F) - No Crossflow.

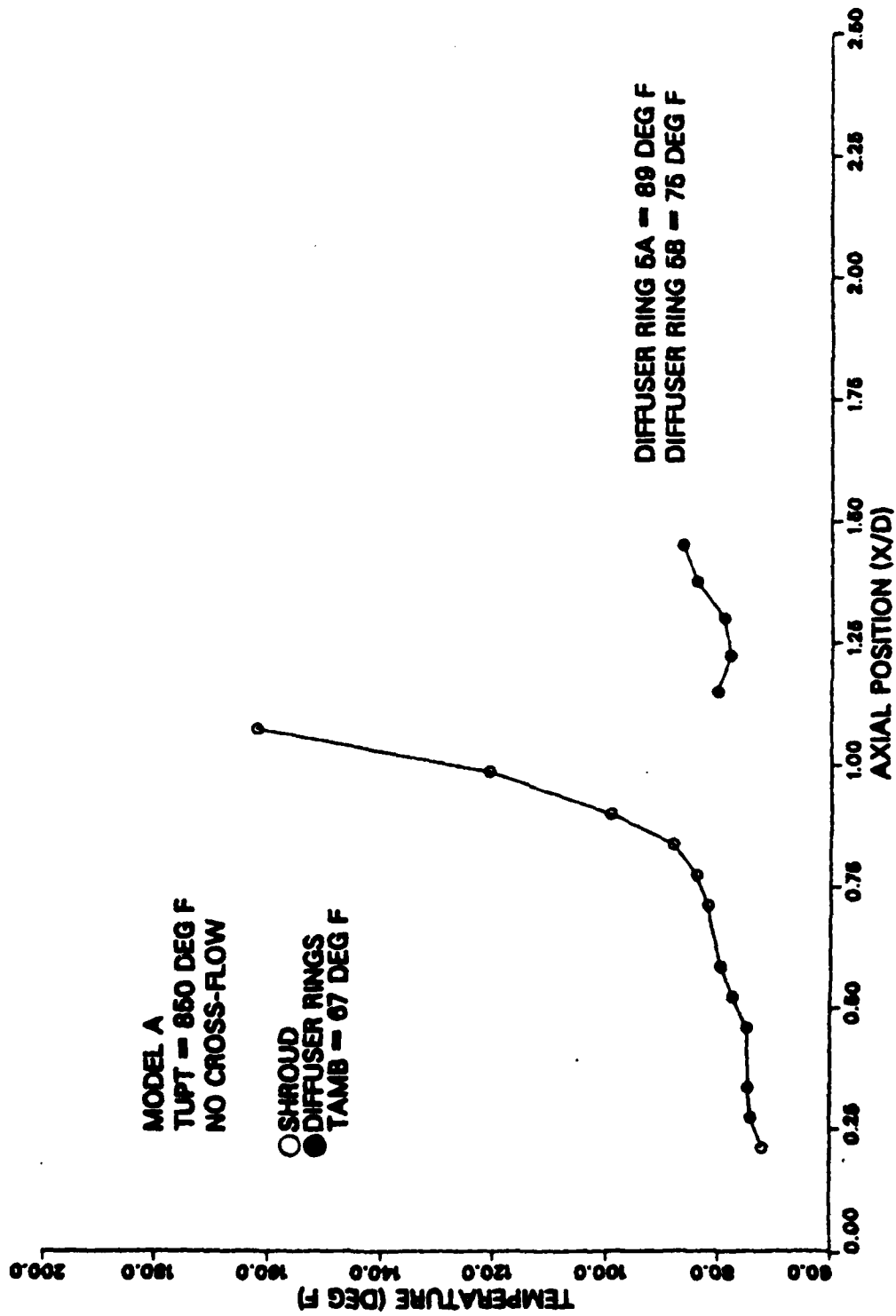


Figure 81. Omega External Temp., Model A (850 F) - No Crossflow.

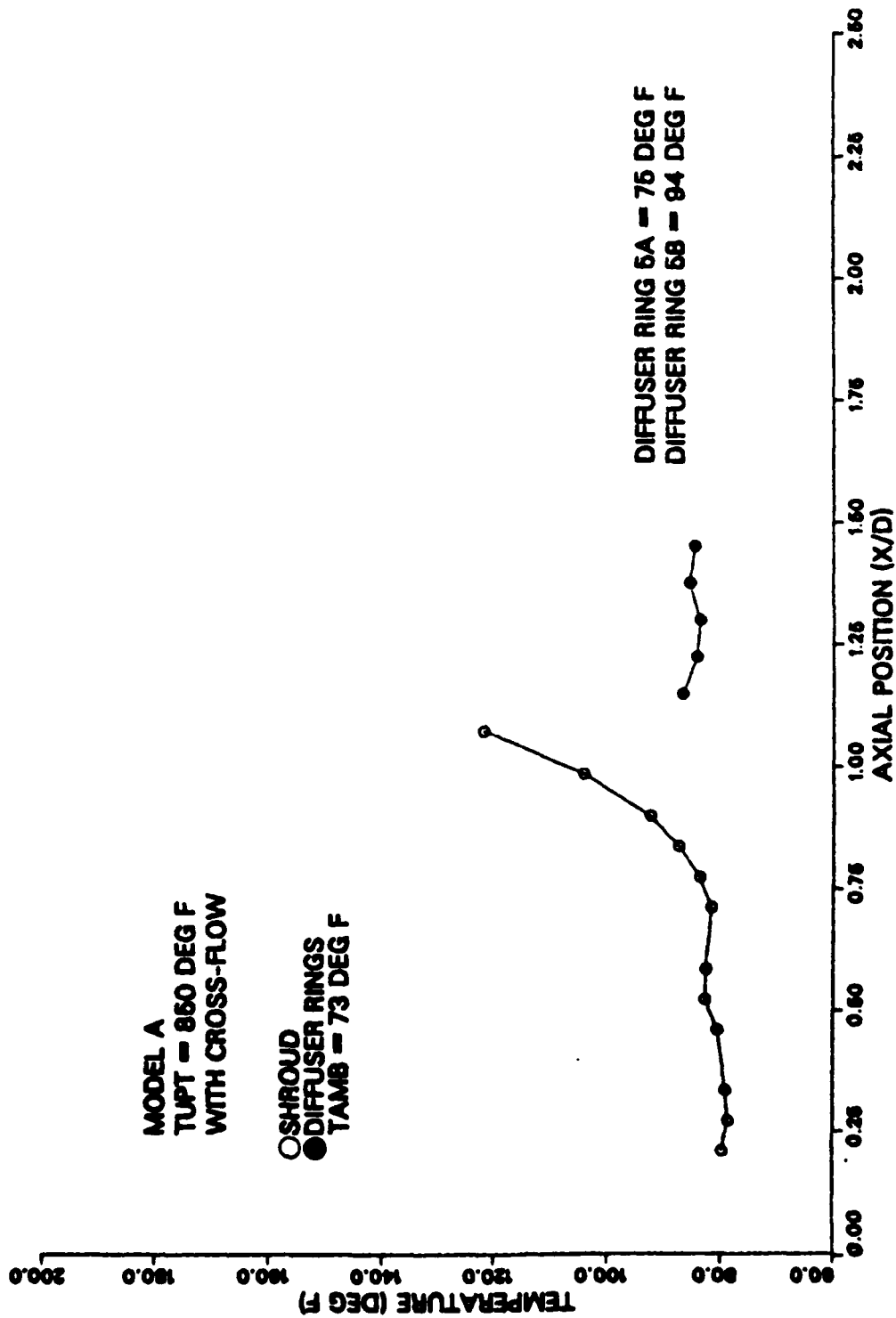


Figure 82. Omega External Temp., Model A (850 F) - Crossflow.

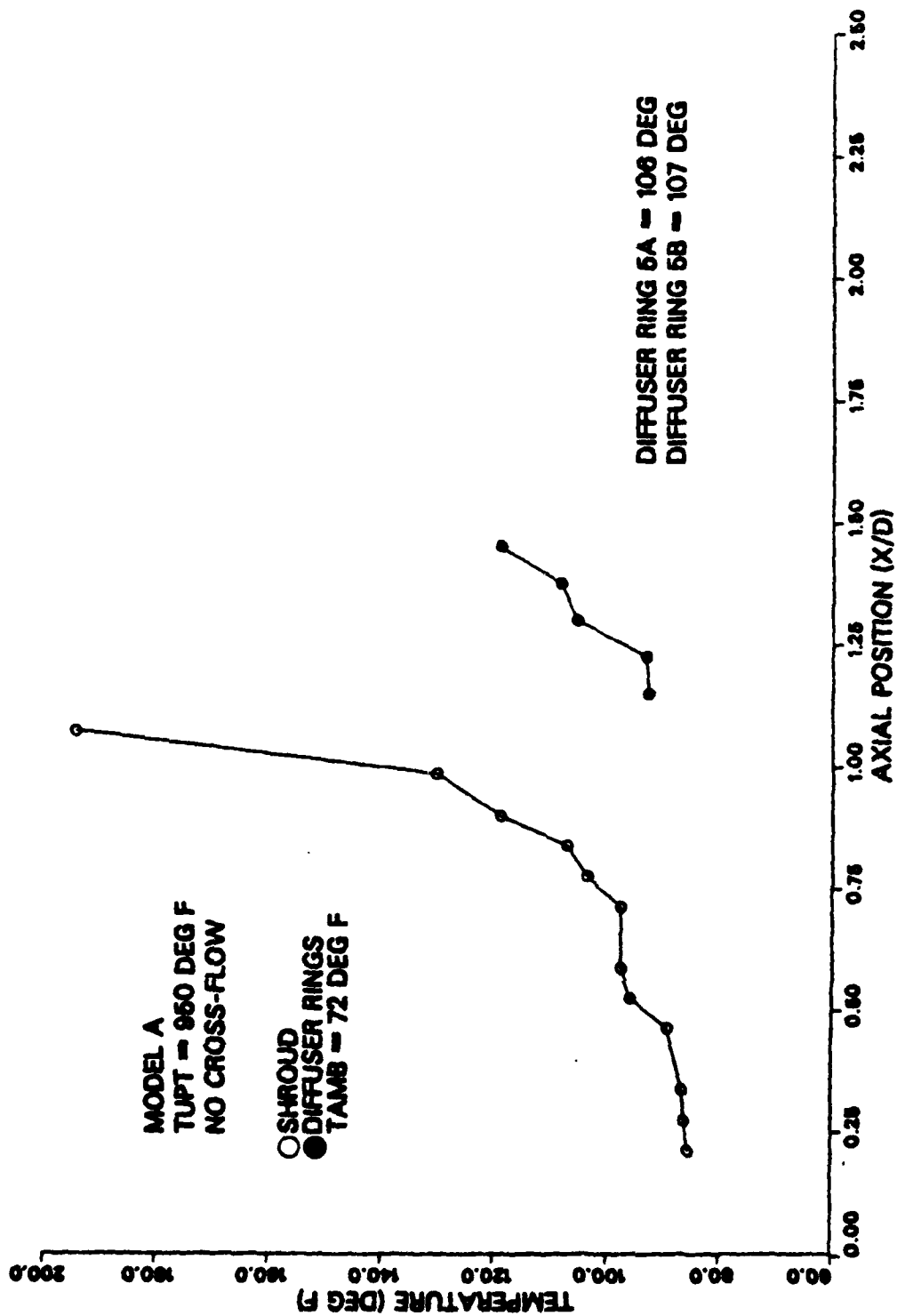


Figure 83. Omega External Temp., Model A (950 F) - No Crossflow.

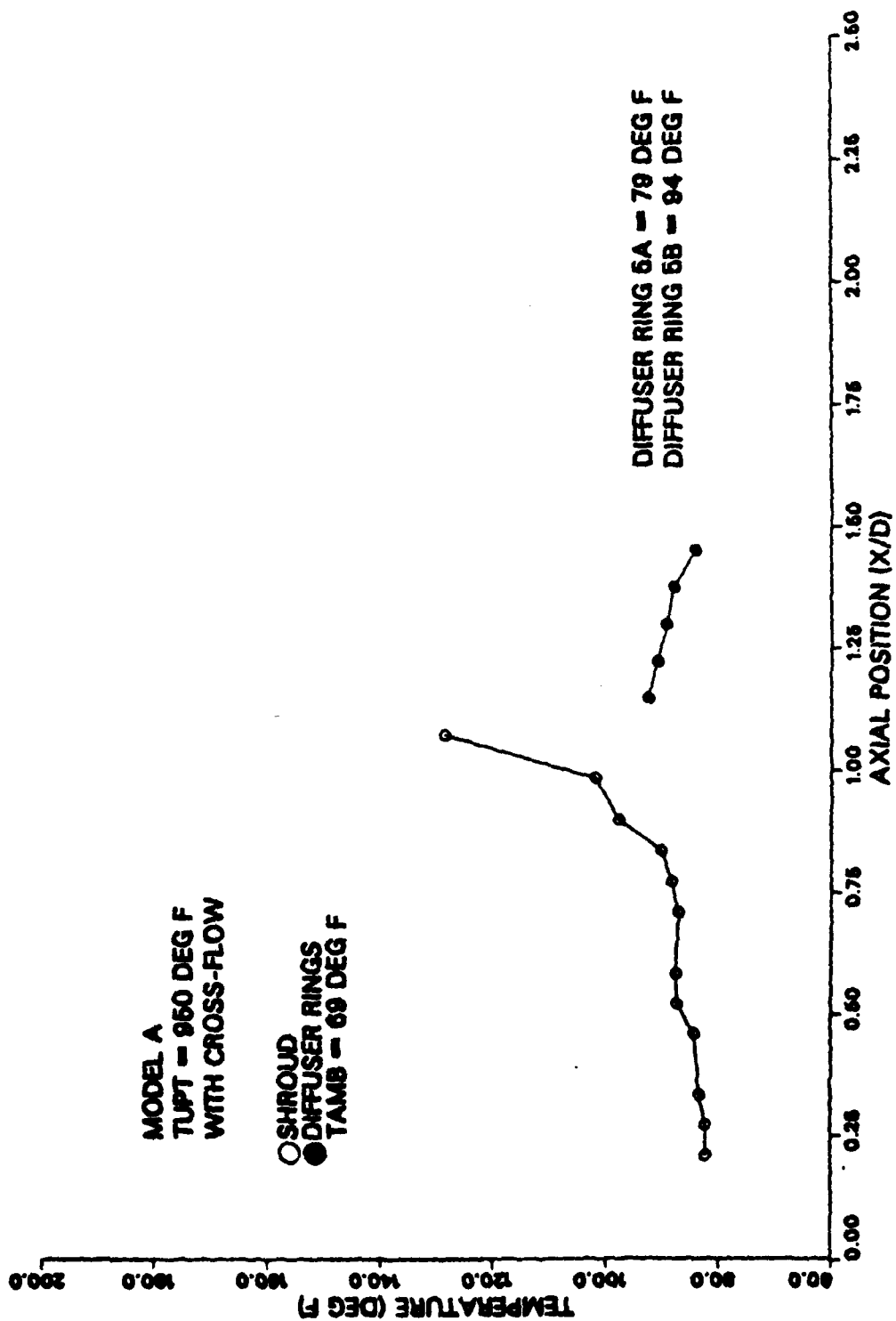


Figure 84. Omega External Temp., Model A (950 F) - Crossflow.

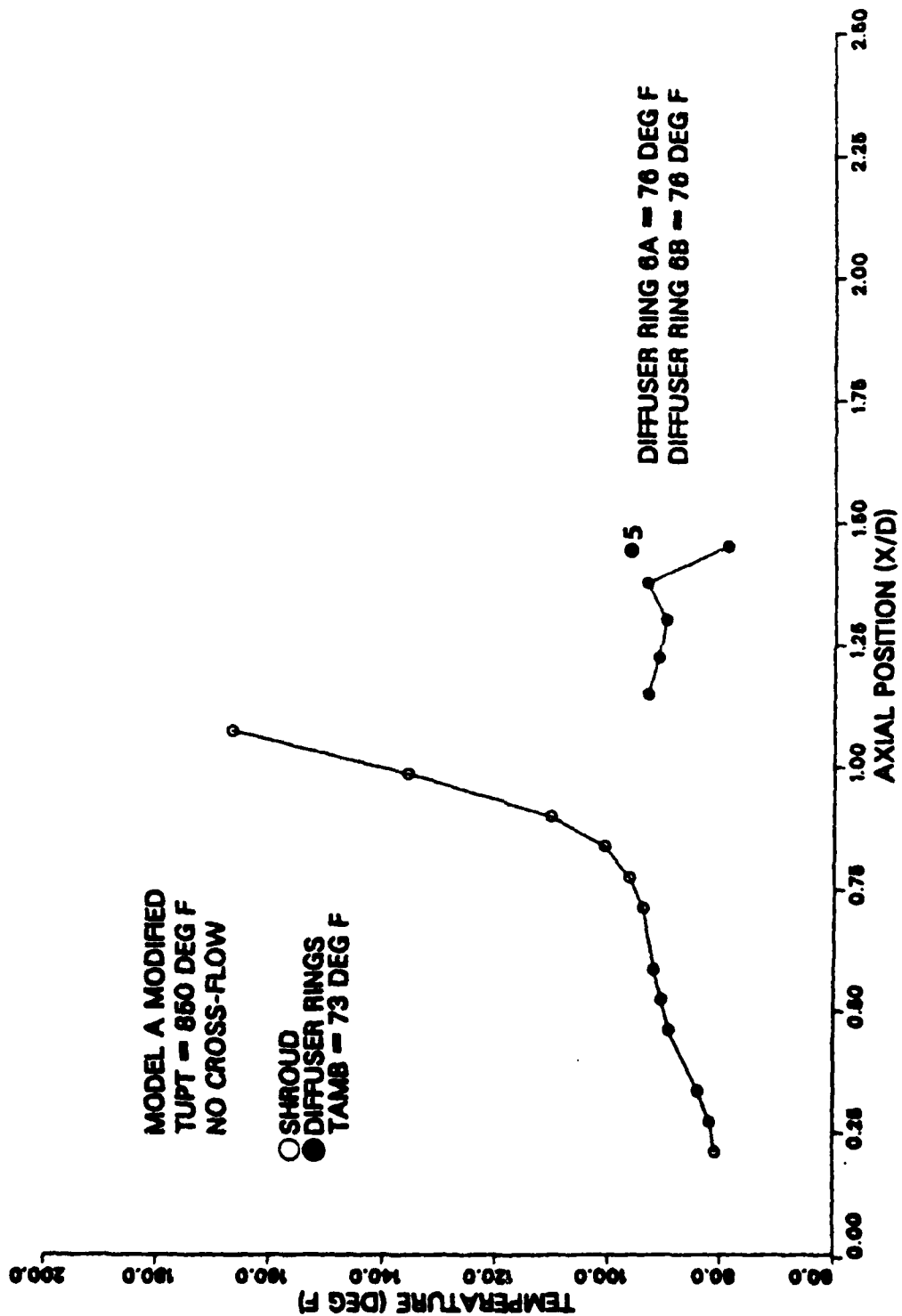


Figure 85. Omega Ext. Temp., Model A Mod (850 F) - No Crossflow.

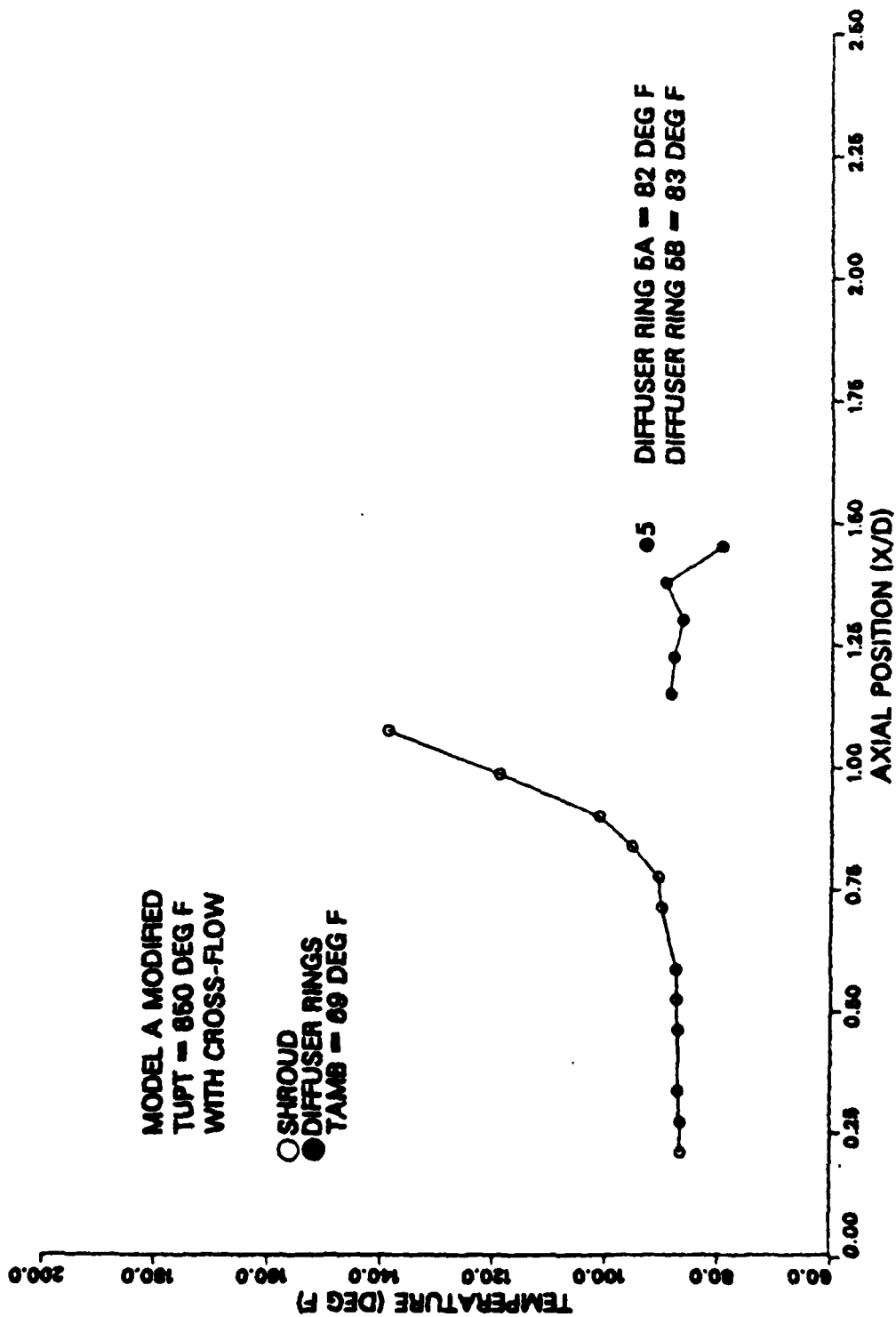


Figure 86. Omega Ext. Temp., Model A Mod (850 F) - Crossflow.

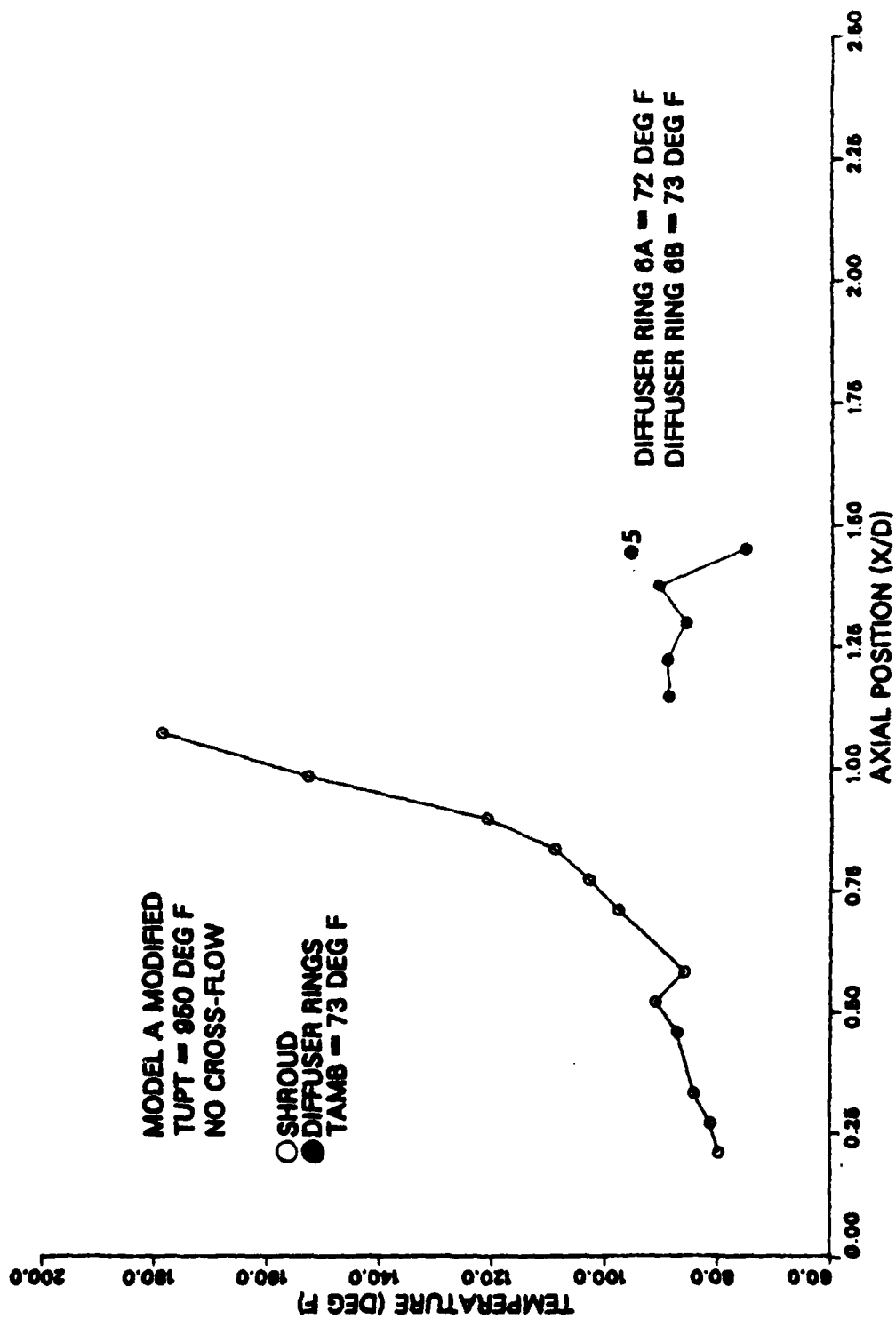


Figure 87. Omega Ext. Temp., Model A Mod (950 F) - No Crossflow.

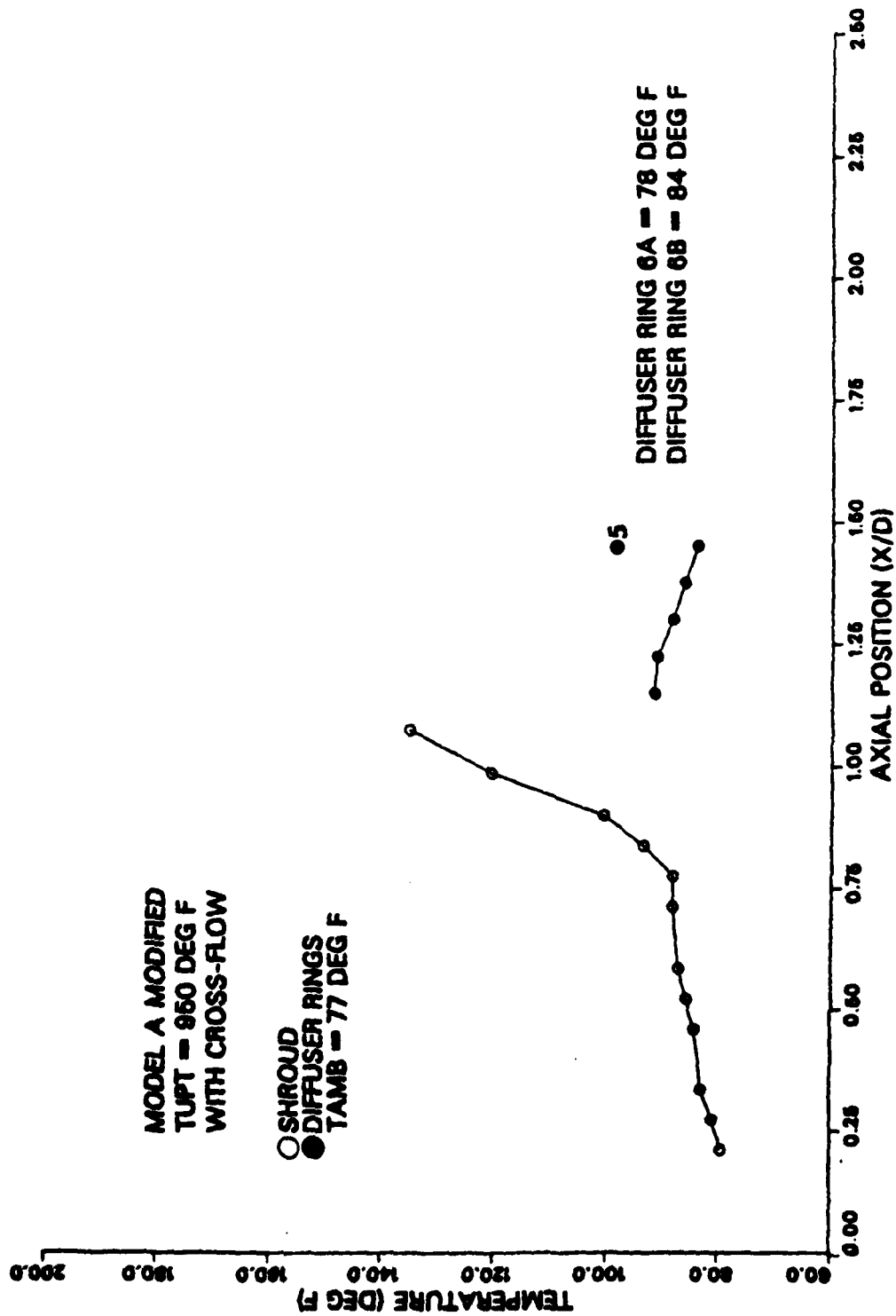


Figure 88. Omega Ext. Temp., Model A Mod (950 F) - Crossflow.

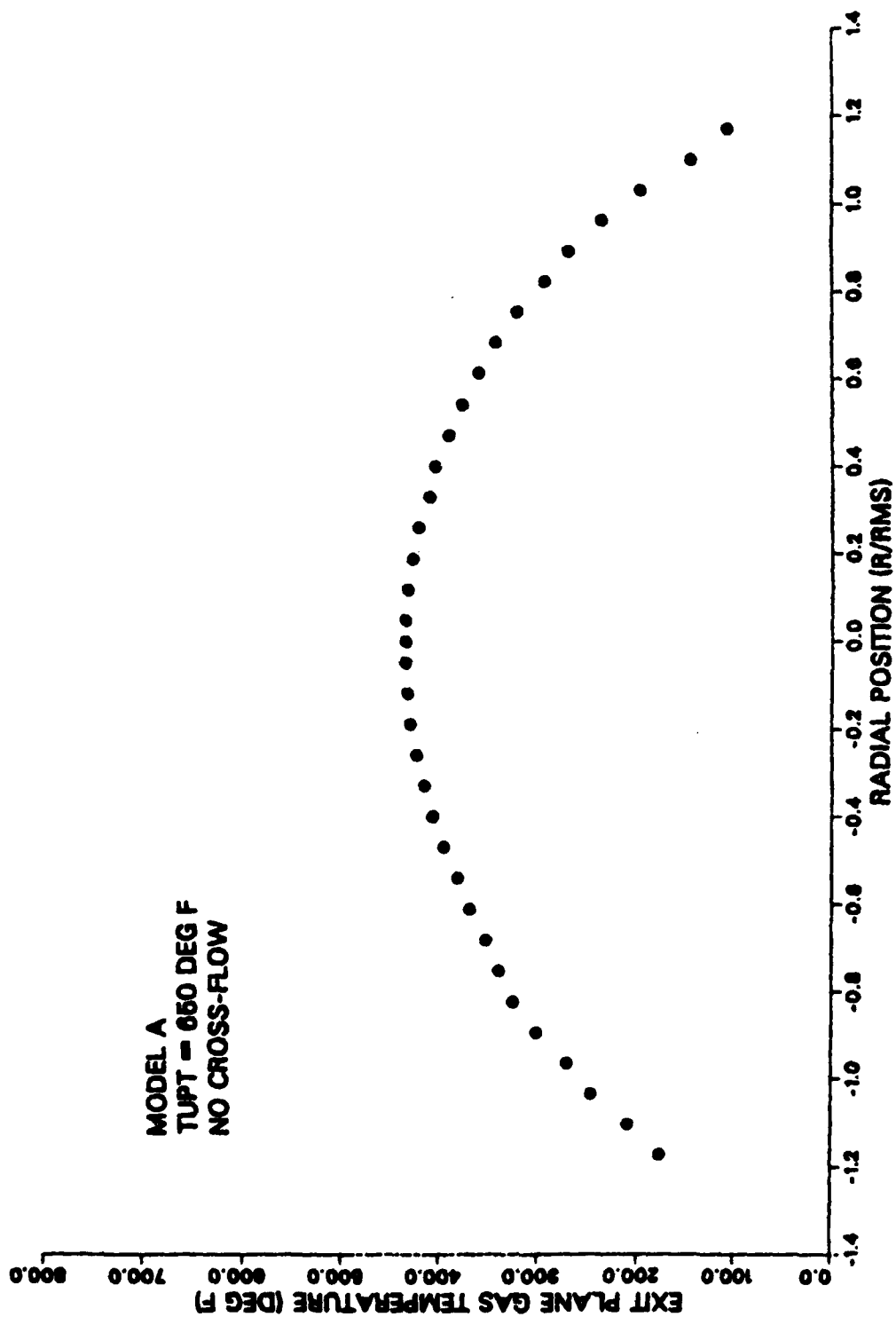


Figure 89. Exit Plane Temp., Model A (650 F) - No Crossflow.

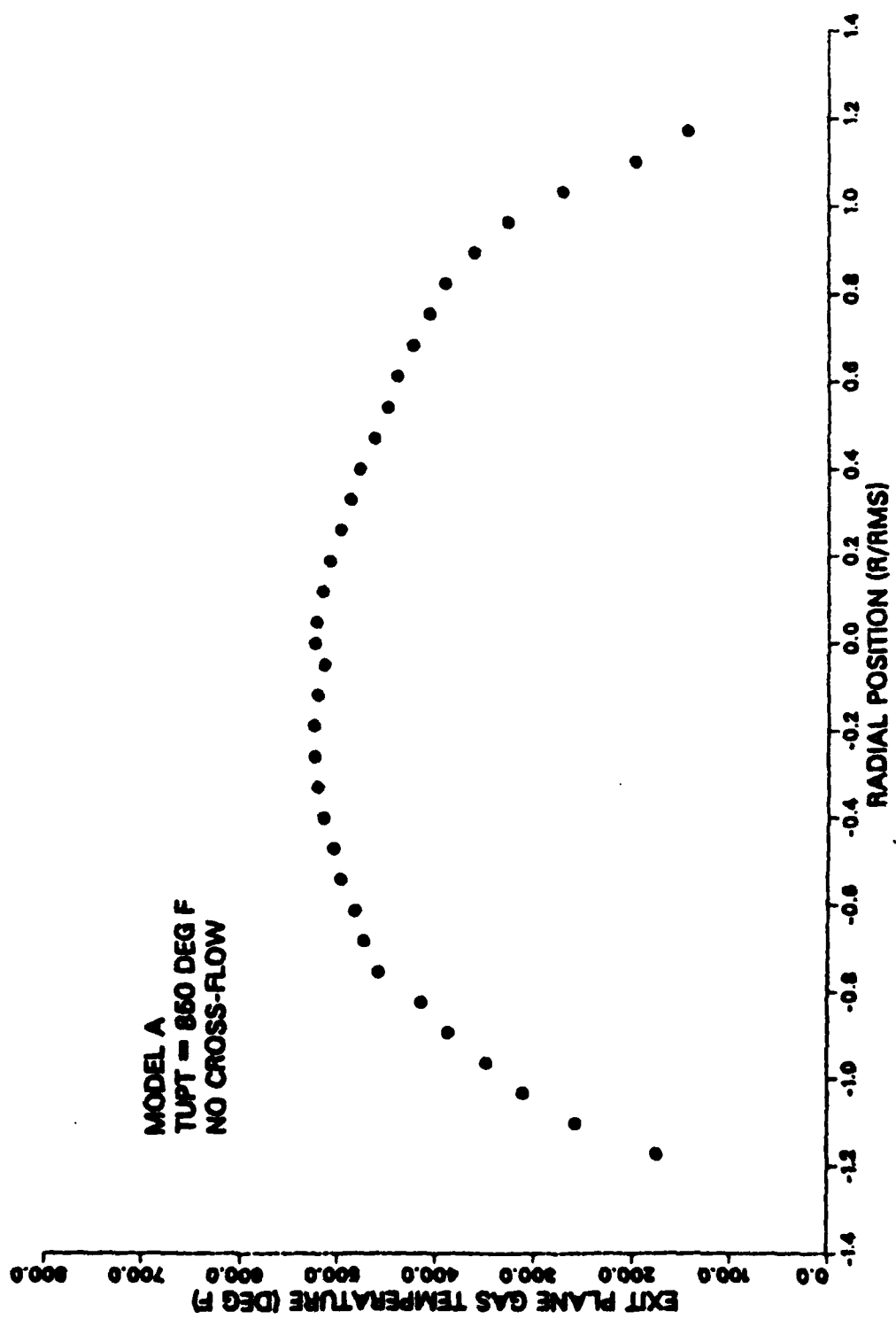


Figure 90. Exit Plane Temp., Model A (850 F) - No Crossflow.

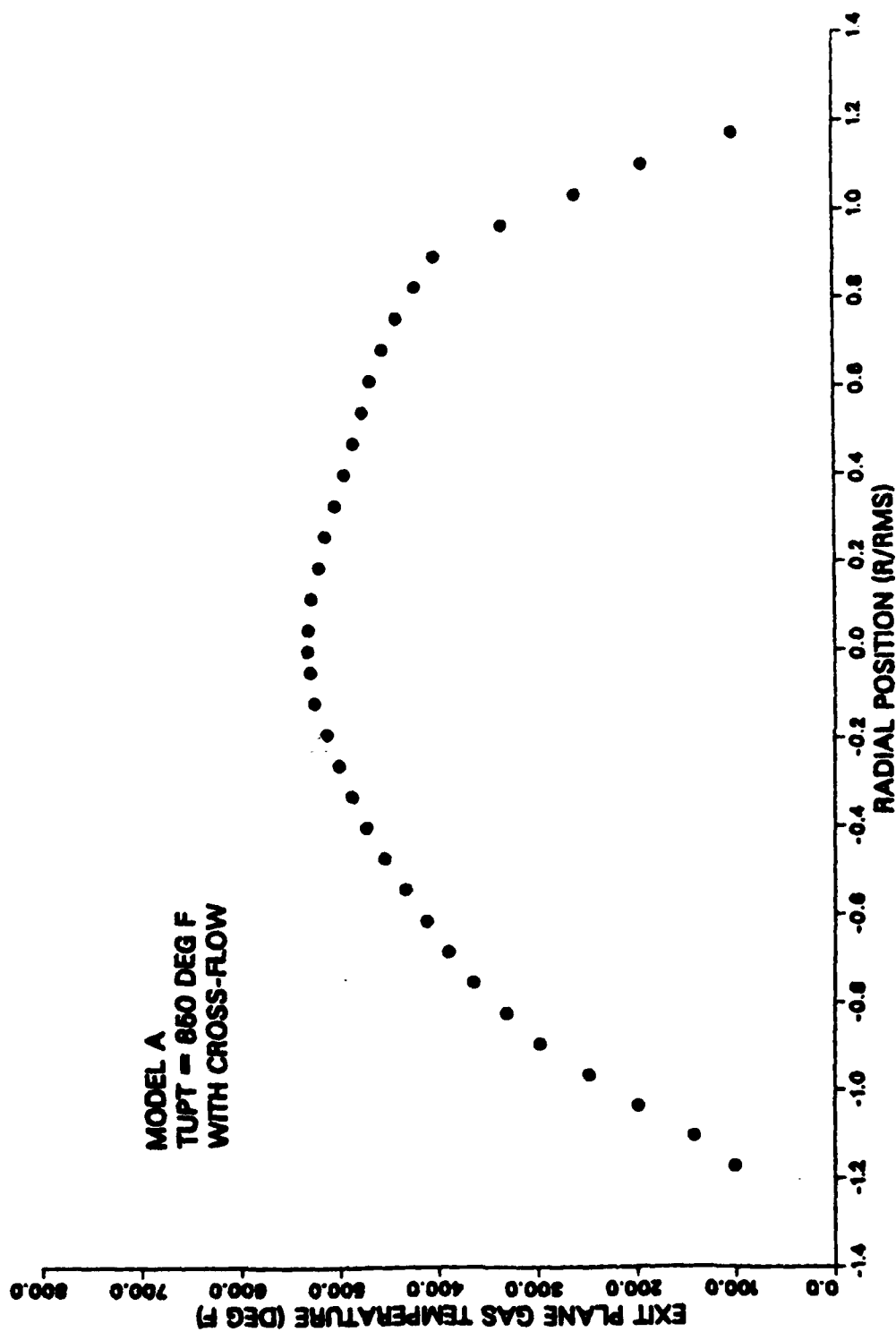


Figure 91. Exit Plane Temp., Model A (850 F) - Crossflow.

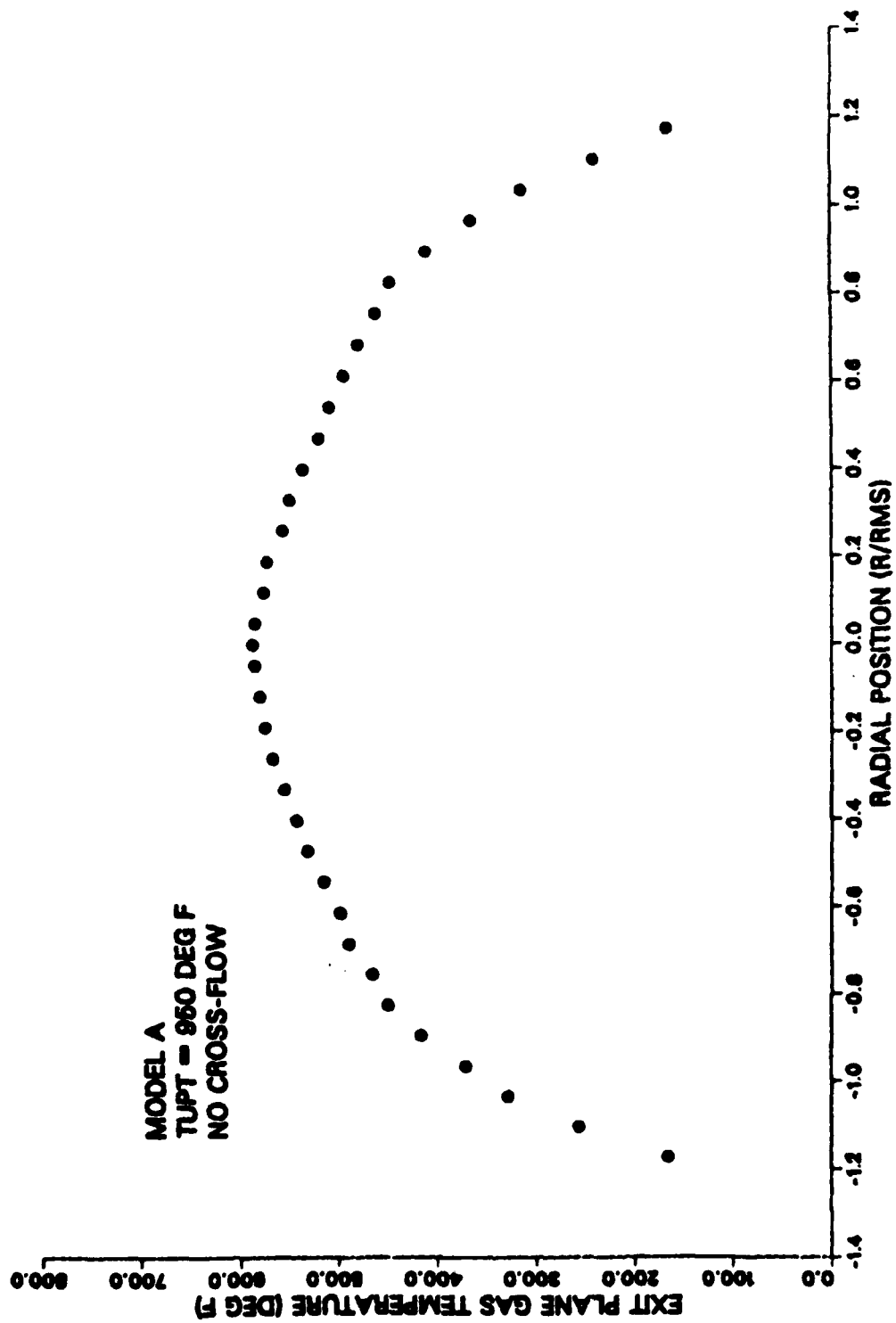


Figure 92. Exit Plane Temp., Model A (950 F) - No Crossflow.

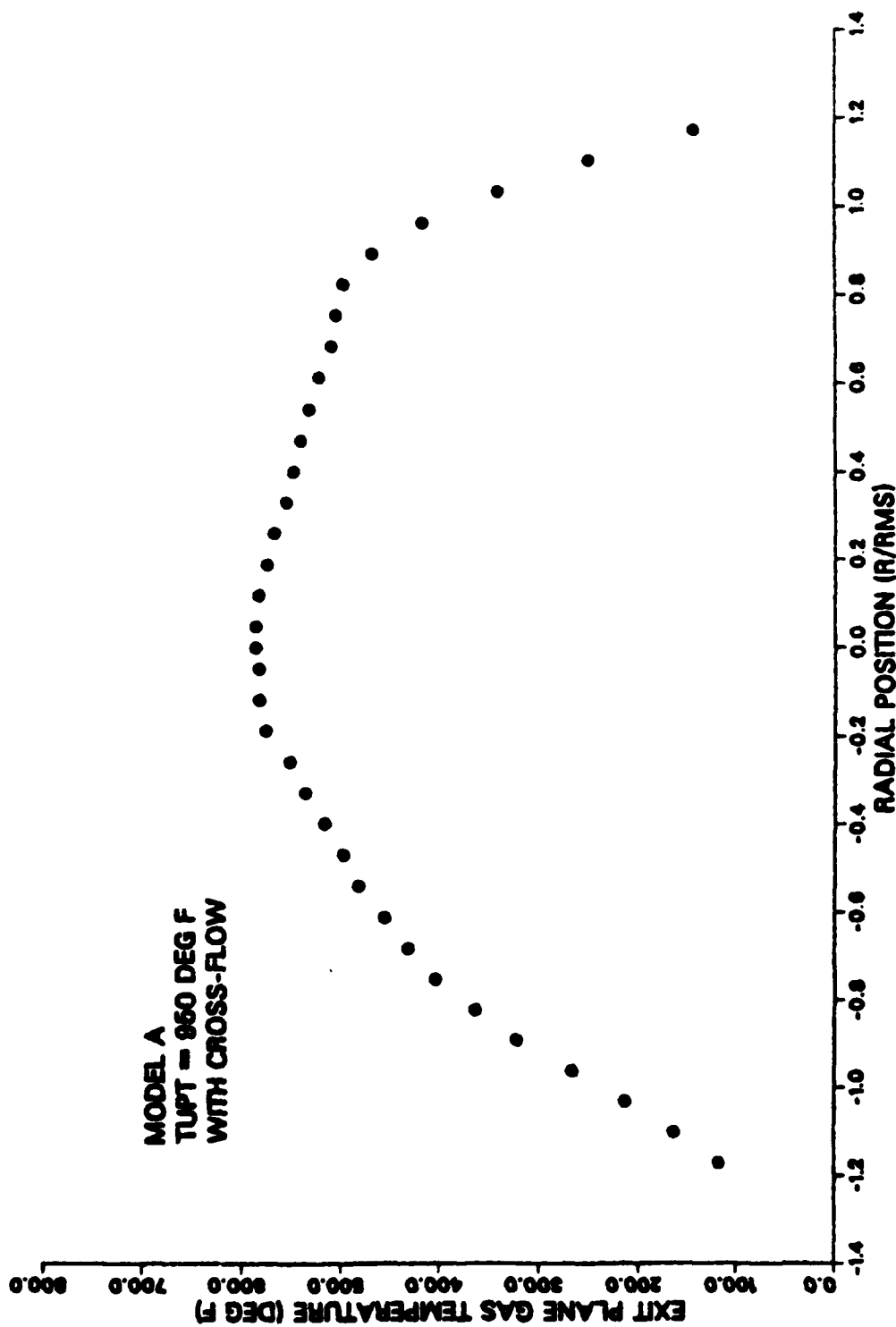


Figure 93. Exit Plane Temp., Model A (950 F) - Crossflow.

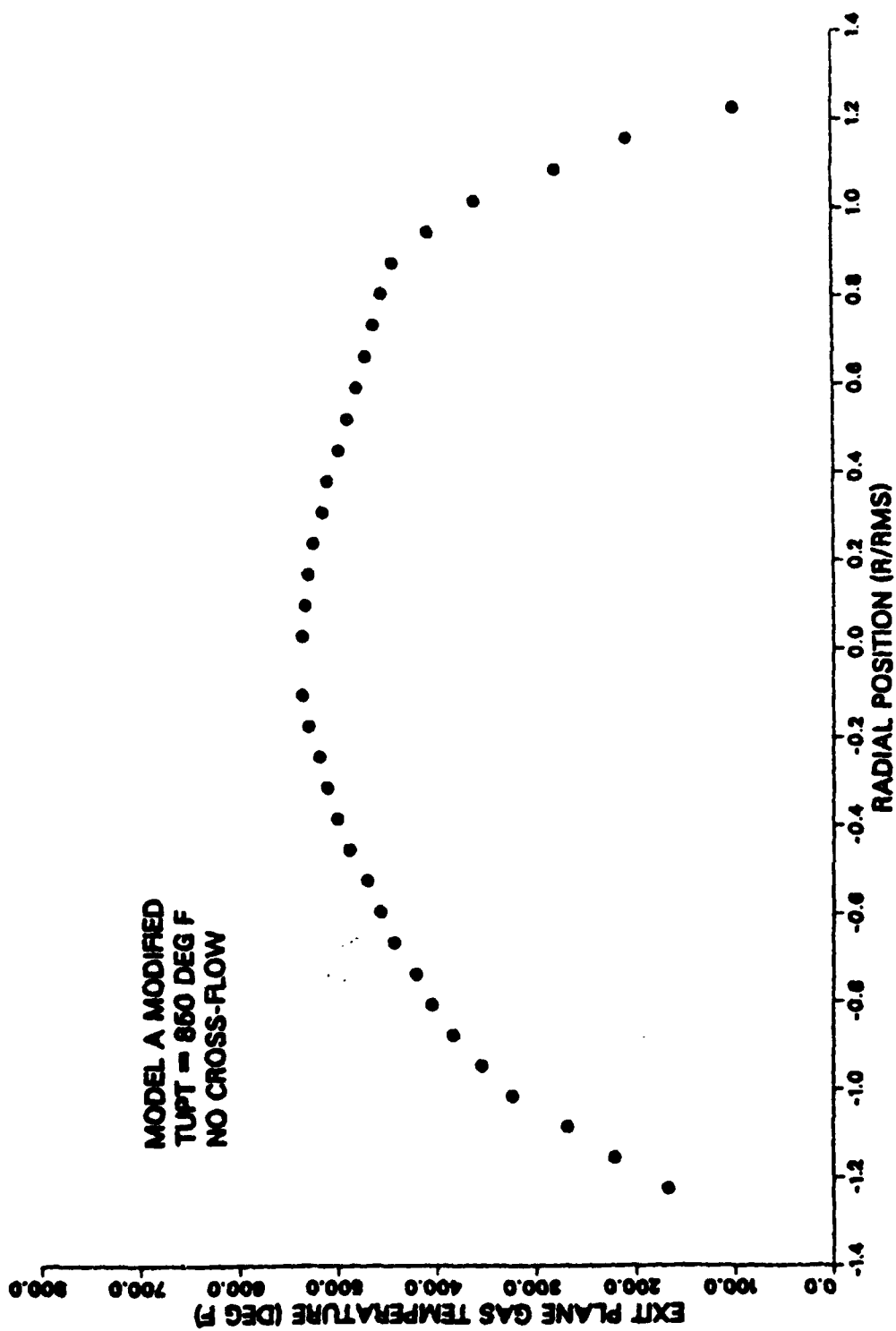


Figure 94. Exit Plane Temp., Model A Mod (850 F) - No Crossflow.

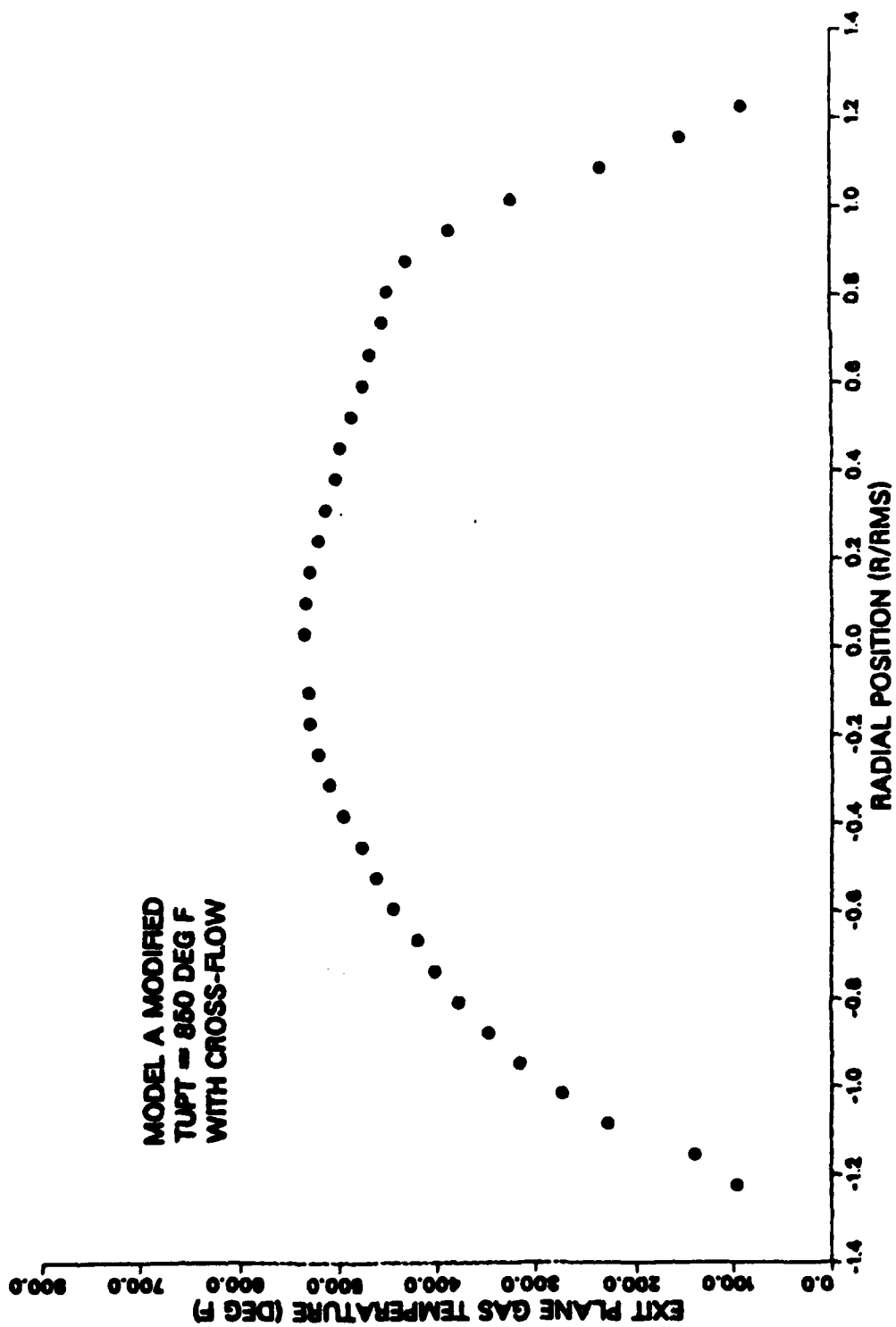


Figure 95. Exit Plane Temp., Model A Mod (850 F) - Crossflow.

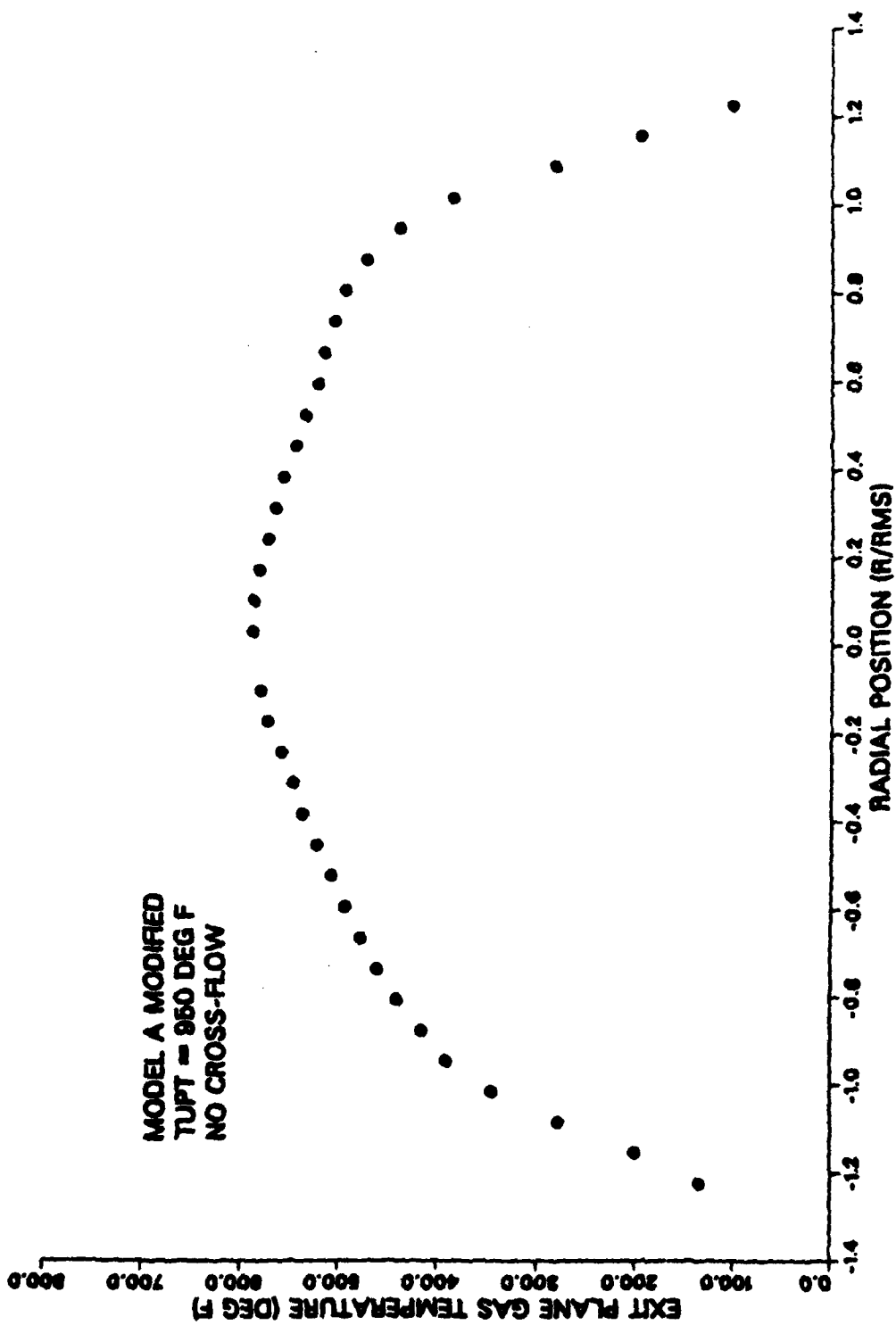


Figure 96. Exit Plane Temp., Model A Mod (950 F) - No Crossflow.

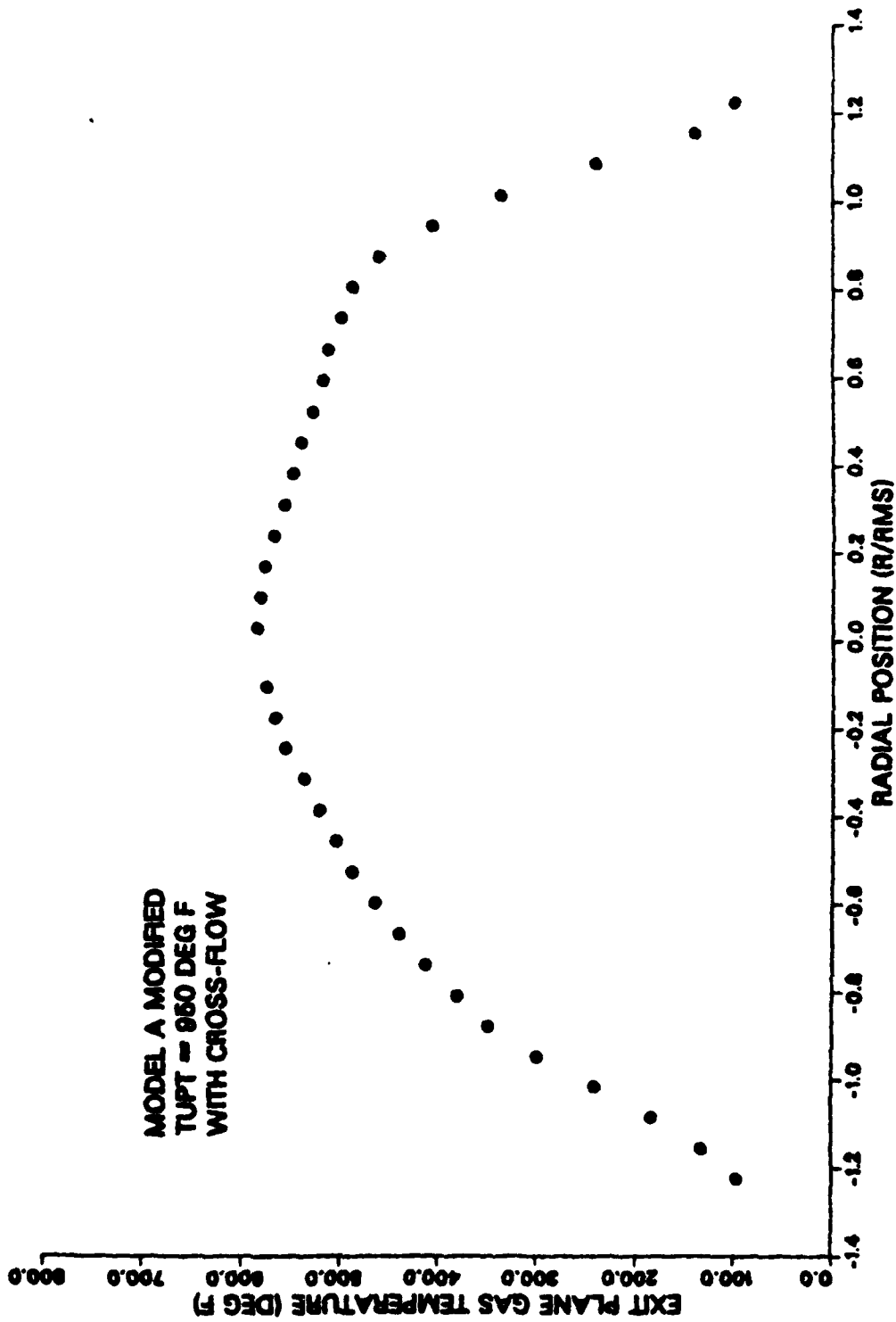


Figure 97. Exit Plane Temp., Model A Mod (950 F) - Crossflow.

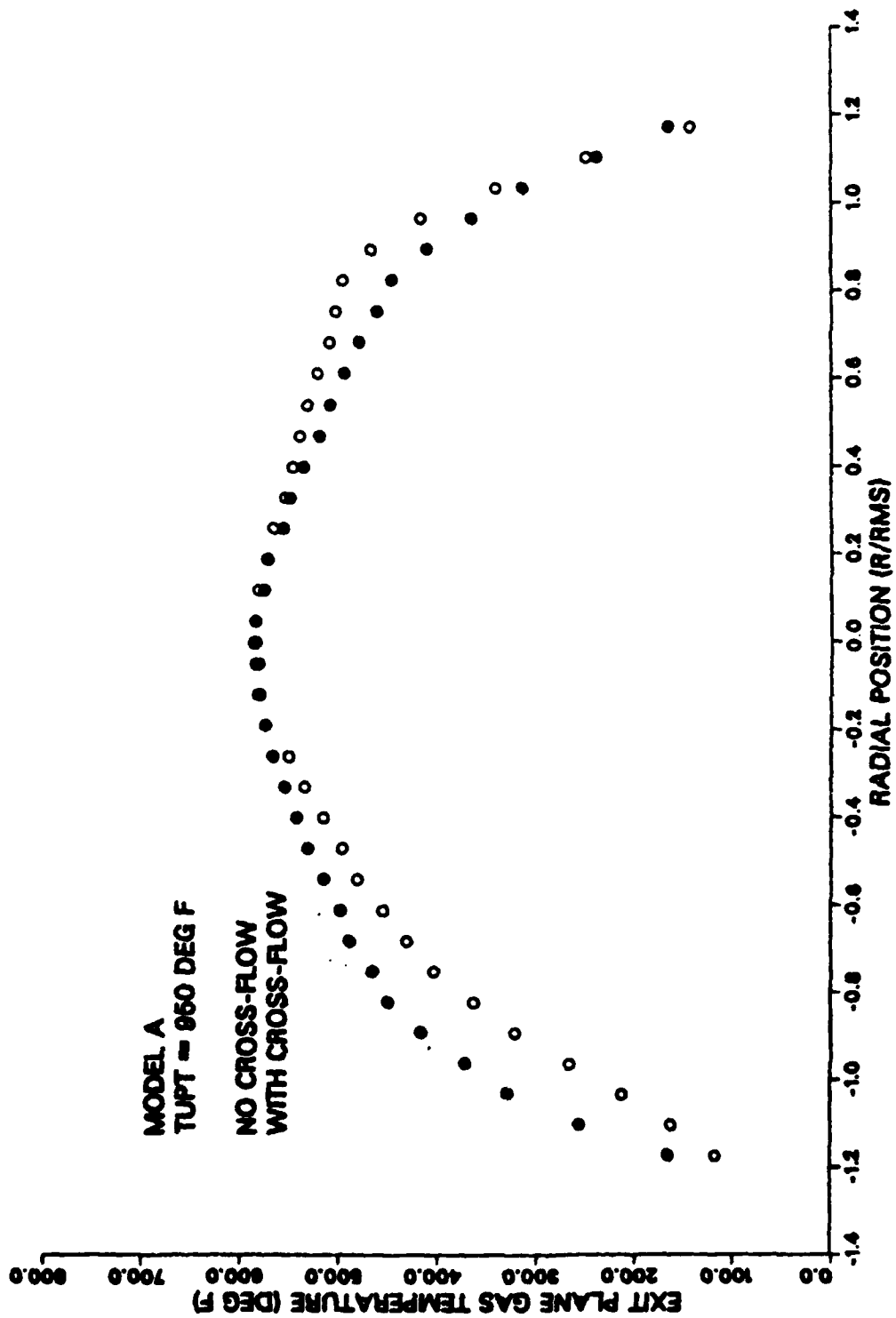


Figure 98. Exit Plane Temp. Comparison, Model A (950 F).

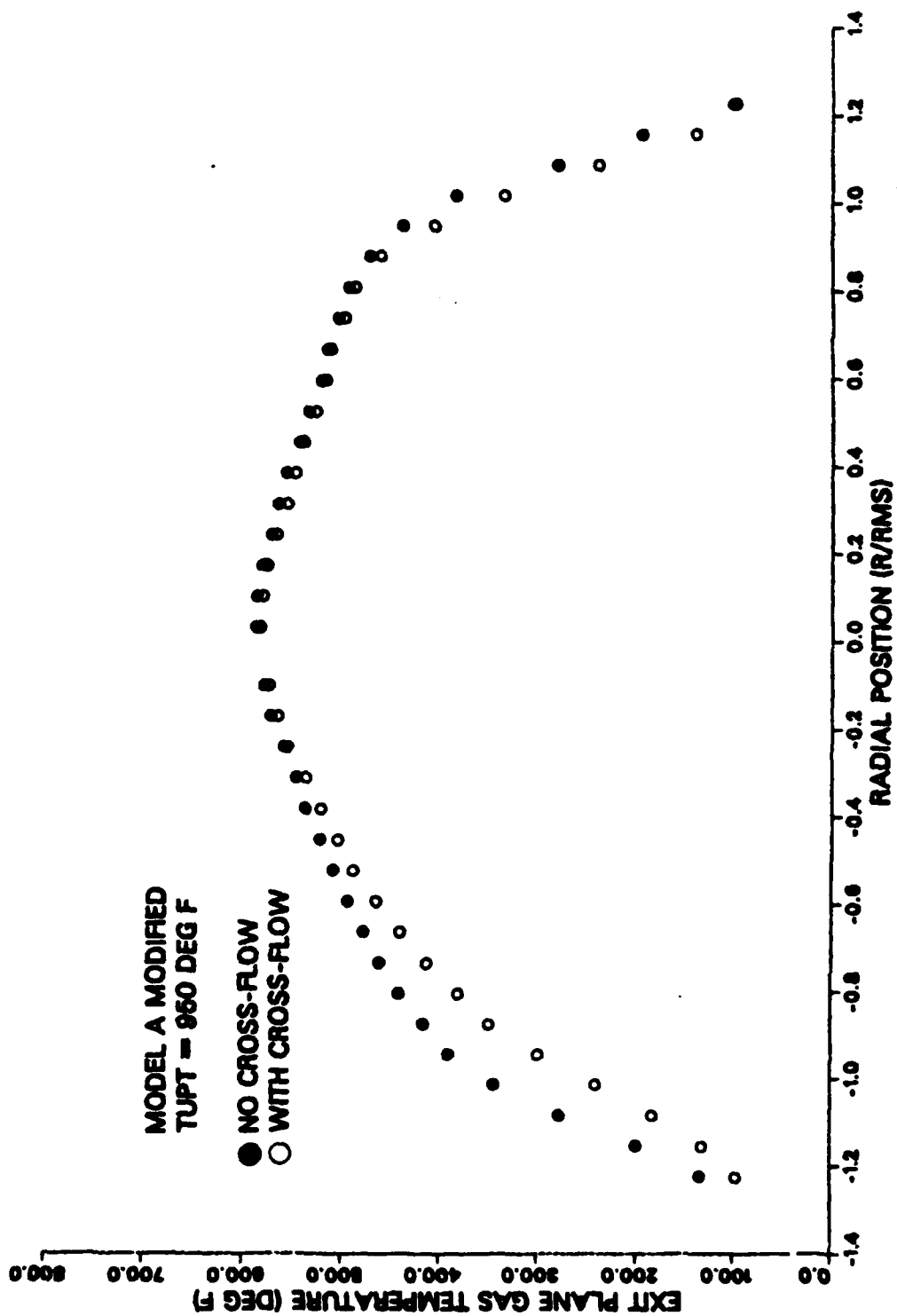


Figure 99. Exit Plane Temp. Comparison, Model A Mod (950 F).

TABLE I
Rotameter Calibration Data

Rotameter Reading	Weight Empty (gr.)	Weight Full (gr.)	Net Weight (gr.)	Time (sec.)	Mass Flow lbm/sec	Flow Rate GPH
08	67.0	29.5	37.5	120	0.689	0.345
09	84.0	30.7	53.3	120	0.979	0.490
10	103.3	31.8	71.5	120	1.314	0.657
15	173.1	31.1	142.0	120	2.609	1.306
20	256.7	31.6	225.1	120	4.136	2.070
25	381.4	31.9	349.5	120	6.421	3.214
30	520.0	31.8	488.2	120	8.696	4.489
35	342.9	32.4	310.5	60	11.41	5.710
40	397.8	32.1	365.7	60	13.44	6.725
43	423.3	32.1	391.2	60	14.37	7.194
40	757.7	32.4	725.3	120	13.33	6.669
35	651.5	31.5	620.0	120	11.39	5.701
34	629.3	32.1	597.2	120	10.97	5.491
33	603.2	32.8	570.4	120	10.48	5.245
32	582.5	32.4	550.1	120	10.11	5.058
31	558.8	32.3	526.5	120	9.613	4.841
30	530.0	32.0	498.0	120	9.149	4.579
29	500.8	32.3	468.5	120	8.607	4.308
28	475.4	32.2	443.2	120	8.142	4.075
27	450.5	31.4	419.1	120	7.700	3.854
26	426.5	32.4	394.1	120	7.240	3.624
25	395.9	31.2	364.7	120	6.700	3.353
20	267.1	32.2	234.9	120	4.316	2.160
15	169.0	31.9	137.1	120	2.519	1.261
10	104.6	31.9	72.7	120	1.336	0.669
08	72.1	31.6	40.5	120	0.744	0.372

NOTES

- 1) Average fuel temperature 61.7° F
- 2) Fuel: Number two diesel; specific gravity = 0.862

TABLE II

Thermocouple Display Channel Assignments, Type K

<u>Channel</u>	<u>Assignment</u>
1	Exit Plane (TEP)
2	Plenum Ambient Temp.
3	Uptake (TUPT)
4	Burner (TBURN)
5	Nozzle box at the position of the removed burner
6	Mixing Stack, Thermocouple (10)
7	Mixing Stack, Thermocouple (5)
8	Mixing Stack, Thermocouple (9)
9	Mixing Stack, Thermocouple (8)
10	Mixing Stack, Thermocouple (12)
11	Mixing Stack, Thermocouple (7)
12	Mixing Stack, Thermocouple (4)
13	Mixing Stack, Thermocouple (1)
14	Mixing Stack, Thermocouple (6)
15	Mixing Stack, Thermocouple (3)
16	Mixing Stack, Thermocouple (11)
17	Mixing Stack, Thermocouple (2)
18	UNUSED

TABLE III

Thermocouple Display Channel Assignments, Type T

<u>Channel</u>	<u>Assignment</u>
1	Fuel Supply
2	Ambient Air (TAMB)
3	Inlet Air Supply (TNH)
4	UNUSED
5	Model A, Diffuser Ring 2
6	Model A, Diffuser Ring 3
7	Model A Shroud, $X/D=0.625$
8	Model A, Diffuser Ring 5
9	Model A Shroud, $X/D=0.750$
10	Model A, Diffuser Ring 5A
11	Model A, Diffuser Ring 5B
12	Model A, Diffuser Ring 1
13	Model A Shroud, $X/D=1.068$
14	Model A Shroud, $X/D=0.125$
15	Model A Shroud, $X/D=0.375$
16	UNUSED
17	Model A, Diffuser Ring 4
18	UNUSED

TABLE IV
Model Characteristics

	<u>Model A</u>	<u>Model A Modified</u>
Mixing Stack Assembly L/D (overall)	1.5	1.5
Mixing Stack Inside Diameter (D)	7.122	7.122
L/D	1.0	1.0
Rows of Film Cooling Slots	4	4
Shroud Start Position (X/D)	0.15	0.15
Diffuser Number of Rings	5	6
Ring Length (L/D)	0.101	0.101
Half Angle	10	10
Film Cooling Clearance	0.188	0.188
Stand-off Distance (S/D)	0.5	0.5
Primary Nozzles Number	4	4
Type	tilted-angled (15/20)	tilted-angled (15/20)
Am/Ap	2.5	2.5

TABLE V

Pumping Coeff. Data, Model A (175 F) - No Crossflow

900 MUT RIG PERFORMANCE 000 TUPH: 174

DATA TAKEN BY R.E. STAPLES
 MIXING STACK LENGTH: 7.22 INCHES
 MIXING STACK DIAMETER: 7.122 INCHES
 MIXING STACK L/D: 1.50
 STANDOFF RATIO: 0.50
 AMBIENT PRESSURE: 29.68 INCHES HG

DATE: 10 SEP 63
 NUMBER OF PRIMARY NOZZLES: 4
 PRIMARY NOZZLE DIAMETER: 2.25 INCHES
 ORIFICE DIAMETER: 7.510 INCHES
 AREA RATIO, ORIF/AN: 2.50
 CAVIT: 1.3901

NO	PMH IN HG	DELPH IN H ₂ O	TAP DEG F	MOFA	TRUEN DEG F	TUPT DEG F	TAMP DEG F	PUPH IN H ₂ O	PPLN IN H ₂ O	SEC AREA SQ IN
1	3.00	12.50	187.1	0.0	181.0	184.0	70.7	5.30	2.90	0.000
2	3.00	12.50	187.1	0.0	181.0	185.0	71.0	5.60	2.55	1.767
3	3.10	12.40	187.4	0.0	181.0	185.0	71.2	5.90	2.25	3.534
4	3.10	12.40	187.4	0.0	181.0	185.0	70.8	6.20	1.95	5.301
5	3.10	12.40	187.9	0.0	181.0	185.0	71.1	6.55	1.55	8.443
6	3.10	12.30	188.0	0.0	181.0	186.0	71.4	6.90	1.25	11.585
7	3.10	12.30	188.1	0.0	181.0	186.0	70.9	7.10	1.00	14.726
8	3.10	12.30	188.0	0.0	181.0	186.0	71.3	7.50	0.50	27.493
9	3.10	12.30	188.4	0.0	181.0	186.0	71.3	7.70	0.30	34.859
10	3.10	12.30	188.5	0.0	181.0	186.0	71.7	7.80	0.20	52.425
11	3.20	12.30	188.8	0.0	181.0	186.0	71.4	7.95	0.10	64.992
12	3.20	12.30	189.4	0.0	182.0	187.0	71.4	8.00	0.00	99.999

NO	WPA LBM/S	WV LBM/S	WS LBM/S	WC	W?	TP	Pp/10	WOTOP-44 FT/S	UP FT/S	UM FT/S	UU FT/S	UPALM
1	1.489	0.000	1.489	0.000	0.000	0.824	0.323	0.000	222.8	88.9	78.4	0.0630
2	1.489	0.000	1.489	0.095	0.233	0.823	0.284	0.059	227.9	93.7	78.4	0.0631
3	1.484	0.000	1.484	0.178	0.207	0.823	0.252	0.110	222.1	97.5	78.2	0.0628
4	1.484	0.000	1.484	0.249	0.180	0.823	0.218	0.154	222.0	100.9	78.1	0.0628
5	1.484	0.000	1.484	0.354	0.143	0.823	0.174	0.219	221.7	105.9	78.0	0.0627
6	1.478	0.000	1.478	0.436	0.116	0.823	0.141	0.271	220.9	109.6	77.8	0.0624
7	1.477	0.000	1.477	0.496	0.093	0.822	0.113	0.308	220.7	112.4	77.7	0.0624
8	1.478	0.000	1.478	0.649	0.047	0.822	0.057	0.403	220.5	119.8	77.6	0.0623
9	1.477	0.000	1.477	0.735	0.024	0.822	0.034	0.456	220.3	123.9	77.6	0.0623
10	1.477	0.000	1.477	0.789	0.019	0.823	0.023	0.490	220.2	126.6	77.5	0.0623
11	1.474	0.000	1.474	0.642	0.009	0.823	0.011	0.429	220.5	121.9	77.6	0.0623
12	1.478	0.000	1.478	0.000	0.000	0.821	0.000	0.000	220.7	88.1	77.7	0.0623

TABLE VI

Pumping Coeff. Data, Model A (650 F) - No Crossflow

TUP1: 650

*** HOT RIG PERFORMANCE ***
5 MIN. DIFFUSERDATA TAKEN BY R.E. STAPLES
WIRING STACK LENGTH: 1.22 INCHES
WIRING STACK DIAMETER: 7.122 INCHES
WIRING STACK L/D: 1.50
WIRING STACK AREA: 0.50
WIRING STACK SURF: 30.51 INCHES MG
WIRING STACK SURF: 30.51 INCHES MGDATE: 10 AUG 63
NUMBER OF PRIMARY NOZZLES: 2.25 INCHES
PRIMARY NOZZLE DIAMETER: 7.510 INCHES
PRIMARY NOZZLE AREA: 4.50
PRIMARY NOZZLE SURF: 2.50
CAMERA: 1.3741

NR	PRN IN MG	VELPH IN H2O	TAN DEC F	WOTA	TQUN DEC F	TUPT DEC F	TAMT DEC F	PUMP IN H2O	PRN IN H2O	SEC AREA SQ IN	UP F1/S	UU F1/S	UPACH
1	3.00	6.20	185.9	25.0	1190.0	654.0	66.8	5.00	2.48	0.000	93.7	0.0578	
2	3.00	6.20	185.7	25.0	1185.0	653.0	67.5	5.30	2.20	1.167	93.5	0.0577	
3	3.10	6.20	186.0	25.0	1190.0	653.0	68.3	5.60	1.93	3.534	93.6	0.0578	
4	3.10	6.20	185.9	25.0	1192.0	654.0	68.9	5.80	1.67	5.301	93.5	0.0577	
5	3.10	6.20	186.3	25.0	1194.0	654.0	69.7	6.10	1.32	8.443	93.4	0.0577	
6	3.10	6.20	186.4	25.0	1192.0	654.0	69.8	6.30	1.08	11.585	93.4	0.0576	
7	3.10	6.20	186.2	25.0	1195.0	654.0	69.7	6.50	0.88	14.720	93.5	0.0577	
8	3.10	6.20	186.5	25.0	1194.0	655.0	69.1	6.90	0.60	27.293	93.6	0.0578	
9	3.20	6.20	186.2	25.0	1192.0	655.0	68.2	7.10	0.25	39.059	93.5	0.0577	
10	3.20	6.20	186.6	25.0	1193.0	656.0	68.0	7.20	0.17	52.425	93.5	0.0577	
11	3.20	6.20	186.3	25.0	1195.0	656.0	68.2	7.20	0.12	64.092	93.3	0.0576	
12	3.20	6.20	186.9	25.0	1195.0	653.0	65.6	7.30	0.00	99.000	93.3	0.0576	
NR	PRN LPM/S	VELPH LPM/S	TAN LPM/S	WOTA LPM/S	TQUN LPM/S	TUPT LPM/S	TAMT LPM/S	PUMP LPM/S	PRN LPM/S	SEC AREA SQ IN	UP F1/S	UU F1/S	UPACH
1	1.049	0.007	1.056	0.000	0.000	0.154	0.473	0.327	0.000	265.6	100.0	93.7	0.0578
2	1.049	0.007	1.056	0.000	0.000	0.137	0.474	0.290	0.001	265.2	110.1	93.5	0.0577
3	1.050	0.007	1.057	0.100	0.154	0.120	0.473	0.254	0.114	265.4	113.9	93.6	0.0578
4	1.050	0.007	1.057	0.235	0.222	0.104	0.473	0.220	0.160	265.5	117.1	93.6	0.0578
5	1.050	0.007	1.057	0.132	0.214	0.085	0.473	0.174	0.226	265.2	121.6	93.5	0.0577
6	1.050	0.007	1.057	0.413	0.191	0.067	0.472	0.142	0.281	265.0	125.3	93.5	0.0577
7	1.050	0.007	1.057	0.473	0.448	0.055	0.473	0.116	0.322	264.9	128.1	93.4	0.0576
8	1.050	0.007	1.057	0.592	0.500	0.025	0.472	0.053	0.440	264.8	131.6	93.5	0.0577
9	1.052	0.007	1.059	0.683	0.445	0.016	0.471	0.031	0.464	264.1	136.1	93.6	0.0577
10	1.051	0.007	1.058	0.741	0.300	0.011	0.471	0.022	0.503	263.2	140.8	93.6	0.0577
11	1.052	0.007	1.059	0.772	0.324	0.007	0.471	0.016	0.524	263.3	142.3	93.6	0.0577
12	1.051	0.007	1.058	0.800	0.300	0.000	0.472	0.000	0.000	264.4	105.5	93.3	0.0576

Pumping Coeff. Data, Model A (850 F) - No Crossflow

168

Pumping Coeff. Data, Model A (850 F) - Crossflow

169

TABLE XI

Pumping Coeff. Data, Model A (950 F) - No Crossflow

TUMT: 950

*** MWT MIC PERFORMANCE ***
S RING DIFFUSER

DATE: 02 SEP 83
 NUMBER OF PRIMARY NOZZLES: 2.25 INCHES
 MIXING NOZZLE DIAMETER: 7.510 INCHES
 MIXING STACK L/D: 1.50
 MIXING STACK LENGTH: 7.122 INCHES
 STANDOFF HEIGHT: 0.50 INCHES
 AMBIENT PRESSURE: 30.58 INCHES HG
 GAMMA: 1.3556

DATA TAKEN BY P.E. STAPLES

IN	QMA IN HG	UELPA IN H2O	YMA DEC F	ROTA	TUWEN DEC F	TUPT DEC F	TAMU DEC F	PUMT IN H2O	PPLN IN H2O	SEC AREA SQ IN	UM FT/S	UW FT/S	UMACM
1	4.10	5.00	184.2	31.5	1255.0	951.0	71.0	6.80	3.00	0.000	107.7	107.7	0.0595
2	4.10	5.00	184.6	31.5	1255.0	950.0	72.2	7.10	2.05	1.767	107.5	107.5	0.0594
3	4.10	5.00	184.7	31.5	1255.0	949.0	72.7	7.40	2.30	3.534	107.4	107.4	0.0593
4	4.10	5.00	184.6	31.5	1257.0	944.0	72.9	7.70	2.05	5.001	107.3	107.3	0.0593
5	4.10	5.00	184.9	31.5	1257.0	950.0	73.5	8.00	1.63	8.443	107.3	107.3	0.0592
6	4.10	5.00	184.9	31.5	1255.0	950.0	71.7	8.30	1.32	11.585	107.2	107.2	0.0592
7	4.20	5.00	184.9	31.5	1255.0	951.0	73.0	8.50	1.08	14.726	107.1	107.1	0.0593
8	4.20	5.00	184.8	31.5	1255.0	953.0	71.5	9.00	0.52	27.293	107.0	107.0	0.0594
9	4.20	5.00	185.1	31.5	1255.0	954.0	73.3	9.10	0.25	39.859	107.0	107.0	0.0593
10	4.20	5.00	185.4	31.5	1255.0	954.0	73.0	9.40	0.20	52.425	107.0	107.0	0.0592
11	4.20	5.00	185.3	31.5	1255.0	953.0	73.5	9.40	0.15	64.492	107.0	107.0	0.0592
12	4.20	5.00	186.0	31.5	1255.0	957.0	73.4	9.50	0.00	86.622	107.0	107.0	0.0592

TABLE X

Pumping Coeff. Data, Model A (950 F) - Crossflow

IUP1: 950

999 MUI RIG PERFORMANCE 999
999 MUI RIG DIFFUSER

IN CROSS-FLOW

DATA TAKEN BY D.E. STAPLES

MIXING STACK LENGTH: 7.22 INCHES
MIXING STACK DIAMETER: 7.122 INCHES
MIXING STACK L/D: 1.50
STANDOFF RATIO: 0.50
AMBIENT PRESSURE: 29.68 INCHES HGDATE: 04 SEP 63
NUMBER OF PRIMARY NOZZLES: 4
PRIMARY NOZZLE DIAMETER: 2.25 INCHES
UNITARY NOZZLE DIAMETER: 7.510 INCHES
STANDOFF RATIO: 0.50
CORRECTION FACTOR: 1.3556

NO	PMH IN HG	DELPH IN H2O	TMH DEC F	MD1A	TMUPH DEC F	TUMT DEC F	TMH DEC F	TMH IN H2O	PHLM IN H2O	SEC AREA SQ IN	UM FT/S	UU FT/S	UWACH
1	4.50	4.90	182.5	31.5	1197.0	953.0	72.4	7.20	3.25	0.000	124.5	109.1	0.0602
2	4.50	4.80	182.6	31.5	1196.0	949.0	71.7	7.50	2.95	1.767	127.8	107.6	0.0594
3	4.50	4.80	182.6	31.5	1196.0	949.0	70.8	7.80	2.60	3.534	132.0	107.5	0.0594
4	4.50	4.80	183.1	31.5	1201.0	950.0	72.2	8.10	2.30	4.801	134.6	107.4	0.0593
5	4.50	4.80	183.1	31.5	1201.0	951.0	72.0	8.40	1.85	8.443	145.9	107.3	0.0592
6	4.50	4.80	183.3	31.5	1204.0	951.0	71.7	8.80	1.50	11.585	149.6	107.3	0.0592
7	4.50	4.80	183.5	31.5	1206.0	952.0	72.0	9.00	1.25	14.726	150.0	107.5	0.0592
8	4.50	4.80	183.7	31.5	1212.0	956.0	72.1	9.60	0.62	27.293	161.7	107.8	0.0593
9	4.50	4.80	183.2	31.5	1215.0	956.0	71.2	9.80	0.35	34.859	163.2	107.6	0.0593
10	4.50	4.80	183.5	31.5	1212.0	957.0	71.5	10.00	0.22	52.425	164.2	107.7	0.0593
11	4.50	4.80	183.3	31.5	1216.0	958.0	71.6	10.00	0.15	64.992	168.2	107.8	0.0593
12	4.50	4.80	184.3	31.5	1216.0	961.0	71.5	10.10	0.00	99.999	172.5	107.8	0.0593

TABLE XI

Pumping Coeff. Data, Model A Mod (850 F) - No Crossflow

UNIT: 850

DATA TAKEN BY R.E. STAPLES											
DATE: 04 SEP 83											
NUMBER OF PRIMARY NOZZLES: 4											
PRIMARY NOZZLE DIAMETER: 2.25 INCHES											
SECONDARY NOZZLE DIAMETER: 7.125 INCHES											
AREA RATIO: 1.3014											
CAMERA: 1.3014											
MIXING STACK LENGTH: 7.22 INCHES											
MIXING STACK DIAMETER: 7.125 INCHES											
MIXING STACK L/D: 1.50											
STANDOFF HEIGHT: 0.50											
AMBIENT PRESSURE: 29.67 INCHES HG											
UNIT: 850											
NR	QPM IN HG	WFLP IN H2O	TRM DEC F	NOIA DEC F	TUUM DEC F	LUPT DEC F	TAMU DEC F	WUPT IN H2O	PPTN IN H2O	SEC AREA SQ IN	UWACH
1	4.10	5.40	189.3	29.5	1202.0	851.0	72.3	6.60	3.10	0.000	0.0602
2	4.10	5.40	189.5	29.5	1202.0	851.0	73.0	6.90	2.70	1.767	0.0602
3	4.10	5.40	189.9	29.5	1206.0	850.0	74.2	7.20	2.35	3.514	0.0601
4	4.10	5.40	190.2	29.5	1206.0	851.0	73.4	7.50	2.08	5.401	0.0600
5	4.10	5.40	190.4	29.5	1213.0	852.0	73.4	7.80	1.67	8.443	0.0600
6	4.10	5.40	190.4	29.5	1214.0	852.0	74.2	8.10	1.35	11.585	0.0600
7	4.10	5.40	190.8	29.5	1207.0	854.0	75.4	8.10	1.10	14.726	0.0600
8	4.20	5.40	190.5	29.5	1207.0	854.0	73.7	8.80	0.55	27.293	0.0600
9	4.20	5.40	190.6	29.5	1215.0	855.0	75.4	9.00	0.30	34.859	0.0600
10	4.20	5.30	190.8	29.5	1201.0	854.0	75.4	9.10	0.20	52.425	0.0600
11	4.20	5.30	190.5	29.5	1196.0	852.0	74.1	9.20	0.15	64.992	0.0600
12	4.20	5.30	190.9	29.5	1196.0	853.0	74.3	9.30	0.00	88.888	0.0600
NR	QPM LBM/S	WFLP LBM/S	TRM LBM/S	NOIA LBM/S	TUUM LBM/S	LUPT LBM/S	TAMU LBM/S	WUPT LBM/S	PPTN LBM/S	SEC AREA LBM/S	UWACH
1	0.977	0.809	0.985	0.000	0.600	0.157	0.406	0.386	0.000	300.6	120.0
2	0.976	0.809	0.985	0.097	0.699	0.137	0.407	0.337	0.067	300.2	124.7
3	0.976	0.809	0.985	0.182	0.885	0.120	0.408	0.294	0.124	299.6	128.6
4	0.976	0.809	0.985	0.262	0.866	0.106	0.407	0.260	0.174	299.6	132.5
5	0.976	0.809	0.985	0.306	0.872	0.085	0.407	0.209	0.230	299.4	137.6
6	0.976	0.809	0.985	0.452	0.853	0.069	0.407	0.169	0.309	299.2	141.8
7	0.975	0.809	0.984	0.518	0.876	0.056	0.407	0.138	0.354	299.4	145.1
8	0.977	0.809	0.986	0.679	0.889	0.028	0.406	0.069	0.463	299.5	153.0
9	0.977	0.809	0.986	0.732	0.842	0.015	0.407	0.034	0.500	299.5	155.7
10	0.967	0.809	0.976	0.786	0.805	0.010	0.407	0.026	0.542	299.3	157.1
11	0.968	0.809	0.976	0.845	0.665	0.008	0.407	0.019	0.582	295.9	159.7
12	0.967	0.809	0.976	0.800	0.600	0.000	0.407	0.000	0.600	295.9	161.8

Pumping Coeff. Data, Model A Mod (850 F) - Crossflow

173

TABLE XIII

Pumping Coeff. Data, Model A Mod (950 F) - No Crossflow

TUMT: 950

000 INUT RIG PERFORMANCE 000

000 INUT RIG PERFORMANCE 000

DATA TAKEN BY R.E. STAPLES
 MIXING STACK LENGTH: 7.22 INCHES
 MIXING STACK DIAMETER: 7.122 INCHES
 MIXING STACK L/D: 1.50
 STANDOFF MATING: 0.50
 AMBIENT PRESSURE: 29.07 INCHES HG

DATE: 00 SEP 83

NUMBER OF PRIMARY NOZZLES: 2.25 INCHES
 PRIMARY NOZZLE DIAMETER: 7.510 INCHES
 AREA RATIO: 2.50
 CAPAC: 1.3550

NR	PMH IN HG	UCLPA IN H2O	1AM DEC F	MOIA	THUAM DEC F	LUPT DEC F	TAMU DEC F	LUPT IN H2O	PULM IN H2O	SEC AREA SQ IN	UP FT/S	UM FT/S	UU FT/S	UMACH
1	4.40	4.80	144.0	31.5	1224.0	952.0	73.0	7.10	3.15	0.000	304.9	121.7	106.7	0.0584
2	4.40	4.80	141.9	31.5	1224.0	951.0	72.1	7.40	2.78	1.167	304.5	124.5	106.6	0.0566
3	4.40	4.80	144.4	31.5	1224.0	953.0	73.4	7.80	2.43	3.534	304.6	130.7	106.6	0.0588
4	4.50	4.80	144.2	31.5	1227.0	952.0	73.4	8.10	2.13	4.801	304.7	133.2	106.7	0.0569
5	4.50	4.80	144.5	31.5	1226.0	952.0	73.0	8.40	1.70	8.443	304.3	139.7	106.6	0.0582
6	4.50	4.80	144.4	31.5	1225.0	952.0	73.3	8.70	1.38	11.545	304.0	143.4	106.5	0.0582
7	4.50	4.80	144.4	31.5	1226.0	952.0	73.4	8.90	0.55	14.726	303.8	147.1	106.4	0.0587
8	4.50	4.80	144.2	31.5	1226.0	953.0	73.2	9.50	0.55	27.293	301.7	154.7	106.4	0.0527
9	4.50	4.80	144.5	31.5	1236.0	955.0	73.3	9.70	0.30	34.854	301.7	157.3	106.4	0.0587
10	4.50	4.80	144.2	31.5	1236.0	956.0	73.2	9.80	0.20	52.425	304.0	160.1	106.5	0.0587
11	4.60	4.80	144.5	31.5	1236.0	956.0	72.9	9.80	0.15	64.992	304.4	163.1	106.7	0.0582
12	4.70	4.80	144.1	31.5	1236.0	956.0	73.2	10.00	0.00	82.000	304.8	171.7	106.8	0.0584

Pumping Coeff. Data, Model A Mod (950 F) - Crossflow

DATE: 05 SEP 83												DATA TAKEN BY H.E. STAPLES											
NUMBER OF PRIMARY NOZZLES: 4												WINDING STACK LENGTH: 7.22 INCHES											
PRIMARY NOZZLE DIAMETER: 2.25 INCHES												WINDING STACK L/D: 1.50											
WINDING DIAMETER: 7.510 INCHES												STANDOFF HEIGHT: 0.50											
AREA RATIO: A/DAP: 2.50												AMBIENT PRESSURE: 29.61 INCHES HG											
GAMMA: 1.3556																							
IN CROSS-FLOW																							
AR	PMH IN HG	DELTA P IN H2O	FM DEC F	NO1A	THURN DEC F	LUFT DEC F	FMH DEC F	PUFT IN H2O	PULN IN H2O	SFC AREA SQ IN	AR	WPA LBM/S	WP LHM/S	WS LBM/S	WS LBM/S	TP	PP/10	WOT/0.00	UP FT/S	UM FT/S	UNIT: 95		
1	4.50	4.90	193.6	31.5	1213.0	951.0	75.6	7.30	3.15	0.000	1	0.930	0.939	0.000	0.000	0.379	0.401	0.000	309.0	123.4	108.		
2	4.50	4.90	193.6	31.5	1231.0	953.0	76.1	7.60	2.80	1.767	2	0.930	0.939	0.099	0.105	0.379	0.356	0.069	309.7	128.4	108.		
3	4.60	4.90	194.0	31.5	1226.0	955.0	76.4	8.00	2.45	3.534	3	0.931	0.940	0.185	0.187	0.379	0.311	0.128	309.7	132.9	108.		
4	4.60	4.90	193.8	31.5	1231.0	956.0	77.0	8.20	2.15	4.801	4	0.931	0.941	0.235	0.250	0.379	0.273	0.163	309.3	135.2	108.		
5	4.60	4.90	194.2	31.5	1231.0	957.0	76.6	8.60	1.72	8.443	5	0.931	0.940	0.370	0.394	0.379	0.218	0.257	309.5	142.0	108.		
6	4.60	4.80	194.3	31.5	1237.0	954.0	76.1	8.90	1.40	11.585	6	0.920	0.930	0.459	0.493	0.378	0.181	0.321	306.4	145.1	107.		
7	4.60	4.80	194.5	31.5	1242.0	959.0	75.5	9.10	1.15	14.776	7	0.920	0.930	0.529	0.568	0.377	0.149	0.370	306.1	148.4	107.		
8	4.60	4.80	194.5	31.5	1243.0	961.0	76.0	9.60	0.55	27.293	8	0.920	0.940	0.609	0.642	0.377	0.071	0.474	306.1	155.8	107.		
9	4.70	4.80	194.9	31.5	1242.0	961.0	76.6	9.90	0.32	39.459	9	0.920	0.940	0.784	0.842	0.377	0.041	0.528	306.1	159.7	107.		
10	4.70	4.80	194.9	31.0	1213.0	950.0	77.0	9.90	0.20	52.825	10	0.921	0.954	0.941	0.981	0.376	0.026	0.551	301.8	160.2	106.		
11	4.70	4.80	195.4	31.0	1213.0	949.0	77.6	10.00	0.15	64.992	11	0.921	0.954	1.081	1.140	0.376	0.020	0.591	301.4	162.9	106.		
12	4.70	4.80	195.6	31.0	1215.0	948.0	77.9	10.00	0.00	80.000	12	0.921	0.956	1.200	1.260	0.376	0.000	0.600	303.0	171.0	106.		

TABLE XV

Mixing Stack Pressure Data, Model A

Uptake Temperature	Axial Position (F)	Mixing Stack Pressure (in. water ref. to atmos.)		
		550	850 (NO CROSSFLOW)	950
Position A	0.00	-0.95	-1.05	-1.05
	0.25	-0.50	-0.55	-0.52
	0.50	-0.15	-0.10	-0.05
	0.75	-0.05	-0.65	-0.10
Position B	0.00	-0.90	-1.05	-1.00
	0.25	-0.25	-0.30	-0.30
	0.50	-0.55	-0.55	-0.55
	0.75	-0.40	-0.25	-0.28
(CROSSFLOW)				
Position A			-1.10	-1.15
			-0.60	-0.60
			-0.15	-0.15
			-0.35	-0.35
Position B			-1.10	-1.15
			-0.32	-0.35
			-0.72	-0.67
			-0.55	-0.50

TABLE XVI

Mixing Stack Pressure Data, Model A Modified

Uptake Temperature	Axial Position (F)	Mixing Stack Pressure (in. water ref. to atmos.)	
		850 (NO	950 CROSSFLOW)
Position A	0.00	-1.10	-1.10
	0.25	-0.55	-0.55
	0.50	-0.15	-0.15
	0.75	-0.25	-0.32
Position B	0.00	-1.02	-1.00
	0.25	-0.28	-0.29
	0.50	-0.55	-0.53
	0.75	-0.25	-0.24
(CROSSFLOW)			
Position A		-1.10	-1.20
		-0.60	-0.60
		-0.15	-0.20
		-0.35	-0.40
Position B		-1.10	-1.15
		-0.32	-0.35
		-0.70	-0.70
		-0.52	-0.50

TABLE XVII

Mixing Stack Temperature Data, Model A

Thermocouple Number	Axial Position	Mixing Stack Temperature (degrees F)				
Uptake Temperature		650 NCF	850 NCF	850 CF	950 NCF	950 CF
6	0.00	101	135	110	150	123
7	0.00	106	139	115	163	129
10	0.41	67	67	79	77	75
9	0.41	195	258	231	297	263
16	0.36	158	234	189	258	231
11	0.46	74	79	87	88	100
12	0.61	198	204	290	342	324
14	0.76	241	314	308	357	343
15	0.89	226	263	283	301	301
8	0.89	230	305	301	345	336
17	0.84	73	74	103	87	91
13	0.94	258	305	314	347	340
Ambient		65	67	75	75	69

NCF - NO CROSSFLOW
CF - CROSSFLOW

TABLE XVIII

Mixing Stack Temperature Data, Model A Mod

Thermocouple Number	Axial Position	Mixing Stack Temperature (degrees F)			
Uptake Temperature		850 NCF	850 CF	950 NCF	950 CF
6	0.00	142	108	162	127
7	0.00	146	113	168	133
10	0.41	76	77	72	77
9	0.41	263	230	299	263
16	0.36	237	192	282	235
11	0.46	88	84	98	91
12	0.61	306	289	343	324
14	0.76	321	309	358	342
15	0.89	272	278	296	299
8	0.89	311	300	348	333
17	0.84	84	93	83	119
13	0.94	312	312	342	336
Ambient		73	69	73	76

NCF - NO CROSSFLOW
CF - CROSSFLOW

TABLE XIX
Shroud and Diffuser Temp. Data, Model A

	AXIAL POSITION	TEMPERATURE					(F)
UPTAKE TEMPERATURE	(X/D)	650 NCF	850 NCF	850 CF	950 NCF	950 CF	
SHROUD	0.125	73.8	78.0	81.8	90.3	88.0	
	0.375	81.1	88.5	86.5	101.4	86.9	
	0.625	87.4	98.0	86.3	111.7	88.9	
	0.750	97.2	108.8	91.5	124.5	95.3	
	1.068	125.4	143.9	108.4	160.3	111.7	
DIFFUSER RING	1	80.6	83.0	96.2	96.3	95.3	
	2	80.7	83.5	104.1	96.5	107.8	
	3	76.5	78.7	94.8	90.6	100.1	
	4	82.9	85.2	101.2	97.6	107.7	
	5	87.9	87.3	99.3	103.0	106.3	
	SA	84.6	90.9	96.9	102.8	102.6	
	SB	92.7	103.5	92.0	114.5	102.0	
AMBIENT		66	67	75	75	69	

NCF - NO CROSSFLOW
CF - CROSSFLOW

TABLE XX
Shroud and Diffuser Temp. Data, Model A Mod

UPTAKE TEMPERATURE	AXIAL POSITION (X/D)	TEMPERATURE (F)			
		850 NCF	850 CF	950 NCF	950 CF
SHROUD	0.125	87.5	77.7	87.4	82.7
	0.375	98.1	86.3	94.9	88.9
	0.625	106.1	97.5	108.5	92.1
	0.750	114.1	104.0	118.3	96.2
	1.068	151.9	108.4	166.2	115.7
DIFFUSER RING	1	91.8	106.0	90.6	93.3
	2	93.0	106.9	91.4	105.2
	3	88.4	99.0	95.6	99.2
	4	94.7	108.2	93.6	104.5
	5	95.8	90.1	94.5	101.4
	5A	95.5	92.2	94.1	98.5
	5B	99.7	93.2	96.2	91.2
AMBIENT		73	69	73	76

NCF - NO CROSSFLOW
 CF - CROSSFLOW

TABLE XXI
Exit Plane Temperature Data, Model A

UPTAKE TEMPERATURE	AXIAL POSITION	R/RMS	TEMPERATURE				
			650 NCF	850 NCF	850 CF	950 NCF	950 CF
	0.00	1.171	177	176	102	107	119
	0.25	1.101	210	259	144	258	165
	0.50	1.031	247	312	201	330	215
	0.75	0.961	271	349	250	372	268
	1.00	0.890	302	388	299	417	323
	1.25	0.820	325	415	332	450	364
	1.50	0.750	339	458	365	466	404
	1.75	0.680	352	473	390	489	431
	2.00	0.610	369	482	412	498	455
	2.25	0.539	381	495	433	515	481
	2.50	0.469	395	504	454	531	496
	2.75	0.399	406	514	472	542	515
	3.00	0.329	415	520	480	554	534
	3.25	0.259	423	523	499	566	550
	3.50	0.188	429	524	511	574	574
	3.75	0.118	432	520	524	579	581
	4.00	0.048	434	513	528	584	581
	4.25	0.000	434	505	529	582	576
	4.25	0.000	435	523	531	586	584
	4.00	0.048	434	521	530	584	584
	3.75	0.118	432	515	527	575	581
	3.50	0.188	427	508	519	572	573
	3.25	0.259	421	497	513	556	566
	3.00	0.329	410	487	503	549	554
	2.75	0.399	404	478	494	536	547
	2.50	0.469	390	463	495	520	540
	2.25	0.539	377	450	476	509	532
	2.00	0.610	360	440	468	495	522
	1.75	0.680	343	425	456	480	510
	1.50	0.750	322	408	442	463	505
	1.25	0.820	294	392	423	448	498
	1.00	0.890	270	363	404	412	469
	0.75	0.961	237	329	336	367	419
	0.50	1.031	197	273	262	316	343
	0.25	1.101	146	200	195	242	253
	0.00	1.171	108	146	103	168	146

TABLE XXII
Exit Plane Temperature Data, Model A Mod

UPTAKE TEMPERATURE	AXIAL POSITION	R/RMS	TEMPERATURE			
			850 NCF	850 CF	950 NCF	950 CF
	0.00	1.171	168	97	135	98
	0.25	1.101	223	141	201	134
	0.50	1.031	270	229	279	185
	0.75	0.961	325	275	345	243
	1.00	0.890	355	317	391	301
	1.25	0.820	394	348	416	350
	1.50	0.750	405	378	441	381
	1.75	0.680	421	402	461	413
	2.00	0.610	443	420	477	440
	2.25	0.539	457	444	493	464
	2.50	0.469	470	461	507	487
	2.75	0.399	486	475	521	503
	3.00	0.329	500	494	536	520
	3.25	0.259	510	508	545	535
	3.50	0.188	516	519	557	554
	3.75	0.118	525	528	571	564
	4.00	0.048	535	529	573	573
	4.25	0.000	535	529	583	580
	4.25	0.000	535	533	586	582
	4.00	0.048	532	532	585	579
	3.75	0.118	529	527	580	575
	3.50	0.188	524	519	571	566
	3.25	0.259	515	512	564	555
	3.00	0.329	510	502	556	547
	2.75	0.399	499	498	543	539
	2.50	0.469	490	486	534	527
	2.25	0.539	481	475	521	517
	2.00	0.610	472	468	515	512
	1.75	0.680	464	455	505	499
	1.50	0.750	456	450	494	489
	1.25	0.820	445	431	473	462
	1.00	0.890	409	388	440	408
	0.75	0.961	362	325	386	338
	0.50	1.031	281	236	284	243
	0.25	1.101	210	155	198	142
	0.00	1.171	101	92	103	101

TABLE XXIII
Exit Plane Horiz. Pitot Traverse Data

PITOT POSITION (IN.)	DYNAMIC PRESSURE (IN. H ₂ O)	VELOCITY (KNOTS)
0.000	0.100	12.53
0.500	0.850	36.52
1.000	0.750	34.50
1.500	0.700	33.14
2.000	0.650	31.54
2.500	0.650	31.54
3.000	0.650	31.54
3.500	0.650	31.54
4.000	0.675	32.55
4.500	0.675	32.55
5.000	0.650	32.55
5.500	0.625	31.32
6.000	0.625	31.32
6.500	0.675	32.55
7.000	0.675	32.55
7.500	0.675	32.55
8.000	0.650	31.54
8.500	0.625	31.32
9.000	0.600	30.69
9.500	0.675	32.55
10.000	0.675	32.55
10.500	0.700	33.14
11.000	0.675	32.55
11.500	0.625	31.32
11.625	0.000	00.00

1

TABLE XXIV
24 in. Standoff -Pitot Horiz. Traverse

PITOT POSITION (IN.)	DYNAMIC PRESSURE (IN. H ₂ O)	VELOCITY (KNOTS)
0.000	0.400	25.06
0.500	0.400	25.06
1.000	0.400	25.06
1.500	0.380	24.42
2.000	0.360	23.77
2.500	0.350	23.44
3.000	0.350	23.44
3.500	0.350	23.44
4.000	0.350	23.44
4.500	0.350	23.44
5.000	0.400	25.05
5.500	0.450	26.53
6.000	0.520	28.57
6.500	0.550	29.38
7.000	0.600	30.69
7.500	0.640	31.69
8.000	0.640	31.69
8.500	0.650	31.94
9.000	0.640	31.69
9.500	0.600	30.69
10.000	0.600	30.69
10.500	0.600	30.69
11.000	0.600	30.69
11.500	0.550	29.38
11.625	0.550	29.38

TABLE XXV
24 in. Standoff - Pitot Vertical Traverse

PITOT POSITION (IN.)	DYNAMIC PRESSURE (IN. H ₂ O)	VELOCITY (KNOTS)
0.000	0.150	15.43
0.500	0.170	16.42
1.000	0.200	17.61
1.500	0.250	19.91
2.000	0.275	20.69
2.500	0.275	20.69
3.000	0.350	23.56
3.500	0.350	23.56
4.000	0.350	23.56
4.500	0.450	26.72
5.000	0.500	28.16
5.500	0.500	28.16
6.000	0.600	30.65
6.500	0.600	30.65
7.000	0.620	31.36
7.500	0.620	31.36
8.000	0.620	31.36
8.500	0.620	31.36
9.000	0.600	30.65
9.500	0.600	30.65
10.000	0.600	30.65
10.500	0.600	30.65
11.000	0.600	30.65
11.500	0.600	30.65
12.000	0.570	30.07
12.500	0.570	30.07
13.000	0.500	28.16
13.500	0.450	26.72
14.000	0.370	24.23
14.250	0.370	24.23

TABLE XXVI
24 in. Standoff -4.5 in Pitot Vert. Traverse

PITOT POSITION (IN.)	DYNAMIC PRESSURE (IN. H ₂ O)	VELOCITY (KNOTS)
0.000	0.300	21.70
0.250	0.300	21.70
0.500	0.230	19.00
0.750	0.325	22.58
1.000	0.480	27.45
1.250	0.550	29.38
1.500	0.600	30.69
1.750	0.610	30.94
2.000	0.610	30.94
2.250	0.610	30.94
2.500	0.610	30.94
2.750	0.590	30.43
3.000	0.580	30.17
3.250	0.560	29.65
3.500	0.550	29.38
3.750	0.530	28.64
4.000	0.510	28.29
4.250	0.500	28.01
4.500	0.470	27.16

TABLE XXVII
Pumping Coefficient Results

FIVE RING DIFFUSER		
TUPT	NO CROSSFLOW (F)	CROSSFLOW
175	0.50 *(0.54)	--
650	0.51	--
850	0.57	0.59
950	0.55	0.61
SIX RING DIFFUSER		
850	0.57	0.59
950	0.58	0.59

*PRITCHARD FROM COLD FLOW TEST

TABLE XXVIII
Air Mass Flow Calibration Data

P_{NH+B} (IN. HG)	ΔP_N (IN. H ₂ O)	$\left[\frac{P_{NH+B} \cdot \Delta P_N}{INHR} \right]^{0.5}$	\dot{m}_a (LBM/SEC)
31.15	2.0	0.319	0.554
31.15	2.0	0.316	0.555
31.15	2.0	0.313	0.591
32.85	4.0	0.459	0.833
32.85	4.0	0.462	0.838
33.85	4.0	0.435	0.852
34.75	6.0	0.582	1.026
35.05	6.0	0.579	1.051
38.65	6.0	0.606	1.126
38.55	8.0	0.706	1.295
39.15	8.0	0.705	1.300
47.65	8.0	0.774	1.477
51.55	9.5	0.827	1.595
47.95	10.0	0.875	1.634
48.75	10.0	0.877	1.643

TABLE XXIX
Air Mass Flow vs. Pressure Product Data

\dot{m}_a (LBM/SEC)	PRESSURE PRODUCT
0.554	0.319
0.555	0.316
0.591	0.319
0.833	0.459
0.838	0.462
0.852	0.435
1.026	0.582
1.051	0.579
1.126	0.606
1.295	0.706
1.300	0.705
1.477	0.774
1.595	0.827
1.634	0.875
1.643	0.877

APPENDIX A

GAS GENERATION OPERATION

I. PRIMARY AIR COMPRESSOR OPERATION The primary air flow for the gas generator is supplied by a Carrier Model 18P352 three stage centrifugal air compressor located in Building 230. The compressor is driven through a Western Gear Model 95HSA speed increasing gearbox by a 300 horsepower General Electric induction motor. The compressor serves various other experiments both in building 230 and 249. Figure (14) is a schematic of the compressor system layout. The cooling water system serves both the Carrier compressor and the Sullivan compressor for the supersonic wind tunnel in building 230.

Lube oil for the compressor and speed increaser bearings is supplied from an external sump by either an attached pump or an electrically driven auxiliary pump. The lube oil is cooled in a closed loop oil to fresh water heater exchanger. Cooling water circulates within its own loop and is cooled in an evaporative cooling tower which stands between buildings 230 and 249. Makeup is automatically provided to the fresh water loop by a float operated valve in the cooling tower.

It is recommended that the lube oil system for the compressor be started approximately one hour prior to

AD-A139 953

OPERATIONAL PERFORMANCE CHARACTERISTICS OF A
MULTIPLY-SHROUDED ANGLED-DIP (U) NAVAL POSTGRADUATE
SCHOOL MONTEREY CA R E STAPLES SEP 83

3/3

UNCLASSIFIED

F/O 21/5

ML

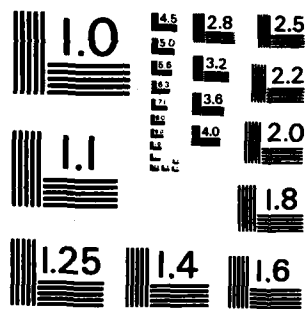
END

DATE

FILMED

84

DT-



MICROCOPY RESOLUTION TEST CHART
NATIONAL BUREAU OF STANDARDS-1963-A

compressor lightoff. This ensures adequate pre-lubrication and warms the oil to some degree, decreasing starting loads. This is critical, as the compressor operates at near the capacity of the breaker in the supplying substation. Should this breaker trip out during the starting sequence it will be necessary to call the trouble desk and have base electricians reset it.

During periods when operations are being conducted daily or when it is desired to operate early in the morning, it is permissible to leave the auxiliary oil pump running overnight with the cooling water system secured. This will maintain the lube oil at a temperature suitable for lightoff and eliminate this delay.

When fully warmed up the compressor supplies air to the gas generator at 170-190°F. It normally takes the compressor about one hour to reach stable operation at this temperature. Although it is possible to obtain a gas generator lightoff with a lower air supply temperature, stable operation enhances data taking and reduces the number of control adjustments required during data runs. It is, therefore, desirable to allow the system to fully stabilize prior to lighting off the gas generator or collecting data. The following lightoff sequence is recommended:

- A) Check the oil level in the compressor's external sump. Oil should be within four inches of the top of the sight glass.
- B) Start the auxiliary oil pump by positioning the "hand-off automatic" switch (Figure 15) in the "hand" position. The electric pump will start and oil pressure should register approximately 30 PSIG. Inspect the system for leaks and note the level in the external sump.
- C) Wait 45 minutes to one hour. During this period the compressor bearing temperatures should rise to approximately 70^oF.
- D) Line up the combustion gas generator for operation.
 - 1) Open the two manometer isolation valves at the pressure taps on either side of the inlet reducing section (Figure 5). Reconnect manometer tubing at the manometers if it has previously been disconnected.
 - 2) Ensure the main air supply butterfly valve is fully closed (Figure 6).
 - 3) Open the air supply bypass globe valve two and one quarter turns (Figure 6).
 - 4) Open the manually operated 4 inch butterfly isolation valve (Figure 5).

- 5) Energize the main power panel (Figure 9) and open the electrically operated burner air supply and cooling air bypass valves fully.
 - 6) Ensure the gas generator exhaust area is clear.
- E) Start the air compressor fresh water cooling system:
- 1) Check the water level in the cooling tower it should be at the level of the inlet line.
 - 2) Vent the cooling water pump casing. Open the petcock on the suction side of the pump casing until all air in the suction line is expelled.
 - 3) Ensure valve "A" to the Sullivan compressor is closed.
 - 4) Open valve "B" to the Carrier compressor.
 - 5) Start the cooling water pump and cooling tower fan (Figure 17). The fan is interlocked with the pump and will not start unless the pump is running.
 - 6) Inspect the cooling tower drip lattice to ensure water is circulating.
- F) Open the drain on the air compressor air cooling bank (Figure 19).

- G) Ensure the compressor air suction valve is fully closed (indicator vertical) (Figure 20).

WARNING When in operation the compressor produces hazardous noise. Ensure all personnel in the vicinity are wearing adequate hearing protection prior to starting the compressor.

- H) Start the air compressor motor (Figure 13), the controller uses an automatic two stage start circuit.
- I) When the compressor is fully up to speed, switch the auxiliary lube oil pump to the "automatic" position. Lube oil pressure should remain about 24-30 PSIG. Oil is now being supplied by the attached pump driven by the speed increasing gearbox. If the oil pressure should fall to 12 PSIG, the auxiliary pump will start automatically.
- J) When compressor operation has stabilized, slowly open the suction valve until the indicator is in

the full open (horizontal) position. Air is now being supplied to the gas generator. Bypass air from the supply to other experiments will also be discharged outside the rear of building 230. Normally it is not necessary to secure this bypass flow, but in unusual circumstances it may be stopped by closing the isolation valve on the cooling bank (Figure 19).

- K) Operation of the air compressor should be monitored periodically.
- 1) Normal oil pressure from the attached pump is 24 PSIG. Specified bearing pressure are 20-25 PSIG.
 - 2) Normal oil pressure from the auxiliary electric pump is 30 PSIG.
 - 3) Normal oil temperature at the outlet of the lube oil cooler is 100-105°F (135°F maximum).
 - 4) Normal Bearing temperatures for the compressor are 140-160°F. Speed increaser oil temperature is normally 120-130°F.
 - 5) Do not allow any bearing temperature to exceed 200°F. In the event bearing temperatures rise above 180°F during normal operation, the oil cooler should be inspected for proper water temperature and flow rate.

II. GAS GENERATOR LIGHT OFF Allow the air compressor to operate for approximately one hour in order for air inlet temperature to the gas generator to stabilize.

- A) Approximately 15 minutes prior to gas generator light off, line up the fuel system and place it in operation.
- 1) Open the fuel tank suction valve (Figure 22) and bulkhead isolation valve (Figure 21).
 - 2) Ensure the solenoid operated emergency fuel cutoff valve is closed and close the HP pump manual discharge valve.
 - 3) Open the nozzle box drain valve.
 - 4) If this is the first time the system is being placed in operation, open both the fuel control valve (Figure 8) and the needle trimmer valve (Figure 24) fully. If the trimmer valve is known to be properly set, it need not be adjusted as described in this and following steps.
 - 5) Start the fuel supply pump. Fuel supply pressure will be 14-16 PSIG.
 - 6) Start the HP pump. With both trimmer and fuel control valves fully open the discharge pressure

will be 25-30 PSIG. With the trimmer valve properly set and the fuel control valve fully open, the HP pump discharge pressure will be 80 PSIG.

- 7) If the trimmer valve is to be adjusted, close the fuel control valve with the trimmer valve fully open. Observing the HP pump discharge pressure, slowly close the trimmer valve until the HP pump pressure reaches 350 PSIG. The trimmer valve is now set and the fuel control valve should provide smooth control over a range of 80-350 PSIG HP pump discharge pressure. All subsequent fuel control adjustments will be made using the fuel control valve.
- 8) Using the fuel control valve, set the HP pump discharge pressure at 200 PSIG and allow the system to recirculate for 10-15 minutes to warm the fuel. This facilitates combustion and ensures a clean lightoff.

B) When the inlet air temperature reaches 170-180°F, the gas generator may be lighted off.

- 1) Adjust inlet air bypass valve to obtain a pressure of approximately 4.0 in Hg at the upstream side of the inlet reducing section (PNH).

- 2) Ensure the burner air valve is fully open.
Adjust the bypass cooling air valve to obtain a pressure drop across the U-tube of 1.60 inches H_2O . In some cases it may be necessary to leave the cooling air bypass valve fully open and reduce the inlet air pressure (PNH) slightly to obtain this setting. The pressure drop across the inlet reducing section (DELPN) will be about 15 inches H_2O . This provides the recommended lightoff air fuel ratio of 20.
- 3) Open the HP pump manual discharge valve fully.
- 4) Set the high temperature (Type K) readout to monitor burner temperature (TBURN). Set the low temperature (Type T) readout to monitor air inlet temperature (TNH).
- 5) Ensure the gas generator exhaust area is clear.
- 6) Adjust the HP pump discharge pressure to 150 PSIG.
- 7) Depress and hold down the spring loaded ignitor switch for 10 seconds.
- 8) While continuing to hold the ignitor switch depressed, open the solenoid operated emergency fuel cutoff valve. Ignition should be observed in 6-12 seconds. If the gas generator fails to light, close the emergency fuel cutoff valve

and release the ignitor switch. Allow the system to purge for 5 minutes or until no raw fuel is being expelled from the primary nozzle. If the gas generator fails to light, raw fuel will be expelled from the primary nozzles and will collect in the base of the secondary plenum. This should be wiped up prior to continuing.

- 9) When ignition is observed, release the ignitor switch.
- 10) Observe the burner temperature. When the burner temperature reaches 1000°F begin reducing fuel pressure toward minimum (70-75 PSIG at the burner nozzle, (PNOZ)) to stabilize burner temperature between 1000 and 1300°F.

WARNING Do not allow burner temperature to exceed 1500°F.

It will be necessary to close the cooling air bypass valve to about 50 percent open to achieve stable operation at the desired burner temperature.

CAUTION Do not allow burner temperature to fall below 1000°F. The gas generator will begin to emit white smoke when the burner temperature falls to about 950°F and combustion will cease at a burner temperature of about 800°F. If combustion ceases there will be a noticable change in sound intensity accompanied by quantities of white smoke and rapidly falling burner temperature; immediately close the emergency fuel cutoff valve. Readjust fuel and air controls to lightoff settings and reinitiate the lightoff sequence.

The prescribed lightoff sequence usually leads to stable operation with an uptake temperature of 400-500°F and an uptake Mach number of about 0.07.

WARNING Do not allow uptake temperature to exceed 1200°F at any time.

- 11) When stable operation has been established, close the nozzle box drain valve prior to attempting to adjust the uptake Mach number.

III. TEMPERATURE/MACH NUMBER CONTROL

The control process consists of a iterative sequence of adjustments in the uptake temperature (TUPT), inlet air pressure (PNH), and bypass cooling air mass flow. Some practice is necessary to achieve reasonable accuracy in the adjustment process. It must be kept in mind that effect of the bypass cooling air valve varies depending on the valve's initial position. When the bypass valve is more than 50 percent open, opening the valve reduces air flow through the burner, increasing burner temperature (TBURN), however, the increase in the proportion of cool bypass air mixing with the combustion gas results in a lower uptake temperature. When a majority of the air flow is already passing through the combustion chamber, that is, when the bypass valve is less than 50 percent open,

and particularly when it is less than 25 percent open, the increase in burner temperature resulting from opening the bypass valve more than offsets the increased proportion of cooling air and the uptake temperature will raise when the bypass valve is opened. With these cautions in mind, the following adjustment procedure is recommended:

- A) Adjust the fuel control valve to obtain the desired uptake temperature. Do not allow burner temperature to fall below 1000°F or to exceed 1300°F during this process.
- B) As burner temperature approaches one of the limits, change air flow through the burner either by adjusting the bypass valve or the inlet globe valve. Choice of control device depends on the prior operating state. If the system has been stabilized at the desired Mach number it is usually best to control burner temperature during transitions by using the inlet globe valve. The key operating parameters are uptake temperature (TUPT) and uptake pressure (PUPT). Burner temperature is monitored to ensure safe combustion is maintained. For operation with uptake an Mach number of approximately 0.065, the values in Table XXII are recommended:

Recommended Initial Control Settings

TUPT (° F)	PUPT (inches H O)
950	13.3
850	11.1
750	10.5
650	9.6
550	9.0
175	8.8

C) Compute the uptake Mach number (UMACH) using the formula:

$$UMACH = 1.037 \times 10^{-1} (TUPTR/\gamma)^{0.5} \times (((PNH - B) \times DELPN / TNHR)^{0.5} - (2.318 \times 10^{-4} \times ROTA) - 2.085 \times 10^{-1}) / (B + (PUPT / 13.5717)))$$

(eqn A.1)

where:

UMACH = Uptake Mach number
TUPTR = Absolute uptake temperature (R)
 γ = Ratio of specific heats for air

Values of the Ratio of Specific Heats for Air

TUPT (°F)	γ
175	1.3991
550	1.3805
650	1.3741
750	1.3677
850	1.3614
950	1.3556

- PNH = Air pressure before the inlet
reducing section (inches Hg)
- B = Corrected atmospheric pressure
(inches Hg)
- DELPN = Pressure drop across the inlet
reducing section (inches H₂O)
- TNHR = Absolute air temperature before the
inlet reducing section (R)
- ROTA = Fuel mass flow rotameter reading
- PUPT = Gas pressure in the uptake section
(inches H₂O)

D) Adjust the uptake temperature and pressure as necessary using a combination of inlet globe valve, cooling air bypass valve, and fuel control valve changes until the desired test Mach number is obtained.

E) If inlet air temperature has been allowed to stabilize prior to gas generator operation, it will be found that, once the desired uptake temperature and Mach number have been set, no adjustments to the system will be required during data runs. Uptake temperature will be maintained within plus or minus four degrees and uptake Mach number will vary less than 0.001 under most circumstances. The largest variations in uptake Mach number observed have been during pumping coefficient runs when changes in secondary flow induce large changes in uptake pressure. If the gas generator is at the operating point prior to closing the plenum, it will be unnecessary to make adjustments for the slight increase (0.0005 to 0.0010) in Mach number which occurs when secondary flow is shut off.

IV. SECURING THE SYSTEM

A) When data runs are complete, shut down the gas generator by reducing the fuel pressure to minimum and immediately closing the solenoid operated emergency fuel cutoff valve.

- 1) Shut off the high pressure fuel pump.
- 2) Shut off the fuel supply pump.
- 3) Open the cooling air bypass valve fully.
- 4) Open the inner bypass glove valve until an inlet pressure (PNH) of 4.0-5.0 inches Hg is obtained.
- 5) Allow the gas generator to run in this manner until the uptake temperature drops to approximately the inlet air temperature.
- 6) Close the fuel system bulkhead and tank isolation valves. It is good practice to refill the fuel service tank at the end of each operating period. Keeping the tank full of fuel reduces moisture buildup from condensation. Any water or sediment which might enter the tank during filling will have time to settle out and can be removed through the stripping connection prior to the next lightoff.

- B) When the gas generator has cooled sufficiently, the air compressor may be shut down.
- 1) Close the compressor suction butterfly valve.
 - 2) Stop the electric motor.
 - 3) When the compressor oil pressure falls below 20 PSIG, switch the auxiliary oil pump control from the "automatic" to the "hand" position.
 - 4) Allow the lube oil system to run for one hour or until the compressor bearing temperatures are less than 80°F.
 - 5) Stop the auxiliary lube oil pump.
 - 6) Stop the cooling tower fan and cooling water pump.
- C) Close the 4 inch butterfly manual isolation valve.
- D) Close the inlet bypass globe valve.
- E) Open the nozzle box drain valve.
- F) Close the manometer isolation valves. It is also good practice to disconnect the inlet air pressure (PNH) and reducing section pressure drop (DELPN) manometers at the manometer. Other users of the compressor operate at pressures sufficient to over-pressurize these instruments. Over-pressurization

of the mercury manometer which measures the inlet pressure could result in a hazardous mercury spill.

- G) De-energize the main power panel and shut off the thermocouple readouts.

APPENDIX B

CALIBRATION

The use of pressure drop data across nonstandard metering devices requires that the flow restrictor be calibrated to a known or well defined measuring standard. In the case of the experimental apparatus used in the conduct of this experimental work, calibration of the entrance nozzle was essential in effective determination of the air mass flow rate.

The entrance nozzle calibration arrangements utilized was that of Ross [Ref. 6]. An ASME standard Hershel-type Venturi was used as the primary flow measuring device. Data was recorded over a range of inlet pressure drop values from 2.0 in. water to a maximum nominal pressure drop of 10.0 in. water. This data is shown in Table XXVIII.

For the Hershel-type Venturi the mass flow rate is given by equation II-III-15C of [Ref. 15]

$$\dot{m}_a = 0.099702 C_d Y_d^2 F (1-\beta^4)^{-0.5} (\rho h_w)^{0.5} \quad (\text{lbm/sec}) \quad (\text{eqn B.1})$$

where " C_d " is the discharge coefficient of the venturi, " Y " is the expansion factor, " d " is the throat diameter (in.), F is the area thermal expansion factor, " β " is the ratio of throat diameter to entrance diameter, " ρ " is the density of the fluid and " h_w " is the differential pressure (in. water).

After analyzing the data recorded in Table XXIX, it was decided that a linear curve fit in the range of mass flow rates most commonly encountered in previous experimental work would provide the best predictor of the actual mass flow conditions. The range of mass flow rates selected was approximately 0.875-1.740 lbm/sec of air which is considered to effectively bracket the range of experimentally encountered mass flows.

The entrance nozzle calibration is shown in Figure 42 with the data utilized being contained in Table XXIX.

The entrance nozzle was modeled as a venturi using the functional relationship

$$\dot{m}_{air} = f (P \cdot \Delta P / T)^{0.5}$$

which is given by equation II-III-15C of [Ref. 15]. Detailed entrance nozzle mass flow calibration calculations are contained in [Ref. 6], Appendix A.

APPENDIX C
UNCERTAINTY ANALYSIS

The determination of the uncertainties in the experimentally determined pressure coefficients and pumping coefficients was made using the methods described by previous researchers. The basic uncertainty analysis for the cold flow eductor model test facility was conducted by Ellin [Ref. 2] and Hill [Ref. 9] follows this development in analysis of the hot flow facility. Hill's analysis has been corrected for changes in the measured uncertainties resulting from the installation of new fuel flow measuring equipment. The uncertainties obtained using the second order equation were applicable to the experimental work conducted during the present research and are listed here.

UNCERTAINTY IN MEASURED VALUES

<u>Parameter</u>	<u>Value</u>	<u>Uncertainty</u>
TAMB	537 R	<u>+1</u>
TUPT	1415 R	<u>+1</u>
B	29.83 in Hg	<u>+0.005</u>
DELPN	6.20 in H ₂ O	<u>+0.05</u>
PUPT	13.6 in H ₂ O	<u>+0.05</u>
ROTA	28.0	<u>+0.2</u>
PNH	5.9 in Hg	<u>+0.05</u>
TNH	649 R	<u>+0.2</u>
PPLN	5.18 in H ₂ O	<u>+0.01</u>

UNCERTAINTY IN CALCULATED VALUES

P^*/T^*	1.7%
$W^*T^{0.44}$	1.4%

LIST OF REFERENCES

1. Charwat, Andrew, "DD-963 Exhaust Stack Studied," University of California at Los Angeles, July 10, 1971.
2. Ellin, C. R., Model Test of Multiple Nozzle Exhaust Gas Eductor Systems for Gas Turbine Powered Ships, Engineer's Thesis, Naval Postgraduate School, June 1977.
3. Pucci, P. F., Simple Eductor Design Parameters, Ph.D. Thesis, Stanford University, September 1954.
4. Moss, C. M., Effects of Several Geometric Parameters on the Performance of Multiple Nozzle Eductor System, Master's Thesis, Naval Postgraduate School, September 1977.
5. Harrell, J. P., Jr., Experimentally Determined Effects of Eductor Geometry on the Performance of Exhaust Gas Eductors for Gas Turbine Powered Ships, Engineer's Thesis, Naval Postgraduate School, September 1981.
6. Ross, P. D., Combustion Gas Generator for Gas Turbine Exhaust Systems Modelling, Master's Thesis, Naval Postgraduate School, December 1977.
7. Welch, D. R., Hot Flow Testing of Multiple Nozzle Exhaust Eductor Systems, Engineer's Thesis, Naval Postgraduate School, September 1978.
8. Lemke, R. J. and Staehli, C. P., Performance of Multiple Nozzle Eductor Systems, Master's Thesis, Naval Postgraduate School, September 1977.
9. Hill, J. A., Hot Flow Testing of Multiple Nozzle Exhaust Eductor Systems, Master's Thesis, Naval Postgraduate School, September 1979.
10. Eick, I. J., Testing of a Shrouded, Short Mixing Stack Gas Eductor Model Using High Temperature Primary Flow, Master's Thesis, Naval Postgraduate School, October 1982.
11. Kavalis, A. E., Effect of Shroud Geometry on the Effectiveness of a Short Mixing Stack Gas Eductor Model, Master's Thesis, Naval Postgraduate School, June 1983.

12. Pritchard, N. D., Jr., Characteristics of a Four Nozzle, Slotting Mixing Stack with Slanted Shroud, Gas Eductor System, Master's Thesis, Naval Postgraduate School, June 1983.
13. Drucker, C. J., Characteristics of a Four-Nozzle, Slotted Short Mixing Stack with Shroud, Gas Eductor System, Master's Thesis, Naval Postgraduate School, March 1982.
14. Holman, J. P., Experimental Methods for Engineers, Third Edition, pp. 253-258, McGraw-Hill, 1978.
15. American Society of Mechanical Engineers Interim Supplement 19.5 of Instrumentation and Apparatus, Fluid Meters, Sixth Edition, 1971.

INITIAL DISTRIBUTION LIST

	No. Copies
1. Defense Technical Information Center Cameron Station Alexandria, Virginia 22314	2
2. Library, Code 0142 Naval Postgraduate School Monterey, California 93943	2
3. Department Chairman, Code 69 Department of Mechanical Engineering Naval Postgraduate School Monterey, California 93943	2
4. Professor Paul F. Pucci, Code 69Pc Department of Mechanical Engineering Naval Postgraduate School Monterey, California 93943	2
5. Dean of Research, Code 012 Naval Postgraduate School Monterey, California 93943	1
6. Commander ATTN: NAVSEA, Code 0331 Naval Sea Systems Command Washington, DC 20362	1
7. Mr. Olin M. Pearcy NSRDC, Code 2833 Naval Ship Research and Development Center Annapolis, Maryland 21402	1
8. Mr. Mark Goldberg NSRDC, 2033 Naval Ship Research and Development Center Annapolis, Maryland 21402	1
9. Mr. Eugene P. Wienert Head, Combined Power and Gas Turbine Branch Naval Surface Ship Engineering Station Philadelphia, Pennsylvania 19112	1
10. Mr. Donald N. McCallum NAVSEC Code 6136 Naval Ship Engineering Center Washington, DC 21362	1

	No. Copies
11. LCDR Ira J. Eick, USN P.O. Box 248 Lebanon, New Jersey 08833	1
12. LT Carl J. Drucker, USN 1032 Marlborough Street Philadelphia, Pennsylvania 19125	1
13. LCDR C. M. Moss, USN 625 Midway Road Powder Springs, Georgia 30073	1
14. LCDR J. P. Harrell, Jr., USNR 1600 Stanley Ardmore, Oklahoma 73401	1
15. LCDR J. A. Hill, USN RFD 2, Box 116B Elizabeth Lane York, Maine 03909	1
16. CDR R. J. Lemke, USN 2902 No. Cheyenne Tacoma, Washington 98407	1
17. LCDR C. P. Staehli, USN 2808 39th St., N.W. Gig Harbor, Washington 98335	1
18. LT R. S. Shaw, USN 147 Wampee Curve Summerville, South Carolina 29843	1
19. LCDR D. L. Ryan, USN 6393 Caminito Luisito San Diego, California 92111	1
20. LCDR C. C. Davis, USN 1608 Linden Drive Florence, South Carolina 29501	1
21. LCDR D. Welch, USN 1036 Brestwick Commons Virginia Beach, Virginia 23464	1
22. Department Chairman Department of Marine Engineering Maine Maritime Academy Castine, Maine 04421	1

No. Copies

1

23. LCDR R. E. Staples, Jr., USN
2440 Broomsedge Trail
Virginia Beach, Virginia 23456

DATE
FILMED
8